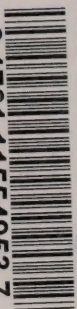


3 1761 11554953 7







Digitized by the Internet Archive  
in 2022 with funding from  
University of Toronto

<https://archive.org/details/31761115549537>







CAI EP321

-77R05

(8)

Pacific Marine Science Report 77-5

Government  
Publications

# TRACE ANALYSIS OF OIL IN SEA WATER BY FLUORESCENCE SPECTROSCOPY

W.J. Cretney  
W.K. Johnson, C.S. Wong



INSTITUTE OF OCEAN SCIENCES, PATRICIA BAY  
Victoria, B.C.





For additional copies or further information please write to:

Department of Fisheries and the Environment

Institute of Ocean Sciences, Patricia Bay

512 - 1230 Government Street

Victoria, B.C.

V8W 1Y4



## Pacific Marine Science Report 77-5

TRACE ANALYSIS OF OIL IN  
SEA WATER BY FLUORESCENCE SPECTROSCOPY

by

W.J. Cretney

W.K. Johnson, C.S. Wong

Institute of Ocean Sciences, Patricia Bay  
Victoria, B.C.

February 1977

This is a manuscript which has received only limited circulation. On citing this report in a bibliography, the title should be followed by the words "UNPUBLISHED MANUSCRIPT" which is in accordance with accepted bibliographic custom.



### Abstract

Several organic compounds were evaluated using fluorescence spectrophotometry as possible standards for the determination of trace amounts of crude oils or residual fuel oils in sea water. Chrysene was selected as the most suitable standard.

Dichloromethane was evaluated as a solvent for the extraction of oil in water at concentrations of a few micrograms per litre and was found suitable for the purpose.

Samples of sea water were collected on Cruise 73-006 of the weather-ship, CCGS Quadra. A portion of each sample was analyzed aboard ship with the remainder being retained for repeat analysis in the shore-based laboratory in Victoria. The average concentration of fluorescent extractable compounds in sea water collected at Ocean Station P (50°N, 145°W) was 0.038 µg/l when expressed as an equivalent concentration of chrysene. The average concentration, expressed as an equivalent concentration of a typical crude oil, would be about 0.4 µg/l.





## Table of Contents

	Page
Introduction.....	1
Selection of a Standard.....	2
Oil and Chrysene Comparison.....	3
Selection of Solvents.....	3
Recovery of Oil from Water.....	4
Field Trial.....	4
Storage of Samples.....	7
Summary.....	8
References.....	9
Figures.....	11
Tables.....	19
Appendices.....	31





## Introduction

A method based on the work of Levy (1971) and Keiser and Gordon (1973) was adopted for the determination of low concentrations of petroleum oil in sea water. In this method oil is extracted from sea water with an organic solvent and its concentration in the sea water is determined by measuring the intensity of fluorescence of the extracted oil in a suitable organic solvent. The method has several attractive features. It is relatively simple to learn and can be carried out quickly, making it suitable for routine analysis. It can be used for both quantitative and qualitative work with the results being only minimally affected by weathering (Coakly, 1973). Because of the high sensitivity of fluorescence spectrophotometers, 1 to 2 litre samples of even the cleanest natural waters are sufficient for analysis, and because of the high selectivity inherent in the fluorescence technique, interferences tend to be less serious than they are in some other methods. A particular disadvantage of the fluorescence method, as herein described, is that only members of certain small groups of compounds present in oils are measurable the bulk of the compounds in oils being undetectable. Thus, a small measurable fraction of an oil is being used as a tracer for the whole and unfortunately, situations do occur where the fate of the tracer is different from the fate of the whole. Consequently, results must be interpreted cautiously.

The measurable groups of compounds in oils have in common the ability to fluoresce; that is, to emit light of longer wavelength than the incident or exciting light. Fluorescence takes place, moreover, generally within microseconds of excitation. Phosphorescence, a related phenomenon, is generally characterized by longer time intervals between excitation and emission.

The polycyclic aromatic hydrocarbons (PAH) constitute a major group of fluorescent compounds in petroleum oils. Many PAH and some related hetero-atom containing polycyclic aromatic compounds are carcinogenic. Teratogenic and/or mutagenic properties may also be displayed. Consequently, the fluorescence measurement of PAH and their hetero-atom containing relatives has a value which transcends its value in locating and tracing probable oil spills.

The spectra, emission or excitation, obtained from a fluorescent compound are characteristic of its electronic structure. Compounds having a different electronic structure give different spectra. Since oils differ in the relative concentrations of fluorescent compounds, the spectra obtained for individual oils, like the spectra obtained for individual compounds, will vary, each oil having distinct emission and excitation spectra. Since oils also vary in the concentration of their fluorescent compounds relative to their non-fluorescent compounds, the fluorescence method is inherently most sensitive for the detection of oils which have the largest relative concentration of fluorescent compounds.

The work described in this report was undertaken in part to familiarize ourselves with the fluorescent characteristics of different types of oils and to assess the applicability of the fluorescence method of analysis of some typical oils in sea water. We also sought a readily available organic compound as a calibration and reference standard so that other laboratories could compare their results with ours. After we had become familiar with the fluorescence method and had found a suitable standard, during August 4 to September 19, 1973, we undertook a study of sea water on Cruise 73-006 (Fig. 1) of the weather ship CCGS Quadra.

### Selection of a Standard

There are many advantages in using a fluorescent compound rather than a fluorescent oil as a reference and calibration standard. A fluorescent compound can be chosen which is obtainable from many sources in unlimited supply. Purification to meet the criteria for a standard does not represent a serious problem. Once it is pure, a fluorescent compound need only be protected against chemical degradation, i.e., oxidation, photolysis, etc., to guarantee homogeneity between and within batches. In contrast, a standard fluorescent oil may be in limited supply from only one source, such as the American Petroleum Institute. Individual batches may vary unless strict attention to homogeneity is observed. Even within a batch homogeneity may be lost if strict handling precautions are not adhered to.

Since we felt that the oils most likely to be encountered would be crude oils, fuel oils or bunker oils, we looked for a standard for these oils rather than one for lighter refined oils. Since heavy oils generally show excitation maxima in the region 290-330 nm and emission maxima in the region 360-400 nm (Appendix 1), these characteristics were taken into consideration in the selection of the standard compound. Nearly two dozen compounds were examined before a choice was made (Appendix 2). For the selection of the trial compounds, a table, "Fluorescence Excitation and Fluorescence Emission Spectra of Model Compounds", compiled by McKay and Latham (1972), was very helpful and is reproduced in Appendix 3. There were, however, some discrepancies between their spectra and our spectra which could be attributed in part to the instruments used. Our instrument, a Perkin-Elmer Model 204, does not have the resolution of the more expensive Perkin-Elmer Model MPF-2A. Variation in detector response shape and source characteristics may also have contributed. It should be noted that the wavelengths of excitation peaks of solutions containing concentrations of over 250 µg/l were not even close to those reported by McKay and Latham. Dilution of these solutions resulted in more favorable comparisons. Intermolecular solute interactions or interference from undissolved solute particles were likely causes of the shift in the excitation peaks of the concentrated (possibly saturated) solutions.

The compound selected for our reference and calibration standard was chrysene. Although it is only slightly soluble in cyclohexane and hexane, it is otherwise particularly well suited as it has numerous peaks (Fig. 2) within the required ranges. Chrysene has excitation maxima at 308 nm and 318 nm (308 nm and 322 nm according to McKay and Latham) and emission maxima at 366 nm, 383 nm, and 400 nm (363 nm, 375 nm, 383 nm and 404 nm according to McKay and Latham). Six pairs of wavelengths could be used for comparison



with heavy oils. The 308 nm, 383 nm pair seemed the best choice since both wavelengths lie in the middle of the desired ranges. Further, our assignment of these wavelengths as the positions of the maxima agrees with that of McKay and Latham. The plot (Fig. 3) of emission intensity against chrysene concentration (in cyclohexane) shows good linearity over the concentration range, 10-50  $\mu\text{g/l}$ , which corresponds to the concentration range, in chrysene equivalents, of the extracts of the oil-spiked water samples which we prepared for study. Good linearity was similarly achieved in the range 1-10  $\mu\text{g/l}$ , which corresponds to the concentration range of extracts of deep ocean sea water samples which are presumably unpolluted.

### Oil and Chrysene Comparison

Chrysene was compared to available oils ranging from heavy fuel oils to outboard motor oils (Table 1 and Table 2). Since wavelengths used were more typical of the heavier oils than the lighter oils, the former gave much higher emission intensities. For example, crude and bunker oils studied exhibited intensities which were 20 to 80 times greater than that of Gulf outboard oil and 10 to 70 times greater than that of Esso diesel oil. The light fuel oils show excitation maxima between 280 nm and 290 nm and emission maxima between 310 nm and 330 nm. Chrysene comparisons, therefore, reflect only the tailing effects of the lighter oils. As chrysene was chosen as a standard for heavy oils, another standard would have to be found if the lighter oils were to be examined. Where possible appropriate spectra of the extracted oil should be used to identify the type of oil being measured and determine the credibility of the standard.

### Selection of Solvents

The decision to use dichloromethane as the extracting solvent was influenced by results obtained by Keiser and Gordon (1973) and verified in our own laboratory. Because dichloromethane is more dense than sea water, multiple extractions using a separatory funnel are easier to carry out than they would be with a lighter-than-water solvent such as hexane. Because it has a low boiling point (40°C), the danger of losing significant amounts of fluorescent compounds during evaporation is minimized. Recoveries of oil from spiked sea water are excellent, being in the range of 90-100% under most conditions (Table 3, Keiser and Gordon, 1973). One drawback, however, is dichloromethane's solubility in water (2% in fresh water). Larger volumes of dichloromethane must therefore be used in the first extraction to compensate for its solubility.

Cyclohexane was used to redissolve the residue after evaporation. It was chosen over pentane, hexane, benzene and dichloromethane. Cyclohexane has the highest boiling point, minimizing concentration changes due to evaporation. It also yielded the highest emission values for spiked samples. Benzene has similar characteristics in both cases, but was rejected because it is a strong absorber of short wavelength ultraviolet light. Cyclohexane proved satisfactory as a storage medium since dissolved oils showed little or no loss of fluorescence even after several months in the dark.

## Recovery of Oil from Water

The recoveries of different oils from waters of various origins were determined (Table 3). Recoveries averaging 92%, for example, were obtained for three different crude oils which had been added to previously extracted surface water from Station P. The loss of fluorescent oil components during roto-evaporation of dichloromethane and during redissolution of the residue in cyclohexane was determined for two oils (Table 4). Since this loss was approximately the same as the overall procedural loss observed for the crude oils in Table 3, the recovery of the crude oils in the extraction step of our procedure appears to have been nearly quantitative. The recovery of refined oil, however, was not quantitative. The reason for the poor recovery of the Esso motorboat oil was not pursued in the study. In this regard, however, it may be noted that the water used, which was surface water obtained from alongside the dock adjacent to the laboratories in Victoria's Inner Harbour, may have contained components, such as surfactants, which interfered with the extraction efficiency of the dichloromethane. Because of our experience with the extraction efficiency of Esso motorboat oil from harbour surface water, we were alerted to the necessity of testing water samples from a study area for the extractability of the pollutant oil, when it is known, in order that concentrations, which are determined by the fluorescence method, can be corrected for extraction efficiency.

Our findings generally agree with those of Keiser and Gordon (1971) who reported average percent recoveries for a No. 6 fuel oil of 99% for the roto-evaporation step and 90% for the extraction step. We found, however, that losses of oil were relatively greater in the roto-evaporation step than in the extraction step. This lack of agreement may reflect differences in the water and oils used in the two studies. In addition, there were procedural differences. We used a higher bath temperature for roto-evaporation of the solvent (55-60°C vs. 30°C) which may have accounted for our greater loss on roto-evaporation. For the extraction we used a 50 ml portion of dichloromethane followed by a 25 ml portion rather than two 40 ml portions. It should also be pointed out, the above arguments notwithstanding, that Keiser and Gordon reported standard deviations of 11% and 7% for the roto-evaporation and the extraction steps, respectively. The differences between their results and our results, which come from a small number of experiments, may therefore be more apparent than real.

## Field Trial

The fluorescence method, as it had evolved by August, 1973, was given a field trial on weathership Cruise No. 73-006. Sea water samples were collected from the port bow with the ship steaming at approximately 5 knots. A solvent washed (distilled water, methanol, and dichloromethane, respectively) five-gallon stainless steel bucket suspended on a nylon line was swung forward at 45° to the ship. At the appropriate instant, determined with practice, the line was allowed to slacken momentarily so that the bucket dropped mouth first into the water. The first two grabs were used as rinses with the third being retained as the sample. (Current practice, however, involves taking the first grab as sample. The reason for this procedural



with heavy oils. The 308 nm, 383 nm pair seemed the best choice since both wavelengths lie in the middle of the desired ranges. Further, our assignment of these wavelengths as the positions of the maxima agrees with that of McKay and Latham. The plot (Fig. 3) of emission intensity against chrysene concentration (in cyclohexane) shows good linearity over the concentration range, 10-50  $\mu\text{g/l}$ , which corresponds to the concentration range, in chrysene equivalents, of the extracts of the oil-spiked water samples which we prepared for study. Good linearity was similarly achieved in the range 1-10  $\mu\text{g/l}$ , which corresponds to the concentration range of extracts of deep ocean sea water samples which are presumably unpolluted.

### Oil and Chrysene Comparison

Chrysene was compared to available oils ranging from heavy fuel oils to outboard motor oils (Table 1 and Table 2). Since wavelengths used were more typical of the heavier oils than the lighter oils, the former gave much higher emission intensities. For example, crude and bunker oils studied exhibited intensities which were 20 to 80 times greater than that of Gulf outboard oil and 10 to 70 times greater than that of Esso diesel oil. The light fuel oils show excitation maxima between 280 nm and 290 nm and emission maxima between 310 nm and 330 nm. Chrysene comparisons, therefore, reflect only the tailing effects of the lighter oils. As chrysene was chosen as a standard for heavy oils, another standard would have to be found if the lighter oils were to be examined. Where possible appropriate spectra of the extracted oil should be used to identify the type of oil being measured and determine the credibility of the standard.

### Selection of Solvents

The decision to use dichloromethane as the extracting solvent was influenced by results obtained by Keiser and Gordon (1973) and verified in our own laboratory. Because dichloromethane is more dense than sea water, multiple extractions using a separatory funnel are easier to carry out than they would be with a lighter-than-water solvent such as hexane. Because it has a low boiling point (40°C), the danger of losing significant amounts of fluorescent compounds during evaporation is minimized. Recoveries of oil from spiked sea water are excellent, being in the range of 90-100% under most conditions (Table 3, Keiser and Gordon, 1973). One drawback, however, is dichloromethane's solubility in water (2% in fresh water). Larger volumes of dichloromethane must therefore be used in the first extraction to compensate for its solubility.

Cyclohexane was used to redissolve the residue after evaporation. It was chosen over pentane, hexane, benzene and dichloromethane. Cyclohexane has the highest boiling point, minimizing concentration changes due to evaporation. It also yielded the highest emission values for spiked samples. Benzene has similar characteristics in both cases, but was rejected because it is a strong absorber of short wavelength ultraviolet light. Cyclohexane proved satisfactory as a storage medium since dissolved oils showed little or no loss of fluorescence even after several months in the dark.

## Recovery of Oil from Water

The recoveries of different oils from waters of various origins were determined (Table 3). Recoveries averaging 92%, for example, were obtained for three different crude oils which had been added to previously extracted surface water from Station P. The loss of fluorescent oil components during roto-evaporation of dichloromethane and during redissolution of the residue in cyclohexane was determined for two oils (Table 4). Since this loss was approximately the same as the overall procedural loss observed for the crude oils in Table 3, the recovery of the crude oils in the extraction step of our procedure appears to have been nearly quantitative. The recovery of refined oil, however, was not quantitative. The reason for the poor recovery of the Esso motorboat oil was not pursued in the study. In this regard, however, it may be noted that the water used, which was surface water obtained from alongside the dock adjacent to the laboratories in Victoria's Inner Harbour, may have contained components, such as surfactants, which interfered with the extraction efficiency of the dichloromethane. Because of our experience with the extraction efficiency of Esso motorboat oil from harbour surface water, we were alerted to the necessity of testing water samples from a study area for the extractability of the pollutant oil, when it is known, in order that concentrations, which are determined by the fluorescence method, can be corrected for extraction efficiency.

Our findings generally agree with those of Keiser and Gordon (1971) who reported average percent recoveries for a No. 6 fuel oil of 99% for the roto-evaporation step and 90% for the extraction step. We found, however, that losses of oil were relatively greater in the roto-evaporation step than in the extraction step. This lack of agreement may reflect differences in the water and oils used in the two studies. In addition, there were procedural differences. We used a higher bath temperature for roto-evaporation of the solvent (55-60°C vs. 30°C) which may have accounted for our greater loss on roto-evaporation. For the extraction we used a 50 ml portion of dichloromethane followed by a 25 ml portion rather than two 40 ml portions. It should also be pointed out, the above arguments notwithstanding, that Keiser and Gordon reported standard deviations of 11% and 7% for the roto-evaporation and the extraction steps, respectively. The differences between their results and our results, which come from a small number of experiments, may therefore be more apparent than real.

## Field Trial

The fluorescence method, as it had evolved by August, 1973, was given a field trial on weathership Cruise No. 73-006. Sea water samples were collected from the port bow with the ship steaming at approximately 5 knots. A solvent washed (distilled water, methanol, and dichloromethane, respectively) five-gallon stainless steel bucket suspended on a nylon line was swung forward at 45° to the ship. At the appropriate instant, determined with practice, the line was allowed to slacken momentarily so that the bucket dropped mouth first into the water. The first two grabs were used as rinses with the third being retained as the sample. (Current practice, however, involves taking the first grab as sample. The reason for this procedural



change is to minimize coating the bucket with material from the ocean's surface microlayer.) A subsample of 1.5 litres was transferred to a 2 litre separatory funnel and extracted with 65 ml of dichloromethane by vigorously shaking the funnel for two minutes. After allowing the layers to separate for approximately five minutes, the dichloromethane was drained into a 250 ml round bottomed flask. A second extraction using 25 ml of dichloromethane was then performed and the extract added to the first. The combined extracts were then evaporated to dryness using a water bath at 55°-60°C aboard ship and a roto-evaporator under reduced pressure with a similar bath at 55°-60°C at our shore laboratory. Care was taken to remove the evaporating flasks from the water bath immediately after evaporation of the solvent. The residue, rarely visible, was then redissolved in 15.0 ml of cyclohexane and compared with chrysene standards using the P.E. Model 204 fluorescence spectrophotometer. Appropriate blank corrections were made. Reagent blanks were prepared by evaporating 90 ml of dichloromethane from the same batch used for the extractions and taking up the residue in 15.0 ml of cyclohexane. All samples, standards, and blanks were compared at six different sets of wavelengths using 308 nm and 318 nm for excitation and 366 nm, 383 nm, and 400 nm for emission.

The average value in chrysene equivalents for all samples collected and analyzed (Table 5) at Station P was 0.038 µg/l with a standard deviation of 0.017 µg/l. Line P samples (Table 6) excluding Station 5 which was obviously contaminated had an average of 0.040 µg/l with a standard deviation of 0.025 µg/l. Of the Line P samples, those from Stations 1 and 2 had comparatively high concentrations. Stations 1 and 2 were over the continental shelf and were also stations of more than normal shipboard activity.

Using the sample (conc. 0.034 µg/l) collected on September 12 as being representative of the samples taken at Station P, the equivalent concentrations (Table 7) of five crude oils and five bunker oils for six wavelength pairs were calculated. The equivalent concentrations vary from oil to oil with the equivalent concentrations of the crude oils being about double those of the bunker or residual fuel oils. This result is a reflection of the greater relative quantities of fluorescent compounds in bunker or residual fuel oils. The amount of variation of the equivalent concentration of a given oil from one wavelength pair to another provides a measure of the similarity of the composition of the fluorescent components of the oil with the composition of the fluorescent components extracted from the sea water. The smaller the variation is, the greater the similarity. No variation would indicate that the oil in question was present, unweathered or otherwise changed, in the sea water. If the relative standard deviation (Table 7) is used as a measure of this variation, then, of the oils studied, B.C. light crude (0.16 R.S.D.) would be most like the sea water extract. With the exception of the Stewart bunker oil, moreover, the sea water extract resembles the crude oils more than it does the bunker oils. Inspection of Table 7 indicates that the equivalent concentration of a given oil may change in a systematic fashion with a change in excitation and emission wavelengths. A general decrease in equivalent oil concentration appears to be linked with an increase in excitation and emission wavelengths. This apparent relationship can be demonstrated more clearly if the equivalent oil concentration is plotted against a function which is the square

root of the sum of the squares of the excitation and emission wavelengths for which the value of the equivalent oil concentration was determined. This function can be regarded as a radius (Appendix 4) and for the purposes of this discussion is designated as  $r$ . In Figure 4 is shown the value of  $r$  for one pair of excitation and emission wavelengths ( $\lambda_{ex} = 308$  nm and  $\lambda_{em} = 366$  nm, respectively). Two plots of equivalent oil concentration against  $r$  are given in Figure 5. The plots show that the equivalent concentration of the "average" crude oil and the "average" bunker oil first decreases and then levels off or increases slightly as  $r$  increases.

Although the plots in Figure 5 are informative, a more useful comparison can be made if the equivalent concentration determined at each pair of wavelengths for a given oil is first divided by the average of all the equivalent concentrations. The ratios which are obtained in this manner can be plotted against  $r$  as shown in Figure 6. Should the equivalent oil concentrations determined at each wavelength pair be the same, then each of the ratios would be equal to 1 and the ratio against  $r$  plot would fall on the horizontal straight line shown in Figure 6. The closer the oil and sea water extract resemble each other (at the wavelengths used in the measurement of the fluorescence), the closer the curve of the equivalent concentration will be to the horizontal straight line. The sea water extract can therefore be seen to more closely resemble the "average" crude oil than the "average" bunker oil. The standard deviation of the ratios from the mean ratio gives a measure of the goodness of fit between the curve of ratios and the horizontal line in Figure 6. It can be easily shown (Appendix 5) that this standard deviation is in fact the relative standard deviation of the equivalent oil concentrations from the mean equivalent oil concentration. The relative standard deviations of the various oils studied are listed, as noted before, in Table 7.

In principle, it should be possible to perform the data analysis described above for a data set based on a much larger number of pairs of wavelengths. For identification purposes an increase in the data base would be much preferred. In this case, however, there may be more than one ratio determined for a given value of  $r$  so that the ratio against  $r$  plots would give a band of variable width and density rather than a line. A simplification can be achieved by using a set of fluorescent measurements determined for a set of points ( $\lambda_{ex}$ ,  $\lambda_{em}$ ) which lie on a diagonal straight line such as the line shown passing through the origin and point (308, 366) in Figure 4. For the above set of points each value of  $r$  would correspond to only one ratio. It would not be difficult to obtain a set of fluorescent measurements for a set of points ( $\lambda_{ex}$ ,  $\lambda_{em}$ ) along the diagonal line as shown in Figure 4. A fluorescence spectrophotometer can be easily modified to scan along such a diagonal line in a process called synchronous excitation of fluorescence emission (Lloyd, 1971a). This process is particularly useful in the analysis of oils and extracts of water which contain oil. More useful information regarding oil composition can be achieved in a single synchronous scan than can be achieved by a single scan with either the excitation or emission wavelength held constant (Gordon and Keiser, 1974; Lloyd, 1971 a, b, c).

On August 20, 1973, a series of sea water samples, which were collected at three hour intervals over a 24 hour period, were analyzed. The results



are given in Table 8. The average equivalent concentration for ( $\lambda_{ex}$ ,  $\lambda_{em}$ ) = (308 nm, 383 nm) was 0.058  $\mu\text{g/l}$  with a standard deviation of 0.021  $\mu\text{g/l}$ . The relative standard deviation was 0.36 which corresponds favourably with the relative standard deviation of 0.63 and 0.45 for Line P and Station P samples, respectively. If the sample taken at 1700 hours, which contained zooplankton were omitted from the analysis, the average would drop to 0.052  $\mu\text{g/l}$  and the relative standard deviation to 0.26. Although further verification would be necessary, the smaller relative standard deviation of samples collected hourly compared to that of samples collected daily indicates that there may be day-by-day variation in the concentration of fluorescent extractable materials at Station P.

### Storage of Samples

Samples were brought back to the laboratory for analysis in three different forms--as sea water, as dichloromethane solutions and as cyclohexane solutions (representing three stages in the analytical work-up). All samples were stored in glass containers with Teflon lined plastic caps. Both the containers and Teflon linings had been previously cleaned with dichloromethane. Some caps also had a liner of dichloromethane-rinsed aluminum foil covering the interior including the threads.

### Sea Water Samples (Table 9)

Samples of approximately three litres were preserved with 60 mg of mercuric chloride and stored in a freezer aboard ship and a cooler ( $<5^{\circ}\text{C}$ ) at the lab until time of analysis. The extractions performed in the lab on these samples yielded slightly lower results;  $0.032 \pm 0.019$   $\mu\text{g/l}$  compared to  $0.038 \pm 0.017$   $\mu\text{g/l}$  for the shipboard analyses. This difference may be due to cleaner experimental conditions in the laboratory rather than loss of fluorescence in the stored sample. Even the significance of the difference is questionable, however, since it is smaller than the standard deviation of either average.

### Dichloromethane

After extraction of the sea water the dichloromethane was stored in a cool, dark place until the time of analysis. Some samples having caps with only Teflon liners were definitely contaminated (Table 10) whereas none of the samples having caps with added aluminum foil were obviously contaminated. The latter samples had an average concentration of  $0.046 \pm 0.016$   $\mu\text{g/l}$  compared to  $0.035 \pm 0.010$   $\mu\text{g/l}$  found for the same sea water samples following analysis on shipboard. The results indicate that there was an increase in fluorescence on storage. A likely source of contamination would be the plastic caps. Simply rinsing the caps with solvent releases greater quantities of fluorescent materials than we have encountered in extracts of sea water.

## Cyclohexane

Upon completion of the extraction with dichloromethane and subsequent evaporation, the residue was taken up in cyclohexane and stored in a dark cooler. The consequences of storing extracts in cyclohexane were similar to those of storing extracts in dichloromethane. Samples in tubes with only Teflon liners became contaminated and those with aluminum foil gave mixed results (Table 10). Conclusions on this small amount of data are hard to make, but it does seem that meticulous care in preparing storage tubes or a more reliable type of sample bottle will be necessary if the samples are to be stored in organic solvents.

## Summary

After an extensive investigation chrysene was chosen as a reference and calibration standard for heavy oils, using its excitation maximum at 308 nm and its emission maximum at 383 nm as the pair of wavelengths to be used for comparison. No problems were encountered at sea that would make performance of the analyses impractical aboard ship except for the ever present possibility of contamination from the ship itself. Storage of samples did pose some problems. There may be some loss of fluorescence if samples of sea water are stored although our results are not definite enough to confirm this. If samples are to be stored in an organic solvent medium, a contaminant-free container must be found as many of our samples were contaminated.

Our results indicated that Station P sea water contained an equivalent of 0.4  $\mu\text{g/l}$  crude oil or 0.2  $\mu\text{g/l}$  bunker oil during the study period. This level is considerably lower than levels reported in the Atlantic. Levy (1972) published results for concentrations of residual oils observed in the northwest Atlantic off the coast of Nova Scotia (January, 1971) which averaged between 1.0 and 2.0  $\mu\text{g/l}$  using bunker C from the ship Arrow as his standard. A few months later (April 1971) using the same standard, Gordon and Michalik (1971) found the average oil concentration in Chedabucto Bay area to be 1.5  $\mu\text{g/l}$ . Further south, Brown, Searl and Elliot (1973) found nonvolatile or persistent hydrocarbons to be generally between 1 and 12  $\mu\text{g/l}$  along well travelled tanker routes. Later Keizer and Gordon (1973), doing a survey from Halifax to Bermuda, found that 77% of their offshore above 200 metre depth samples contained less than 2  $\mu\text{g/l}$  of oil using Venezuelan crude as a calibration standard. It should be noted that the samples from the Atlantic were taken closer to shore and in areas of higher ship activity than those collected for our study.

The concentrations we found must only be regarded as estimates of the maximum possible quantities of petroleum in sea water since there is no evidence to support the supposition that the fluorescent components in the extracts are petroleum derived. Even when an extract can be compared to standards from a probable oil source, the accuracy may be limited by weathering effects or the presence of other fluorescing materials in sea water.



## References

- Brown, R.A., T.D. Searl and J.J. Elliot, B.B. Phillips, D.E. Brandon and P.H. Monaghan, 1973: Distribution of heavy hydrocarbons in some Atlantic ocean waters. Proc. Joint Conf. Prevention and Control of Oil Spills, American Petroleum Institute, Washington, D.C., 505-519.
- Coakly, W.A., 1973: Comparative identification of oil spills by fluorescence spectroscopy fingerprinting. Proc. Joint Conf. Prevention and Control of Oil Spills, American Petroleum Institute, Washington, D.C., 215-222.
- Gordon, D.C., Jr. and P.A. Michalik, 1971: Concentration of Bunker C fuel oil in the waters of Chedabucto Bay, April 1971. J. Fish. Res. Board Canada, 28, 1912-1914.
- Gordon, D.C., Jr. and P.D. Keiser, 1974: Estimation of petroleum hydrocarbons in sea water by fluorescence spectroscopy: Improved sampling and analytical methods. Fisheries and Marine Service Tech. Report No. 457. Bedford Institute of Oceanography, Dartmouth, N.S.
- Keiser, P.D. and D.C. Gordon, Jr., 1973: Detection of trace amounts of oil in sea water by fluorescence spectroscopy. J. Fish. Res. Board Canada, 30, 1039-1046.
- Levy, E.M., 1971: The presence of petroleum residues off the east coast of Nova Scotia, in the Gulf of St. Lawrence and the St. Lawrence River. Water Res., 5, 723-733.
- Levy, E.M., 1972: Evidence for the recovery of the waters off the east coast of Nova Scotia from the effects of a major oil spill. Water Air Soil Pollut., 1, 144-148.
- Lloyd, J.B., 1971a: The nature and evidential value of the luminescence of automobile engine oil and related materials. I. Synchronous excitation of fluorescence emission. J. Forens. Sci. Soc., 11, 83-94.
- Lloyd, J.B., 1971b: The nature and evidential value of the luminescence of automobile engine oil and related materials. II. Aggregate luminescence. J. Forens. Sci. Soc., 11, 153-170.
- Lloyd, J.B., 1971c: The nature and evidential value of the luminescence of automobile engine oils and related materials. III. Separated luminescence. J. Forens. Sci. Soc., 11, 235-253.
- McKay, J.F. and D.R. Latham, 1972: Fluorescence spectrometry in the characterization of high-boiling petroleum distillates. Anal. Chem., 44, 2132-2137.





## FIGURES

1. Chart showing Line P station positions.
2. (a) Scan of fluorescence emission ( $\lambda_{\text{ex}} = 308 \text{ nm}$ ) of a  $114 \mu\text{g/l}$  solution of chrysene in cyclohexane and (b) Scan of fluorescence excitation ( $\lambda_{\text{em}} = 383 \text{ nm}$ ) of  $114 \mu\text{g/l}$  solution of chrysene in cyclohexane.
3. Linearity of response of Perkin Elmer Model 204 fluorescence spectrophotometer.
4. Rectangular coordinate system showing the distance  $r$  to the point (308, 366) and the section in which fluorescent measurements are made.
5. Plot of equivalent oil concentration against  $r$ .
6. Plot against  $r$  of the ratio of equivalent oil concentration (measured at the six pairs of wavelengths) to the average equivalent concentration.





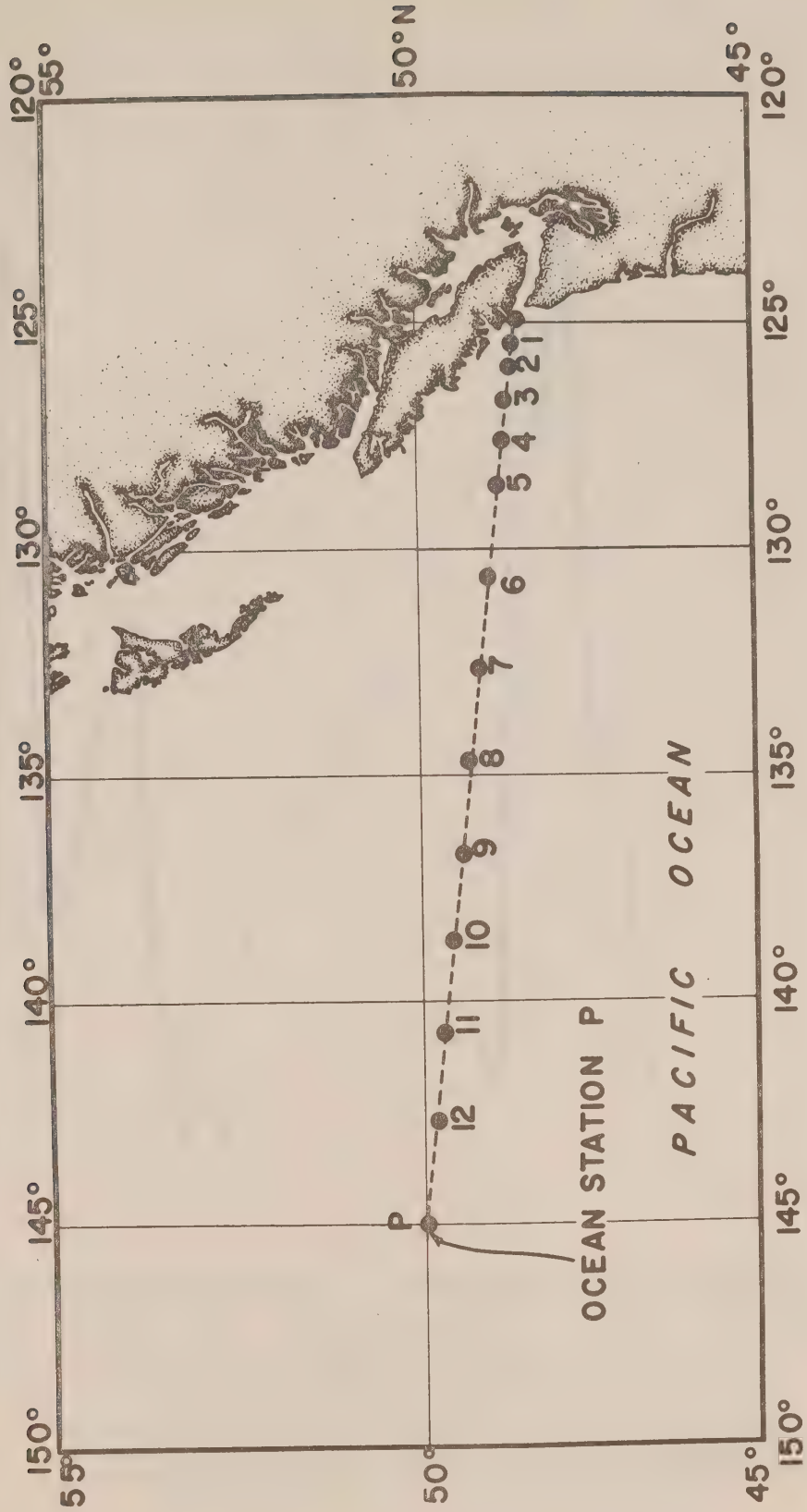


Figure 1. Chart showing Line P station positions.

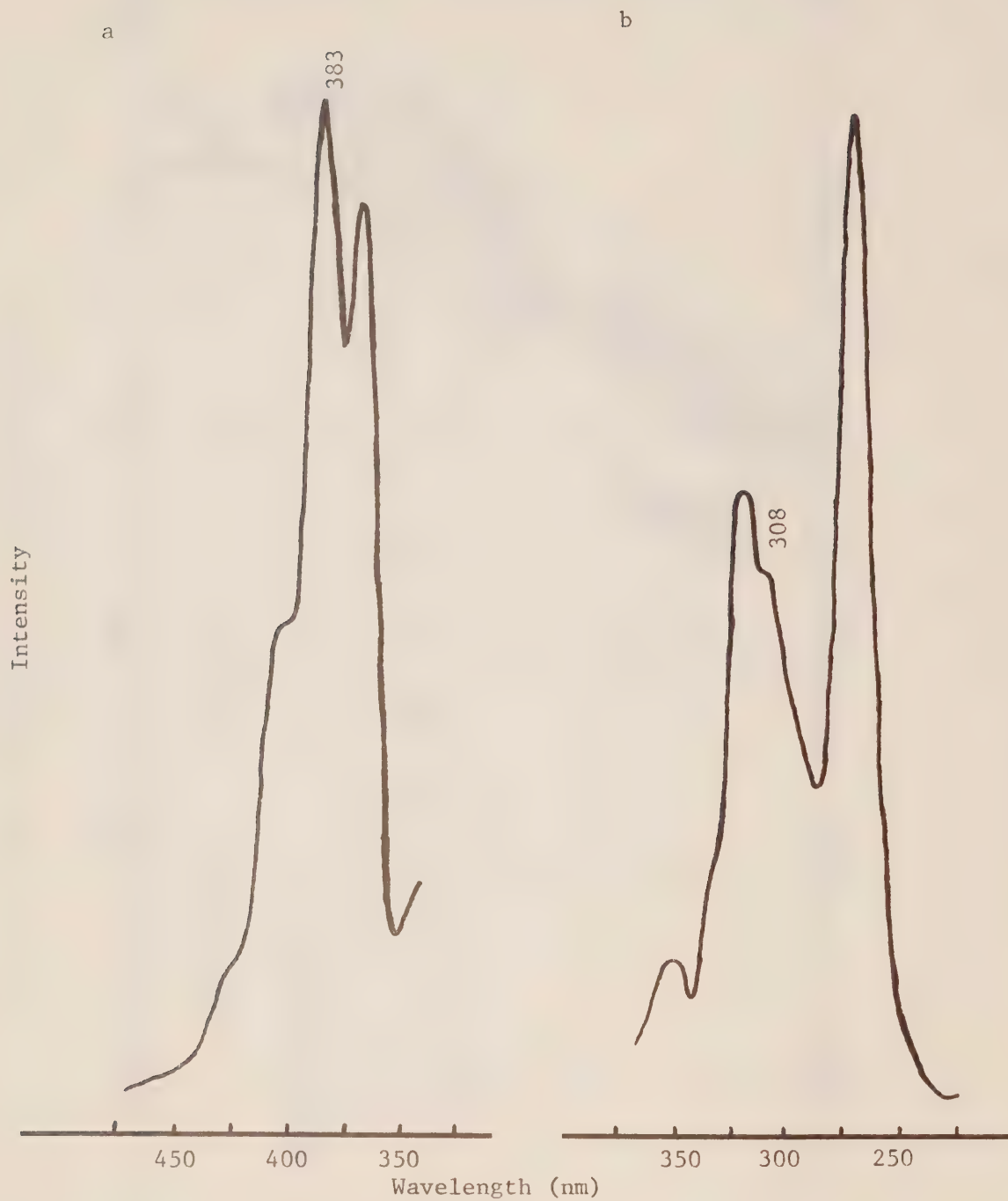


Figure 2. (a) Scan of fluorescence emission ( $\lambda_{\text{ex}} = 308 \text{ nm}$ ) of a  $114 \mu\text{g/l}$  solution of chrysene in cyclohexane and (b) Scan of fluorescence excitation ( $\lambda_{\text{em}} = 383 \text{ nm}$ ) of  $114 \mu\text{g/l}$  solution of chrysene in cyclohexane.



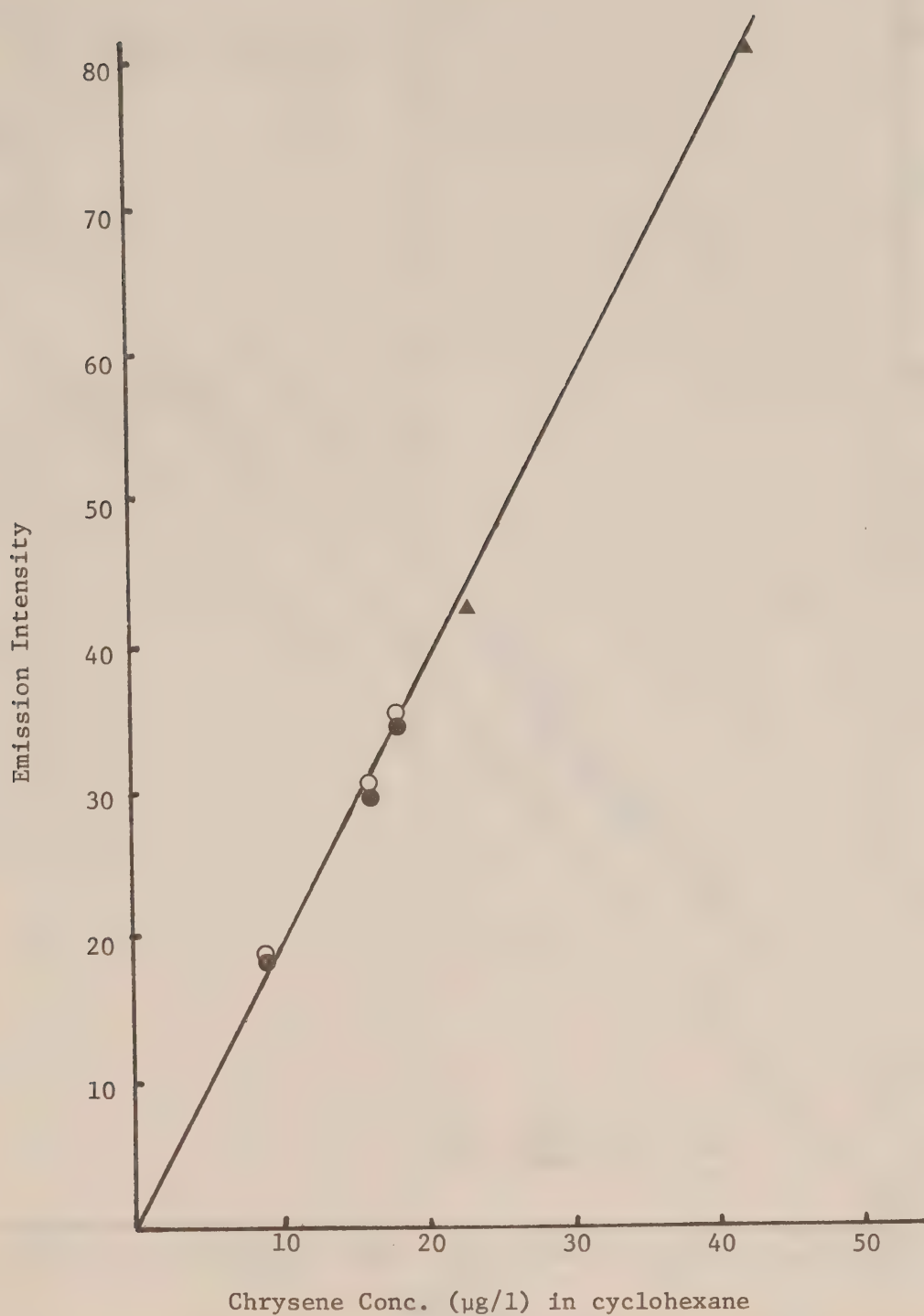


Figure 3. Linearity of response of P.E. Model 204 fluorescence spectrometer,  $\lambda_{\text{ex}} = 308 \text{ nm}$ ,  $\lambda_{\text{em}} = 383 \text{ nm}$ , (●) 1st run, (▲) 2nd run, (○) 3rd run.

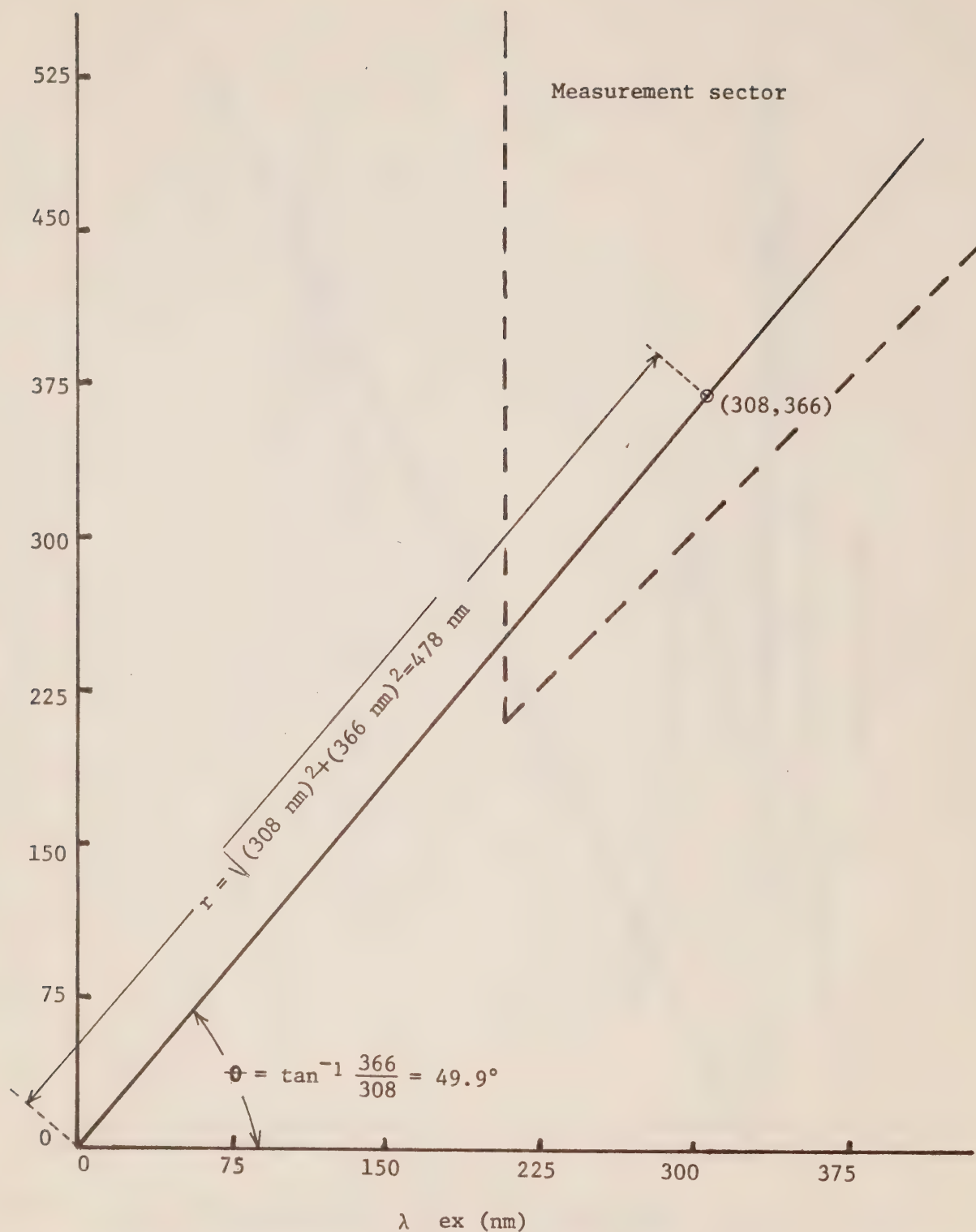


Figure 4. Rectangular coordinate system showing distance  $r$  to the point (308 nm, 366 nm) and the sector in which fluorescent measurements are constrained by the requirements of the instrument ( $\lambda_{ex} \geq 220 \text{ nm}$ ) and the fluorescence process ( $\lambda_{em} \geq \lambda_{ex}$ ).



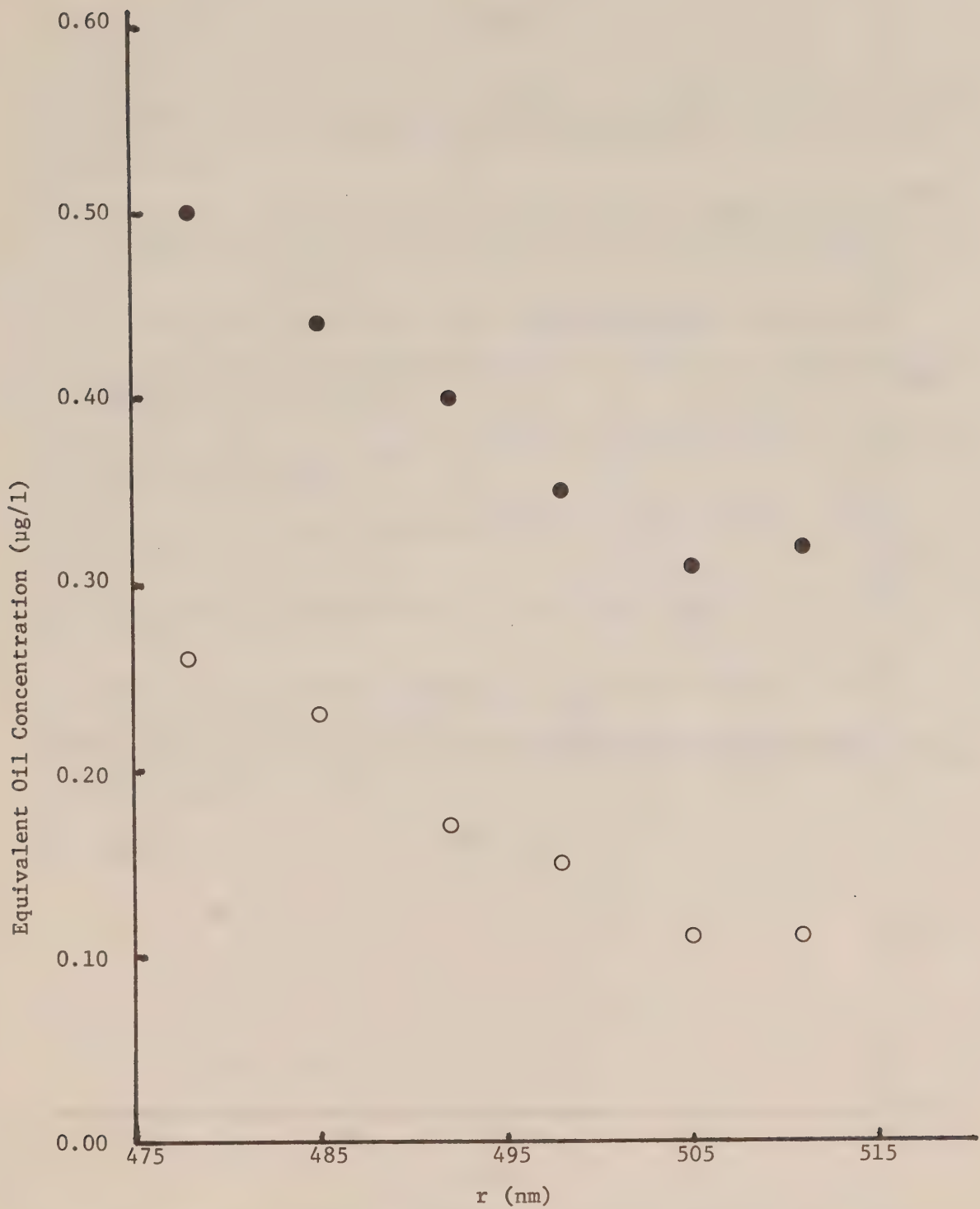


Figure 5. Plot of equivalent oil concentration against  $r$ . (●) "average" crude oil. (○) "average" bunker oil.

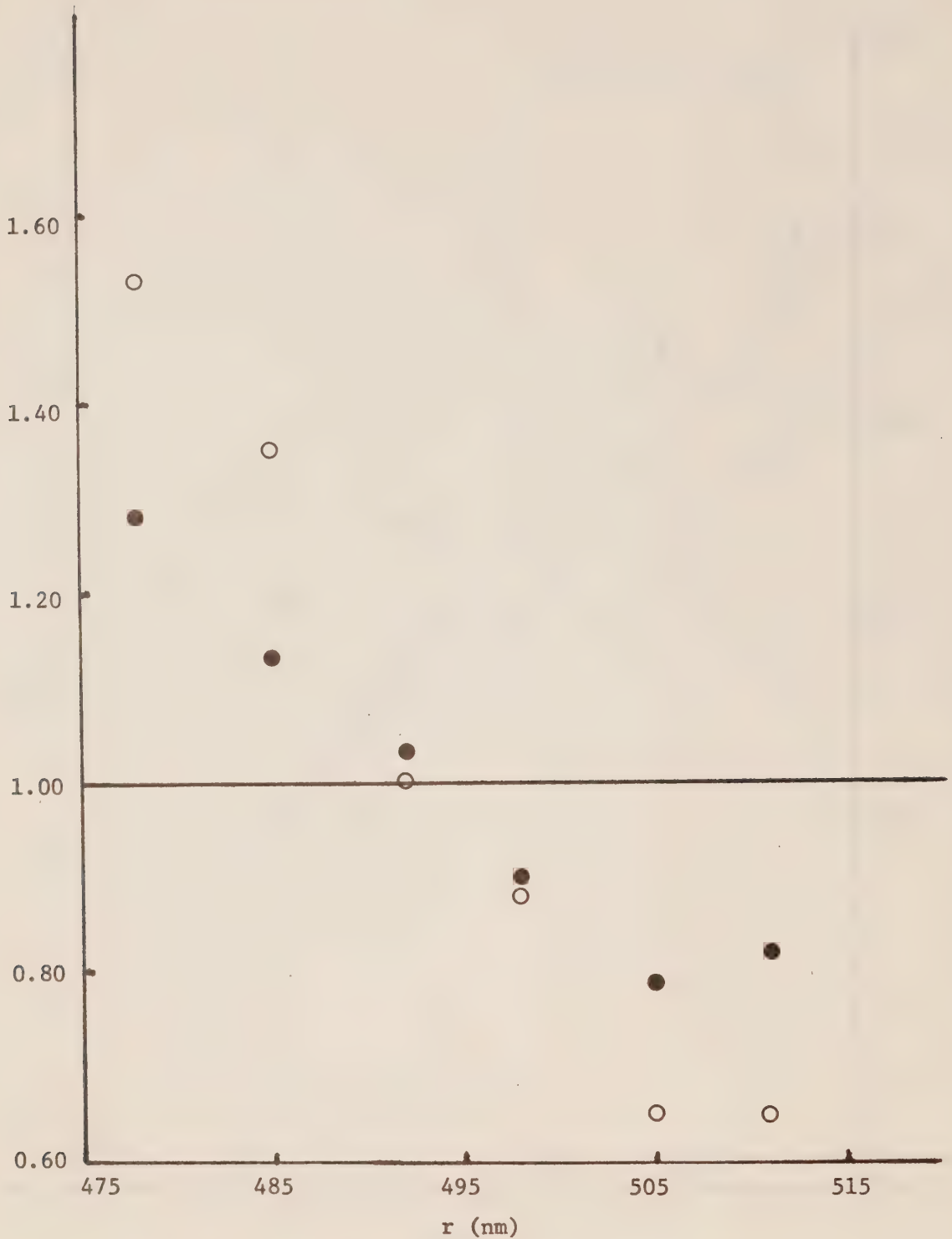


Figure 6. Plot against  $r$  of the ratio of equivalent oil concentration (measured at the six pairs of wavelength) to the average equivalent oil concentration. (●) "average" of crude oil (○) "average" bunker oil.



## TABLES

1. The Concentration of Chrysene which has the Same Fluorescent Intensity at Selected Pairs of Excitation and Emission Wavelengths as 1 mg/l of a Given Oil
2. The Concentration of a Given Oil which has the Same Fluorescent Intensity at Selected Pairs of Excitation and Emission Wavelengths as 1 mg/l of Chrysene
3. Recovery of Oil from Water using Dichloromethane as Extractant
4. Recovery of Oil from Dichloromethane following Roto-evaporation and Redissolution in Hexane
5. Equivalent Chrysene Concentrations of Sea Water Samples Analyzed on Shipboard at Station P
6. Equivalent Chrysene Concentrations of Sea Water Samples Analyzed on Shipboard Along Line P
7. Equivalent Oil Concentrations of Sea Water Samples Collected on September 12, 1973
8. Equivalent Chrysene Concentrations of Sea Water Samples During 24 Hour Time Series on August 20, 1973
9. Equivalent Chrysene Concentrations of Sea Water Samples Brought Back to Laboratory for Analysis
10. Comparison of Sample Storage Methods





TABLE 1

The Concentration<sup>a</sup> of Chrysene which has the Same Fluorescent Intensity at Selected Pairs of Excitation and Emission Wavelengths as 1 mg/l<sup>a</sup> of a Given Oil<sup>b</sup>

$\lambda$ ex (nm)	308	318	308	318	308	318
$\lambda$ em (nm)	366	366	383	383	400	400
Type of Oil	Equivalent Chrysene Conc., $\mu\text{g/l}$					
Cod liver	0.0002	0.0002	0.0003	0.0003	0.0006	0.0005
Gulf outboard	0.0087	0.0066	0.0047	0.0038	0.0055	0.0046
Esso diesel	0.024	0.015	0.009	0.006	0.007	0.005
B.C. light crude	0.051	0.045	0.038	0.034	0.060	0.051
Peace River crude	0.078	0.068	0.063	0.056	0.104	0.091
Esso crude	0.119	0.103	0.095	0.084	0.163	0.144
Red Water Gulf crude	0.120	0.104	0.100	0.089	0.174	0.149
Boundary Bay crude	0.120	0.109	0.100	0.091	0.164	0.142
Esso No. 46	0.185	0.168	0.183	0.166	0.366	0.318
CCGS <sup>c</sup> Vancouver, bunker	0.185	0.164	0.178	0.163	0.374	0.346
CCGS <sup>c</sup> Quadra, bunker	0.193	0.173	0.192	0.170	0.376	0.315
Esso bunker C	0.235	0.205	0.217	0.190	0.437	0.381
CSS <sup>d</sup> Stewart, bunker	0.279	0.268	0.231	0.221	0.407	0.389

<sup>a</sup>In cyclohexane.

<sup>b</sup>The crude oils were samples of pipeline feed oils obtained from the Imperial Oil Refinery, Ioco, B.C. The bunker oils obtained from the ships were not identified. The other oils were purchased.

<sup>c</sup>Canadian Coast Guard Ship.

<sup>d</sup>Canadian Survey Ship.

TABLE 2

The Concentration of a Given Oil which has the Same Fluorescent Intensity at Selected Pairs of Excitation and Emission Wavelengths as  $1 \mu\text{g/l}^a$  of Chrysene

$\lambda$ ex (nm)	308	318	308	318	308	318
$\lambda$ em (nm)	366	366	383	383	400	400
Type of Oil	Equivalent Oil Conc., $\mu\text{g/l}$					
B.C. light crude	19.6	22.6	26.3	29.4	16.7	19.6
Red Water Gulf crude	8.3	9.6	10.3	11.2	5.7	6.7
Boundary Bay crude	8.3	9.2	10.0	11.0	6.1	7.0
Esso crude	8.4	9.7	10.5	11.9	6.1	6.9
Peace River crude	12.8	14.7	15.9	17.8	9.6	11.0
CCGS Quadra, bunker	5.2	5.8	5.2	5.9	2.7	3.2
CCGS Vancouver, bunker	5.4	6.1	5.6	6.1	2.7	2.9
CSS Stewart, bunker	3.6	3.7	4.3	4.5	2.5	2.6
Esso bunker C	4.3	4.9	3.7	5.2	2.3	2.6
Esso No. 46	5.4	6.0	5.5	6.0	2.7	3.1

<sup>a</sup>In cyclohexane

TABLE 3

Recovery of Oil from Water using Dichloromethane as Extractant

Medium	Oil Added	Conc., $\mu\text{g}/\text{l}$	% Recovery <sup>a</sup>
Extracted Stn. P sea water	Peace River crude <sup>b</sup>	3.1	90, 96
	Esso crude <sup>b</sup>	4.7	96, 94
	Red Water Gulf crude <sup>b</sup>	14.0	88
Victoria Harbour <sup>d</sup> sea water, 5 m	Boundary Bay crude <sup>b</sup>	4.0	99, 92
		2.0	78
	Boundary Bay crude <sup>c</sup>	4.0	90, 86
		2.0	84
Distilled water	Boundary Bay crude <sup>c</sup>	2.0	68, 102, 97, 99
Victoria Harbour <sup>d</sup> sea water, surface	Esso outboard <sup>c</sup>	19.5	55, 52, 38
		39.0	56, 49

<sup>a</sup> Recovery after extraction of 1 liter of water with dichloromethane (50 ml, 25 ml), roto-evaporation and dissolution in <sup>b</sup> cyclohexane or <sup>c</sup> hexane.

<sup>d</sup> Filtered using Whatman No. 1 filter paper.

TABLE 4

Recovery of Oil from Dichloromethane following Roto-evaporation<sup>a</sup> and Redis-solution in Hexane

Oil	Recovery (%)	Average Loss (%)
Esso outboard	93, 91, 87	10
Peace River crude	85, 91	12

<sup>a</sup> Water aspirator, water bath at 55°-60°C.



TABLE 5

Equivalent Chrysene Concentrations of Sea Water Samples Analyzed on Ship-board at Station P

$\lambda_{ex}$ (nm)	308	318	308	318	308	318
$\lambda_{em}$ (nm)	366	366	383	383	400	400
1973 Sample Date	Equivalent Chrysene Conc., $\mu\text{g/l}$					
August 8	0.11	0.11	0.080	0.080	0.080	0.11
August 11	0.075	0.062	0.048	0.041	0.041	0.066
August 14	0.031	0.024	0.019	0.014	0.014	0.024
August 17	0.048	0.025	0.031	0.024	0.024	0.044
August 20	0.082	0.067	0.054	0.046	0.046	0.077
August 23	0.060	0.049	0.040	0.035	0.035	0.062
August 26	0.076	0.056	0.039	0.031	0.031	0.043
August 29	0.044	0.037	0.027	0.025	0.025	0.038
September 1	0.026	0.022	0.016	0.013	0.013	0.026
September 4	0.037	0.031	0.031	0.025	0.025	0.058
September 7	0.049	0.039	0.031	0.025	0.025	0.045
September 12	0.053	0.044	0.034	0.027	0.027	0.045
September 15	0.066	0.053	0.045	0.039	0.039	0.074

TABLE 6

Equivalent Chrysene Concentrations of Sea Water Samples Analyzed on Ship-board Along Line P

$\lambda$ ex (nm)		308	318	308	318	308	318
$\lambda$ em (nm)		366	366	383	383	400	400
1973							
Station	Sample Date	Equivalent Chrysene Conc., $\mu\text{g/l}$					
2	August 4	n.d. <sup>a</sup>	n.d.	0.069	n.d.	n.d.	n.d.
5	August 4	0.19	0.17	0.17	0.14	n.d.	0.26
6	August 4	0.048	0.074	0.035	0.031	0.047	0.046
7	August 4	0.058	0.085	0.038	0.035	0.051	0.051
12	August 6	0.045	0.033	0.026	0.022	0.034	0.030
12	September 16	0.032	0.024	0.021	0.015	0.033	0.032
10	September 17	0.042	0.033	0.028	0.024	0.049	0.046
9	September 17	0.026	0.023	0.022	0.019	0.036	0.040
8	September 17	0.055	0.043	0.034	0.026	0.046	0.045
7	September 18	0.026	0.020	0.015	0.013	0.026	0.023
4	September 18	0.076	0.060	0.044	0.039	0.060	0.057
3	September 18	0.031	0.022	0.018	0.015	0.027	0.029
2	September 19	0.12	0.10	0.089	0.085	0.14	0.13
1	September 19	0.10	0.10	0.085	0.078	0.13	0.12

<sup>a</sup> not determined.

TABLE 7

Equivalent Oil Concentrations of Sea Water Samples Collected on September 12, 1973<sup>a</sup>

$\lambda$ ex (nm)	308	318	308	318	308	318	308	318	Avg. Conc.	318	R.S.D.
$\lambda$ em (nm)	366	366	383	383	400	400	400	400	$\mu\text{g/l}$	400	S.D.
Type of Oil	Equivalent Oil Conc., $\mu\text{g/l}$										
B. C. light crude	1.1	0.98	0.89	0.79	0.75	0.78	0.88	0.14	0.16		
Red Water Gulf crude	0.44	0.44	0.34	0.30	0.26	0.27	0.34	0.081	0.24		
Boundary Bay crude	0.44	0.40	0.34	0.30	0.27	0.28	0.34	0.079	0.23		
Esso crude	0.45	0.43	0.36	0.32	0.27	0.28	0.35	0.076	0.22		
Peace River crude	0.68	0.51	0.54	0.48	0.43	0.44	0.51	0.092	0.18		
"Average" crude	0.50	0.44	0.40	0.35	0.31	0.32	0.39	0.074	0.19		
CCGS Quadra, bunker	0.28	0.26	0.18	0.16	0.12	0.13	0.19	0.067	0.35		
CCGS Vancouver, bunker	0.29	0.27	0.19	0.16	0.12	0.12	0.19	0.074	0.39		
CSS Stewart, bunker	0.19	0.16	0.15	0.12	0.11	0.10	0.14	0.034	0.24		
Esso bunker	0.23	0.22	0.13	0.14	0.10	0.10	0.15	0.058	0.39		
Esso No. 46	0.29	0.26	0.19	0.16	0.12	0.12	0.19	0.072	0.38		
"Average" bunker	0.26	0.23	0.17	0.15	0.11	0.11	0.17	0.062	0.36		

<sup>a</sup>Shipboard analysis (Table 5)



TABLE 8

Equivalent Chrysene Concentrations of Sea Water Samples during 24 Hour Time Series on August 20, 1973

$\lambda$ ex (nm)	308	318	308	318	308	318
$\lambda$ em (nm)	366	366	383	383	400	400
Time	Equivalent Chrysene Conc., $\mu\text{g/l}$					
0200	0.085	0.076	0.060	0.058	0.10	0.086
0500	0.10	0.081	0.067	0.054	0.10	0.078
0800	0.095	0.080	0.063	0.050	0.086	0.072
1100 <sup>a</sup>	0.058	0.045	0.037	0.031	0.052	0.047
1400	0.082	0.067	0.056	0.046	0.077	0.071
1700 <sup>b,c</sup>	0.16	0.12	0.10	0.085	0.12	0.12
2000 <sup>b</sup>	0.086	0.071	0.051	0.037	0.072	0.052
2300 <sup>b</sup>	0.053	0.040	0.031	0.028	0.041	0.040

<sup>a</sup>Paint chips in sample.

<sup>b</sup>Stored overnight in test tubes (cyclohexane medium) with Teflon lined plastic caps.

<sup>c</sup>Zooplankton in subsample.

TABLE 9

Equivalent Chrysene Concentrations of Sea Water Samples Brought Back to the Laboratory for Analysis

$\lambda$ ex (nm)		308	318	308	318	308	318
$\lambda$ em (nm)		366	366	383	383	400	400
1973							
Station	Sample Date	Equivalent Chrysene Conc. $\mu\text{g/l}$					
2	August 4	0.86	0.068	0.069	0.057	0.13	0.11
P	August 8	0.12	0.090	0.071	0.054	0.10	0.76
P	August 11	0.065	0.049	0.035		0.041	0.035
P	August 14	0.050	0.038	0.031	0.026	0.043	0.041
P	August 17	0.051	0.036	0.032	0.022	0.035	0.035
P	August 20	0.048	0.032	0.027	0.021	0.036	0.031
P <sup>a</sup>	August 23	0.086	0.072	0.060	0.052	0.11	0.10
P	August 26	0.061	0.046	0.035	0.029	0.046	0.040
P	August 29	0.033	0.023	0.018	0.013	0.021	0.022
P	September 1	0.033	0.025	0.017	0.014	0.022	0.022
P	September 1 Duplicate	0.037	0.017	0.013	0.010	0.015	0.017
P	September 4	0.030	0.017	0.013	0.010	0.018	0.014
P	September 4 Duplicate	0.025	0.014	0.011	0.007	0.013	0.010
P	September 7	0.026	0.019	0.012	0.010	0.016	0.017
P	September 12	0.044	0.029	0.025	0.019	0.034	0.032

<sup>a</sup>Aluminum foil liner corroded - flakes in sample.

TABLE 10  
Comparison of Sample Storage Methods

Place of Analysis: Storage Medium: Container: Seal:	Shore-based Laboratory			
	Sea water, HgCl <sub>2</sub> Gallon jugs Teflon lined screw caps	Organic solvent Glass test tubes Teflon lined screw caps	Organic solvent Glass test tubes Aluminum foil and Teflon lined screw caps	
Sample Date 1973	Equivalent Chrysene Conc., µg/l			
August 8	0.080	0.071	n.d.	n.d.
August 11	0.048	0.035	0.34 <sup>b</sup>	0.064 <sup>c</sup>
August 14	0.019	0.031	1.60 <sup>b</sup>	0.043 <sup>c</sup>
August 17	0.031	0.032	n.d.	0.041 <sup>c</sup>
August 20	0.054	0.027	0.16 <sup>c</sup>	n.d.
August 23	0.040	0.060	n.d.	0.054 <sup>c</sup>
August 26	0.039	0.035	n.d.	0.051 <sup>c</sup>
August 29	0.027	0.018	0.037 <sup>b</sup>	0.024 <sup>c</sup>
September 1	0.016	0.017	0.053 <sup>c</sup>	n.d.
September 4	0.031	0.013	0.081 <sup>c</sup>	0.034 <sup>b</sup>
September 7	0.031	0.012	0.13 <sup>c</sup>	0.084 <sup>b</sup>
September 12	0.034	0.025	n.d.	0.026 <sup>c</sup>
September 15	0.045	n.d.	n.d.	0.066 <sup>c</sup>

<sup>a</sup> Fluorescence measured at  $\lambda$  ex = 308 nm,  $\lambda$  em = 383 nm.

<sup>b</sup> Stored in cyclohexane.

<sup>c</sup> Stored in dichloromethane.





## Appendices

1. Fluorescence Excitation and Fluorescence Emission Spectra of Specific Oils
2. Fluorescence Excitation and Fluorescence Emission Spectra of Model Compounds--This Study
3. Fluorescence Excitation and Fluorescence Emission Spectra of Model Compounds--McKay and Latham
4. Transformation from Rectangular to Polar Coordinates
5. Relationship between Relative Standard Deviation of Equivalent Concentrations and Standard Deviation of Ratios





## Appendix 1

Fluorescence Excitation and Fluorescence Emission Spectra of Specific Oils<sup>a</sup>

Oils	Fluorescence Excitation Wavelength, nm	Fluorescence Emission Wavelength, nm
Boundary Bay crude	315	370
Red Water Gulf crude	300	363
B.C. light crude	300	337, <u>358</u>
Peace River crude	308	<u>366</u> , 398
CCGS Vancouver, bunker C	310	350, 383, <u>410</u>
Tar Ball #15 Transpac 72	330	383
Stewart, bunker	323	370
CCGS Quadra, bunker C	310, <u>340</u>	385
Esso diesel	290	333
Esso fuel #46	<u>340</u> , 309, 359	<u>387</u> , 384, 405, 405
Esso crude	<u>330</u> , 305	<u>369</u> , 378, 363, 376
Esso, bunker C	<u>338</u> , 307, 358	<u>386</u> , 382, 405, 405
Outboard motor oil	237	342

<sup>a</sup>Underlined wavelength indicates maximum peak

# Appendix 2

## Fluorescence Excitation and Fluorescence Emission Spectra of Model Compounds<sup>a</sup>

	Excitation Peaks (nm)	Emission Peaks (nm)	Solubility in	
			Hexane	(ppm range)
1-Methylnaphthalene (1020 ppm)	316	336	Miscible	
1-Ethylnaphthalene (20 ppm)	291	337	Miscible	
Dibenzothiophene	287, <u>321</u>	338, <u>344</u>	Fair	
m-Terphenyl (582 ppm)	306	339	Fair	
2,3,5-Trimethylnaphthalene	300	340	Fair	
N-Ethylcarbazole (5.3 ppm)	265, <u>290</u> , 333, 340	350, 364	Poor	
N-Phenylcarbazole	275, 300(s), <u>335</u>	350(s), <u>358</u>	Fair	
Phenanthrene (28 ppm)	291	355(s), <u>366</u> , 383(s)	Fair	
Triphenylene (2.1 ppm)	264(s), <u>284</u>	357, 370	Fair	
Sym-Dibenzocyclooctatetraene	316	358	Fair	
Chrysene (236 ppb)	268, 308(s), 318	366, <u>383</u> , 401	Poor	
1,2,5,6-Dibenzanthracene (800 ppm)	270, 317, 368	368, 398, 420	Poor	
2-Phenylindole	297(s), <u>330</u>	355, 370(s)	Poor	
1,2,7,8-Dibenzphenanthrene (Picene) (2.4 ppm)	285, 300, 325	380, 398, 419	Poor	
Bibenzyl (3 ppm & 150 ppm in MeOH)	294, 319, 331(s), 350	397, 420	Fair	
Decacyclene	270, 300, 335, 380, 402	408, 432, 478, 506		
2,3,6,7,-Dibenzanthracene(280 ppb)	305, 324, 342	398, 421, 450, 487	Poor	
9,10-Dimethyl- 1,2-benzanthracene	336, 350, <u>388</u>	413, 427	Fair	
Cod Liver Oil (240 ppb)	330	480	Miscible	
Indene (in Benzene)	298, 327, <u>384</u>	<u>481</u> , 510	Insoluble	
Tetraphenylethylene	No spectra obtained		Very poor	
9,9-Bifluorene	No spectra obtained			
Biphenylene	No spectra obtained			

<sup>a</sup>A wavelength underlined was the most intense. Shoulders are indicated by (s).

Table I. Fluorescence Excitation and Fluorescence Emission Spectra of Model Compounds<sup>a</sup>

Compound	Fluorescence excitation spectra, wavelength, nm						Fluorescence emission spectra, wavelength, nm					
Fluorene	268	275(s)	293	303			303	310				
Naphthalene	269	278	288				324	338	350			
9-Methylcarbazole ( <i>N</i> -Methylcarbazole)	249	293	322				334	349	365(s)	378(s)		
Carbazole	249	293	320				335	351	364(s)			
2-Methylcarbazole	250	297	319				335	350	365(s)	385(s)		
3-Methylcarbazole	252	296	325				342	358	372(s)	378(s)		
11 <i>H</i> -Benzo[ <i>b</i> ]fluorene (2,3-Benzofluorene)	270	288	306	319	326	342	342	351	359	369		
11 <i>H</i> -Benzo[ <i>a</i> ]fluorene (1,2-Benzofluorene)	255	265	296	306	318		347	365	382(s)			
Triphenylene	262	277	288				354	364	373	381(s)	391(s)	
11 <i>H</i> -Benzo[ <i>a</i> ]carbazole (1,2-Benzocarbazole)	255	279	306				354	372	392	413		
7 <i>H</i> -Benzo[ <i>c</i> ]carbazole (3,4-Benzocarbazole)	263	286	324				362	369	381	402		
Chrysene	261	271	297	308	322		363	375	383	404	427	
Phenanthrene	261	278	285	296			348	357	365	385		
7 <i>H</i> -Dibenzo[ <i>c,g</i> ]carbazole (3,4,5,6-Dibenzocarbazole)	278	303	350	363			367	386	405			
Dibenz[ <i>a,c</i> ]anthracene (1,2,3,4-Dibenzanthracene)	269(s)	279	289				377	388	398	409(s)		
Picene (1,2,7,8-Dibenzphenanthrene)	287	304	328				377	398	421	449		
Anthracene	260	312	325	341	358	377	380	401	424	451		
13 <i>H</i> -Dibenzo[ <i>a,i</i> ]carbazole (1,2,7,8-Dibenzocarbazole)	290	321	334	348			380	401	425			
Pyrene	308	322	337				374	379	384	389	395	
Benz[ <i>a</i> ]anthracene (1,2-Benzanthracene)	255	271	280	290	317	329	387	408	435	462		
Benzo[ <i>b</i> ]chrysene (2,3,7,8-Dibenzphenanthrene)	255	289	305				394	418	444	470(s)		
Dibenzo[ <i>g,p</i> ]chrysene (1,2,7,8-Dibenzochrysene)	280	292	303	340	353		395	409				
Dibenz[ <i>a,i</i> ]anthracene (1,2,5,6-Dibenzanthracene)	301	324	335	351			396	407	418	446	473	
Naphtho[1,2,3,4- <i>def</i> ]chrysene (1,2,4,5-Dibenzopyrene)	276	293	305	330	342	358	397	408	420	446		
Benzo[ <i>c</i> ]acephenanthrylene (3,4-Benzofluoroanthene)	255	299	310				403	413	429	459	489(s)	
Benzo[ <i>a</i> ]pyrene (1,2-Benzopyrene)	256	269	286	300	333	349	405	410	429	457		
Dibenzo[ <i>c,g</i> ]phenanthrene (3,4,5,6-Dibenzophenanthrene)	239	272	312	332			405	424	446(s)			
Benzo[ <i>ghi</i> ]perylene (1,12-Benzoperylene)	291	302	331	348	364	385	399	408	420	446		
Dibenzo[ <i>def,mno</i> ]chrysene (Anthanthrene)	260	296	308	384	401	407	432	459	494			
Benzo[ <i>rst</i> ]pentaphene (3,4,9,10-Dibenzopyrene)	247	274	285	297	316	332	434	450	462	480	494	
Perylene	255	370	388	410	438		440	466	500	540(s)		
Coronene	292	303	324	340			411	422	428	435	446	
Dibenzo[ <i>b,h,def</i> ]chrysene (3,4,8,9-Dibenzopyrene)	272	300	312	399	422	448	451	480	518			
Fluoranthene	241	256	266	280	290	311	409(s)	418(s)	436	463		
Ovalene	314	328	342	399	422	448	450	462	475	482	490	
									503	509	514	
										539		

<sup>a</sup> The most intense peak in each spectrum is in italic type. Shoulders are indicated by (s).



## Appendix 4

## Transformation from Rectangular to Polar Coordinates

A rectangular coordinate system is shown in Figure 4 with emission wavelengths ( $\lambda_{em}$ ) marked along the ordinate and with excitation wavelengths ( $\lambda_{ex}$ ) marked along the abscissa. Each point in the plane has rectangular coordinates ( $\lambda_{ex}$ ,  $\lambda_{em}$ ) and represents a single pair of wavelengths. The distance  $r$  from the origin (0,0) to the point ( $\lambda_{ex}$ ,  $\lambda_{em}$ ) is given by the Theorem of Pythagoras:

$$r = \sqrt{\lambda_{ex}^2 + \lambda_{em}^2}$$

The distance  $r$  may also be regarded as the radius of a circle with centre (0,0) passing through the point ( $\lambda_{ex}$ ,  $\lambda_{em}$ ). Whether  $r$  is regarded as a distance or a radius, however, a given value of  $r$  does not correspond to a unique wavelength pair or point ( $\lambda_{ex}$ ,  $\lambda_{em}$ ). For example, in Figure 4 the point (308 nm, 366 nm) has a value of  $r$  equal to 478 nm, but this value of  $r$  could correspond as well to any other point of the same distance from the origin. The point (308 nm, 366 nm) is uniquely determined by the value 478 nm and the value and angle  $\theta$  shown in Figure 4. This value of  $\theta$  is  $49.9^\circ$  and is determined using the formula:

$$\theta = \tan^{-1} \frac{\lambda_{em}}{\lambda_{ex}}$$

Thus, the point (308 nm, 366 nm) can be also represented as (478 nm,  $49.9^\circ$ ) which are called the polar coordinates of the point.

## Appendix 5

Relationship between Relative Standard Deviation of Equivalent Concentrations  
and Standard Deviation of Ratios

$$s = \sqrt{\frac{1}{n-1} \sum_{i=1}^n (x_i - \bar{x})^2} \quad \text{by definition}$$

$$\frac{s}{\bar{x}} = \sqrt{\frac{1}{n-1} \sum_{i=1}^n \frac{(x_i - \bar{x})^2}{\bar{x}^2}}$$

$$= \sqrt{\frac{1}{n-1} \sum_{i=1}^n \left( \frac{x_i}{\bar{x}} - 1 \right)^2}$$

$$= \sqrt{\frac{1}{n-1} \sum_{i=1}^n (R_i - 1)^2}$$

but

$$\bar{R} = \frac{1}{n} \sum_{i=1}^n R_i$$

$$= \frac{1}{n} \sum_{i=1}^n \frac{x_i}{\bar{x}}$$

$$= \frac{\frac{1}{n} \sum_{i=1}^n x_i}{\bar{x}}$$

$$= \frac{\bar{x}}{\bar{x}} = 1$$

$$\frac{s}{\bar{x}} = \sqrt{\frac{1}{n-1} \sum_{i=1}^n (R_i - \bar{R})^2} = s^1$$

where

$s$  = standard deviation of equivalent concentrations about the mean equivalent concentration

$n$  = number of equivalent concentrations

$x_i$  =  $i^{\text{th}}$  equivalent concentration

$\bar{x} = \frac{1}{n} \sum_{i=1}^n x_i$  = mean equivalent concentration

$\frac{s}{\bar{x}}$  = relative standard deviation of the equivalent concentrations about the mean equivalent concentration

$R_i = \frac{x_i}{\bar{x}} = i^{\text{th}}$  ratio

$\bar{R}$  = mean ratio

$s^1$  = standard deviation of ratios about the mean ratio.







CAI EP 321

-77R06

Government  
Publications

# THE INTERACTION OF CHLORINE AND SEAWATER

R.W. Macdonald and C.S. Wong



INSTITUTE OF OCEAN SCIENCES, PATRICIA BAY  
Victoria, B.C.



For additional copies or further information please write to:

Department of Fisheries and the Environment  
Institute of Ocean Sciences, Patricia Bay  
512 - 1230 Government Street  
Victoria, B.C.  
V8W 1Y4

THE INTERACTION OF CHLORINE AND SEAWATER

by

R.W. Macdonald and C.S. Wong

Institute of Ocean Sciences, Patricia Bay  
Victoria, B.C.  
February, 1977

This is a manuscript which has received only limited circulation.  
On citing this report in a bibliography, the title should be followed  
by the words "UNPUBLISHED MANUSCRIPT" which is in accordance with  
accepted bibliographic custom.



## Abstract

An examination of the interaction of chlorine and seawater has been made with particular emphasis on those aspects most pertinent to a spill or leak of liquid chlorine in seawater. This has been done in order to be able to predict the results of a rupture of the chlorine tank cars lost in Malaspina Strait early in 1975.

The appropriate phase diagrams have been constructed from information available in the literature, and small scale release experiments from the submersible, Pisces, confirm that the behavior of chlorine when released at various depths conforms rather closely to thermodynamic prediction. Depending on depth or temperature, four phases are possible: liquid chlorine, gaseous chlorine, liquid water (with chlorine dissolved in it), and chlorine hydrate (solid).

Literature data has been used to predict the effect of chlorine on such seawater parameters as alkalinity, pH, and Eh, and the speciation which should occur with various chlorine in seawater mixtures.

Results of experiments performed here show that, at low concentrations (5 mg chlorine/l seawater) seawater has a natural demand of about 1.5 mg/l in half an hour, and 3 mg/l after a day or so. Sediments can also destroy chlorine with 5 g (wet weight) removing 5 mg of chlorine from a liter flask of stirred seawater within four hours.

Consideration of critical data on chlorine, and a review of our release experiments show that gaseous explosion will not occur when liquid chlorine and seawater are mixed under conditions possible in Georgia Straits.

In the event of a chlorine leakage from a tank car resting on the bottom, liquid chlorine and chlorine hydrate will tend to fall being denser than seawater, and stay near the bottom. At depths less than 40 meters it is possible that gaseous chlorine could form. Depending on depth, much of the gaseous chlorine would not reach the atmosphere but would be tied up as an hydrate and remain in the seawater. Eventually after sufficient dilution, the natural chlorine demand of seawater and sediments will remove the chlorine through oxidation reactions. Mixing will help this process. Secondary toxic products formed by chlorination (or bromination) of organics should not be a problem in a clean area such as Malaspina Strait.



## Table of Contents

	Page
Acknowledgements.....	iii
Introduction.....	1
Thermodynamics.....	2
Implications of the Phase Diagram.....	3
Speciation.....	4
Effect of Chlorine on Alkalinity and pH.....	6
Effect of Chlorine on Redox Potential.....	7
Kinetics.....	9
Chlorine Demand on Seawater.....	10
Gaseous Explosion.....	14
Chlorine Release in Seawater.....	15
Chlorine Release in the Atmosphere.....	17
Toxicity (Marine Environment).....	18
Toxicity (Atmospheric).....	19
Conclusions.....	20
References.....	22
Tables.....	26
Figures.....	28





## Acknowledgements

The authors wish to express their thanks to Colin Jackson of Ocean Chemistry for handling the photography of the under water chlorine releases, and Lloyd Twaites of Chemex for providing the excellent photographs of the gaseous chlorine release in Howe Sound.

We are deeply indebted to Environmental Engineering for the loan of their amperometric titrator and thank W. Bailey and J. Duffield for their generous cooperation. Lucien Sitwell performed the chlorine demand experiments.

The crew of the Pisces deserves our gratitude for their courteous and knowledgeable assistance in setting up the chlorine release experiments.

Finally we thank Joyce Aavik for her patient typing and retyping of the manuscript.



## Introduction

On February 19, 1975, four tank cars filled with liquid chlorine were lost from a barge being towed in the vicinity of Malaspina Strait in B.C. coastal waters (Fig. 1). Although a series of searches was carried out (A.D. O'Connor, March 1975, November, 1976 and others), the exact location of the sunken cars has not as yet been determined. Each tank car carried approximately 94 metric tons<sup>1</sup> of liquid chlorine with a 10% void space padded to 6.9 bars with air.

Although there has been no evidence to date which might indicate that chlorine has leaked from the cars, it is only a matter of time before corrosion leads to failure of the tanks. How long this will take is an open question since it is not known exactly what condition the cars were in when they were lost or what sort of damage they might have received as a result of the accident.

The tank cars are constructed of five circumferential sections of 2 cm steel with two layers of 5 cm cork for insulation and a 0.3 cm steel jacket on the outside. The steel should not crack on impact, but rather deform. Strain introduced in this manner should not significantly accelerate corrosion, and the outside of the tank car should degrade rather slowly, of the order of .5 mm per year. Corrosion will not take place on the inside of the tank car provided water does not leak in, since a protective chloride layer is formed by interaction of the chlorine and iron. The cars are apparently quite rugged, and it is reported that when two cars fell down an incline east of Prince George, one car punctured the other car, but the second car survived the fall and was retrieved intact (anonymous).

The most vulnerable area for corrosion is around the hot rolled monel valve seat. Small scratches in a good coat of paint would lead to pit corrosion in the iron in close contact with the seat. How quickly this could cause penetration depends very strongly on how well the valve body and steel were coated with paint. A minimum time of two to three years has been estimated, while 10-20 years is more likely. Once a pinhole is formed it should expand rapidly since the acidic chlorine water mixture is quite corrosive (Carson, 1975). Since rupture is inevitable it was decided to examine the chemical aspects of the chlorine-seawater system in order to predict the likely sequence of events following tank car failure.

The study was initiated by a literature search out of which the appropriate phase diagrams have been constructed. Further, the likely speciation of chlorine and its effect on pH and pE have been estimated. In order to fill in gaps in our knowledge of the chlorine seawater system, we ran some chlorine demand experiments in seawater obtained from Saanich Inlet and on surface sediment from the Strait of Georgia.

---

<sup>1</sup>SI units are used throughout this report. Conversion factors to other commonly used units are to be found in Table I.

Before relying on thermodynamic predictions we thought it would be worthwhile to carry out some small scale chlorine releases at various depths of the water column to get some visual verification of the behaviour of chlorine in seawater. This was done from the submersible, Pisces IV, in Saanich Inlet.

### Thermodynamics

The phase diagram for the chlorine-water mixture forms a three dimensional system with the variables composition, pressure and temperature. Figures 2-5 present some two dimensional aspects of the phase diagram which cover conditions likely to be encountered in Malaspina Strait.

In order to calculate the position of the lines on the phase diagrams, data was extracted from Ketelaar (1967) for the chlorine rich side, and from Fernandez et al (1967) for the remainder of the diagram. Vapour pressures of chlorine were drawn from the Matheson Gas Data Book (1966). In making the various equilibrium calculations it was assumed that only a two-component system existed, that is, seawater (35‰) and chlorine. Therefore, it cannot be rigorously applied to the case where other atmospheric components such as nitrogen and oxygen are included. If an atmosphere of fixed composition were also included, there would be four dimensions on the phase diagram and the possibility of a gas phase even at high pressures. This does not limit the utility of these phase diagrams since, as a first approximation, chlorine and seawater mixtures below the surface are essentially isolated from the atmosphere. With an unlimited volume of atmosphere in intimate contact with the chlorine-water system it is expected that chlorine would partition into the atmosphere according to its vapour pressure. This may be considered as a possible removal path of chlorine from seawater. Chemical reactions in the water column will also lead to chlorine removal.

A brief description of how the phase diagrams were calculated is included below to make clear the estimates and assumptions which have been used.

In considering water solubility in liquid chlorine, chlorine solubility in water and the composition of the hydrate it is assumed that over a range of 0-20 bars, hydrostatic pressure does not cause any appreciable effects. It is also assumed that hydrostatic pressure does not significantly alter vapour pressure. It can be shown that this is justifiable since

$$\frac{dP}{dP_s} = \frac{\bar{V}_{\text{liquid}}}{\bar{V}_{\text{vapour}}} \quad (1)$$

where  $P$  is the vapour pressure,  $P_s$  is the total pressure (including hydrostatic and other contributions) and the  $\bar{V}$ 's are the respective molal volumes. For water vapour, increasing the total pressure from 1-10 bars results in less than a 1% increase in vapour pressure.



Vapour pressures for water over seawater (35‰) were taken from Sverdrup, Johnson and Fleming (1942). The mole fraction of water in the saturated gas phase was estimated as

$$\frac{P_{H_2O}}{P_{H_2O} + P_{Cl_2}} \approx \frac{P_{H_2O}}{P_{Cl_2}} = X_{H_2O} \quad (2)$$

Vapour pressure of water over hydrate was estimated from the data of Ketelaar (1967).

Equilibrium between chlorine gas and water was calculated from the data of Bozzo in Fernandez et al (1967) on chlorine solubility in pure water NaCl solutions at various pressures and temperatures. (A salting-out coefficient for 35‰ seawater based on the NaCl solutions was calculated to be about 0.7) Chlorine solubilities in the hydrate region were obtained from Bozzo's Figure 7 in Fernandez et al (1967). The solubilities of chlorine in water outside the hydrate region at 9 bars pressure were extrapolated for various temperatures from Bozzo's Table IV taking into consideration the salting-out effect. Figure 6 summarizes the solubility of chlorine in seawater as a function of pressure and temperature.

The solubilities of water in liquid chlorine were taken from the data provided by Ketelaar (1967) for both the liquid water and hydrate regions. Here it was assumed that the influence of salt on the activity of water was negligible. (This assumption is quite acceptable since the activity of the water is directly related to its vapour pressure, and only a relatively small vapour pressure lowering is observed on going from distilled water to seawater.)

Fernandez et al (1967), using the Miller-Strong method, determined that the formula for chlorine hydrate was  $Cl_2 \cdot 6.2 H_2O$  and this composition has been assumed for the phase diagrams presented here. Roozeboom (1918) gave the upper invariant point for the hydrate (quadruple point) as 28.7°C, and a pressure of 6.08 bars. Recent measurements of Fernandez et al (1967) indicate that the quadruple point should be at 28.3°C with a pressure of about 8.1 bars. The recent data is probably more accurate and so has been adopted here. Salt depresses the temperature of the upper invariant point, and this effect can be taken into consideration by reference to Bozzo's Figure 6 in Fernandez et al (1967). The temperature at which the hydrate becomes unstable at 1 bar was also determined from this source.

#### Implications of the Phase Diagram

The phase diagram can be used to predict a possible sequence of events if chlorine is injected at some point into the water column. Since the phase diagrams are based on equilibrium calculations, conclusions can only be drawn as to what is possible, or thermodynamically acceptable. Other aspects such as very slow kinetic behaviour may prevent thermodynamic equilibrium from being obtained. With this in mind, let us consider two

possibilities, a spill at the surface (1.01 bar) and a spill at 80 meters (9 bars).

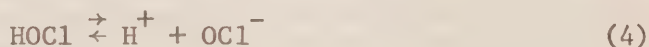
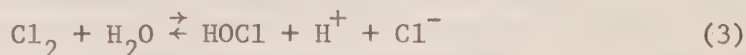
Reference to Figure 2 shows that at 1 bar, pure chlorine can form a gas phase over the whole range of temperatures from 0-30°C. On mixing chlorine with water in a mole ratio of 99:1 there will be a possibility of obtaining chlorine gas over a chlorine saturated water solution, or chlorine gas over a solid hydrate (crystalline yellow) if the temperature is below about 8°C. Further dilution with water will not result in any phase changes until the molar ratio of water to chlorine exceeds 6.2:1 at which point a water phase in equilibrium with the hydrate is possible provided the temperature is sufficiently low. Eventually, when the mole fraction of water exceeds .998, only a water phase will be present with some dissolved chlorine forming a seawater "bleach". This will occur when there are 10 g or less of chlorine dissolved in 1 litre of seawater.

Reference to Figure 3 shows that at 9 bars pressure one does not expect a gaseous phase over the 0-30° temperature range. Following the dilution path of chlorine, a liquid chlorine phase is anticipated initially. With sufficient water the hydrate will start to form (below 26°C) or chlorine and liquid water will coexist above that temperature. Further dilution will eventually result in dissolution of the hydrate or liquid chlorine.

If the bulk of seawater at Malaspina Strait is at or near 8°C (Crean and Ages, 1968) reference to Figure 4 will give a rough idea of the various possibilities. Only in a very small region is a gas phase possible, and it is anticipated that initially liquid chlorine and hydrate would occur (below 40 m) and after further dilution only hydrate and water would be thermodynamically stable. Eventually all hydrate would dissolve given a sufficient quantity of water.

#### Speciation

Chlorine reacts with water very quickly to form hypochlorous acid which can then further dissociate



The equilibrium constant for Equation 3 has been measured by at least two groups and their results have been reviewed by White (1972). At 25°C,

$$K_H = \frac{[\text{H}^+][\text{Cl}^-][\text{HOCl}]}{[\text{Cl}_2]} = 4.47 \times 10^{-4} \quad (5)$$

The dissociation of hypochlorous acid in seawater has recently been examined by Sugam and Helz (1976) and the apparent ionization constant  $K'_1$  has been given as a function of salinity and temperature.

$$K'_1 = \frac{[\text{OCl}_t^-] \bar{a}_H}{[\text{HOCl}]} \quad (6)$$

Where  $\text{OCl}_t^-$  is the total concentration of hypochlorite, and  $\bar{a}_H$  is the operational hydrogen ion activity obtained from a pH measurement with a glass electrode and a reference electrode with liquid junction. Figure 7 shows the fraction  $\frac{\text{OCl}_t^-}{\text{HOCl}}$  as a function of pH and temperature.

On a recent cruise on the CSS Vector (November 29 - December 3, 1976) a pH profile was determined at two stations. Measurements were made with a glass electrode and a reference electrode with liquid junction. The method of measurement was based on the experimental design given by Zirino (1975) for shipboard determinations. The pH's measured at 25°C have been corrected to in situ values by using Table VI.3 in Strickland and Parsons (1972). Figure 8 shows the in situ pH as a function of depth, and the station locations are marked on Figure 1. As can be seen, the pH of the deeper water is at about 7.7, while the pH of the surface water (above 30 m) is slightly higher at about 7.9. In seasons where biological productivity is higher, some  $\text{CO}_2$  will be removed from the water, and it is anticipated that the pH could rise to about 8.3, at least in the surface waters. The temperature of the deep water varies between 8° and 9°C, while surface waters drop to as low as 5°C in winter and rise to 15°C in summer (Crean and Ages, 1968). The inset area in Figure 7 shows the region normally expected in unpolluted water. For sufficiently dilute chlorine the  $\text{OCl}_t^-$  form will dominate with the  $\frac{\text{OCl}_t^-}{\text{HOCl}}$  ratio varying from 3 to 10. The higher value is to

to be expected in surface waters particularly when the pH is higher. This is of some importance since evidence shows that the non-ionized form is more toxic to bacteria (Fair et al, 1968) and also more reactive in the formation of toxic secondary products (Morris, 1967 and Farkas et al, 1949).

There is, however, another factor which should be considered. The addition of chlorine to seawater will cause a pH change according to Equation 3 and Equation 4 since each mole of chlorine produces initially one mole of HCl, and further ionization of hypochlorous acid can potentially liberate a second proton.

Consideration simultaneously of both Equation 3 and 4 allows the equilibrium concentration of the chlorine species to be calculated as a function of pH. The ratio of each species to the total chlorine present is shown in Figure 9 where

$$\alpha_0 = \frac{[\text{Cl}_2]}{[\text{Cl}_2] + [\text{HClO}] + [\text{ClO}_t^-]} \quad (7)$$

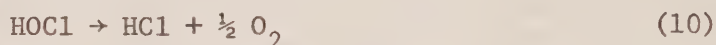


$$\alpha_1 = \frac{[\text{HClO}]}{[\text{Cl}_2] + [\text{HClO}] + [\text{ClO}_t^-]} \quad (8)$$

$$\alpha_2 = \frac{[\text{ClO}_t^-]}{[\text{Cl}_2] + [\text{HClO}] + [\text{ClO}_t^-]} \quad (9)$$

Consideration has been taken of the chloride concentration in seawater, which tends to shift Equation 3 to the left on going from fresh water to seawater. From Figure 9 it is important to note that  $\text{ClO}_t^-$  comprises 10% or more of the chlorine species in seawater only when the pH is greater than 6. From pH 4 to 6 the  $\text{HClO}$  form is most important, while chlorine becomes significant below pH 4.5.

Oxidation reactions involving  $\text{HClO}$  or  $\text{ClO}^-$  can also liberate protons which no longer have an associated chlorine species as shown in Equation 10.



(There is of course a chloride generated by this reaction). When some of the chlorine has been lost by this route, it will appear as if a strong acid,  $\text{HCl}$ , has been added along with the remaining chlorine.

#### The Effect of Chlorine on Alkalinity and pH

According to Equation 3, the addition of chlorine to seawater can be considered as a titration of seawater with a strong acid. Hydrogen ions can also be added through the secondary ionization of  $\text{HOCl}$ . (This secondary reaction will not affect the titration alkalinity since for each mole of protons added, one mole of the conjugate base  $\text{OCl}^-$  is also added. Titration to a pH 4 endpoint will cause all of the  $\text{OCl}^-$  to be converted back to  $\text{HOCl}$ . As mentioned above, oxidation reactions removing the  $\text{OCl}^-$  form (Equation 10) will lower the alkalinity). There may also be a further titrational effect dependant on the pH of the end point since some chlorine will be formed at lower pH's. Reference to Figure 9 will illustrate this clearly.

In the long term, once all of the active chlorine species have been reduced to chloride, two moles of  $\text{H}^+$  will have been generated for each mole of  $\text{Cl}_2$  added to the seawater. Consider the tank cars which contain a total of 376 metric tons of chlorine. If we accept an alkalinity change of 2% as being relatively insignificant, simple calculations show that dilution with  $2 \times 10^8 \text{ m}^3$  of seawater are required.

Let us now consider the influence of adding  $\text{Cl}_2$  to seawater on the pH of seawater. A "typical" sample of seawater might have a total  $\text{CO}_2$  of about  $2.2 \times 10^{-3} \text{ mol/l}$  and a pH of 7.9. Using the apparent dissociation constants for the  $\text{CO}_2$  system (Horne, 1968) and  $K_w$  taken from Culberson and Pytkowicz (1973) for  $8^\circ\text{C}$  and  $35\text{‰}$  salinity, it is possible to



calculate what additions of strong acid are required to cause the pH to change to any specified value in a closed system (i.e.,  $\text{CO}_2$  is not allowed to escape to an atmosphere). Figure 10 shows the titration curve calculated for  $C_T = 2.2 \times 10^{-3}$  mol/l. Keeping the initial pH at 7.9 and allowing effect shown in Figure 10.

Titration with chlorine has some similarities to titration with a strong acid, but cognizance must be taken of both Equation 3 and 4. Using the appropriate equilibrium constants of Sugam and Helz (1976), and White (1972), the titration curve has been calculated and is shown on Figure 9 along with the speciation curves. The interesting features are that at high pH (6.5-7.9) the system is buffered to a certain extent by  $\text{OCl}^-$ , particularly at about pH 7.4 when  $[\text{OCl}^-] = [\text{HOCl}]$ . The pH, therefore, does not change as rapidly in this region with the addition of chlorine as it does when most of the  $\text{OCl}^-$  is converted to  $\text{HOCl}$  below pH 6. Below pH 3.5  $\text{Cl}_2$  becomes an important species, since the equilibrium of Equation 3 is shifted to the left. Addition of large amounts of chlorine here do not have a great influence on pH. This is particularly dramatic since the logarithm of chlorine added is plotted as the ordinate.

The measured pH values in Malaspina Straits are fairly uniform with depth (Fig. 8) indicating that at least at these two stations at the time of sampling no anomalous behaviour attributable to chlorine was determined.

#### Effect of Chlorine on Redox Potential

The redox potential of a system at equilibrium is expressed as a dimensionless quantity pE. Somewhat analogous to pH, pE is the negative logarithm of electron activity. It is referenced to a conventional zero assigned to the standard hydrogen electrode.

$$\text{pE} = -\log\{e\} = \frac{F}{2.3} \frac{E_h}{RT} = \frac{E_h}{.059} \quad (11)$$

where F is the Faraday, R the gas constant (8.31 joules/°Cmole and T the absolute temperature. The redox potential is normally discussed in terms of both pE and  $E_h$ , the interrelation being demonstrated in Equation 11.

For oxic seawater the measured pE is found to be approximately 8.5 suggesting that pE is controlled by the  $\text{O}_2/\text{H}_2\text{O}_2$  couple (Breck, 1975).

The addition of chlorine to seawater would be expected to upset this precariously poised system, chlorine being a strong oxidant. If it is assumed that the seawater system becomes controlled by the  $\text{Cl}_2/\text{Cl}^-$  couple then



From fundamental thermodynamics

$$\Delta G^\circ = -nFE^\circ = -RT \ 2.3 \log K \quad (13)$$

where  $\Delta G^\circ$  is the standard free energy change and  $K$  is the equilibrium constant associated with the respective reaction.

For Equation 12,  $\Delta G^\circ = -13.12 \text{ KJ/mol}$

$$\log K = 23.02 \quad (14)$$

$$\log K = \log \left[ \frac{\{Cl^-\}}{P_{Cl_2}^{1/2} \{e\}} \right] = \log \{Cl^-\} + pE - \frac{1}{2} \log P_{Cl_2} \quad (15)$$

For seawater of 35‰ salinity

$$\{Cl^-\} = [Cl^-] \quad Cl^- = 0.55 \times .66 = .36 \quad (16)$$

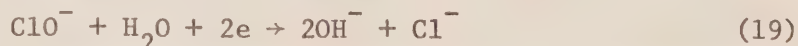
(  $Cl^-$  was taken from Whitfield, 1976)

$$23.02 = -.044 + pE - \frac{1}{2} \log P_{Cl_2} \quad (17)$$

$$pE = 23.46 + \frac{1}{2} \log P_{Cl_2} \quad (18)$$

Variation of  $P_{Cl_2}$  from 0.1 to 10 bars will not cause a large change in  $pE$  and therefore  $pE = 23.5$  should be sufficiently accurate when the couple in Equation 12 controls the redox potential. This indicates in more precise terms what we already intuitively suspected; that chlorine is strongly oxidizing. Reversing the procedure, it obtains directly from Equation 18 that normal oxic seawater with a  $pE$  of 8.5 has a negligibly small  $P_{Cl_2}$  since  $\log P_{Cl_2} \sim -30$ .

Perhaps a more useful way of looking at the redox potential of chlorinated seawater is to consider the hypochlorite ion.



$$E^\circ = 0.89 \text{ (Horne, 1968)}$$

$$\Delta G^\circ = -171.5 = -RT \ 2.3 \log K \quad (20)$$

$$\log K = 20.14 = 2 \log\{\text{OH}^-\} + \log\{\text{Cl}^-\} + 2\text{pE} - \log\{\text{H}_2\text{O}\} - \log\{\text{ClO}^-\} \quad (21)$$

$$= 2[\log K_w^{\text{Sw}} + \text{pH}] + \log\{\text{Cl}^-\} + 2\text{pE} - \log\{\text{H}_2\text{O}\} - \log\{\text{ClO}^-\} \quad (22)$$

$$= 26.40 + 2\text{pH} - 0.44 + 2\text{pE} + .008 - \log\{\text{ClO}^-\} \quad (23)$$

( $K_w^{\text{Sw}}$  has been taken from Culberson and Pytkowicz (1973), for a temperature of  $25^\circ\text{C}$  and salinity of  $35\text{‰}$ . The activity of water in seawater has been estimated from the vapour pressure lowering of  $35\text{‰}$  seawater, Sverdrup et al, 1942).

Therefore

$$\text{pE} = 28.49 - \text{pH} + \frac{1}{2}\log\{\text{ClO}^-\} \quad (24)$$

Using the approximation given by Sugam and Helz (1976), for the activity coefficient of the hypochlorite ion in seawater

$$\text{OCl}^- = 0.64 = \frac{+}{-}\text{KCl} \quad (25)$$

$$\text{pE} = 28.39 - \text{pH} + \frac{1}{2}\log[\text{ClO}_t^-] \quad (26)$$

Equation 26 is simply a different formulation of Equation 18, but it is easier to see the influence of chlorine on pE because by reference to the titration curve in Figure 9 it is now possible to estimate pH.

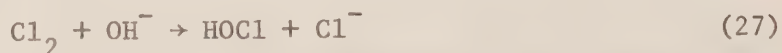
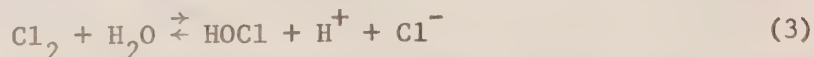
Use of Equation 5 and 6 along with the estimated value for pH yields pE as a function of chlorine added. This curve is shown in the top part of Figure 9 where it can be seen that pE does not vary greatly over a wide range of total chlorine concentrations. This curve was generated by assuming that no chlorine was removed through oxidation reactions. As indicated earlier, oxidation processes will remove chlorine, but will not remove the HCl generated and therefore a variety of time-concentration paths are possible along the pH and pE curves. These paths will be more or less independent depending on how much oxidizable material there is in seawater.

Equation 18 and 26 are also useful in determining the oxidation state of the elements or compounds in seawater at equilibrium, and for instance, it can be shown that bromide should be converted to bromine at equilibrium in the presence of chlorine.

### Kinetics

There is general agreement that the adsorption of chlorine by water (Equation 3) is extremely fast (Shilov and Solodushenkov, 1936,

Morris and Carrell, 1946, Spalding, 1962). In fact, Shilov and Solodushenkov (1936) found the reaction to be almost complete in less than one second at 1°C, a temperature somewhat lower than any expected in Georgia Strait waters. Spalding (1962) considered two possible reactions



His results indicated that between pH 3 and 10.5 the first equation applied, and considering a copious quantity of water is available, Equation 3 can be kinetically treated as a first order equation. Spalding measured a first order rate constant of 20.9/sec at 25°C with an activation energy of 62.8 KJ/mol. The half life of the reaction at 8°C can be calculated at about .1 sec, and therefore conversion of  $\text{Cl}_2$  to HOCl is very rapid.

The production of chlorine hydrate ( $\text{Cl}_2 \cdot 6.2 \text{H}_2\text{O}$ ) appears to be transport controlled with the slowest step occurring at the chlorine-water interface (de Graauw and Rutten, 1970). Therefore, agitation or turbulence will encourage the production of the hydrate.

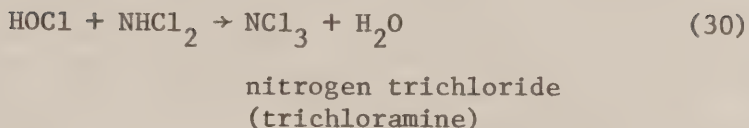
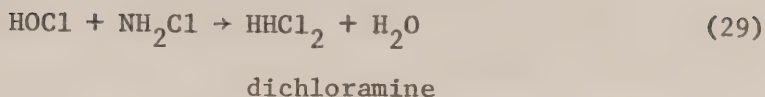
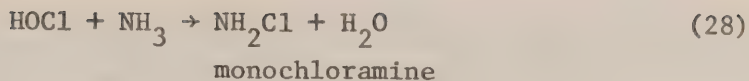
#### The Chlorine Demand of Seawater

So far we have considered the various equilibrium reactions of chlorine in water assuming that no removal mechanism were operating. This, of course, is not the case in nature and a variety of removal paths are available. Given sufficient time and mixing, all of the chlorine with a +1 valence will eventually be removed through redox reactions. A variety of compounds naturally present in seawater will be important in the removal of chlorine, some of which are listed below (White, 1972).

1. Ammonia
2. Amino Acids
3. Proteins
4. Organic Carbon
5. Nitrite
6. Iron
7. Manganese
8. Sulphide

Many of the listed compounds are produced and regulated by biological processes, and are contained in dead or living material. The most important group of compounds with regard to short term chlorine interaction are those containing nitrogen (1, 2, 3 and 5 of the above list), especially ammonia. The reaction of chlorine and ammonia in dilute solutions leads to the formation of the chloramines.





The above reactions are not redox reactions in that chlorine still maintains its +1 valance and these compounds still have oxidizing, disinfecting and biocidal capacity. An excellent and very complete review of the interaction of chlorine with ammonia and also other compounds is given by White (1972), to which the reader is referred for more detail than is provided here. Jolley (1973) has also collected together much data on the speciation and exchange reactions involving chlorine in water.

Chlorine which is tied up by ammonia or nitrogen compounds is known as "combined available chlorine residual" or just "combined residual". Residual chlorine existing as hypochlorite ions or as hypochlorous acid is termed "free available chlorine residual" or "free residual" (ASTM Standards, 1976). In addition to the interaction of chlorine with nitrogen compounds, other reactions are possible with the substances listed above. Reducing agents such as  $\text{H}_2\text{S}$ ,  $\text{Mn}^{2+}$ ,  $\text{Fe}^{2+}$  and organic carbon can be oxidized and so remove chlorine quickly from the water. Loss of chlorine in this manner is referred to as the "chlorine demand" of the water (Singley, 1973). Chlorine demand, then, is that amount of chlorine which the water can remove by reducing the  $\text{Cl}^{+1}$ , to  $\text{Cl}^{-1}$  or irretrievably tying up the chlorine in some organic compound. Operationally, demand is defined as the "difference between the amount of chlorine applied to a treated supply, and the amount of free combined or total available chlorine remaining at the end of a contact period" (APHA, 1971).

With respect to chlorination, seawater has one important difference from fresh water. It contains an appreciable quantity of bromide, with 67.3 mg/Kg in seawater of 35‰ salinity (Wilson, 1975). As mentioned while discussing the effect of chlorine on the pE of seawater, it is thermodynamically possible for chlorine to displace the bromide in seawater with a loss of about 30 mg/Kg of chlorine, and a production of about 67.3 mg/Kg bromine in 35‰ seawater. Bromine is then free to react in an analogous manner to chlorine producing hypobromous acid and the bromamines. Most instrumental methods do not differentiate bromine and chlorine contributions, and therefore seawater measurements have commonly been referred to in terms of the chlorine demand. A method which reportedly could differentiate between chloramines and bromamines was devised by Johannesson (1958), but Duursma and Parsi (1976) could not obtain satisfactory results in their laboratory. In the remainder of this report we shall refer to all measurements in terms of chlorine, tacitly realizing that some bromine or brominated species will be contributing.

Griffin (1944) in experimenting with higher than normal residuals used for water treatment, discovered the so called "breakpoint" phenomenon. Measured chlorine residuals initially increase with the amount of chlorine added, but suddenly drop off. This behaviour is caused by the interaction of chlorine and ammonia. After the minimum, or "breakpoint" free residual chlorine can be measured.

A breakpoint curve was determined for some 2 m seawater obtained in Howe Sound from the ship M.V. Pandora II during an Ocean Chemistry cruise in July, 1976. Various amounts of chlorine were added to the seawater and the total residual was determined amperometrically after 30 minutes. (The amperometric determination of free and combined residual chlorine is well documented by the ASTM Handbook (1976) and the Fischer and Porter Instruction bulletin for the amperometric titrator made by that company. The reader is referred to these for details of the method. The Fischer and Porter Model 1771010 Amperometric Titrator was used for all chlorine determinations, and does not distinguish between chlorine and bromine contributions.) Figure 11 shows the essential features of this breakpoint curve and several aspects should especially be considered. The curve does not pass through the origin due to some initial chlorine demand caused by some species in seawater which are readily oxidized within the half hour chlorination period. The first part of the curve lies in the region where most of the chlorine is tied up as monochloramine. After the maximum, dichloramine may be formed, an important compound since it participates in further reactions which lead to the eventual oxidation of ammonia by deamination. The downward slope in Figure 11 results in a measured increase in chlorine demand. The minimum is the breakpoint beyond which free chlorine residual exists. In fresh water there is also a small portion of dichloramine and trichloramine present. Duursma and Parsi (1976) in some very recent investigations measured the interaction of ammonia and chlorine in seawater with relatively high doses of both chlorine and ammonia (up to 710 mg/Kg  $\text{Cl}_2$ ). Their experiments point out some fundamental differences between the formation of chloramines in seawater and in fresh water. It would appear that the breakpoint in seawater is obtained at lower ratios of chlorine to ammonia than in fresh water, and that the dichloramine does not persist in detectable quantities. Oxidation of ammonia via the chloramines can result in various possible nitrogen species including  $\text{N}_2$ ,  $\text{NO}_3^-$ ,  $\text{N}_2\text{O}$ , and NO (White, 1972).

While investigating the chlorine demand of water as a function of time, Taras (1953, 1950) found that chlorine demand could be expressed by the equation

$$D = kt^n \quad (31)$$

where D is chlorine demand, t is contact time, and k and n are constants determined experimentally.

The exponent n relates to the speed of the chlorine consuming reactions, and as such helps to define which species are responsible for the chlorine demand observed. The higher the exponent, the slower the reaction, and also the more complicated the reacting species.



Some experiments were made on the chlorine demand of seawater as a function of time on samples obtained in August 1976 from Saanich Inlet in the vicinity of the small CEPEX enclosures. Both a 2 meter and a 30 meter sample are shown in Figure 12 (each seawater sample was chlorinated with 5 mg/l chlorine initially). The first chlorine demand measurement appears to be low possibly due to experimental error or perhaps due to an induction period peculiar to the seawater system. (The 2 m sample also had the first point somewhat lower than might be expected.) The exponent of  $t$  was found to be .22 for the 30 m sample and .20 for the 2 m sample, indicating that compounds other than ammonia are also responsible for some of the chlorine demand. Water with the nitrogen component mainly due to ammonia have exponents in the .01-.08 range (White, 1972). A Taras plot (Fig. 13) was also made for a sample of surface sediment obtained in Georgia Strait several miles off Point Grey. In this case 5.2 grams of sediment (wet weight) were placed in 5 litres of demand-free water which was then chlorinated to 5 mg/l. The sample was continuously stirred by a magnetic stirrer with a Teflon stirring bar throughout the measurements. Figure 12 shows that again, the early measurement was depressed, while the exponent of  $t$  calculated from the later points was .28 indicating the likely occurrence of more complicated nitrogenous compounds than ammonia. The 5 g sample also had a fairly high demand removing all of the chlorine in the 5 litre flask within four hours. (All demand experiments were run under ambient laboratory light conditions.)

These experiments show that seawater may be expected to have a short term demand of about 1.5 mg/l (Fig. 11). Sediment appears to have a fairly high demand with 1 g (wet weight) of surficial mud capable of quickly removing 2 mg of chlorine from a 1 litre volume. This agrees well with the estimate given by White (1972) for the 10 minute demand of seawater of 1.5 mg/l. In any event the chlorine demand should not exceed 3 mg/l unless some organic pollution has taken place. Examination of Figure 12 shows that after two days only 3 mg/l chlorine had been removed from the 30 m seawater sample. The same was true for the 2 m sample.

Duursma and Parsi (1976) investigated the persistence of chlorine in seawater using far higher concentrations of chlorine than used in our studies, with chlorine doses of over 1600 mg/l. They found that under these circumstances a more or less rapid loss of chlorine was often seen with the higher dose during the first few minutes. Aeration augmented this effect causing a seawater solution initially dosed with 1400 mg/l of chlorine to fall to about 1100 mg/l after ten hours. They hypothesized that some of the chlorine may have been removed by gas bubbling, an unlikely mechanism since at the pH of their chlorinated seawater (greater than 10) the amount of free chlorine is very low (see Fig. 9). There does not at present appear to be any reasonable explanation for this behaviour, and their investigations at lower doses of chlorine (below 600 mg/l) do not show this loss.

A possible direct removal of chlorine from seawater is possible by a light stimulated reaction



Duursma and Parsi (1976) studied the effect of light on persistence of chlorine in seawater with chlorine concentrations below 35 mg/l. They found no significant difference in chlorine behaviour between the light and dark conditions, and suggest that formation of bromine may be responsible since the bromine reaction analogous to Equation 32 was not photochemically mediated under the experimental conditions.

### Gaseous Explosion

When a liquified gas is spilled onto or injected into a second fluid, there is a possibility of forming superheated liquid drops. In this case, the temperature of the drop is elevated above its normal boiling point.

Under the usual circumstances when a liquid exposed to a gas phase (the atmosphere) is raised to its boiling point it will simply boil and maintain a constant temperature. Bubble formation during boiling results from nucleation on the walls of the vessel, or from impurities in the boiling liquid where microscopic irregularities trap or adsorb gas and present a gas-liquid interface where a bubble can be formed. Even this process is sometimes not sufficient to prevent superheating, and most chemists are familiar with the phenomenon of "bumping" while attempting a distillation. The use of boiling chips with rough porous surfaces can prevent this by introducing a large gas-liquid interface. Kinetic analysis shows that the probable formation of a bubble within a liquid (homogeneously) at the normal boiling temperature is very low. Small bubbles tend to collapse before they reach a critical size where surface tension effects are not so important.

In the case where an immiscible drop of liquified gas is placed into another fluid at a temperature in excess of the boiling point of the liquified gas, the drop can remain stable even at remarkably high temperatures. For example, several authors have been able to reproducibly heat n pentane to 146-147°C at atmospheric pressure (Reid, 1976). This is over 100 C° in excess of its normal boiling point.

There is, however, a definite limit to which a liquid can be heated called the "superheat" or "cavitation" limit, above which a superheated liquid can explode with violence.

Since the boiling point of chlorine is -34.5°C at atmospheric pressure, and the temperature of seawater in Georgia Strait may be expected in the 5-15°C temperature range, the injection of liquid chlorine into the water will result in the formation of superheated drops. It is important to ascertain the likelihood of an explosion or explosions following rupture of the tank cars. This discussion applies only to that part of the water column where chlorine gas is thermodynamically stable. At depths where chlorine would normally remain a liquid, gaseous explosion will never be a problem.

Thermodynamic stability analysis shows that for a pure liquid the superheat limit occurs when (Beegle et al., 1974)



$$\left(\frac{\partial P}{\partial V}\right)_T = 0 \quad (33)$$

Using this thermodynamic criterion and the Redlich-Kwong (1949) equation of state, Reid (1976) has provided a generalized curve of reduced pressure ( $P/P_C$ ) as a function of the reduced superheat limit  $\left(\frac{T_{SL}}{T_C}\right)$

where  $P_C$  and  $T_C$  are the critical pressure and temperatures respectively. This curve gives a very adequate representation of experimental observations on many gases.

Based on this curve and the critical pressure (76.8 bars) and critical temperature (144°C) of chlorine, the water temperature would have to be in excess of 100°C before explosion could take place at atmospheric pressure. Clearly, this rules out gaseous explosion as a result of mixing chlorine with Georgia Strait water.

#### Chlorine Release in Seawater

On August 20, 1976, some small-scale chlorine release experiments were performed in Saanich Inlet at a series of depths from 25 m to 145 m. A small size cylinder (10 cm diameter x 36 cm length, Canadian Liquid Air) was half filled with liquid chlorine and padded to 35 bars pressure with nitrogen. The outlet was connected through a short length (1 meter) of .3 cm OD stainless steel tubing, acting as a flow restrictor, to a Whitey ball valve. After the ball valve, a short piece of .6 cm stainless steel tubing was connected with a one way check valve at the end, and a short piece of .6 cm OD Teflon was connected last. The ball valve was opened and closed outside the Pisces by a Whitey valve actuator with spring return. The actuator was connected through a hydraulic reduction valve (14 bars) to the Pisces hydraulic system (69 bars) which was operated from within the Pisces. Figure 14 gives a schematic diagram of the equipment, and Figure 15 shows how the system was arranged on the outside of the Pisces.

During the release experiments visual examination, colour 35 mm slides and super 8 movies were used to document the behaviour of chlorine at various depths when released into the water. In the following description it will be assumed that every 10 meters depth of seawater is approximately equivalent to 1 bar of pressure so that, for example, 80 meters would have a total pressure of 9 bars, atmospheric pressure being included. This should not be in error by more than about 2%. Accurate interconversion of pressure and depth can be made provided salinity and temperature data are available (Saunders and Fofonoff, 1976).

Initially on the dive, the Pisces descended to the bottom of Saanich Inlet about 190 m. Although the order for the cylinder specified padding the void space with 35 bars (500 psi) of  $N_2$ , chlorine did not come out at this depth. It is possible that the cylinder was not padded to sufficient pressure or, more likely, some of the  $N_2$  dissolved in the chlorine causing

a reduction in pressure according to Henry's law. The first chlorine emerged at 145 m (15.7 bars) as green liquid drops, some running down the tube as a thick syrup-like fluid and some squirting out and then quickly descending in drops about 1/2 cm in diameter (Fig. 16). No hydrate was seen although the chlorine rapidly disappeared from sight below the Pisces windows before mixing to any degree with the water. As suggested in the section on kinetics, the hydrate formation process is transport controlled at the chlorine-water interface and slow mixing here probably slowed down hydrate formation even though the hydrate is thermodynamically stable (Fig. 5).

At 90 meters the chlorine emerged more vigorously (due to reduced hydrostatic pressure) and could be observed for a longer time period than before. Figure 17 shows the green liquid coming up out of the tube, and then rapidly descending. Some yellowish hydrate could be seen forming on a few of the liquid chlorine drops, and fine white flakes of hydrate were clearly seen, dispersed through the water a short time after the chlorine had been released. These flakes appeared to have almost neutral buoyancy neither rising nor falling at an observable rate. The density of the hydrate is 1.23 g/cc which indicates that it could eventually sink at a rate dependent on particle size. Figure 17, also taken at 90 m, shows more clearly the liquid chlorine-hydrate clumps which formed shortly after injection into the water. These clumps slowly sunk below the Pisces windows.

At 60 meters depth the chlorine shot out in a fairly dispersed plume and formed hydrate more readily than at 90 meters probably due to turbulent mixing, and a finer dispersion of chlorine into small drops. Figure 19 shows the chlorine plume, and some of the liquid drops with hydrate attached are visible to the right of the tube and level with it. Some small bubbles were also seen, but these were probably due to  $N_2$  being released from the chlorine similar to the release of  $CO_2$  on opening a carbonated drink.

At 45 meters a similar behaviour was observed but the liquid chlorine-hydrate clumps which formed initially had occluded or attached bubbles which caused them to rise quite rapidly. At this depth, liquid chlorine, hydrate and gaseous chlorine were all seen although the gaseous chlorine formed slowly. Fine flakes of hydrate were seen shortly after chlorine injection as shown in Figure 20.

At 25 meters no liquid was observed at all, and the chlorine came out as a steady gas plume (Fig. 21). Outgassing and expansion of dissolved  $N_2$  may have contributed to this, but the general colour showed that a large portion of the gas was chlorine. Since liquid chlorine still remained in the cylinder (which was inverted) at the end of the experiment, the gas seen at this level was generated from liquid chlorine, and not from gas coming directly from the cylinder. No hydrate was seen in the water near the injection point, but it could possibly have formed further up in the water column as the gas plume rose. How far the gas bubbles rose was impossible to tell from inside the Pisces. Some gas was sighted near the surface, but only when the Pisces had cleared its ballast tanks. There was no direct evidence of chlorine at the surface. In accordance with the theory given in the section on gaseous explosion, no violent explosions were seen at any point in the water column during the chlorine releases.



Some experiments on chlorine-seawater interaction were performed by Macmillan-Bloedel (R.W. Cunningham, 1975) in which chlorine was released into seawater in the laboratory, and into the surface water in Burrard Inlet. They used a 25 litre chlorine cylinder inverted, so that only liquid chlorine was released (The tank was not pressurized with air or  $N_2$ .) Gaseous chlorine and the hydrate formed during all of the experiments, some of the gas apparently reaching the surface from a depth of 20-30 cm. Much of the chlorine was tied up in "golf ball" sized lumps of hydrate which came to the surface and dissociated into the aqueous phase within a couple of minutes. (The surface temperature of the water was probably less than  $10^\circ C$ .)

The physical behaviour of chlorine in seawater conforms quite closely with thermodynamic prediction (Fig. 2-5). Gas forms above 45 meters and the hydrate clumps rise due to attached bubbles above the depth. In the event of a large spill of chlorine at less than 45 meters, it is impossible to give an exact estimate of the behaviour, but the majority of chlorine should be tied up as a hydrate before reaching the surface. At very shallow depths, some chlorine gas could break the surface and escape to the atmosphere, but how much would escape depends directly on the magnitude of the leak, the depth of the water and the temperature. Lumps of hydrate buoyed by occluded gas could also float to the surface, but would tend to dissolve into the water rather than release chlorine to the atmosphere.

#### Chlorine Release in the Atmosphere

During an Ocean Chemistry Cruise on the CSS Vector we had the opportunity of observing first hand an accidental release of a mixture and hydrochloric acid from FMC Co. at Squamish on November 29, 1976. The Vector, which at the time of release was on station about 500 meters off shore directly in front of FMC was forced off station for about two hours while the chlorine dispersed. It was estimated that a mixture consisting of 76 kg of chlorine and 4.5 kg of hydrochloric acid was lost during the discharge. The amount of chlorine lost corresponds to less than 0.1% of that contained in one of the tank cars. Winds at the time were light (about 3 knots) and from the west. Initially, a yellowish-white cloud was seen at the FMC site (Fig. 22) but soon it spread across the water toward Darrell Bay as an elongated whitish mist (Fig. 23). The whitish mist, or remnants of it were visible along the eastern side of Howe Sound for over three hours after the release (Fig. 24), and on returning to station after two and a half hours there was still a strong chlorine smell in the air. Since the chlorine which was released was mixed with some hydrochloric acid, the whitish mist was most likely caused by the interaction of HCl with water vapour in the air. Pure chlorine when released might not be so visible, although water vapour could lead to the production of HCl by way of Equation 3.

Two researchers on a field trip were conducting a sampling program throughout the night (November 29-30) on the tidal flats in front of FMC. They both detected chlorine in the air at times, and reported that on occasions it smelled strongly while at other times they did not notice it

depending on the wind direction. Both developed sore throats as a result of the exposure (Thomas and Erickson, 1976).

### Toxicity (Marine Environment)

As has been shown in the previous sections, the chemistry of chlorine in seawater can be fairly complex, and prediction of reaction products in the natural environment is virtually impossible (Mattice and Zittel, 1976). In spite of this, it appears that toxicity can be fairly well predicted provided the correct type of information is available.

After water has been chlorinated, only three basic forms of chlorine need be considered for toxic effects.

1. Free residual chlorine existing as either  $\text{HOCl}$ ,  $\text{OCl}^-$  or even as free  $\text{Cl}_2$ . The equilibrium between these three species has already been dealt with in some detail, and it suffices here to repeat that the system is very pH dependent (Fig. 9).
2. Combined residual chlorine, specifically the chloramines but also compounds formed with more complex nitrogenous substances such as proteins and amino acids.
3. Apparent chlorine demand chlorine. This category covers that chlorine which has been removed from the system by redox reactions resulting largely in the formation of chlorides. Operationally, it is the difference between the chlorine added, and the "active" chlorine determined by some suitable technique.

Of these three forms the third contributes almost nothing to toxicity in seawater. In the case of polluted waters containing high concentrations of anthropogenic materials some toxic secondary products may be formed, for example cyanogen chloride (Allen, et al., 1946, 1948) chlorophenols (Parker, 1935; Hopkins and Bean, 1966) 5-chlorouracil and 4-chlororesorcinol (Jolley, 1973). These compounds should not be important in open ocean water and it will be considered here that chlorine removed by chlorine demand has been effectively destroyed.

A further consideration peculiar to seawater is the possibility of producing brominated compounds due to the displacement of bromide from the seawater by chlorine. Toxicity studies of chlorine in seawater have traditionally not been concerned about the generation of bromine, but operationally this should not cause problems since toxicity measured as a function of chlorine addition will cover combined effects of chlorine and bromine. The bromide in seawater may indeed explain observed differences in toxicity of chlorinated fresh water and chlorinated seawater. In the remainder of this section reference will be made only to chlorine while it is realized that some or all of the chlorine may be converted to bromine in seawater.

The combined and free residual chlorine cause almost all of the toxic effects in natural waters so that it is important to consider chlorine remaining in both of these two forms after chlorination, rather than the



original dose of chlorine added (Merkens, 1958; Doudoroff and Katz, 1950).

Whether the chlorine is in the free or combined form does not seem to matter greatly as far as toxicity is concerned, with both free chlorine and the chloramines exhibiting the same order of magnitude of effects (Brungs, 1973). Evidence has been presented that free chlorine is more toxic (Merkens, 1958; Rosenberger, 1971) and that the chloramines are more toxic (Holland, et al., 1960). The experiments were not strictly comparable, and it is probable that other environmental factors must be considered in determining which form is more toxic. The concentration of total residual chlorine (free and combined) appears to be both necessary and sufficient to determine toxicity (Brungs, 1973; Mattice and Zittel, 1976). (The total residual chlorine is best determined by the amperometric, or ferrous DPD method. The orthotolidene method has been criticized as inaccurate by Mattice and Zittel, 1976.)

So far we have mentioned that the total concentration of available chlorine is most important when considering toxic effects. Of equal importance is the time of exposure. Therefore, when talking about toxicity of chlorine, it is most important to consider the dose-time anticipated. Mattice and Zittel (1976) in their recent review have taken all of the literature data and have constructed a most useful dose-time curve for the toxicity of chlorine both in fresh water and in seawater. Acute and chronic toxicity thresholds have been estimated from a statistical analysis of the compiled data, and are shown in Figure 24. The chronic toxicity threshold is the level of chlorine below which no toxic effects result regardless of exposure time. The acute toxicity threshold is constructed from consideration of dose-time effects, where high concentrations can be endured for shorter time periods. There is probably a limit on the acute threshold curve where higher concentrations of chlorine do not shorten death time.

From Figure 24 it can be seen that the chronic toxicity threshold of chlorine in the marine environment is about .02 mg/l. Since the threshold is a statistical creation, we cannot say that there will be no toxic effects from concentrations below this, but we can say that the chance of mortality is very small, and becomes smaller the further below the threshold line the total residual chlorine concentration is.

Exposure to higher chlorine concentrations can be endured by a wide spectrum of life forms for a short time period with a .1 mg/l level for one minute not contributing too great a hazard.

These toxicity thresholds have been generated by reference to tests on many different animals in a variety of developmental stages. As a result the thresholds tend to represent the safety limit for the most sensitive species, and will in general err on the side of safety.

#### Toxicity (Atmospheric)

Chlorine is an extremely irritating substance to mucous membranes and the respiratory system. The minimum concentration causing slight irritation is about 1  $\mu$ l/l (Matheson Gas Data Book, 1966) but chlorine cannot be detected

in the atmosphere by smell until it reaches a level of about 3.5  $\mu\text{l/l}$ . The maximum level which can be breathed for one hour without causing damage is 4  $\mu\text{l/l}$ . A detectable odour of chlorine therefore indicates that there is a safety hazard, and steps should be taken to reduce chlorine inhalation. At a level of 15  $\mu\text{l/l}$  there is an immediate throat irritation, and levels of 50  $\mu\text{l/l}$  are dangerous even for short exposures (less than 30 minutes) (Dangerous Properties of Industrial Materials, 1975). Levels of 1000  $\mu\text{l/l}$  are likely to be fatal after a few deep breaths. Chlorine when inhaled reacts with water to form HCl and nascent oxygen both of which attack tissue and can result in pulmonary edema.

### Conclusions

1. Thermodynamics show that four phases may be expected when chlorine and water are mixed, gaseous chlorine, liquid chlorine, chlorine hydrate (solid) and water. With sufficient dilution chlorine will dissolve completely in water forming a "bleach". Above 50 meters gaseous chlorine can form at the anticipated range of temperatures.
2. Chlorine interacts with water on dissolving to form several species.  $\text{Cl}_2$ ,  $\text{HOCl}$ , and  $\text{OCl}^-$ . The equilibrium involving these species will be important in considering the effect of chlorine on pH, alkalinity and even toxicity.
3. Chlorine solutions in seawater will be much more strongly oxidizing than normal oxalic seawater, and it is likely that the 67.3 mg/l bromide in 35‰ salinity seawater will be converted to bromine.
4. Most of the chlorine speciation reactions are rapid, and hydrate formation is very fast, being transport controlled. It is, therefore, anticipated that given mixing, most of the chlorine will quickly form hydrate which can then dissolve on further dilution with water. Even if tank car rupture occurs in shallow water, most of the chlorine should be tied up as a hydrate.
5. The chlorine demand of seawater is about 1.5 mg/l (half hour) and about 3 mg/l after two days. Dilution of chlorine to 3 mg/l should result in it being removed via redox processes within a couple of days.
6. Chlorine release experiments show that the chlorine-seawater system conforms very well to thermodynamic prediction, at least for small releases.
7. Gaseous explosion caused by localized superheating of liquid chlorine is not expected to be a problem at the anticipated water temperatures.

8. Chlorine is expected to exhibit toxic effects when present above .02 mg/l, but should not cause problems below that level. Once the chlorine has been removed by the natural demand of seawater it is effectively out of the system. Secondary toxic products should not become a problem in a relatively unpolluted area such as Malaspina Strait. If the tank cars are in deep water, leaked chlorine should settle to the bottom and toxic water formed from mixing the chlorine with seawater should thereafter remain in deep water until sufficient dilution removes the chlorine below toxic levels.

## References

1. Allen, L.A. et al., 1946, Toxicity to Fish of Chlorinated Sewage Effluents , Surveyor, 105, 298.
2. Allen, L.A. et al., 1948, Formation of Cyanogen Chloride During Chlorination of Certain Liquids: Toxicity of Such Liquids to Fish, J. Hyg., 46, 184.
3. A.P.H.A., 1971, Standard Methods for the Examination of Water and Waste Water, 13th ed.
4. ASTM, 1976, Annual Book of ASTM Standards, Part 31, Water.
5. Beegle, B., M. Modell and R.C. Reid, 1974, Thermodynamic Stability Criterion for Pure Substances and Mixtures, A.I.Ch.E.J., 20, 1200-06.
6. Birtwell, I., 1975, personal communication.
7. Breck, W.G., 1974, Redox Levels in the Sea. In: The Sea, V. 5 Edited by E.D. Goldberg, J. Wiley and Sons Ltd.
8. Brungs, W.A., 1973, Effects of Residual Chlorine on Aquatic Life, Journal W.P.C.F., 45, 2180-93
9. Carson, J., 1975, personal communication.
10. Crean, P.B., and A.B. Ages, 1968, Oceanographic Records from Twelve Cruises in the Strait of Georgia and Juan de Fuca Strait, V. 1-5 Dept. of Energy, Mines and Resources.
11. Culberson, C.H. and R.M. Pytkowicz, 1973, Ionization of Water in Seawater, Marine Chemistry, 1, 306-16.
12. Cunningham, R.W., 1975, personal communication.
13. de Graauw, J. and J.J. Rutten, 1970, The Mechanism and Rate of Hydrate Formation, Third International Symposium on Fresh Water from the Sea, V. 3, 103-116.
14. Doudoroff, P. and Katz, M., 1950, Critical Review of Literature on the Toxicity of Industrial Wastes and Their Components to Fish, Sew. and Ind. Wastes, 22, 1432.
15. Duursma, E.K. and Parsi, P., 1976, Persistence of Total and Combined Chlorine in Sea Water, Netherlands J. of Sea Res., 10, 192-214.
16. Fair, G.M., J.C. Morris, S.I. Chang, I. Weil, and R.P. Burdeu, 1948, Air Water Works Assoc. J., 40, 1051-61.



17. Farkas, L., M. Lewin and R. Bloch, 1949, The Reaction between Hypochlorite and Bromides, J. Am. Chem. Soc., 71, 1988-91.
18. Fernandez, R., W.W. Carey, A.T. Bozzo and A.J. Barduhn, 1967, Thermodynamics and Kinetics in the Hydrate and Freezing Processes, Research and Development Progress Report No. 229, United States Department of the Interior.
19. Fischer and Porter, Instruction for Model 1711010 Amperometric Titrator, Warminster Pennsylvania (Revision 1).
20. Griffin, 1944, Chlorine for Ammonia Removal, In:Fifth Annual Water Conf., Proc. Engrs. Soc., Western Penn, 27.
21. Holland, G.A., et al., 1960, Toxic Effects of Organic and Inorganic Pollutants on Young Salmon and Trout, State of Wash., Dept. of Fisheries, Res. Bull., No. 5, 198.
22. Hopkins, E.S. and Bean, E.L., 1966, Water Purification Control, Williams and Wilkins Co., Baltimore, Md.
23. Horne, R.A., 1969, Marine Chemistry, Wiley-Interscience, N.Y., 568 p.
24. Johannesson, J.K., 1958, The Determination of Monobromamine and monochloramine in Water, Analyst, Lond., 83, 155-59.
25. Jolley, R.L., 1973, Chlorination Effects on Organic Constituents in Effluents from Domestic Sanitary Sewage Treatment Plants. Univ. of Tennessee, Oak Ridge, ORNL-TM-4290, 342pp (Thesis).
26. Ketelaar, J.A.A., 1967, The Drying and Liquification of Chlorine and the Phase Diagram  $\text{Cl}_2 - \text{H}_2\text{O}$ , Electrochem. Tech., 5, 143-7.
27. The Matheson Gas Data Book, 1966, Matheson Co. Inc., 4th Edition, 500 pp.
28. Mattice, J.S. and Zittel, H.E., 1976, Site-Specific Evaluation of Power Plant Chlorination, Journal W. P. C. F., 48, 2284-2308.
29. Merkens, J.C., 1958, Studies on the Toxicity of Chlorine and Chloramines to the Rainbow Trout, Water and Waste Treatment Journal, 7, 150.
30. Morris, J.E., 1967, Kinetics of Reactions Between Aqueous Chlorine and Nitrogen Compounds. In: Principles and Applications of Water Chemistry, S.D. Faust and J.V. Hunter, Eds.,pp. 23-53.
31. Morris, J.C., 1946, The Mechanism of Hydrolysis of Chlorine, Am. Chem. Soc. J., 68, 1692-4.
32. O'Connor, A., 1975, The Chlorine Tank Car Search. Technical Report. Victoria, Canadian Hydrographic Service.

33. Parker, A., 1935, Some Problems of Water Supply, J. Soc. Chem. Ind.,  
34, 49.
34. Redlich, O. and Kwong, J.N.S., 1949, On the Thermodynamics of Solutions,  
V., Chem. Rev., 44, 233-44.
35. Reid, R.C., 1976, Superheated Liquids, American Scientist, 64, 146-56.
36. Roozeboom, H.W.B., 1918. In: Die Heterogenen Gleichgewichte  
II , Vol. 2 by E.H. Buchner, p. 191, F. Viewcg und Sohn,  
Braunscheweig.
37. Rosenberger, D.R., 1971, The Calculation of Acute Toxicity of Free  
Chlorine and Chloramines to Coho Salmon by Multiple Regression  
Analysis, Michigan State Univ., East Lansing (Thesis).
38. Saunders, P.M. and N.P. Fofonoff, 1976, Conversion of Pressure to  
Depth in the Ocean, Deep-Sea Res., 23, 109-111.
39. Sax, N.I., 1975, Dangerous Properties of Industrial Materials, 4th  
Edition, Van Nostrand Reinhold Co., 1258 pp.
40. Shilov, E.A. and S.N. Solodushendov, 1936, The Velocity of Hydrolysis  
of Chlorine. Comptrend. Acid Sci. URSS, 3, 15 .
41. Singley, J.E., 1973, Chemical and Physical Purification of Water  
and Waste Water in Water and Water Pollution Handbook,  
ed. L.L. Ciaccio, Marcel Dekker.
42. Spalding, C.W., 1962, Reaction Kinetics in the Absorption of  
Chlorine into Aqueous Media, A. I. Ch. E. Journal, 8, 685-89.
43. Strickland, J.D.H. and Parsons, T.R., 1972, A Practical Handbook of  
Seawater Analysis, Fisheries Res. Board of Canada, Ottawa, 310 pp.
44. Sugam, R. and George R. Helz, 1976, Apparent Small Ionization  
Constant of Hypochlorous Acid in Seawater, Environ. Sci. and Tech.,  
10, 384-6.
45. Sverdrup, H.U., M.W. Johnson and R.H. Fleming, 1942, The Oceans,  
Their Physics Chemistry and General Biology Prentice-Hall Inc.,  
1087 pp.
46. Taras, M.J., 1953, Effect of Free Residual Chlorine on Nitrogen  
Compounds in Water, J. A.W.W.A., 45, 37 and 1950 Chlorine Demand  
Studies, J. A.W.W.A., 42, 462.
47. Thomas, D. and P. Erickson, 1976, personal communication.

48. White, G.C., 1972, Handbook of Chlorination, Van Nostrand, 744 pp.
49. Wilson, T.R.S., 1975, Salinity and Major Elements of Sea Water.  
In: Chemical Oceanography, Riley and Skirrow, 2nd Ed. Academic Press, Volume 1, p. 365-408.
50. Zirino, A., 1975, Measurement of the apparent pH of seawater with a combination microelectrode, Limnology and Oceanography, 20, Q1-Q4.

TABLE I

## Conversion of Common Units to SI Units

To Convert From Common Unit	To SI Unit	Multiply By
Atmosphere (Atm)	Bar	1.0133
Calories (Cal)	Joules (j)	4.184
pounds/sq inch (psi)	Bar	.06895
Tons (long)	Metric Tons	1.106



TABLE II

## Selected Properties of the Chlorine Water System

Chlorine

Molecular Weight	70.9 g/mol	
Boiling Point	-34.5°C	1
Specific Gravity (liquid) 0-20°C	1.47-1.41	1
Latent Heat of Vaporization 28.3°C	60.6 cal/g	1
Specific Heat (liquid)	0.226 cal/g	1
Specific Heat Cp (gas)	0.114 cal/g	1

Hydrate

Composition ( $\text{Cl}_2 \cdot n \text{H}_2\text{O}$ )	$n = 6.2$	2
Critical Decomposition Temperature	28.3°C	2
Specific Gravity	1.23	3

## Heats of Reaction

a) $\text{Cl}_2 (\text{g}) + n \text{H}_2\text{O} (\text{l}) \rightarrow \text{Cl}_2 \cdot n \text{H}_2\text{O} (\text{Cal/mol at } 28.3^\circ\text{C})$	16,550	2
b) $\text{Cl}_2 (\text{l}) + n \text{H}_2\text{O} (\text{l}) \rightarrow \text{Cl}_2 \cdot n \text{H}_2\text{O} (\text{Cal/mol at } 28.3^\circ\text{C})$	12,253	2
c) $\text{Cl}_2 (\text{l}) + \text{H}_2\text{O} (\text{l}) \rightarrow \text{HClO}_{\text{ag}} + \text{HCl}_{\text{ag}} (\text{Cal/mol at } 25^\circ\text{C})$	4,420	3

<sup>1</sup>Matheson Gas Data Book<sup>2</sup>Fernandez, et al.<sup>3</sup>CRC Handbook of Chemistry and Physics, 50th edition, 1970.

## List of Figures

1. The area where the tank cars are thought to be lost. Included on the chart are the two station locations where pH profiles were determined, vulnerable biological resources, and the areas which have been searched.
2. Phase diagram for the chlorine-water system at 1 bar pressure (surface).
3. Phase diagram for the chlorine-water system at 9 bars pressure (approximately 80 meters depth).
4. Phase diagram for the chlorine-water system at 8°C.
5. Phase diagram for the chlorine-water system at the hydrate composition.
6. Solubility of chlorine in seawater as a function of pressure and temperature.
7. Speciation of hypochlorous acid as a function of pH and temperature.
8. In situ pH measured as a function of depth for two stations in Malaspina Strait (see Fig. 1).
9. The speciation of chlorine in seawater as a function of pH. Shown also is the titration curve expected when chlorine is added to seawater, and the redox potential as a function of chlorine added.
10. Titration curve for seawater with a strong acid (HCl) for seawater with an initial pH of 7.9, and at total carbonate concentration from  $2.0 \times 10^{-3}$  mol/l to  $2.4 \times 10^{-3}$  mol/l.
11. Breakpoint curve for the chlorination of seawater.
12. Chlorine demand as a function of time for 30 meters seawater.
13. Chlorine demand as a function of time for some Georgia Strait surface sediment.
14. Schematic diagram of the equipment used to release small amounts of chlorine from the Pisces at various depths.
15. A picture of the equipment on the outside of the Pisces.
16. Liquid chlorine drops sinking in seawater at about 145 meters depth.
17. Liquid chlorine drops sinking in seawater at about 90 meters. Yellowish hydrate can be seen forming on some of the drops.
18. Chlorine in seawater at 90 meters a short time after injection. Clumps of liquid chlorine and hydrate can be seen in the water.

19. Chlorine plume at 60 meters. Liquid chlorine drops with hydrate attached are visible to the right of the tube above and below the nozzle.
20. Fine flakes of hydrate generated shortly after chlorine release at 45 meters. Flakes similar to these were also seen at 60 meters and 90 meters.
21. Plume of gaseous chlorine at 25 meters.
22. Chlorine "cloud" at Squamish shortly after an accidental discharge from FMC.
23. Elongated chlorine cloud about half an hour after the release.
24. Chlorine mist hanging above the waters of Howe Sound about three hours after the release.
25. Acute and chronic toxicity thresholds for chlorine in seawater.

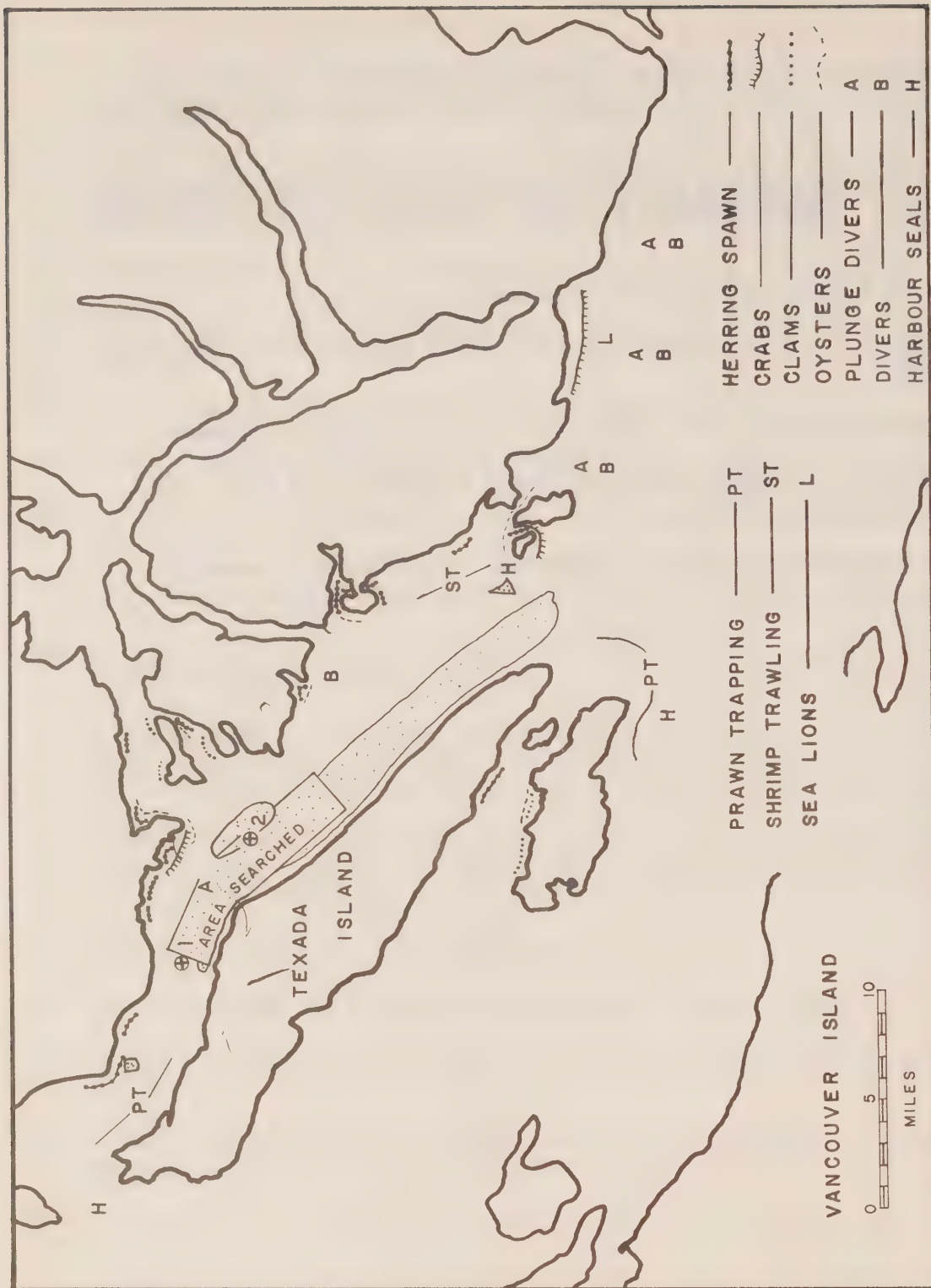


Figure 1. The area where the tank cars are thought to be lost. Included on the chart are the two station locations where pH profiles were determined, vulnerable biological resources, and the areas which have been searched.



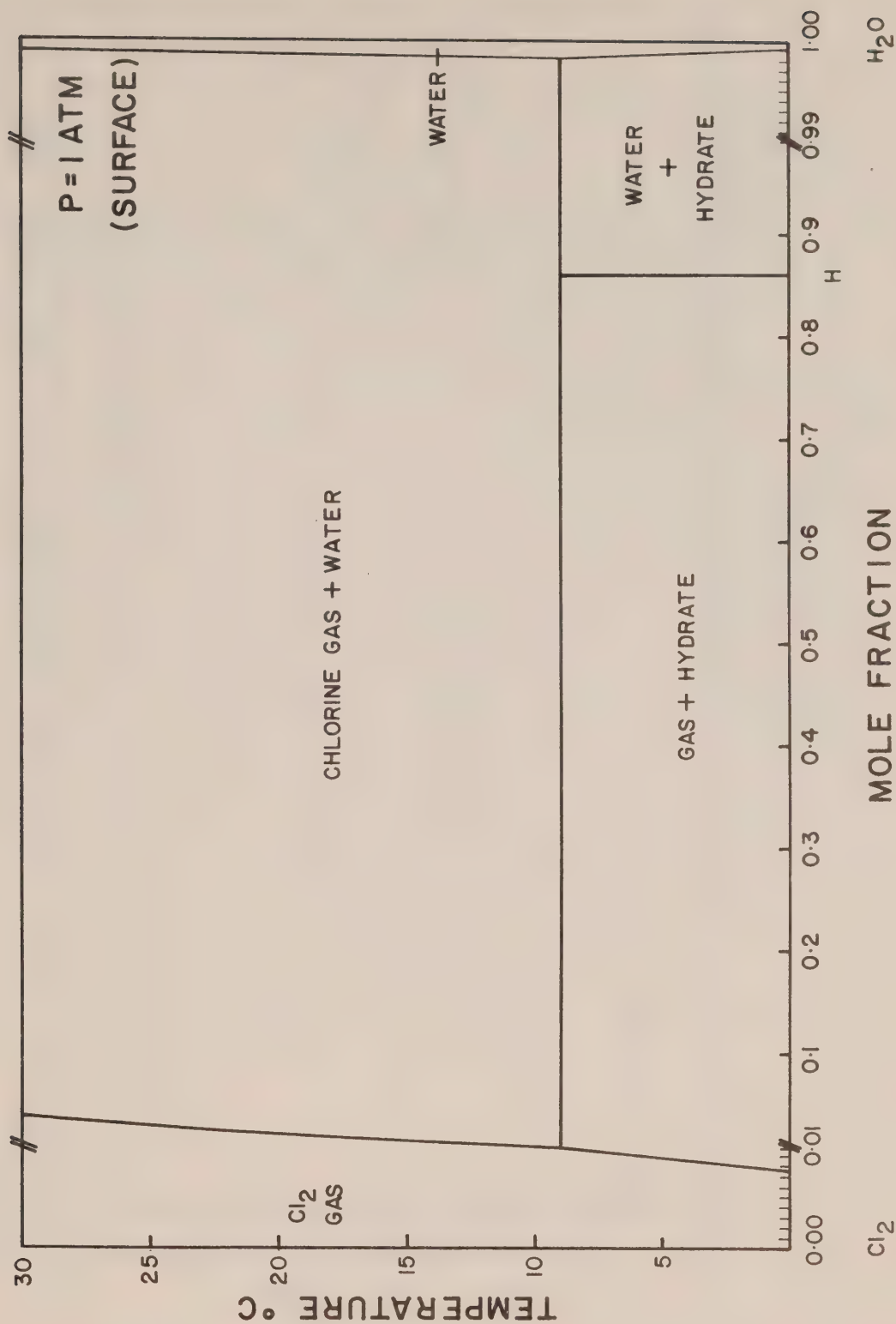


Figure 2. Phase diagram for the chlorine-water system at 1 bar pressure (surface).

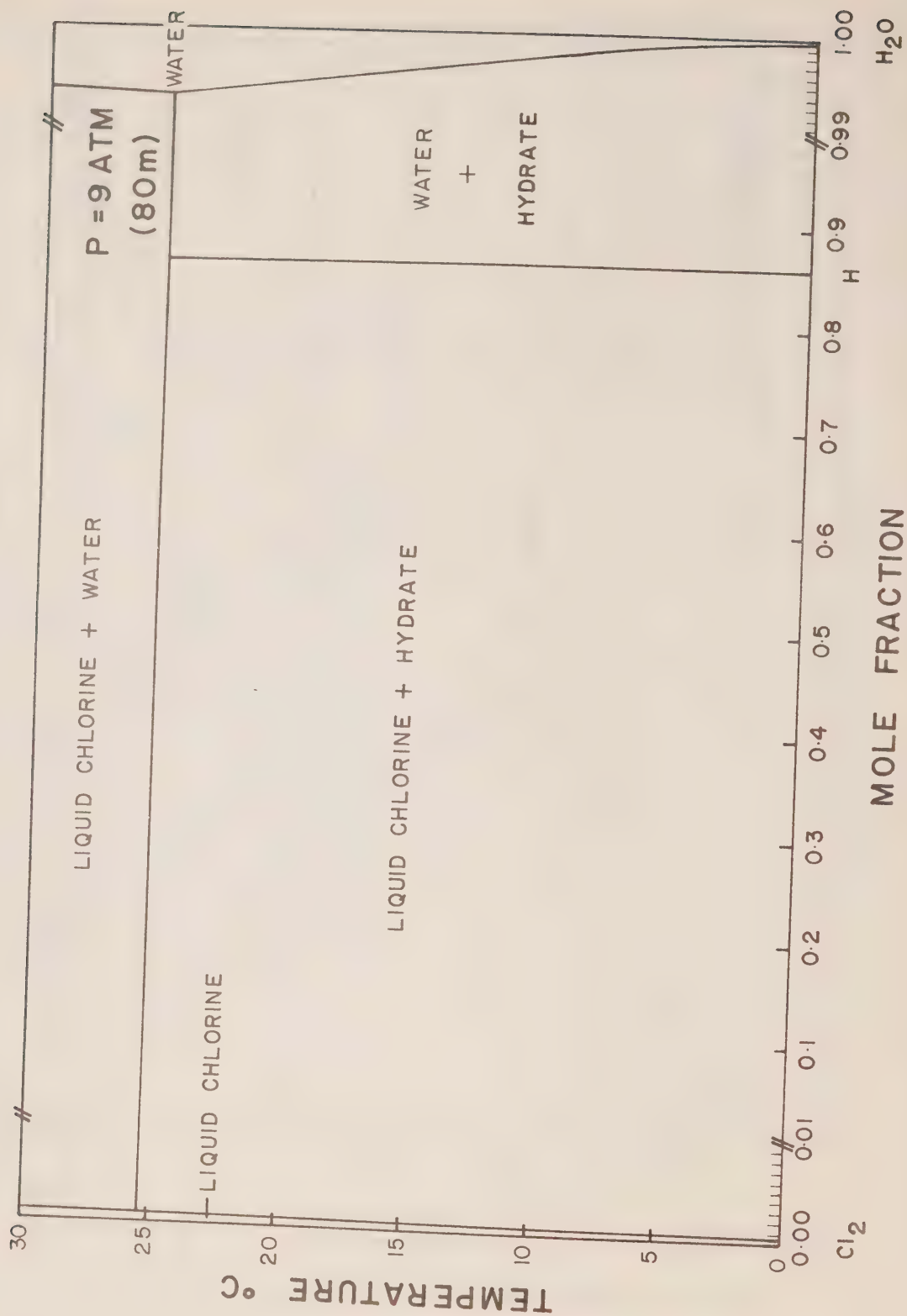


Figure 3. Phase diagram for the chlorine-water system at 9 bars pressure (approximately 80 meters depth).

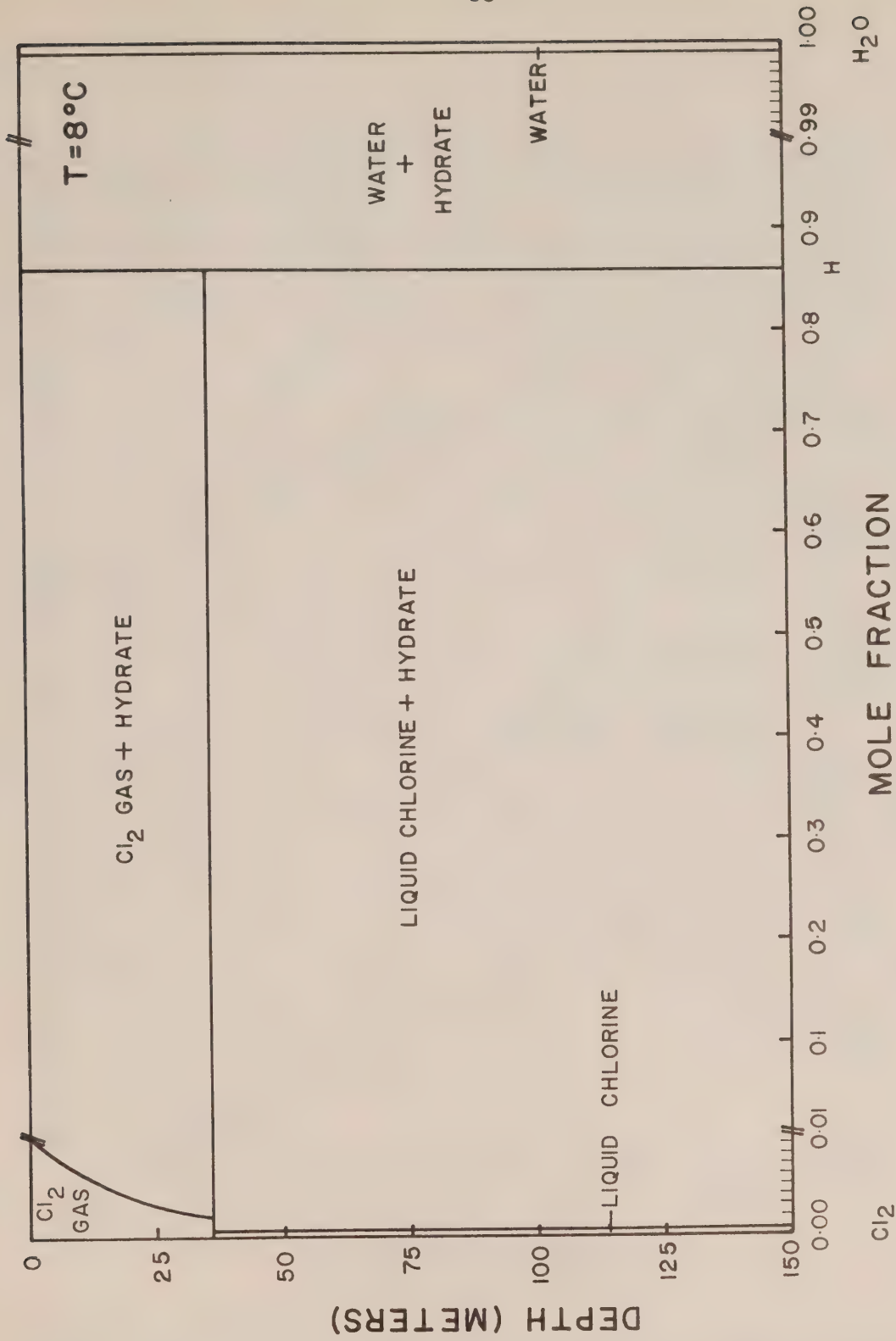


Figure 4. Phase diagram for the chlorine-water system at  $8^{\circ}\text{C}$ .

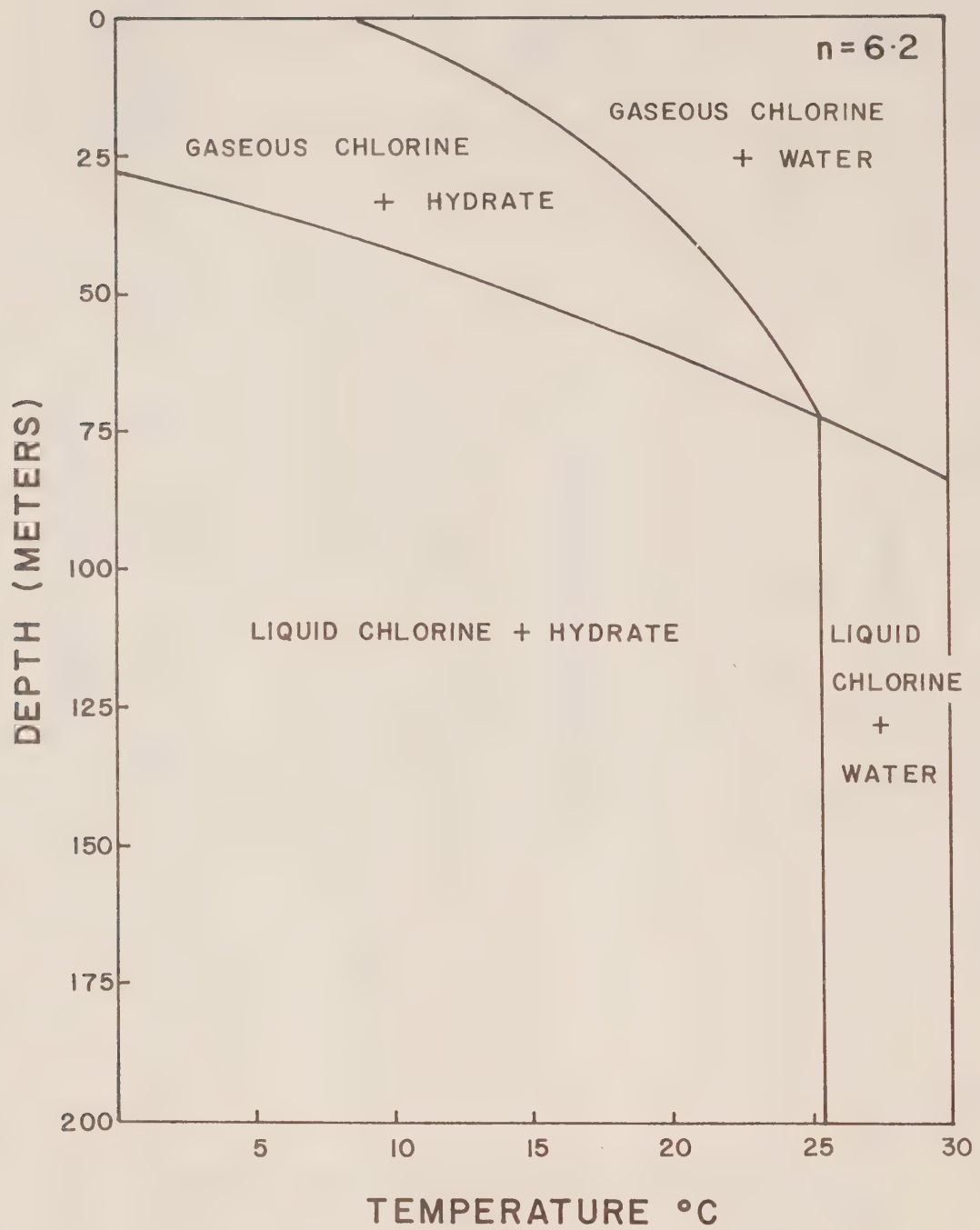


Figure 5. Phase diagram for the chlorine-water system at the hydrate composition.



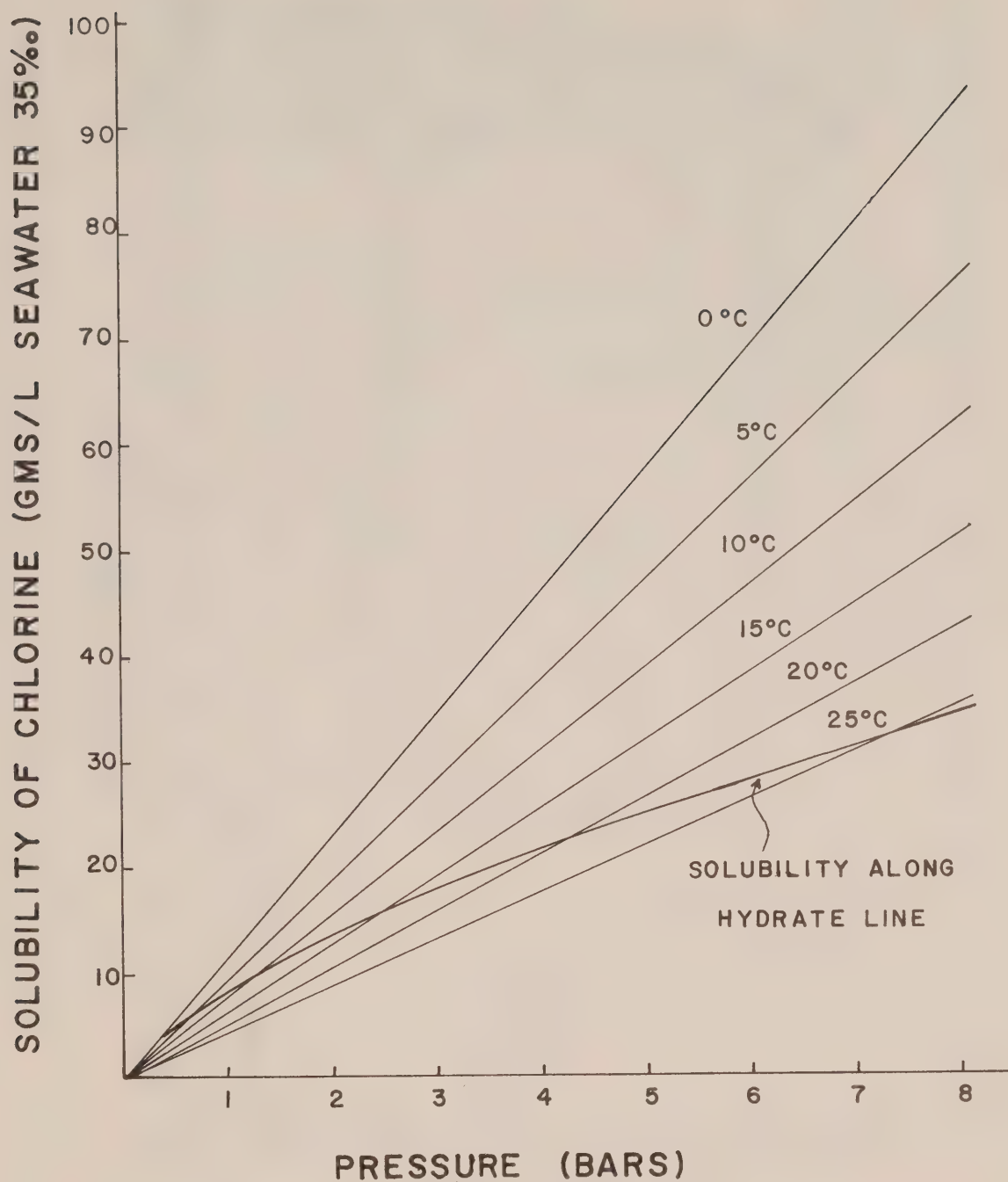


Figure 6. Solubility of chlorine in seawater as a function of pressure and temperature.

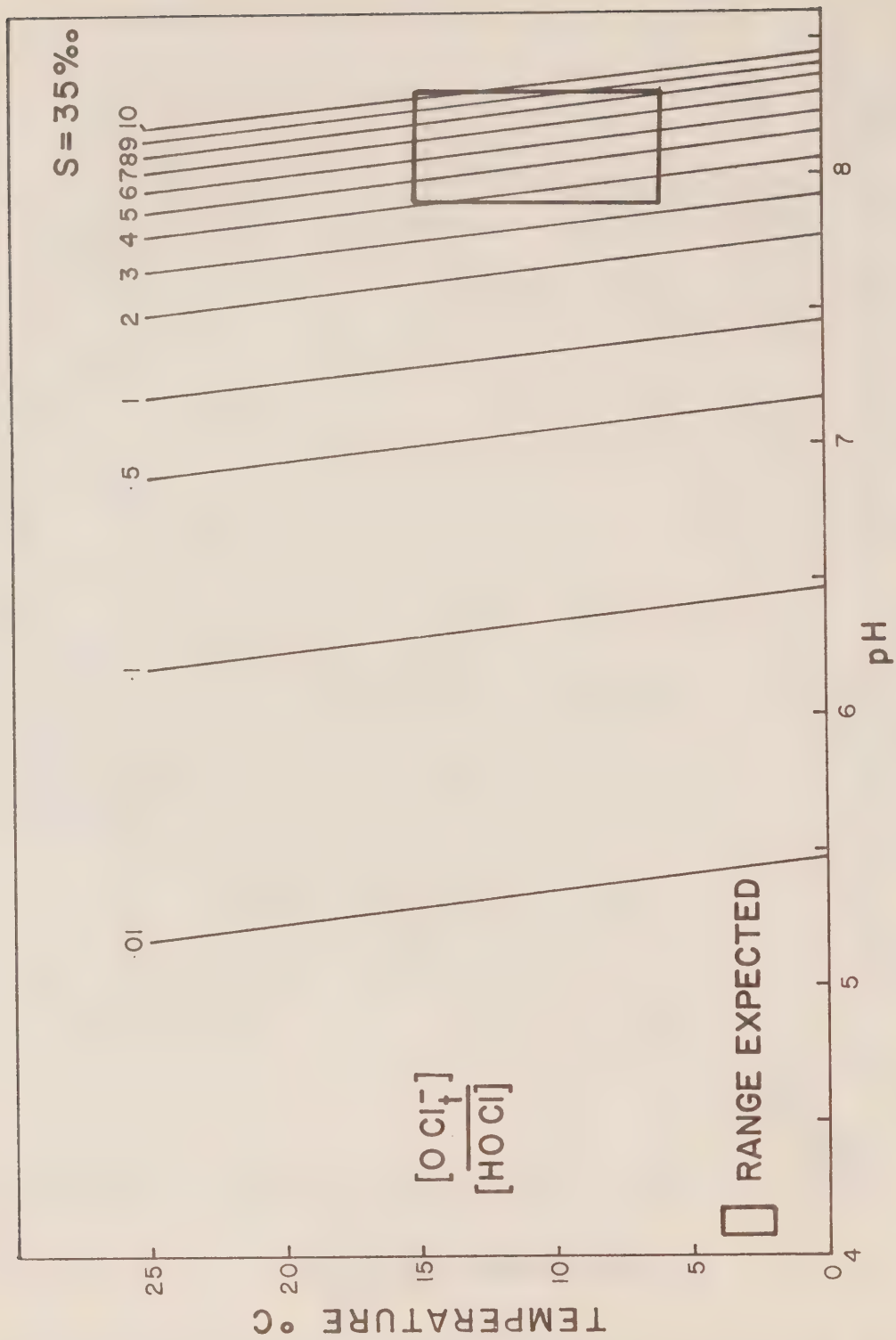


Figure 7. Speciation of hypochlorous acid as a function of pH and temperature.

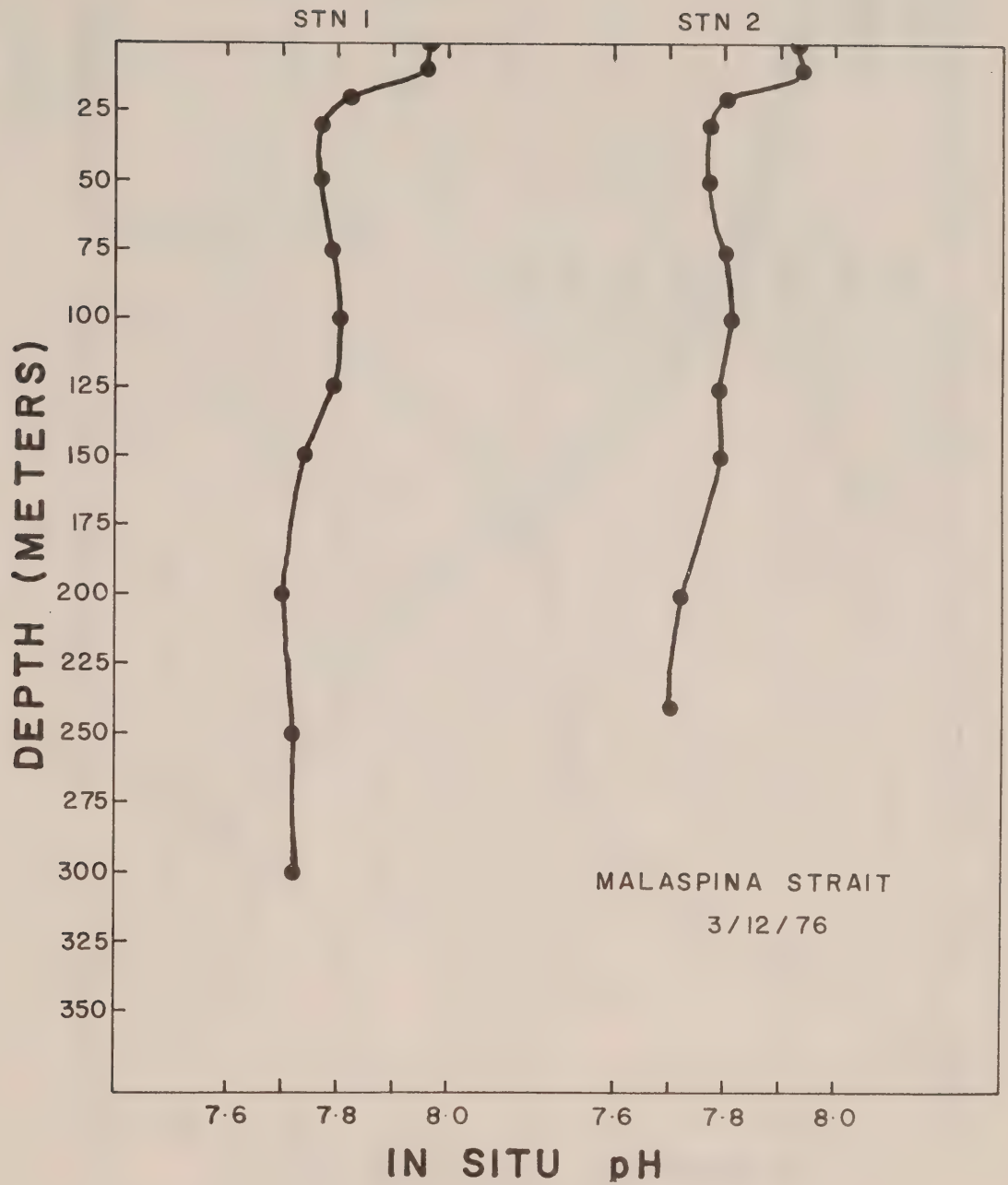


Figure 8. In situ pH measured as a function of depth for two stations in Malaspina Strait (see Fig. 1).

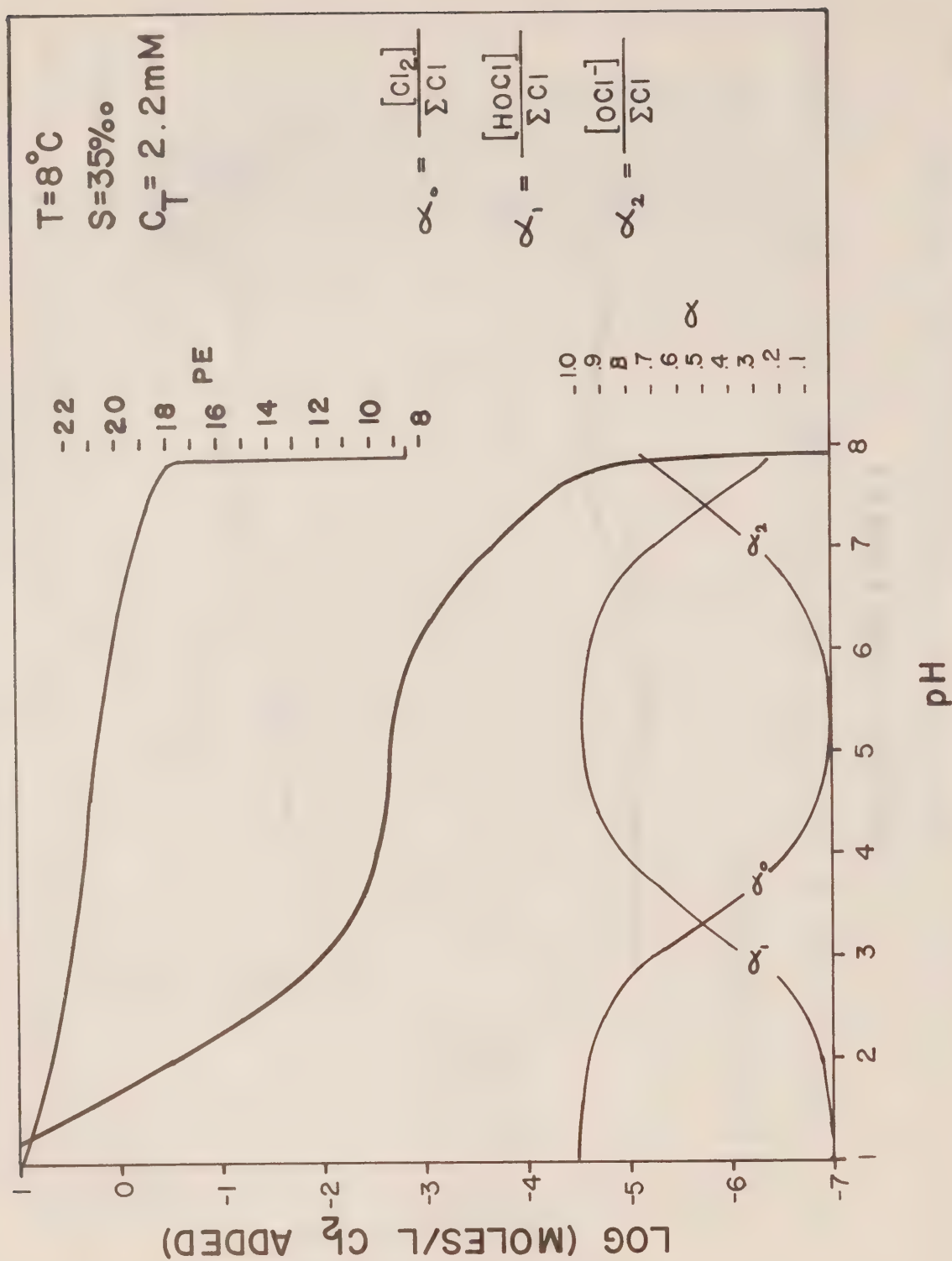


Figure 9. The speciation of chlorine in seawater as a function of pH. Shown also is the titration curve expected when chlorine is added to seawater, and the redox potential as a function of chlorine added.



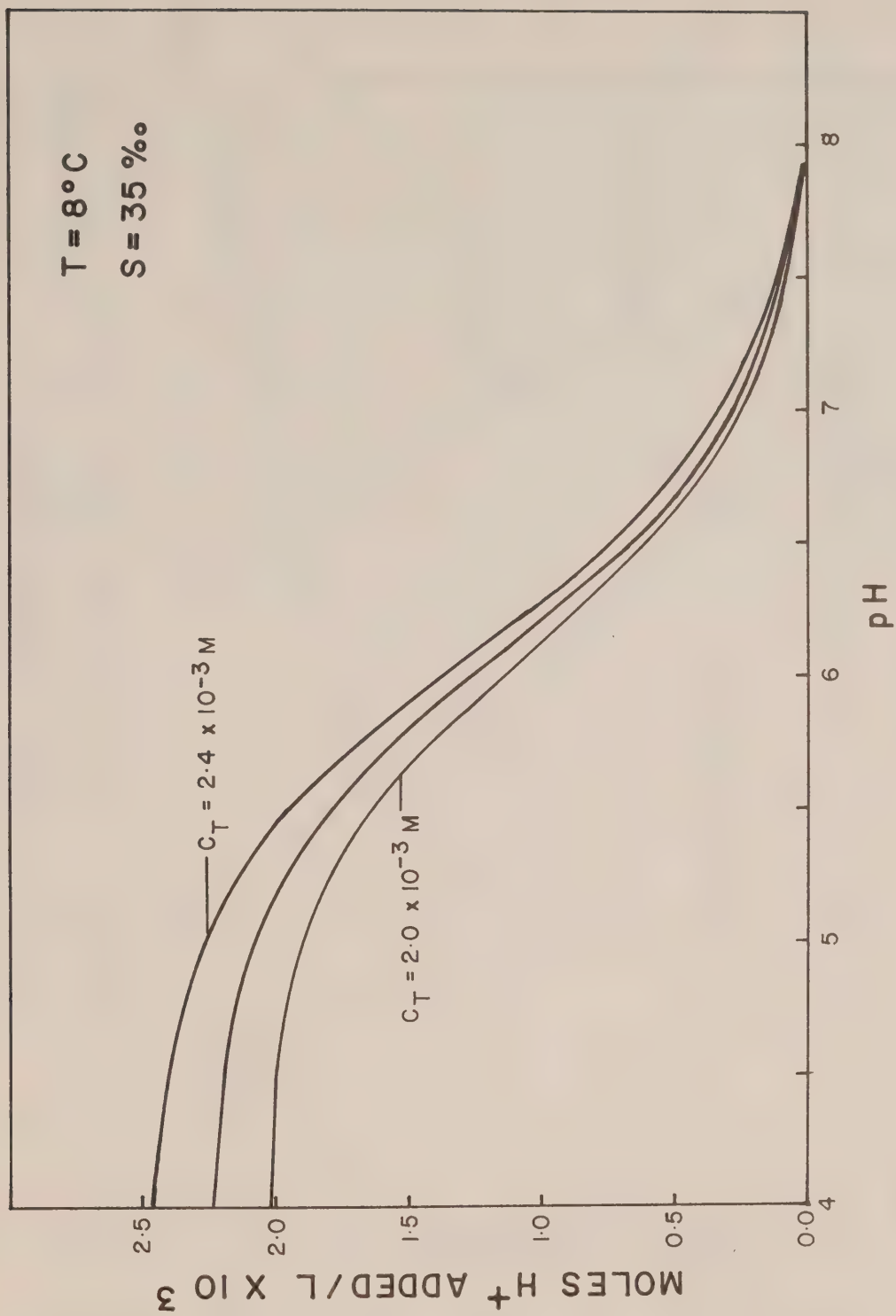


Figure 10. Titration curve for seawater with a strong acid (HCl) for seawater with an initial pH of 7.9, and a total carbonate concentration from  $2.0 \times 10^{-3}$  mol/l to  $2.4 \times 10^{-3}$  mol/l.

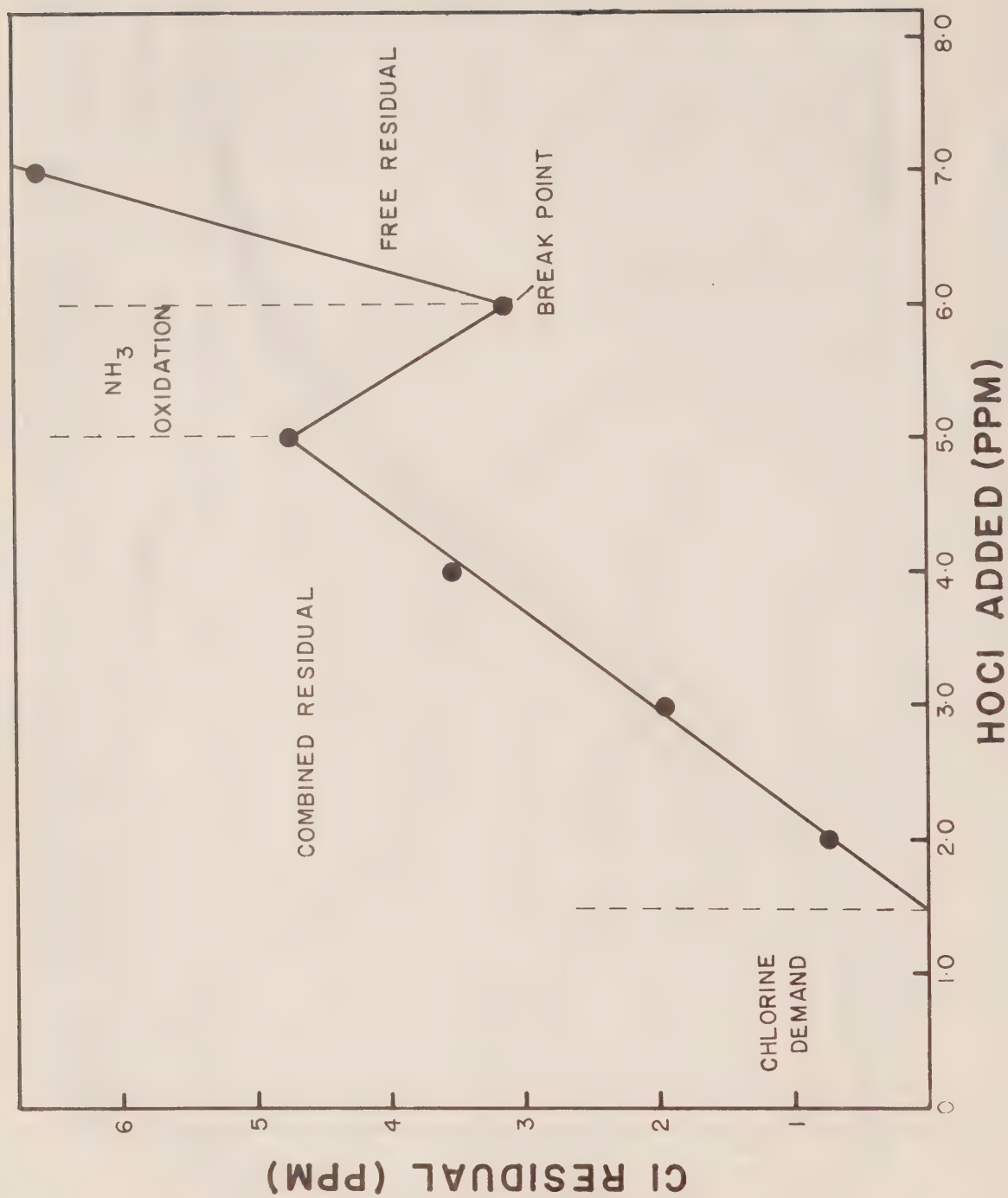


Figure 11. Breakpoint curve for the chlorination of seawater.

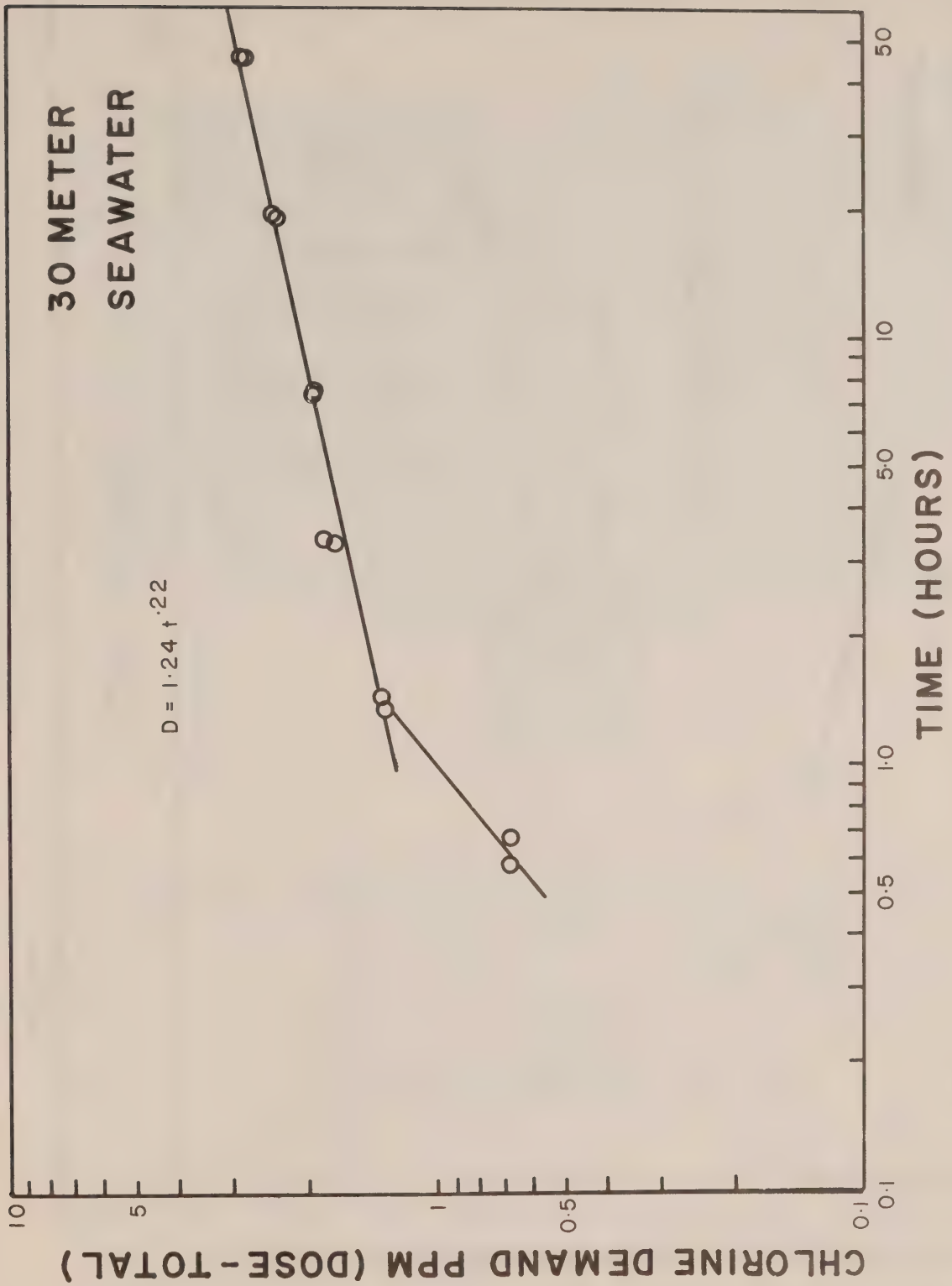


Figure 12. Chlorine demand as a function of time for 30 meters seawater.

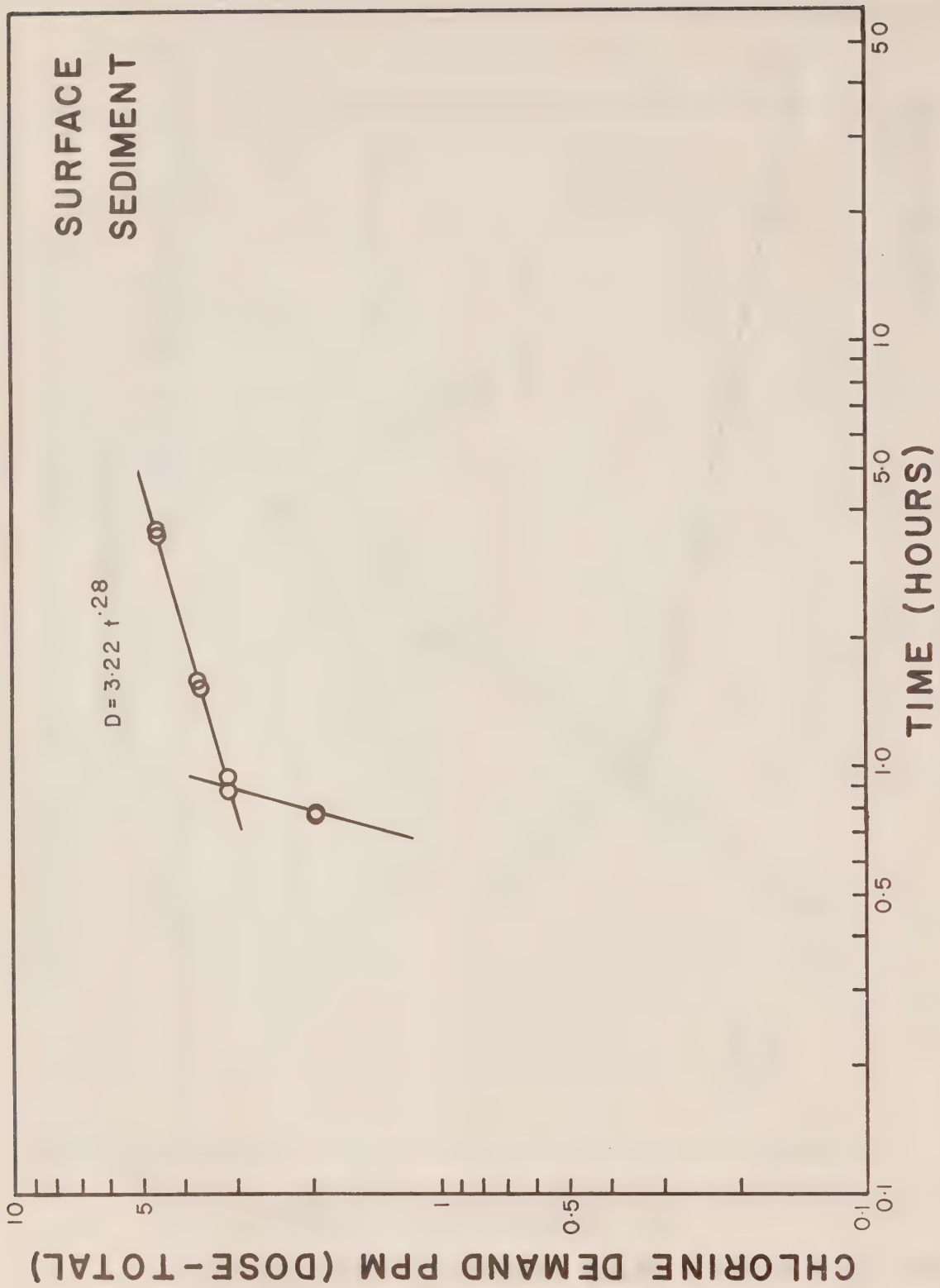


Figure 13. Chlorine demand as a function of time for some Georgia Strait surface sediment.



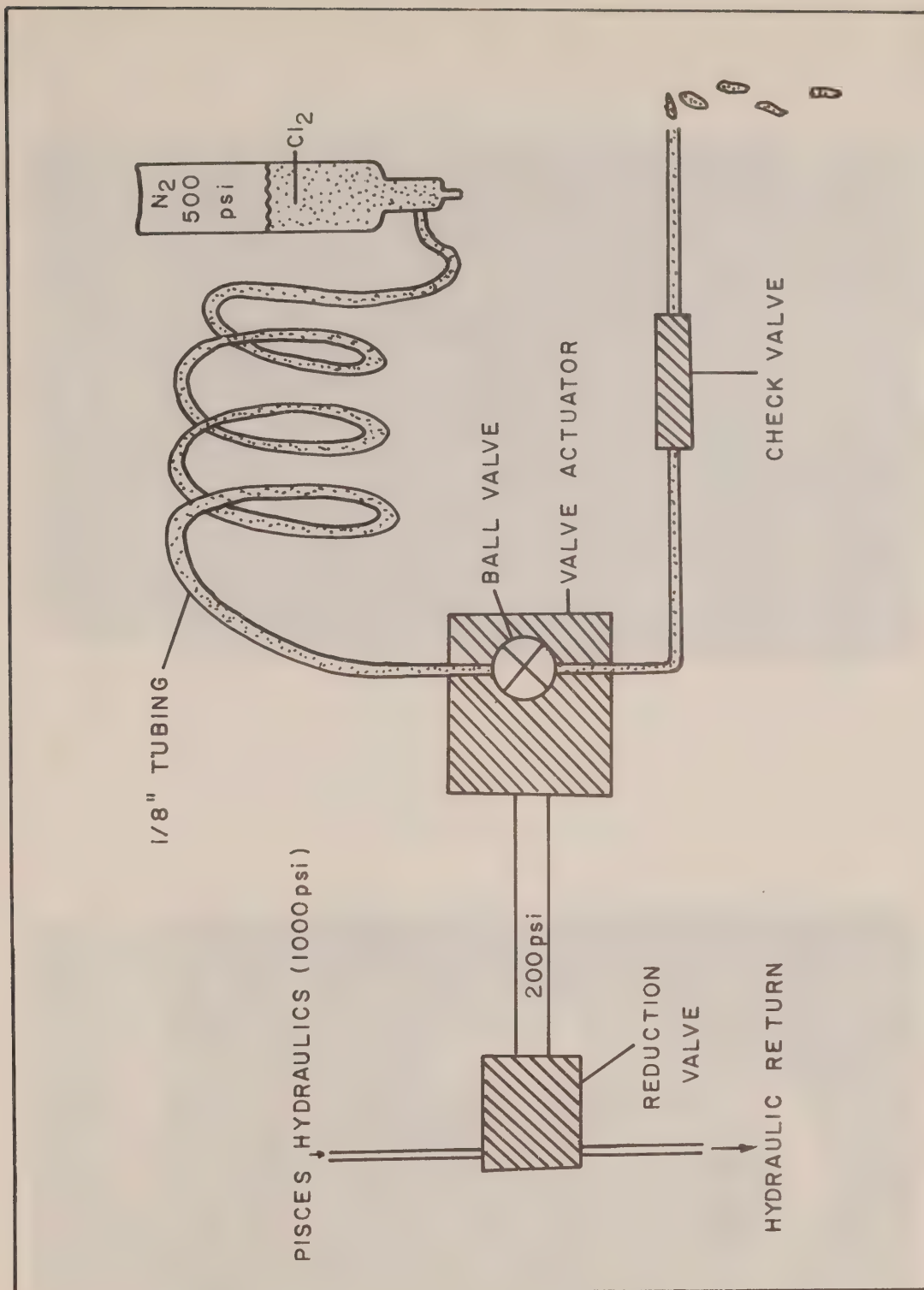


Figure 14. Schematic diagram of the equipment used to release small amounts of chlorine from the Pisces at various depths.

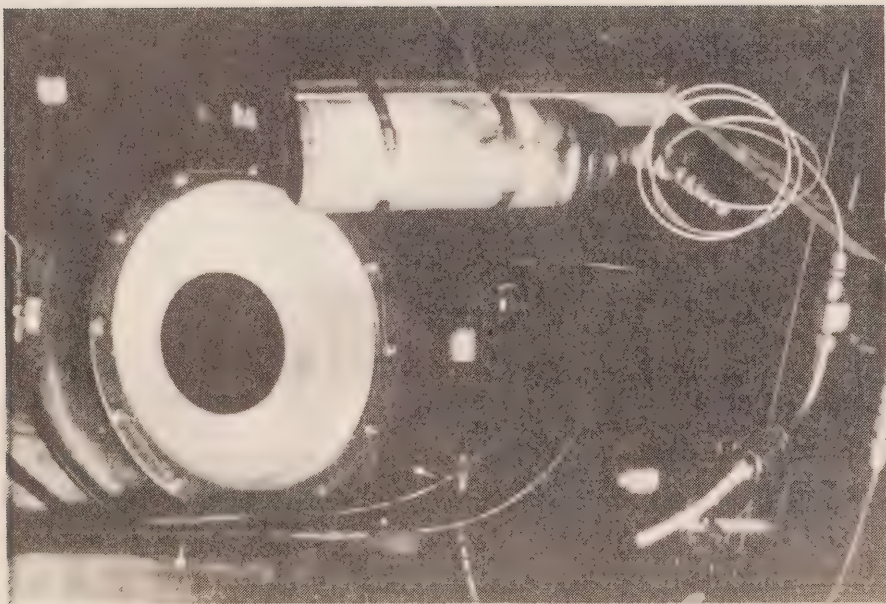


Figure 15. A picture of the equipment on the outside of the Pisces.

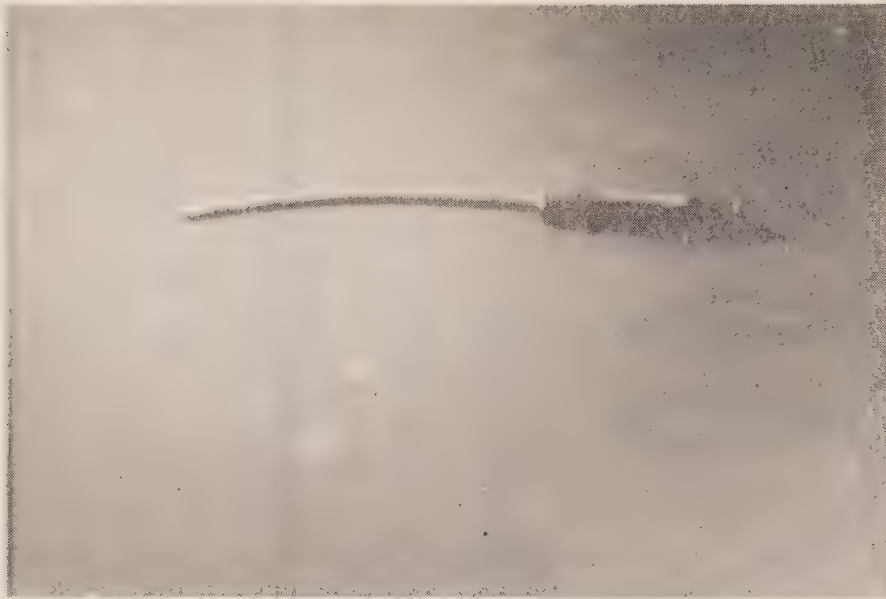


Figure 16. Liquid chlorine drops sinking in seawater at about 145 meters depth.

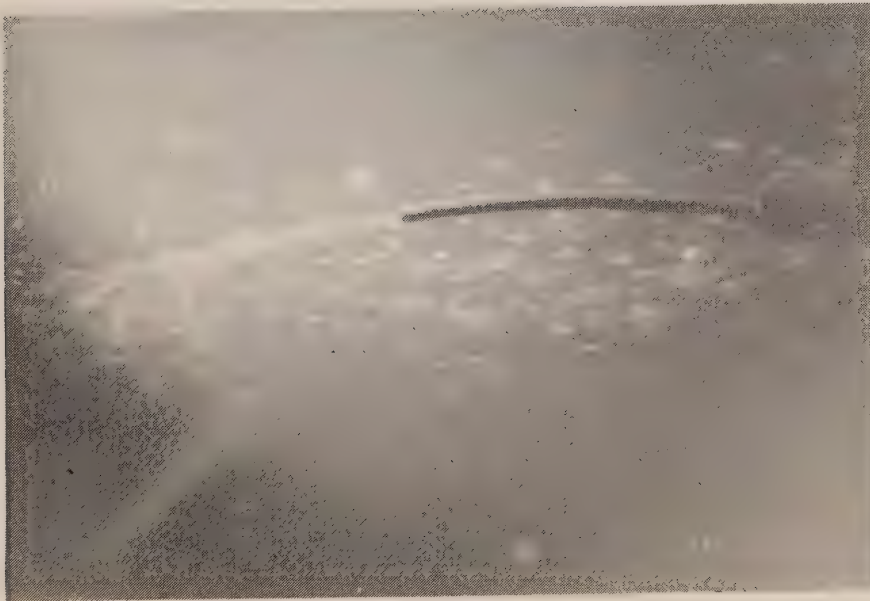


Figure 17. Liquid chlorine drops sinking in seawater at about 90 meters. Yellowish hydrate can be seen forming on some of the drops.



Figure 18. Chlorine in seawater at about 90 meters a short time after injection. Clumps of liquid chlorine and hydrate can be seen in the water.

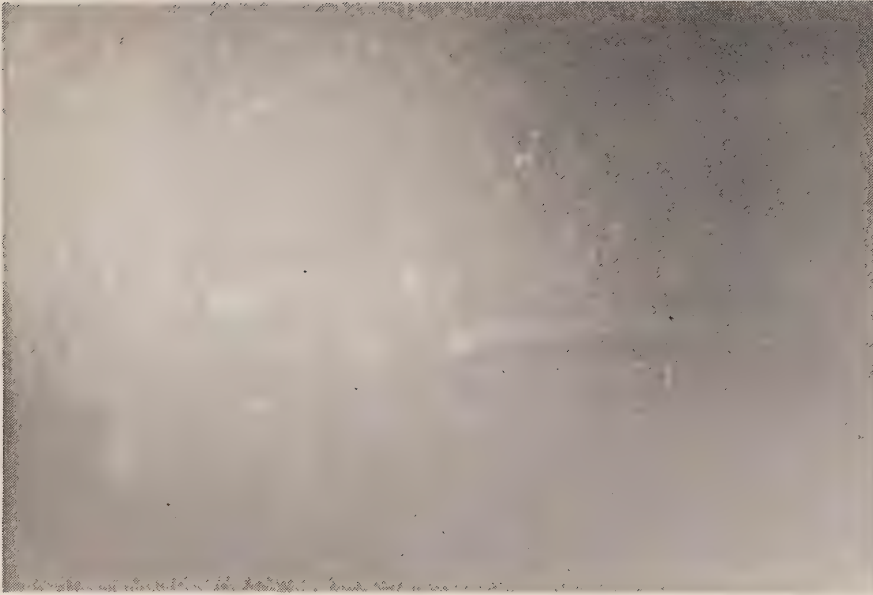


Figure 20. Fine flakes of hydrate generated shortly after chlorine release at 45 meters. Flakes similar to those also seen at 60 meters and 90 meters.

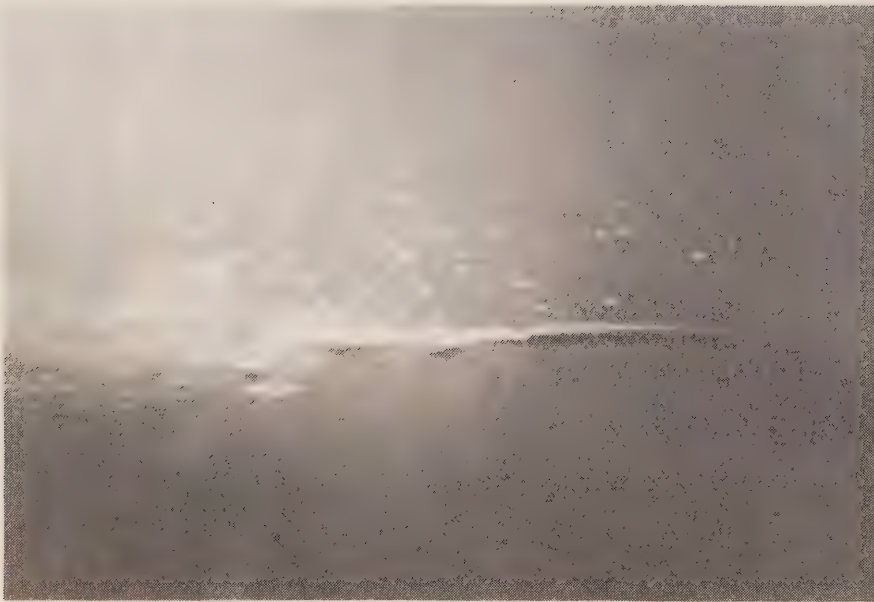


Figure 19. Chlorine plume at 60 meters. Liquid chlorine drops with hydrate attached are visible to the right of the tube above and below the nozzle.





Figure 21. Plume of gaseous chlorine at 25 meters.

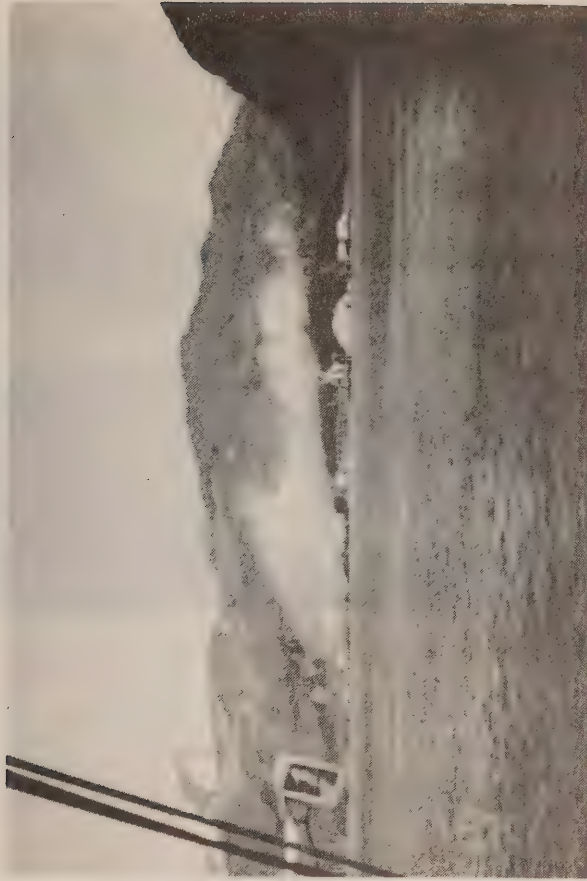


Figure 22. Chlorine "cloud" at Squamish shortly after an accidental discharge from FMC.



Figure 23. Elongated chlorine cloud about half an hour after the release.



Figure 24. Chlorine mist hanging above the waters of Howe Sound about three hours after the release.

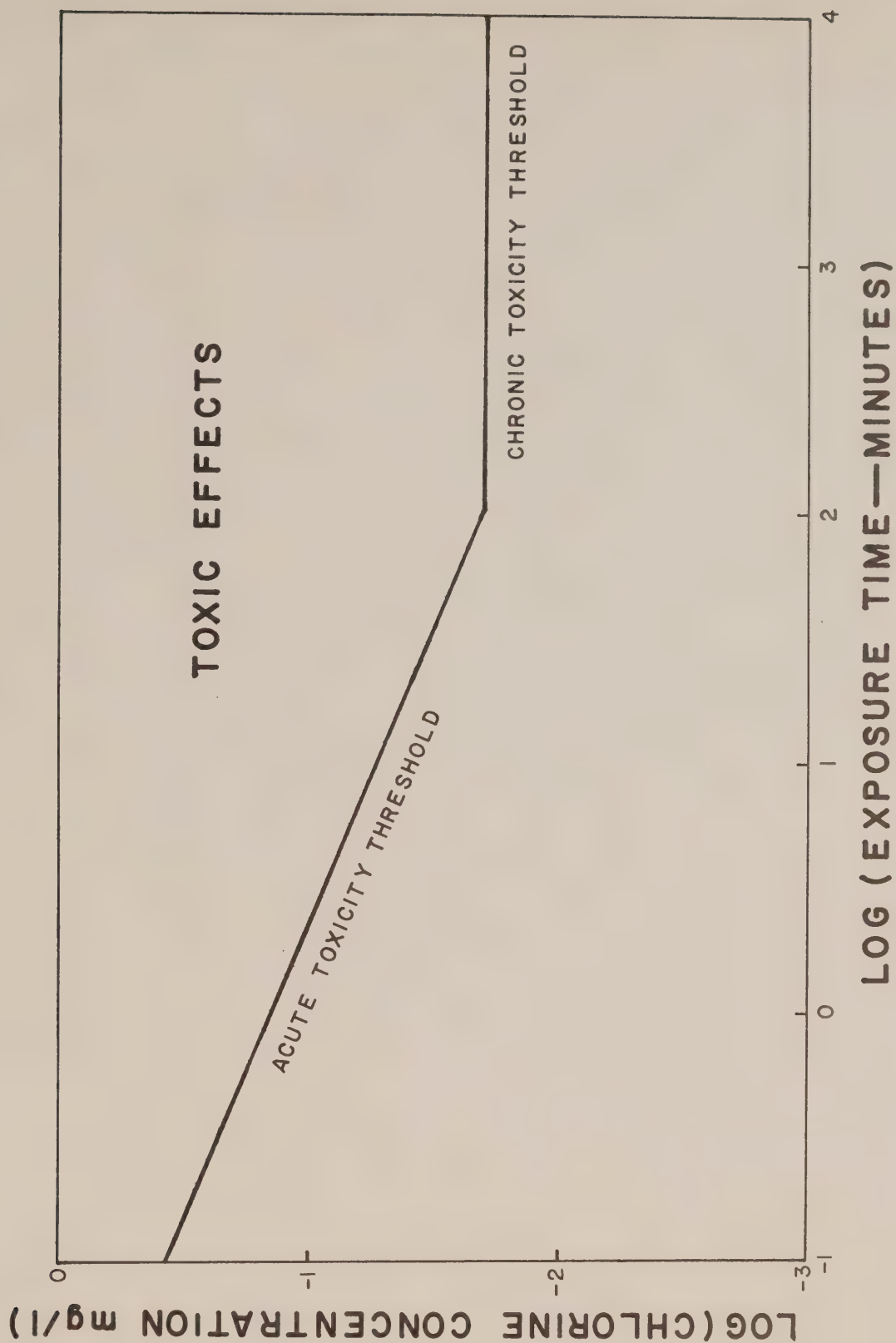


Figure 25. Acute and chronic toxicity thresholds for chlorine in seawater.









CA1 EP 321

-77R07

Pacific Marine Science Report

C-77-7  
university  
Publications

**OCEANOGRAPHIC OBSERVATIONS AT OCEAN STATION P**

**(50° N., 145° W.)**

**Volume 78**

**3 December 1976 – 13 January 1977**

**Seakem Oceanography Ltd.**

**INSTITUTE OF OCEAN SCIENCES, PATRICIA BAY  
Victoria, B.C.**



For additional copies or further information please write to:

Department of Fisheries and The Environment  
Institute of Ocean Sciences, Patricia Bay  
512 - 1230 Government Street  
Victoria, B.C.  
V8W 1Y4



OCEANOGRAPHIC OBSERVATIONS AT OCEAN STATION P (50°N, 145°W)

Volume 78

3 December 1976 - 13 January 1977

by

Seakem Oceanography Ltd.

Institute of Ocean Sciences, Patricia Bay  
Victoria, B.C.

March 1977

This is a manuscript which has received only limited circulation. On citing this report in a bibliography, the title should be followed by the words "UNPUBLISHED MANUSCRIPT" which is in accordance with accepted bibliographic custom.

#### ABSTRACT

Physical, chemical and biological oceanographic observations are made from the weathership at Ocean Weather Station Papa, and between Esquimalt and Station Papa, on a routine continuing basis. Physical oceanography data only are shown, including surface observations and profiles obtained with bottle casts and conductivity-temperature-pressure instruments.





## INTRODUCTION

Canadian operation of Ocean Weather Station P (Latitude  $50^{\circ}00'N$ , Longitude  $145^{\circ}00'W$ ) was inaugurated in December, 1950. The station is occupied primarily to make meteorological observations of the surface and upper air and to provide an air-sea rescue service. The station is manned by two vessels operated by the Marine Services Branch of the Ministry of Transport. They are the CCGS Vancouver and the CCGS Quadra. Each ship remains on station for a period of six weeks, and is then relieved by the alternate ship, thus maintaining a continuous watch.

Bathythermograph observations have been made at Station P since July 1952. A program of more extensive oceanographic observations commenced in August 1956. This was extended in April 1959, by the addition of a series of oceanographic stations along the route to and from Station P and Swiftsure Bank. These stations are known as Line P stations. The number of stations on Line P has been increased twice and now consists of twelve stations (Fig. 1). Bathythermograph observations and surface salinity sample collections, in addition to being made on Line P oceanographic stations, are also made at odd meridians at  $40'$ , i.e.  $139^{\circ}40'W$ ,  $141^{\circ}40'W$ , etc. These stations are known as Line P BT stations. Data observed prior to 1968 has been indexed by Collins et al (1969).

The present record includes hydrographic, continuously sampled STP and surface salinity and temperature data collected from the CCGS Quadra during the period 3 December 1976 to 13 January 1977.

All physical oceanographic data have been stored by the Canadian Oceanographic Data Centre (CODC), 615 Booth Street, Ottawa, Ontario, Canada. Requests for these data should be directed to CODC.

Biological and productivity data are published in the Manuscript Report series of the Fisheries Research Board of Canada (FRB), Pacific Biological Station, Nanaimo, British Columbia, Canada. Requests for these data should be directed to FRB.

Marine geochemical data are for the Ocean Chemistry Group, Ocean and Aquatic Sciences, Environment Canada, 512-1230 Government Street, Victoria, British Columbia, Canada.

PROGRAM OF OBSERVATION FROM CCGS QUADRA, 3 DECEMBER 1976 - 13 JANUARY 1977  
(P-76-9) (CODC Ref. No. 15-76-009)

Oceanographic observations were made by Mr. B. Whitehouse of Seakem Oceanography Ltd., Victoria, B.C.

En route to Station P, Line P Stations 2 to 12 were occupied and an STD profile made to near bottom or 1500 metres. One hydrocast to 1500 m was done at Station 10.

Samples for salinity, nitrate, nutrient, alkalinity and total CO<sub>2</sub> were taken from the seawater loop at all whole and half stations except 12½. Surface bucket salinities were taken at all whole and half stations. Surface bucket temperatures were taken at all whole stations.

Surface tarball tows were made at Stations 2, 4, 6, 8, 10 and 12.

The thermosalinograph, surface temperature recorder and PCO<sub>2</sub> system were run continuously (though the thermosalinograph produced erratic traces).

Mechanical BT's or XBT's were taken at all whole and half stations.

No samples were collected at Station 12½ since the bridge did not inform the oceanographer of the ship's position.

At Station P the oceanographic program was carried out as follows:

I. Physical Oceanography

- 1) Profiles of salinity, temperature and oxygen were obtained from 3 hydrocasts to near bottom (4200 metres); one cast was to 600 m only.
- 2) 6 STD profiles to 1500 metres and 14 to 300 metres were obtained.
- 3) BT's or XBT's were taken every three hours to coincide with meteorological observations, encoded and transmitted according to the ICOSS format.
- 4) Salinity samples were collected daily at 0000 hrs GMT from the seawater loop.

II. Marine Geochemistry

- 1) Nutrient and salinity samples were collected daily at 0000 hrs GMT from the seawater loop. One 24 hour series of nutrient samples was taken each hour from the seawater loop. One profile for nutrients to 500 m and one profile for tritium to 500 m were taken.

- 2) Alkalinity and total CO<sub>2</sub> samples were taken every 2 to 4 days from the seawater loop and in addition 2 profiles to 500 m were taken.
- 3) Air CO<sub>2</sub> samples were taken in quadruplicate at weekly intervals.
- 4) 4 surface tarball tows were completed.
- 5) 3 seawater C-14 samples were extracted from 45 gallons of seawater taken from the seawater loop along with 3 seawater C-13 and 3 air C-13 samples.
- 6) 6 hydrocarbon samples were obtained.
- 7) PCO<sub>2</sub> carboys were filled 10 times while on station.

### III. Biological and Productivity

Samples were obtained as follows:

- 1) 11 - 150 metre vertical plankton hauls.  
     1 - 300 metre vertical plankton haul.  
     2 - 1500 metre vertical plankton hauls.
- 2) 2 profiles to 200 metres for each of plant pigment, nitrate and C<sub>14</sub> productivity were obtained.

En route from Station P, an STD was made at Stations 12 to 1 and one hydrocast was done at Station 6. Nutrient, nitrate, alkalinity and total CO<sub>2</sub> samples were taken from the seawater loop at Stations 12 to 1. Salinity samples were taken at all whole and half stations 12½ to 1. Surface bucket temperatures were taken at all whole stations. Tarball tows were taken at Stations 12, 10, 8, 6, and 2. Mechanical BT's or XBT's were taken at all whole and half stations.

### Observations for Other Agencies

- 1) Marine mammal observations were made by the ship's officers for Mr. I. McAskie, Fisheries Research Board of Canada, Pacific Biological Station, Nanaimo, B.C., Canada.
- 2) Bird observations were made by the ship's officers for Mr. M. Myres, University of Alberta, Calgary, Alberta, Canada and Mr. J. Guiguet, Curator of Birds and Mammals, Provincial Museum, Department of Provincial Secretary and Travel Industry, Victoria, British Columbia, Canada.
- 3) Air CO<sub>2</sub> samples weekly in duplicate for Scripps Institution of Oceanography, La Jolla, California, U.S.A.

Data was processed for publication by Ms. M. Sainsbury of Seakem Oceanography Ltd., Victoria, B.C.



## OBSERVATIONAL PROCEDURES

Observations for salinity, oxygen and temperature from all hydrographic casts, including the surface, were obtained with Niskin water sample bottles equipped with either Richter and Wiese and/or Yoshino Keiki Co. reversing thermometers. Two protected thermometers were used on all bottles and one unprotected thermometer was used on each bottle at depths of 300 m or greater. The accuracy of protected reversing thermometers is believed to be  $\pm 0.02^{\circ}\text{C}$ .

The daily surface water temperatures were measured from a bucket sample using a deck thermometer of  $\pm 0.1^{\circ}\text{C}$  accuracy. The daily surface salinity samples were obtained from the seawater loop. When the seawater loop was not operational these samples were obtained with a bucket, and are indicated with a 'b' in this data record.

Salinity determinations were made aboard ship with either an Autolab Model 601 Mark III inductive salinometer or a Hytech Model 6220 lab salinometer. Accuracy using duplicate determinations is estimated to be  $\pm 0.003^{\circ}/\text{oo}$ .

Depth determinations were made using the "depth difference" method described in the U. S. N. Hydrographic Office Publication No. 607 (1955). Depth estimates have an approximate accuracy of  $\pm 5$  m for depths less than 1000 m, and  $\pm 0.5\%$  of depth for depths greater than 1000 m.

The dissolved oxygen analyses were done in the shipboard laboratory by a modified Winkler method (Carpenter, 1955).

Line P engine intake continuous temperature on both ships were recorded by a Honeywell Electronik 15 Recorder. The temperature probe is at a depth of approximately 3 metres below the sea surface and the instrument accuracy is believed to be  $\pm 0.1^{\circ}\text{C}$ .

Each ship is equipped with a Plessey Model 6600-T thermosalinograph which is used, on Line P, for continuous recording of surface temperatures and salinities from ship's seawater loop. The temperature probe is mounted at the seawater loop intake (approximately 3 metres below the surface) and the salinity probe and recorder are situated in the dry lab. The accuracy of this instrument is believed to be  $\pm 0.1^{\circ}\text{C}$  for temperature and  $\pm 0.1^{\circ}/\text{oo}$  for salinity.

STD profiles were taken with a Plessey Model 9006 STD system.

## COMPUTATIONS

All hydrographic data were processed with the aid of an IBM 370 computer. Reversing thermometer temperature corrections, thermometric depth calculations and accepted depth from the "depth difference" method were computed. Extraneous thermometric depths caused by thermometer malfunctions were automatically edited and replaced. A Calcomp 565 Offline Plotter was used to plot temperature-salinity, and temperature-oxygen diagrams, as well as plots of temperature, salinity, and dissolved oxygen vs  $\log_{10}$  depth. These plots were used to check the data for errors.



Missing hydrographic data were obtained using a weighted parabolas interpolation method (Reiniger and Ross, 1968). These data are indicated with an asterisk in this data record.

Data values which we suspect but which we have included in this data record are indicated with a plus. These data have been removed from punch card and magnetic tape records.

Analog records from the salinity-temperature-pressure instrument have been machine digitized, then replotted using the Calcomp plotter.

Digitization was continued until original and computer plotted traces were coincident. Temperature and salinity values were listed at standard pressures; integrals (depths, geopotential anomaly, and potential energy anomaly) were computed from the entire array of digitized data.

The headings for the data listings are explained as follows:

PRESS	is pressure (decibars)
TEMP	is temperature (degrees Celsius)
SAL	is salinity (parts per thousand)
DEPTH	is reported in metres
SIGMA-T	is specific gravity anomaly
SVA	is specific volume anomaly
THETA	is potential temperature (degrees Celsius)
SVA (DEPTH)	is potential specific volume anomaly
DELTA D	is geopotential anomaly (J/kg)
POT EN	is potential energy in units of $10^8$ ergs/cm <sup>2</sup>
OXY	is the concentration of dissolved oxygen expressed in millilitres per litre
SOUND	is the velocity of sound in m/sec

#### REFERENCES

- Carpenter, J.H., 1965. The Chesapeake Bay Institute technique for the Winkler dissolved oxygen method. *Limnol. and Oceanogr.* 10: 141 - 143.
- Collins, C.A., R.L. Tripe, D.A. Healey and J. Joergensen, 1969. The time distribution of serial oceanographic data from the Ocean Station P programme. *Fish. Res. Bd. Can. Tech. Rept. No.* 106.
- Reiniger, R.F. and C.K. Ross, 1968. A method of interpolation with application to oceanographic data. *Deep Sea Res.* 15: 185 - 193.
- U. S. N. Hydrographic Office, 1955. *Instruction Manual of oceanographic observations*, Publ. No. 607.

LIST OF FIGURES

- Figure 1. Chart showing Line P station positions.
- Figure 2. Composite plot of temperature vs  $\log_{10}$  depth for Line P stations. P-76-9.
- Figure 3. Composite plot of salinity vs  $\log_{10}$  depth for Line P stations. P-76-9.
- Figure 4. Composite plot of temperature vs  $\log_{10}$  depth for Station P. P-76-9.
- Figure 5. Composite plot of salinity vs  $\log_{10}$  depth for Station P. P-76-9.
- Figure 6. Composite plot of oxygen vs  $\log_{10}$  depth for Station P. P-76-9.
- Figure 7. Salinity difference between hydro data and STP. P-76-9.
- Figure 8. Temperature difference between hydro data and STP. P-76-9.

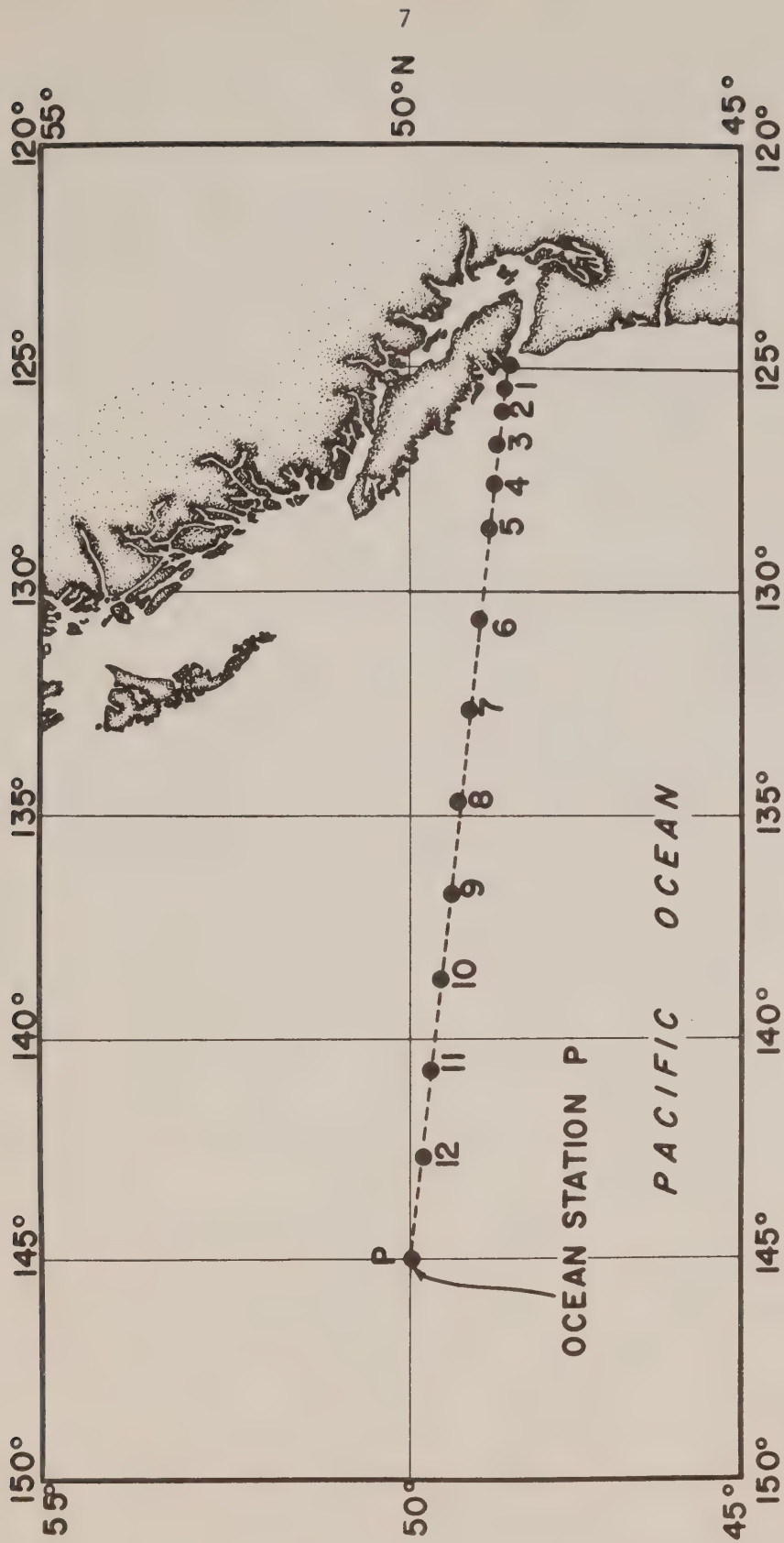


Fig. 1 Chart showing Line P station positions.





Oceanographic Data Obtained on Cruise P-76-9  
(CODC Reference No. 15-76-009)



Results of Hydrographic Observations

(P-76-9)

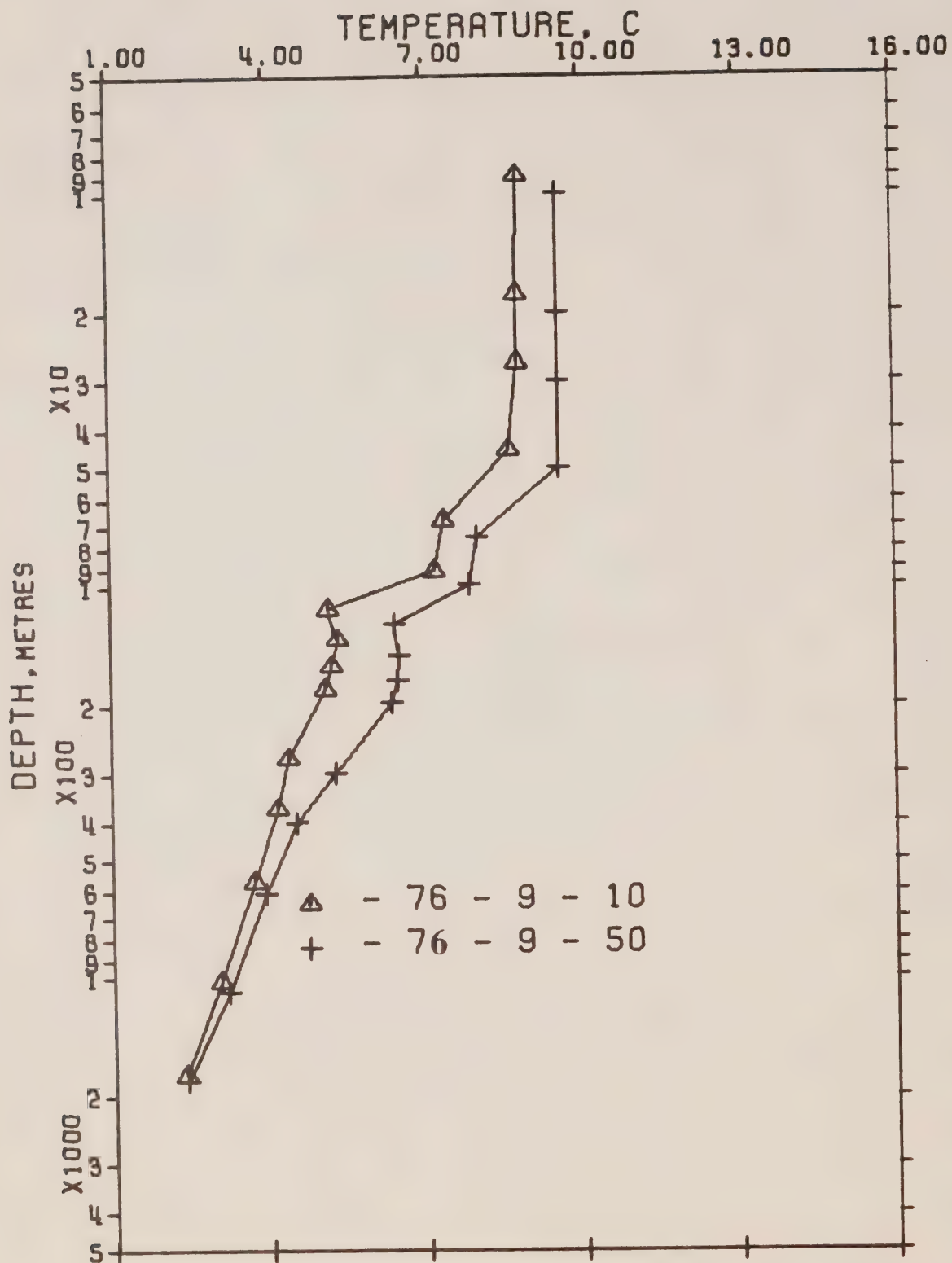


Figure 2. Composite plot of temperature vs  $\log_{10}$  depth for Line P stations. P-76-9.



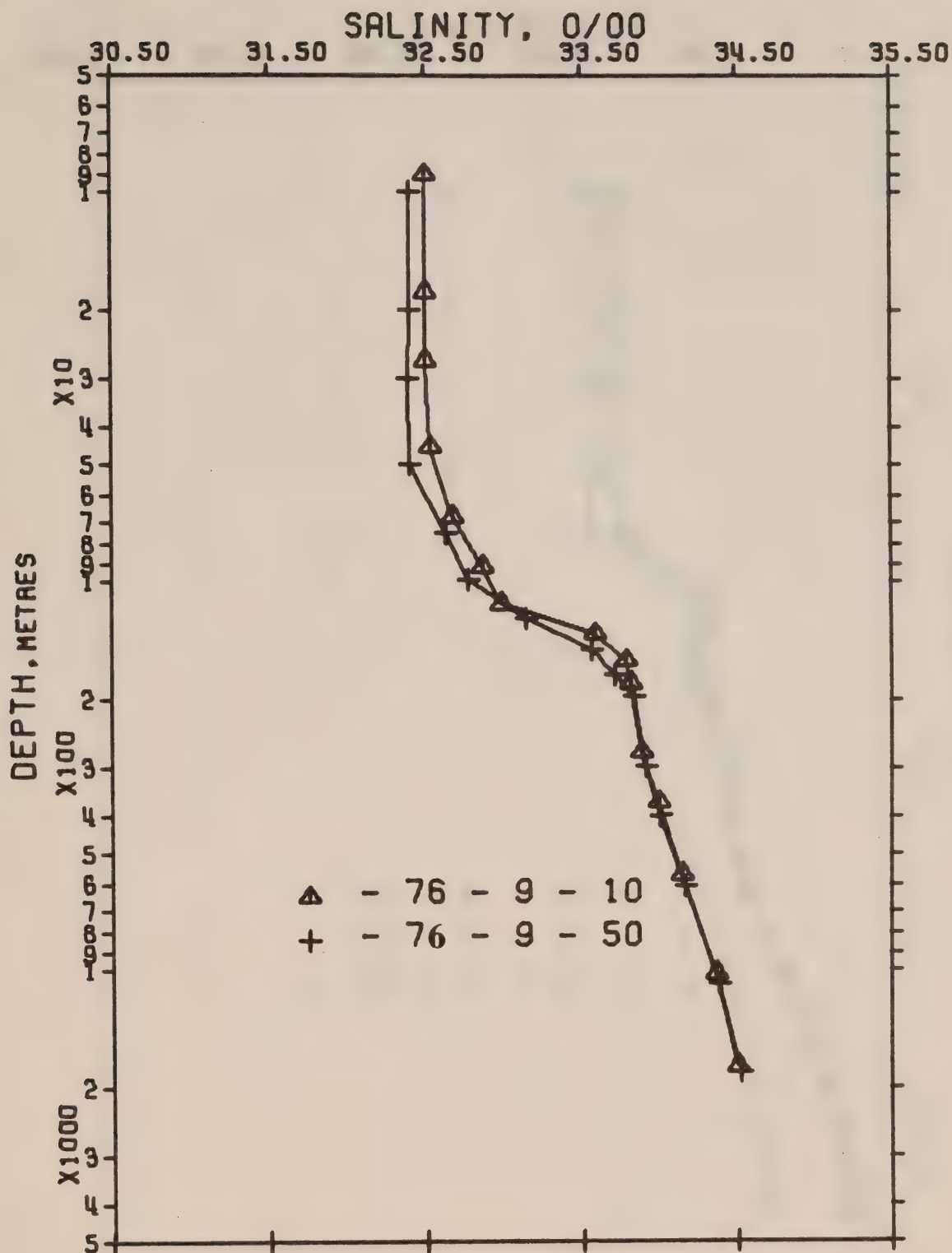


Figure 3. Composite plot of salinity vs  $\log_{10}$  depth for Line P stations. P-76-9.

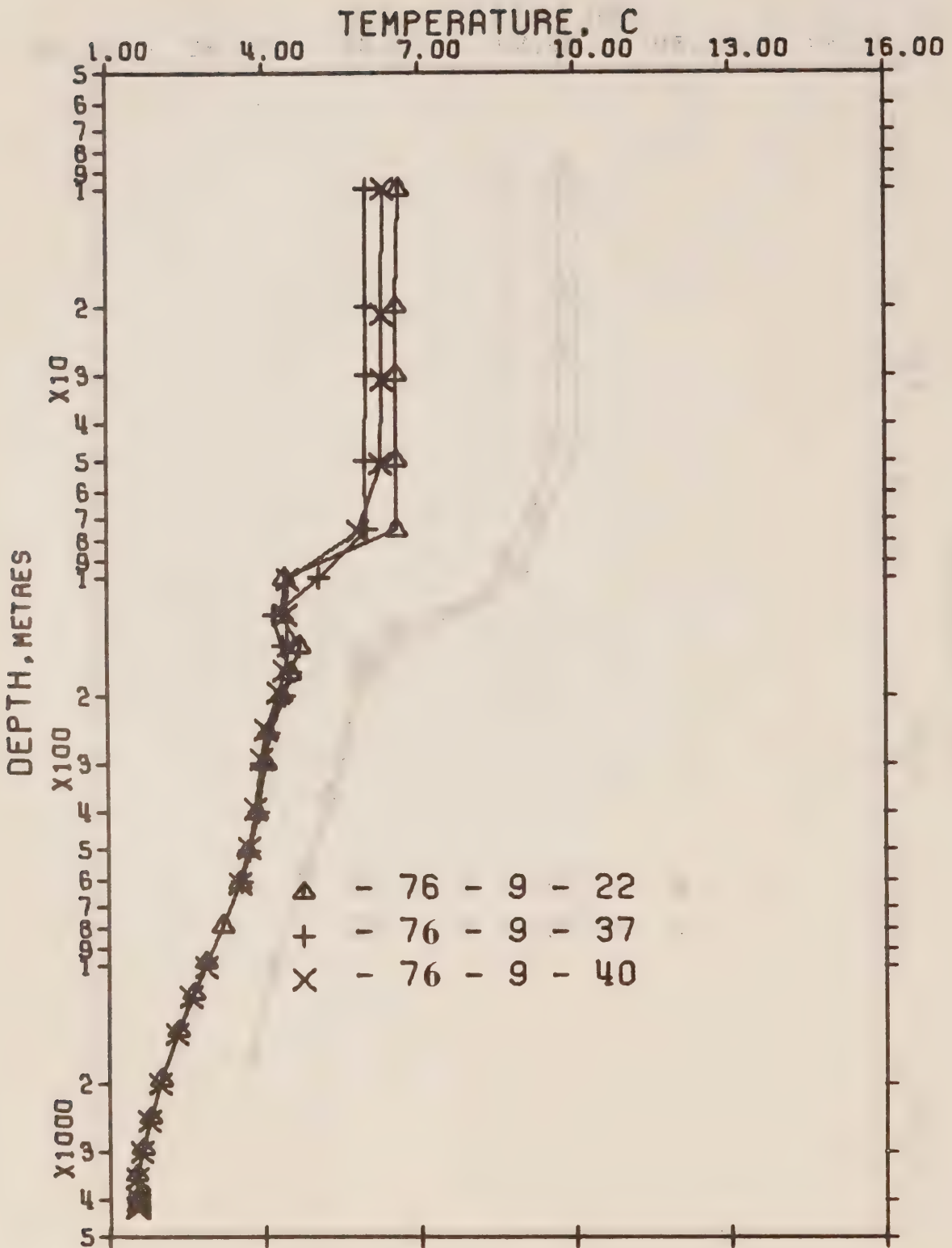


Figure 4. Composite plot of temperature vs  $\log_{10}$  depth for Station P. P-76-9.

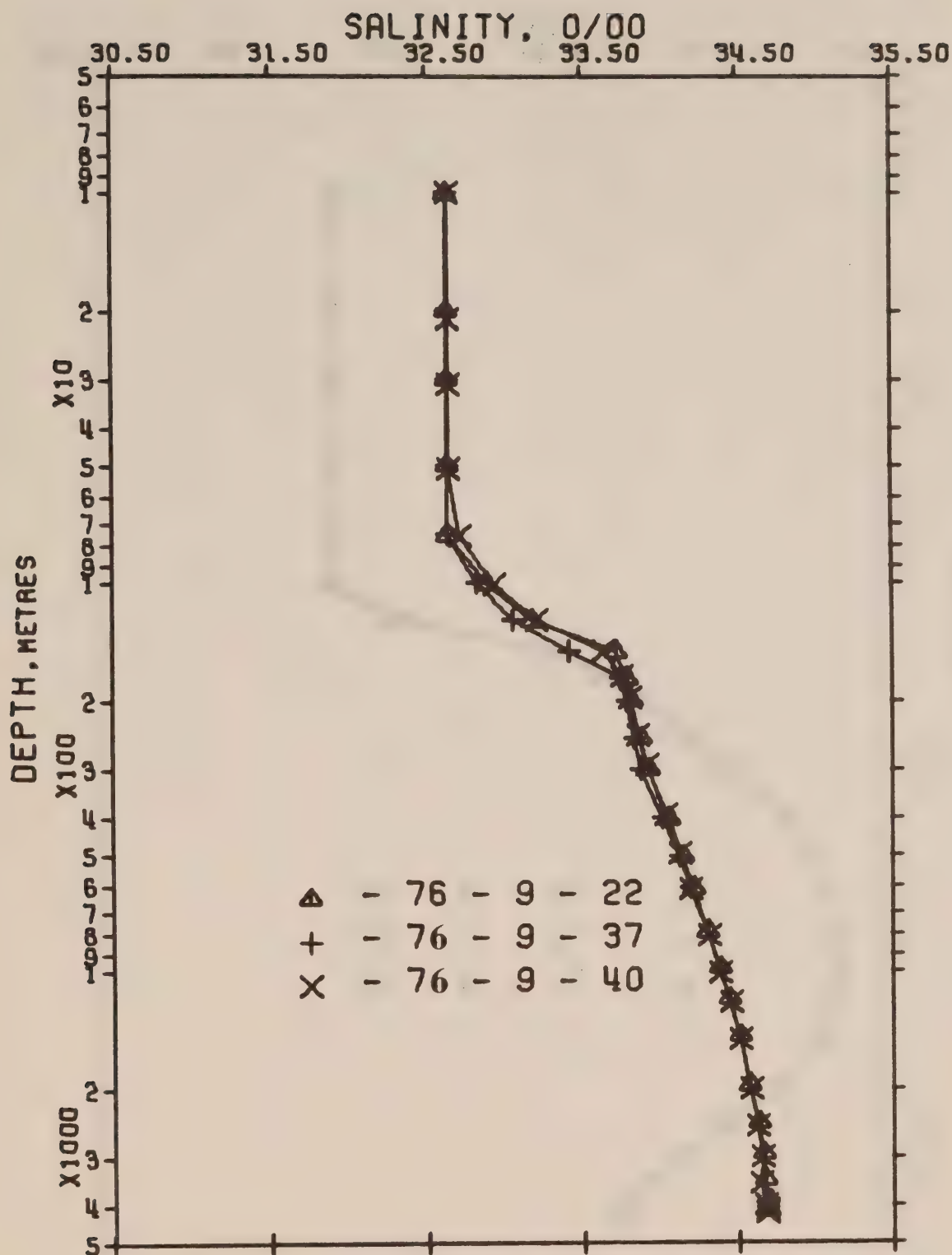


Figure 5. Composite plot of salinity vs  $\log_{10}$  depth for Station P. P-76-9.

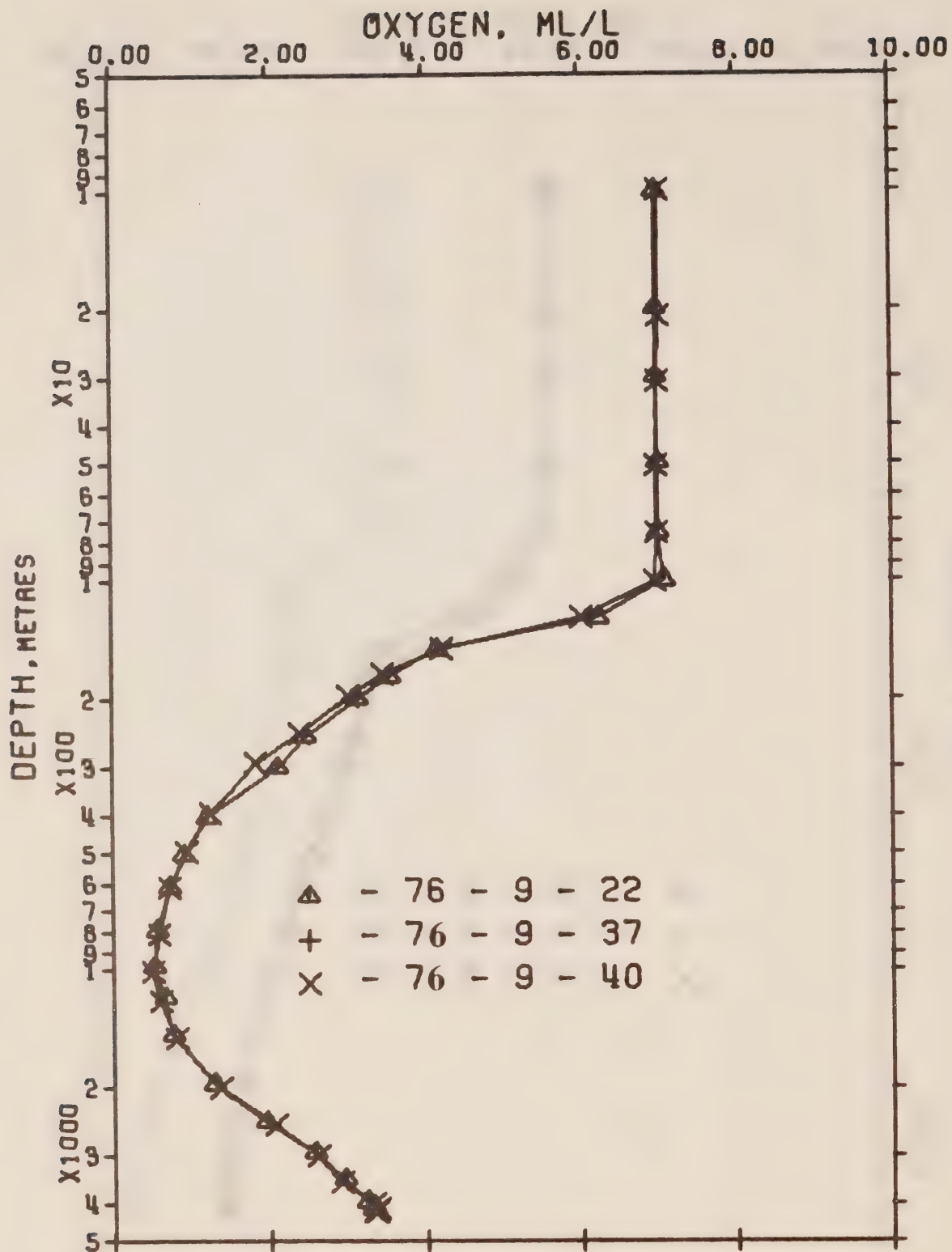
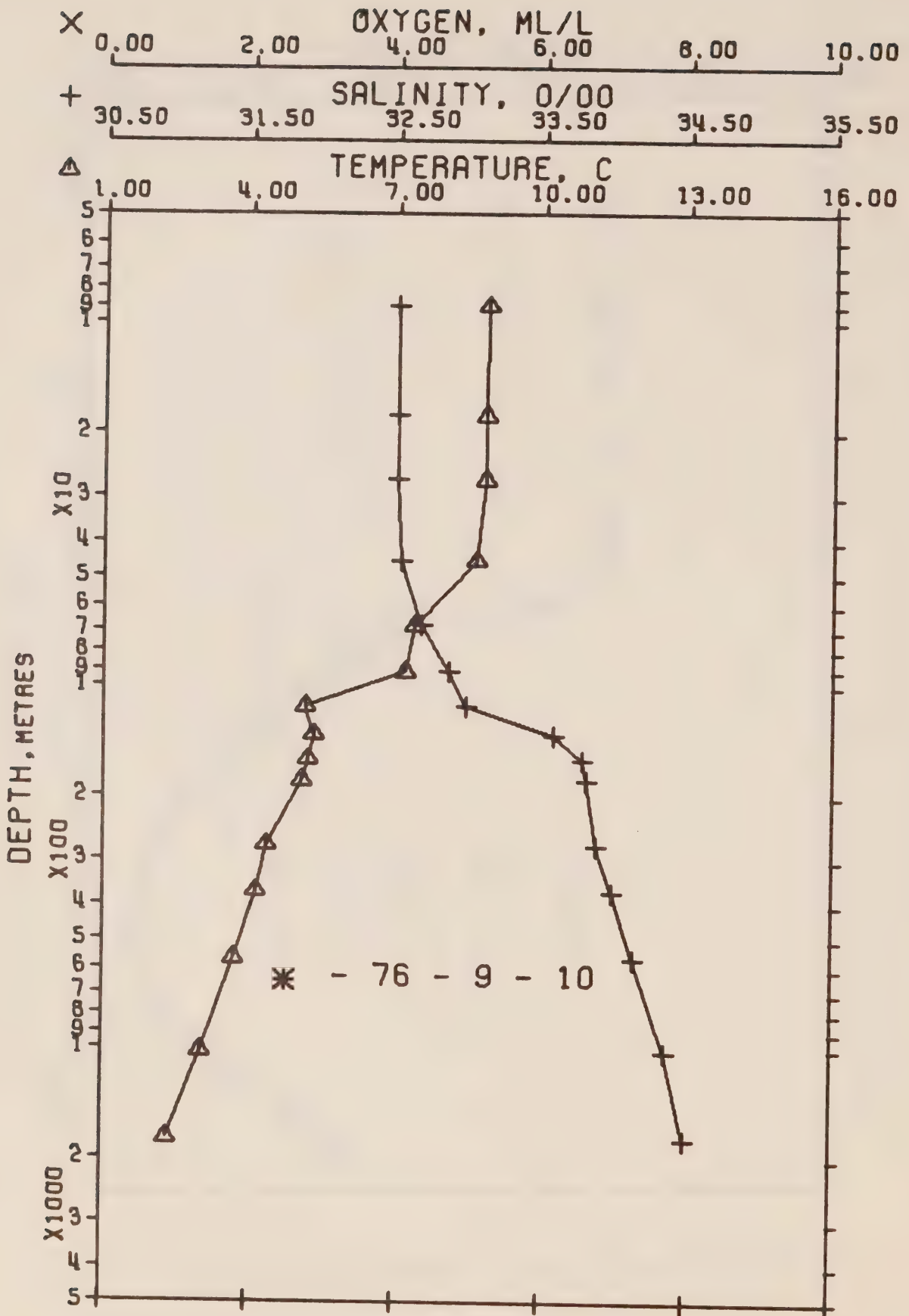


Figure 6. Composite plot of oxygen vs  $\log_{10}$  depth for Station P. P-76-9.







## OFFSHORE OCEANOGRAPHY GROUP

REFERENCE NO. 76- 9- 10

DATE 5/12/76

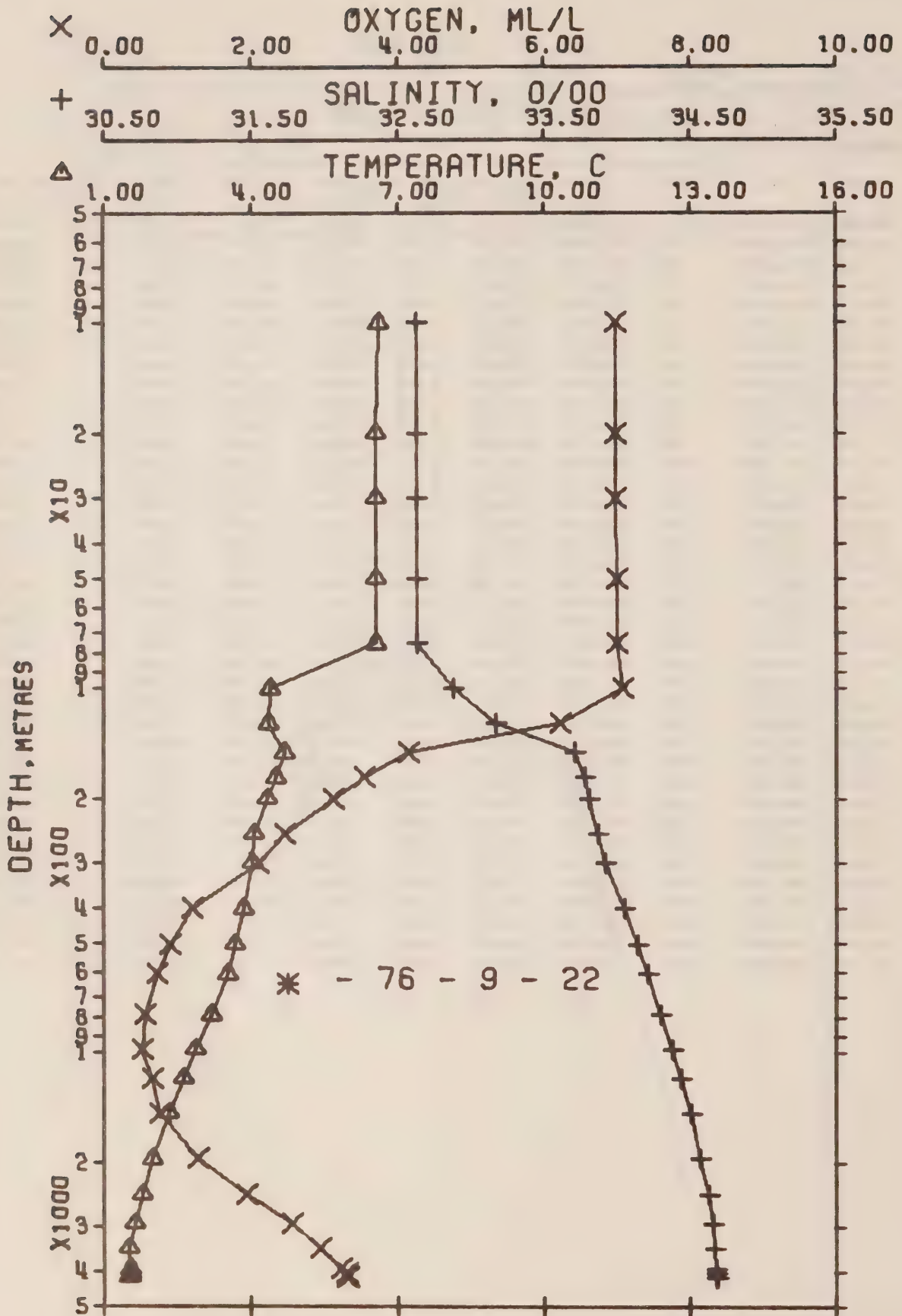
GMT 20.5

POSITION 49-34.0 N, 138-40.0 W

STATION 10

## HYDROGRAPHIC CAST DATA

PRESS	TEMP	SAL	DEPTH	SIGMA T	SVA	THETA	SVA (THETA)	DELTA D	POT. EN	CHY	SOUND
0	8.84	32.504	0	25.215	276.5	8.84	276.3	0.0	0.0		1493.
9	8.82	32.504	9	25.218	276.4	8.82	275.9	0.25	0.01		1493.
10*	8.82	32.504	10	25.218	276.3	8.82	275.9	0.28	0.01		1493.
18	8.81	32.504	18	25.220	276.4	8.81	275.8	0.50	0.05		1493.
20*	8.81	32.504	20	25.220	276.3	8.81	275.7	0.55	0.06		1493.
27	8.80	32.505	27	25.222	276.2	8.80	275.6	0.75	0.10		1493.
30*	8.76	32.509	30	25.231	275.5	8.75	274.7	0.83	0.13		1493.
45	8.61	32.526	45	25.267	272.2	8.61	271.2	1.25	0.29		1493.
50*	8.31	32.560	51	25.339	265.5	8.31	264.4	1.38	0.35		1492.
68	7.37	32.668	68	25.558	244.8	7.36	243.5	1.84	0.63		1479.
75*	7.31	32.729	75	25.614	239.6	7.31	238.3	2.00	0.75		1479.
92	7.19	32.861	91	25.734	228.3	7.18	226.8	2.39	1.08		1478.
100*	6.39	32.908	100	25.877	214.8	6.38	213.3	2.58	1.26		1476.
115	5.15	32.981	114	26.084	194.9	5.14	193.5	2.88	1.59		1471.
125*	5.23	33.273	125	26.305	174.1	5.22	172.5	3.07	1.83		1472.
137	5.32	33.581	136	26.539	152.1	5.31	150.3	3.27	2.08		1473.
150*	5.26	33.697	149	26.638	142.9	5.24	140.9	3.46	2.36		1473.
160	5.21	33.779	159	26.709	136.4	5.20	134.2	3.60	2.59		1473.
175*	5.12	33.799	174	26.735	133.9	5.10	131.7	3.80	2.93		1473.
183	5.07	33.810	182	26.749	132.7	5.06	130.3	3.91	3.13		1473.
200*	4.92	33.825	202	26.778	130.0	4.91	127.5	4.13	3.56		1472.
225*	4.72	33.846	228	26.817	126.5	4.70	123.9	4.45	4.25		1472.
250*	4.54	33.865	252	26.852	123.4	4.52	120.6	4.76	5.01		1472.
276	4.37	33.882	274	26.884	120.5	4.35	117.6	5.08	5.86		1471.
300*	4.31	33.912	301	26.914	117.8	4.29	114.6	5.36	6.70		1472.
371	4.16	33.990	368	26.992	111.0	4.13	107.3	6.17	9.47		1472.
400*	4.08	34.016	403	27.021	108.4	4.05	104.5	6.49	10.72		1472.
500*	3.83	34.092	505	27.106	100.9	3.80	96.3	7.54	15.51		1473.
570	3.69	34.137	565	27.156	96.6	3.65	91.5	8.23	19.27		1474.
600*	3.63	34.157	605	27.177	94.8	3.59	89.5	8.52	20.99		1474.
700*	3.46	34.215	723	27.240	89.4	3.41	83.5	9.44	27.09		1475.
800*	3.31	34.265	826	27.295	84.7	3.26	78.2	10.31	33.74		1476.
900*	3.18	34.310	916	27.343	80.7	3.12	73.6	11.13	40.90		1477.
1000*	3.06	34.350	997	27.385	77.1	2.99	69.6	11.92	48.54		1478.
1030	3.03	34.361	1020	27.397	76.0	2.96	68.5	12.15	50.91		1479.
1200*	2.85	34.399	1227	27.444	72.2	2.76	64.0	13.41	65.19		1481.
1500*	2.58	34.454	1530	27.512	66.8	2.47	57.4	15.49	93.81		1485.
1793	2.36	34.498	1772	27.565	62.4	2.23	52.2	17.33	125.48		1489.





## OFFSHORE OCEANOGRAPHY GROUP

REFERENCE NO. 76- 9- 22

DATE 16/12/76

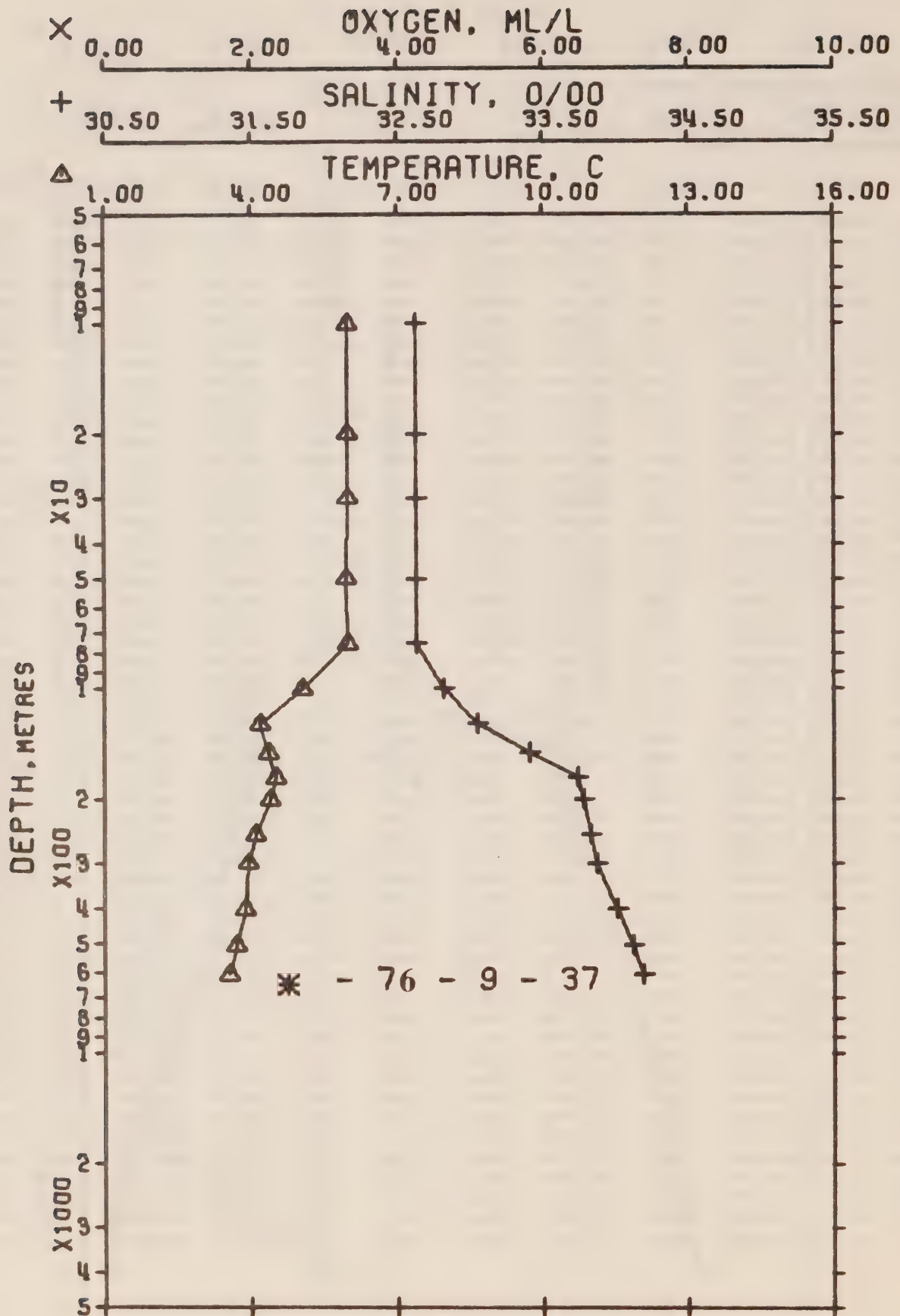
GMT 18.3

POSITION 50- 0.0 N. 145- 0.0 W

STATION P

## HYDROGRAPHIC CAST DATA

PRESS	TEMP	SAL	DEPTH	SIGMA T	SVA	THETA	SVA (THETA)	DELTA D	POT. EN	OXY	SOUND
0	6.55	32.634	0	25.641	236.0	6.55	235.7	0.0	0.0	6.96	1474.
10	6.60	32.634	10	25.635	236.7	6.60	236.4	0.24	0.01	6.97	1475.
20	6.56	32.634	20	25.640	236.3	6.56	235.8	0.48	0.05	6.98	1475.
30	6.56	32.634	30	25.640	236.4	6.56	235.8	0.71	0.11	6.98	1475.
50	6.54	32.634	50	25.642	236.5	6.54	235.6	1.19	0.31	6.99	1475.
75	6.55	32.634	75	25.641	236.9	6.54	235.6	1.79	0.69	7.00	1475.
100*	4.44	32.878	99	26.081	195.0	4.43	193.9	2.33	1.17	7.08	1467.
101	4.39	32.884	100	26.090	194.1	4.38	193.0	2.34	1.18	7.08	1467.
125*	4.37	33.166	124	26.316	172.8	4.36	171.5	2.78	1.69	6.24	1463.
126	4.37	33.175	125	26.323	172.2	4.36	170.9	2.79	1.71	6.22	1463.
150*	4.68	33.688	149	26.697	137.2	4.67	135.4	3.17	2.24	4.21	1470.
151	4.69	33.708	150	26.711	135.8	4.68	133.9	3.19	2.26	4.13	1470.
175*	4.51	33.781	174	26.788	128.7	4.50	126.6	3.50	2.78	3.56	1470.
176	4.50	33.784	175	26.792	128.3	4.49	126.3	3.51	2.80	3.53	1470.
200*	4.33	33.810	199	26.831	124.8	4.32	122.6	3.81	3.38	3.15	1470.
201	4.32	33.811	200	26.833	124.6	4.31	122.5	3.83	3.42	3.13	1470.
225*	4.20	33.838	225	26.867	121.5	4.18	119.1	4.12	4.05	2.80	1470.
250*	4.08	33.864	248	26.900	118.6	4.06	116.0	4.42	4.77	2.48	1470.
252	4.07	33.866	250	26.902	118.3	4.05	115.8	4.44	4.83	2.46	1470.
300*	4.02	33.922	298	26.952	114.1	4.00	111.2	5.00	6.40	2.11	1470.
302	4.02	33.924	300	26.954	113.9	4.00	110.9	5.03	6.48	2.10	1470.
400*	3.87	34.044	397	27.065	104.1	3.84	100.3	6.09	10.30	1.23	1472.
404	3.86	34.049	401	27.069	103.7	3.83	99.8	6.14	10.48	1.19	1472.
500*	3.69	34.133	497	27.153	96.4	3.66	91.9	7.09	14.87	0.93	1473.
507	3.68	34.139	503	27.159	95.9	3.64	91.4	7.16	15.23	0.91	1473.
600*	3.53	34.206	596	27.227	90.0	3.49	84.8	8.02	20.10	0.75	1474.
613	3.51	34.215	608	27.236	89.3	3.47	83.9	8.14	20.83	0.73	1474.
700*	3.35	34.260	699	27.287	84.8	3.30	79.1	8.90	25.88	0.64	1475.
793	3.19	34.302	786	27.335	80.6	3.14	74.5	9.67	31.75	0.56	1475.
800*	3.18	34.305	793	27.339	80.3	3.12	74.1	9.72	32.19	0.56	1476.
900*	3.01	34.348	897	27.389	76.0	2.94	69.3	10.50	38.95	0.54	1476.
989	2.87	34.383	979	27.429	72.5	2.80	65.5	11.16	45.28	0.53	1477.
1000*	2.85	34.387	991	27.434	72.0	2.79	65.1	11.24	46.11	0.53	1478.
1185	2.61	34.440	1173	27.498	66.5	2.53	58.9	12.52	60.32	0.65	1480.
1200*	2.59	34.444	1189	27.502	66.2	2.51	58.5	12.62	61.52	0.66	1480.
1482	2.33	34.506	1466	27.574	60.0	2.23	51.5	14.39	85.75	0.75	1483.
1500*	2.32	34.509	1486	27.577	59.8	2.21	51.2	14.50	87.37	0.78	1484.
1981	2.00	34.575	1957	27.656	53.3	1.86	43.6	17.20	135.33	1.28	1490.
2000*	1.99	34.577	1978	27.658	53.1	1.85	43.3	17.30	137.38	1.31	1491.
2486	1.77	34.626	2453	27.714	48.6	1.59	37.8	19.77	193.66	1.94	1493.
2500*	1.77	34.627	2468	27.715	48.5	1.59	37.7	19.83	195.37	1.96	1498.
2994	1.64	34.657	2951	27.749	46.3	1.42	34.3	22.21	262.00	2.56	1506.
3000*	1.64	34.657	2957	27.749	46.2	1.42	34.2	22.24	262.79	2.57	1506.
3500*	1.52	34.668	3446	27.766	45.2	1.25	32.3	24.48	337.07	2.93	1514.
3505	1.52	34.668	3450	27.767	45.2	1.25	32.3	24.50	337.84	2.93	1514.
4000*	1.54	34.682	3934	27.776	45.9	1.22	31.0	26.75	423.80	3.21	1523.
4017	1.54	34.682	3950	27.776	45.9	1.21	31.0	26.83	427.05	3.22	1523.
4100*	1.53	34.683	4031	27.778	46.0	1.20	30.8	27.21	442.78	3.28	1525.
4120	1.53	34.683	4050	27.778	45.9	1.19	30.7	27.30	446.63	3.29	1525.
4200*	1.52	34.685	4128	27.780	45.9	1.13	30.6	27.66	462.20	3.30	1526.
4212	1.52	34.685	4140	27.780	45.9	1.17	30.5	27.72	464.64	3.30	1526.
4223	1.53	34.686	4150	27.780	46.0	1.18	30.5	27.77	466.67	3.31	1527.



## OFFSHORE OCEANOGRAPHY GROUP

REFERENCE NO. 76- 9- 37

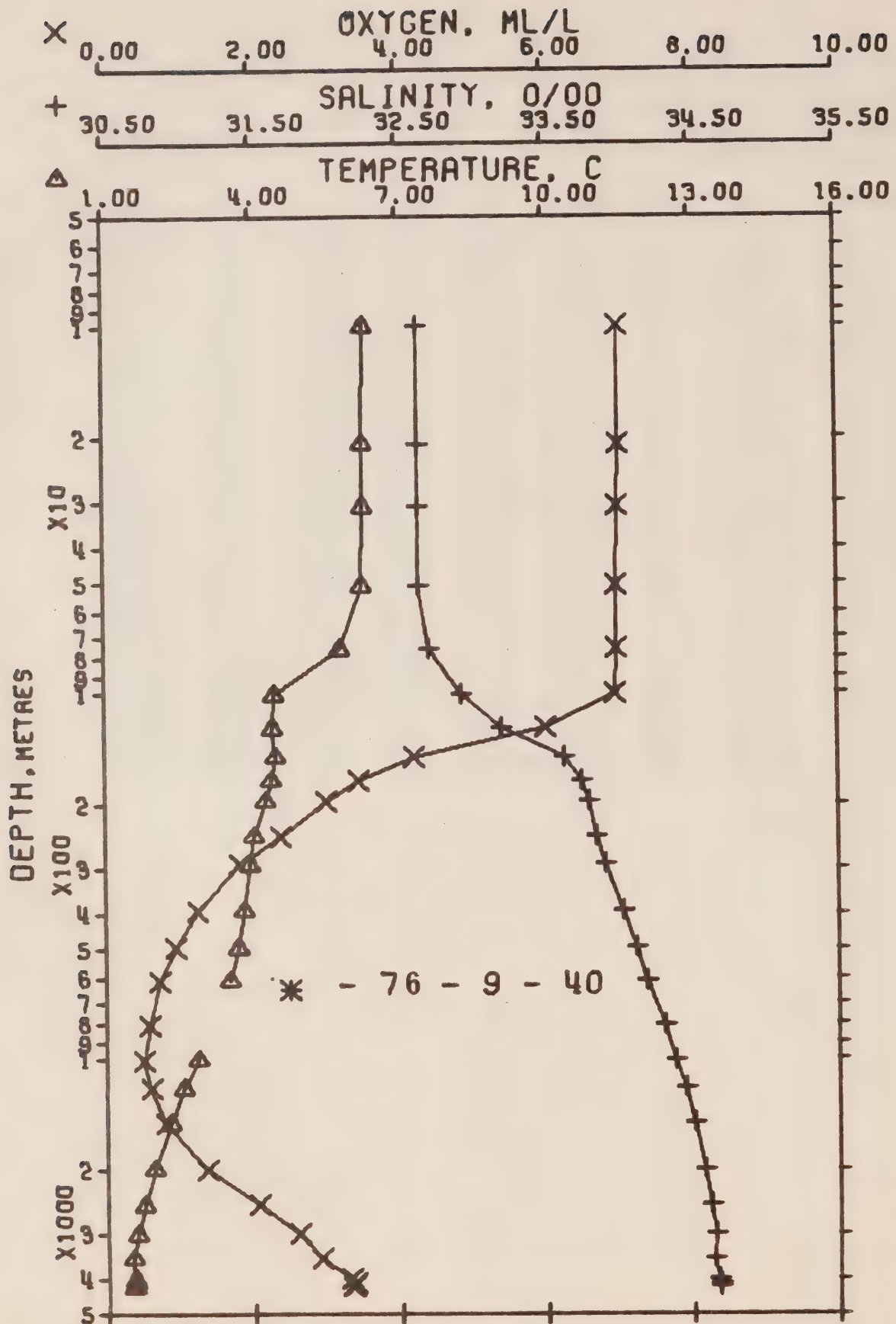
DATE 2/ 1/77 GMT 18.1

POSITION 50- 0.0 N, 145- 0.0 W

STATION P

## HYDROGRAPHIC CAST DATA

PRESS	TEMP	SAL	DEPTH	SIGMA T	SVA	THETA	SVA (THETA)	DELTA D	POT. EN	OXY	SOUND
0	5.99	32.627	0	25.706	229.8	5.99	229.6	0.0	0.0		1472.
10	5.99	32.628	10	25.707	229.8	5.99	229.5	0.23	0.01		1472.
20	5.98	32.626	20	25.706	229.9	5.98	229.5	0.46	0.05		1472.
30	5.98	32.628	30	25.708	229.9	5.98	229.4	0.69	0.11		1472.
50	5.95	32.629	50	25.712	229.7	5.95	228.9	1.16	0.30		1473.
75	5.97	32.628	75	25.709	230.4	5.96	229.2	1.74	0.67		1473.
100*	5.07	32.819	99	25.965	206.1	5.06	204.8	2.28	1.15		1470.
101	5.05	32.823	100	25.971	205.5	5.04	204.3	2.29	1.16		1470.
125*	4.22	33.045	124	26.236	180.4	4.21	179.1	2.76	1.71		1457.
126	4.19	33.052	125	26.244	179.6	4.18	178.3	2.79	1.73		1457.
150*	4.35	33.393	149	26.498	155.9	4.34	154.3	3.18	2.29		1469.
151	4.36	33.406	150	26.507	155.0	4.35	153.3	3.20	2.32		1469.
175*	4.50	33.728	174	26.747	132.5	4.49	130.6	3.54	2.89		1470.
176	4.51	33.743	175	26.759	131.5	4.50	129.5	3.56	2.92		1470.
200*	4.39	33.777	199	26.798	127.9	4.38	125.7	3.86	3.50		1470.
202	4.38	33.780	201	26.802	127.6	4.37	125.4	3.89	3.57		1470.
225*	4.25	33.804	225	26.835	124.6	4.23	122.3	4.18	4.19		1470.
250*	4.11	33.827	248	26.867	121.7	4.10	119.1	4.48	4.93		1470.
253	4.10	33.830	251	26.871	121.3	4.08	118.8	4.52	5.02		1470.
300*	3.96	33.869	298	26.916	117.4	3.94	114.5	5.08	6.60		1470.
303	3.95	33.871	301	26.919	117.1	3.93	114.2	5.12	6.72		1470.
400*	3.87	34.004	397	27.032	107.2	3.85	103.4	6.20	10.61		1472.
405	3.87	34.010	402	27.037	106.7	3.84	102.9	6.26	10.84		1472.
500*	3.72	34.114	497	27.135	98.2	3.69	93.6	7.23	15.32		1473.
509	3.71	34.123	505	27.143	97.4	3.67	92.8	7.32	15.78		1473.
600*	3.56	34.186	596	27.208	91.9	3.52	86.7	8.18	20.62		1474.
614	3.54	34.195	609	27.217	91.0	3.50	85.7	8.31	21.43		1474.





## OFFSHORE OCEANOGRAPHY GROUP

REFERENCE NO. 76- 9- 40

DATE 7/ 1/77

GMT 18.5

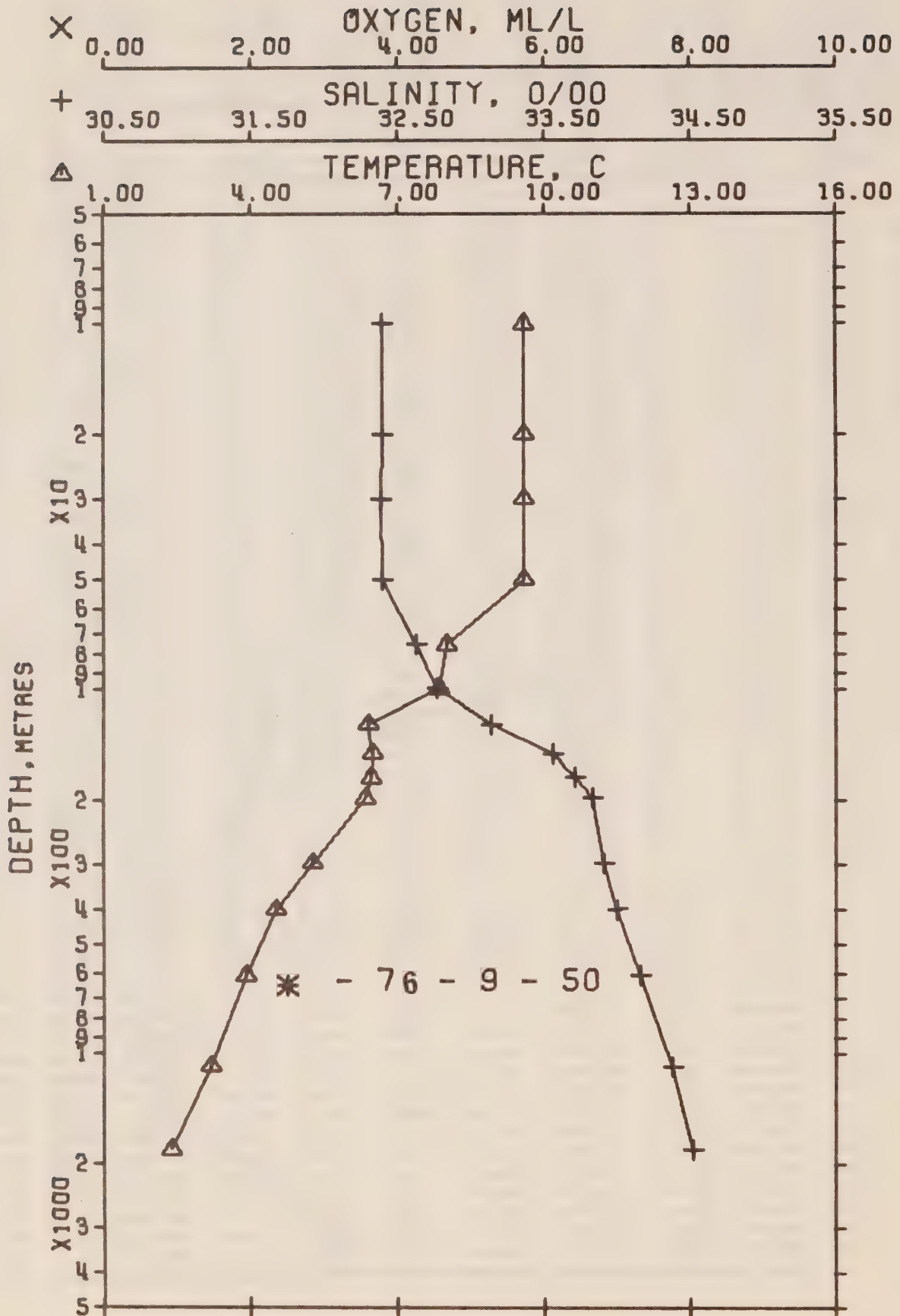
POSITION 50- 0.0 N, 145- 0.0 W

STATION

P

## HYDROGRAPHIC CAST DATA

PRESS	TEMP	SAL	DEPTH	SIGMA T	SVA	THETA	SVA (THETA)	DELTA D	POT. EN	OXY	SOUND
0	6.29	32.637	0	25.676	232.6	6.29	232.4	0.0	0.0	7.02	1473.
10	6.30	32.638	10	25.676	232.7	6.30	232.4	0.23	0.01	7.01	1473.
20*	6.29	32.637	20	25.676	232.8	6.29	232.4	0.47	0.05	7.01	1473.
21	6.29	32.637	21	25.676	232.9	6.29	232.4	0.49	0.05	7.01	1473.
30*	6.27	32.641	30	25.682	232.4	6.27	231.8	0.70	0.11	7.00	1474.
31	6.27	32.641	31	25.682	232.4	6.27	231.7	0.73	0.12	7.00	1474.
50*	6.25	32.645	50	25.687	232.1	6.25	231.3	1.16	0.30	6.98	1474.
51	6.25	32.645	51	25.688	232.1	6.25	231.2	1.19	0.31	6.98	1474.
75*	5.82	32.711	75	25.792	222.4	5.82	221.3	1.73	0.66	6.97	1473.
76	5.80	32.714	76	25.798	221.9	5.79	220.8	1.77	0.68	6.97	1472.
100*	4.54	32.914	100	26.098	193.3	4.53	192.2	2.26	1.13	6.96	1463.
102	4.46	32.926	101	26.116	191.7	4.45	190.5	2.29	1.16	6.95	1463.
125*	4.43	33.195	124	26.333	171.3	4.42	170.0	2.71	1.05	6.02	1463.
126	4.43	33.204	125	26.340	170.6	4.42	169.2	2.73	1.67	5.99	1463.
150	4.49	33.632	149	26.673	139.3	4.48	137.7	3.10	2.19	4.20	1470.
174	4.38	33.753	173	26.780	129.3	4.37	127.4	3.42	2.72	3.44	1470.
175*	4.38	33.755	174	26.782	129.2	4.36	127.2	3.43	2.74	3.42	1470.
198	4.27	33.798	197	26.828	125.1	4.26	122.9	3.73	3.31	2.39	1470.
200*	4.26	33.800	199	26.830	124.8	4.25	122.7	3.75	3.35	2.97	1470.
225*	4.14	33.826	225	26.863	121.8	4.12	119.6	4.06	4.01	2.04	1470.
248	4.04	33.847	246	26.890	119.4	4.02	116.9	4.33	4.68	2.38	1470.
250*	4.04	33.850	248	26.893	119.2	4.02	116.7	4.36	4.74	2.35	1470.
296	3.94	33.908	294	26.949	114.2	3.92	111.3	4.90	6.24	1.32	1470.
300*	3.94	33.913	298	26.954	113.7	3.91	110.9	4.94	6.37	1.80	1470.
396	3.83	34.030	393	27.057	104.7	3.80	101.0	5.99	10.09	1.25	1471.
400*	3.83	34.034	397	27.061	104.4	3.80	100.8	6.03	10.25	1.24	1471.
500*	3.71	34.118	496	27.139	97.7	3.68	93.2	7.04	14.88	0.95	1473.
501	3.71	34.119	497	27.140	97.6	3.67	93.2	7.05	14.94	0.94	1473.
600*	3.55	34.186	596	27.208	91.7	3.51	86.6	7.98	20.18	0.75	1474.
615	3.53	34.195	610	27.218	90.9	3.49	85.7	8.12	21.05	0.72	1474.
700*	3.35	34.246	701	27.275	85.9	3.31	80.1	8.87	26.07	0.66	1475.
800*	3.17	34.299	794	27.335	80.7	3.12	74.5	9.70	32.43	0.60	1475.
814	3.15*	34.306	807	27.343	80.1	3.09	73.7	9.82	33.39	0.59	1476.
900*	3.01	34.340	897	27.382	76.6	2.95	69.9	10.49	39.24	0.55	1477.
1000*	2.87	34.377	992	27.424	73.0	2.80	66.0	11.24	46.47	0.51	1478.
1015	2.85	34.382	1005	27.430	72.5	2.78	65.3	11.35	47.58	0.51	1478.
1200*	2.59	34.441	1189	27.500	66.3	2.51	58.6	12.63	62.04	0.59	1480.
1216	2.57	34.446	1204	27.506	65.8	2.49	58.1	12.74	63.38	0.60	1480.
1500*	2.31	34.507	1485	27.577	59.8	2.21	51.2	14.51	87.98	0.79	1484.
1520	2.29	34.511	1503	27.581	59.4	2.19	50.9	14.63	89.79	0.80	1484.
2000*	1.97	34.576	1979	27.660	52.9	1.83	43.2	17.30	137.69	1.33	1491.
2030	1.95	34.580	2005	27.664	52.5	1.81	42.8	17.46	140.93	1.36	1491.
2500*	1.76	34.621	2471	27.711	48.8	1.58	38.1	19.83	195.70	2.00	1498.
2543	1.74	34.624	2509	27.715	48.5	1.56	37.7	20.04	201.11	2.06	1499.
3000*	1.62	34.646	2961	27.741	46.9	1.40	35.0	22.21	262.44	2.55	1506.
3058	1.61	34.648	3013	27.744	46.7	1.38	34.7	22.48	270.78	2.61	1507.
3500*	1.52	34.643	3450	27.746	47.0	1.25	34.2	24.54	339.72	2.86	1514.
3571	1.51	34.642	3515	27.747	47.1	1.23	34.2	24.88	351.82	2.90	1515.
4000*	1.54	34.669	3937	27.766	46.7	1.21	31.9	26.89	429.43	3.23	1523.
4082	1.54	34.674	4013	27.770	46.7	1.21	31.6	27.27	445.19	3.29	1524.
4100*	1.54	34.674	4031	27.770	46.7	1.20	31.5	27.35	448.70	3.31	1525.
4184	1.54	34.676	4112	27.772	46.8	1.20	31.3	27.75	465.20	3.36	1525.
4200*	1.54	34.676	4128	27.772	46.7	1.19	31.3	27.82	468.48	3.35	1526.
4275	1.52	34.677	4201	27.774	46.6	1.17	31.0	28.17	483.50	3.31	1527.
4284	1.53	34.676	4210	27.772	46.9	1.17	31.2	28.21	485.38	3.33	1528.



## OFFSHORE OCEANOGRAPHY GROUP

REFERENCE NO. 76- 9- 50

DATE 11/ 1/77

GMT 21.8

POSITION 49- 2.0 N, 130-40.0 W

STATION 6

## HYDROGRAPHIC CAST DATA

PRESS	TEMP	SAL	DEPTH	SIGMA T	SVA	THETA	SVA (THETA)	DELTA D	POT. EN	DOXY	SOUND
0	9.57	32.395	0	25.015	295.6	9.57	295.3	0.0	0.0		1485.
10	9.59	32.397	10	25.013	295.8	9.59	295.4	0.30	0.02		1486.
20	9.58	32.396	20	25.014	296.0	9.58	295.3	0.59	0.06		1486.
30	9.57	32.394	30	25.014	296.1	9.57	295.3	0.89	0.14		1486.
50	9.58	32.397	50	25.015	296.5	9.57	295.3	1.49	0.38		1486.
75	7.99	32.635	75	25.444	255.8	7.98	254.3	2.19	0.83		1481.
100	7.84	32.772	99	25.573	243.9	7.83	242.0	2.79	1.37		1481.
125	6.40	33.143	124	26.061	197.7	6.39	195.7	3.35	2.00		1476.
150	6.49	33.558	149	26.376	168.1	6.49	165.7	3.81	2.64		1478.
175	6.45	33.711	174	26.502	156.5	6.43	153.8	4.21	3.32		1473.
199	6.33	33.827	198	26.609	146.7	6.31	143.6	4.58	4.01		1478.
200*	6.32	33.828	199	26.610	146.5	6.30	143.4	4.59	4.03		1478.
225*	6.01	33.853	228	26.670	141.1	5.99	137.8	4.95	4.81		1477.
250*	5.73	33.875	253	26.722	136.3	5.71	132.9	5.29	5.65		1477.
300	5.25	33.914	298	26.811	128.3	5.23	124.4	5.96	7.51		1475.
400*	4.52	33.998	397	26.960	114.6	4.49	110.3	7.16	11.80		1474.
402	4.51	34.000	399	26.962	114.4	4.48	110.0	7.18	11.90		1474.
500*	4.21	34.081	507	27.059	105.9	4.17	100.8	8.26	16.86		1475.
600*	3.95	34.148	597	27.139	98.9	3.91	93.2	9.28	22.58		1475.
614	3.92	34.157	609	27.149	98.0	3.87	92.2	9.42	23.44		1475.
700*	3.76	34.208	716	27.206	93.1	3.71	86.7	10.24	28.94		1476.
800*	3.59	34.261	826	27.264	88.1	3.53	81.1	11.15	35.86		1477.
900*	3.44	34.307	922	27.315	83.8	3.38	76.3	12.01	43.30		1478.
1000*	3.31	34.348	1009	27.361	79.9	3.24	71.8	12.83	51.22		1479.
1091	3.20	34.382	1080	27.398	76.8	3.12	68.3	13.53	58.78		1481.
1200*	3.05	34.406	1216	27.431	74.1	2.97	65.1	14.36	68.40		1482.
1500*	2.72	34.463	1532	27.507	67.7	2.61	57.8	16.48	97.60		1485.
1858	2.39	34.518	1836	27.579	61.6	2.26	50.9	18.79	137.05		1490.





Results of STP Observations

(P-76-9)

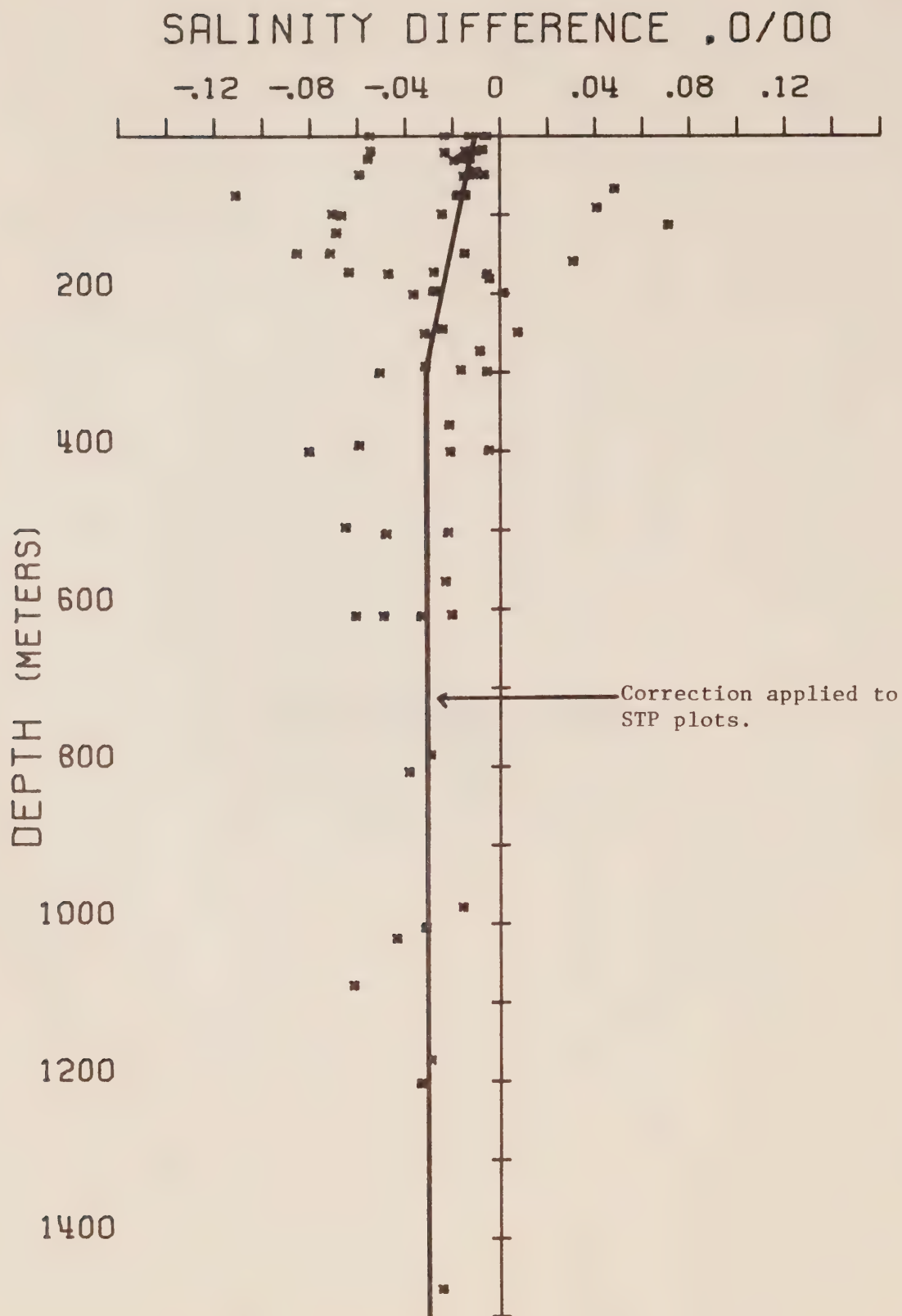


Figure 7. Salinity difference between hydro data and STP. P-76-9.

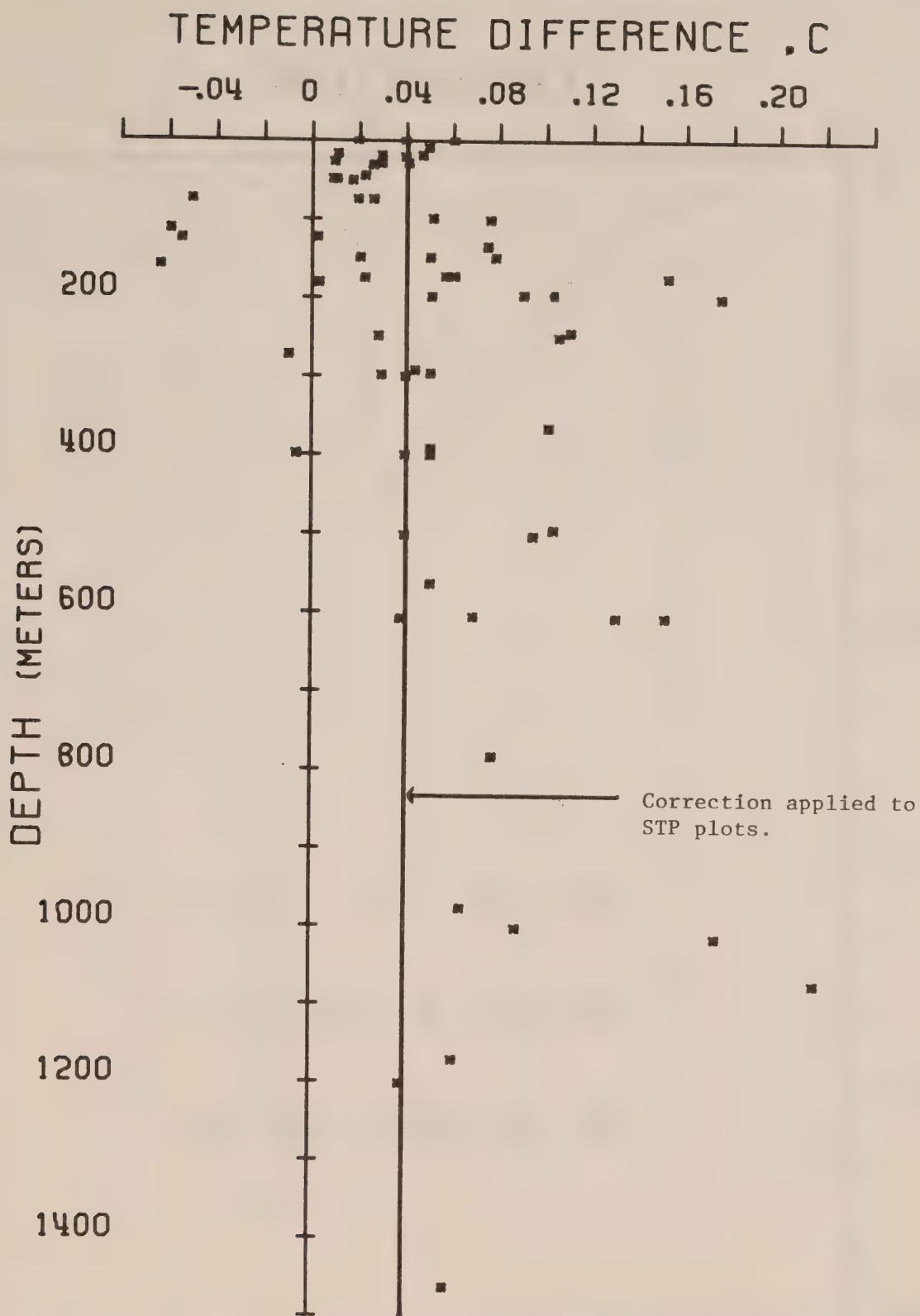
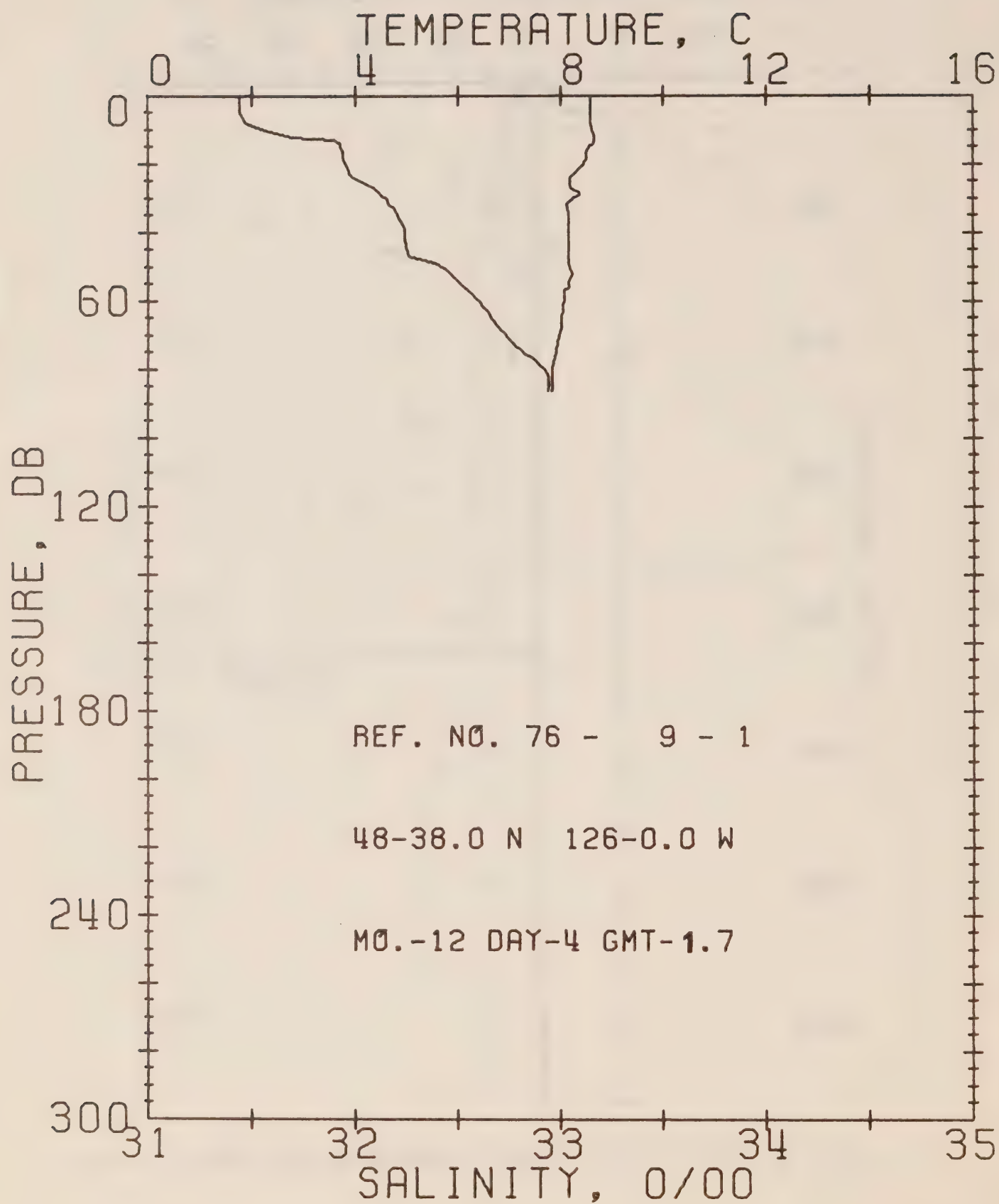


Figure 8. Temperature difference between hydro data and STP. P-76-9.





## OFFSHORE OCEANOGRAPHY GROUP

REFERENCE NO. 76- 9- 1

DATE 4/12/76

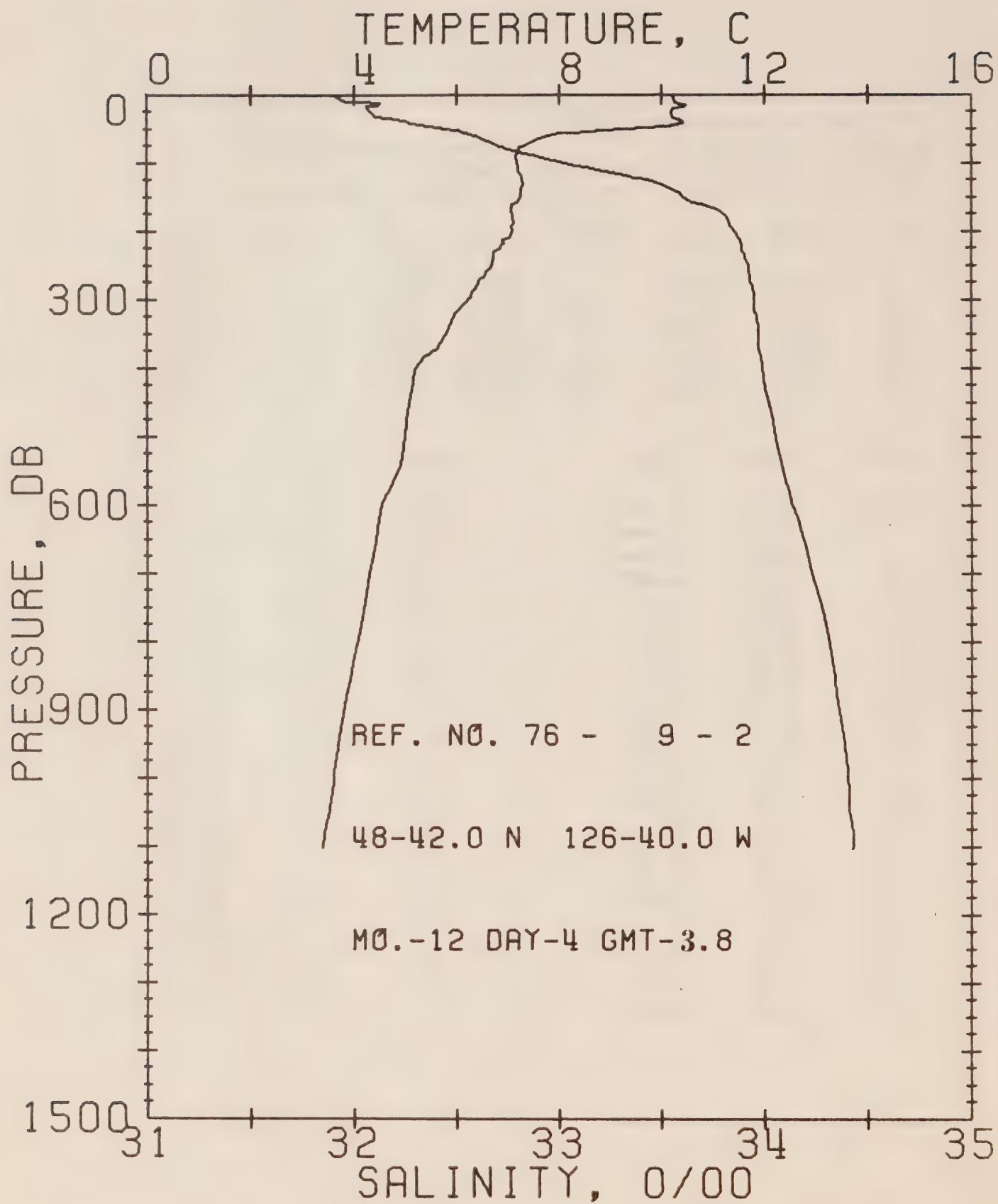
STATION 2

POSITION 48-38.0N, 126- 0.0W GMT 1.7

RESULTS OF STP CAST 45 POINTS TAKEN FROM ANALOG TRACE

PRESS	TEMP	SAL	DEPTH	SIGMA T	SVA	DELTA D	PST. EN	SOUND
0	8.58	31.44	0	24.42	351.6	0.0	0.0	1431.
10	8.62	31.56	10	24.51	343.7	0.35	0.02	1431.
20	8.45	31.95	20	24.84	312.5	0.67	0.07	1431.
30	8.23	32.15	30	25.03	294.5	0.98	0.14	1431.
50	8.18	32.41	50	25.24	274.4	1.55	0.33	1431.
75	7.92	32.82	75	25.60	241.0	2.19	0.79	1431.

DEPTH	TEMP	SAL	DEPTH	TEMP	SAL
0.	8.58	31.44	47.	8.16	32.23
3.	8.58	31.44	48.	8.16	32.33
5.	8.58	31.44	49.	8.16	32.39
8.	8.58	31.47	51.	8.20	32.44
10.	8.62	31.56	52.	8.23	32.46
12.	8.66	31.69	55.	8.17	32.51
13.	8.66	31.90	56.	8.15	32.53
14.	8.64	31.93	57.	8.08	32.55
15.	8.55	31.93	59.	8.07	32.58
17.	8.50	31.94	63.	8.04	32.64
19.	8.51	31.94	65.	8.03	32.66
21.	8.40	31.96	68.	8.02	32.70
23.	8.27	31.97	72.	7.96	32.76
24.	8.20	31.99	75.	7.92	32.82
27.	8.19	32.09	77.	7.90	32.87
28.	8.32	32.11	78.	7.88	32.89
29.	8.37	32.12	80.	7.85	32.92
30.	8.23	32.15	82.	7.85	32.94
32.	8.11	32.17	83.	7.85	32.94
33.	8.13	32.19	84.	7.85	32.94
35.	8.15	32.20	85.	7.85	32.94
39.	8.15	32.24	86.	7.85	32.94
42.	8.15	32.24			



## OFFSHORE OCEANOGRAPHY GROUP

REFERENCE NO. 76- 9- 2

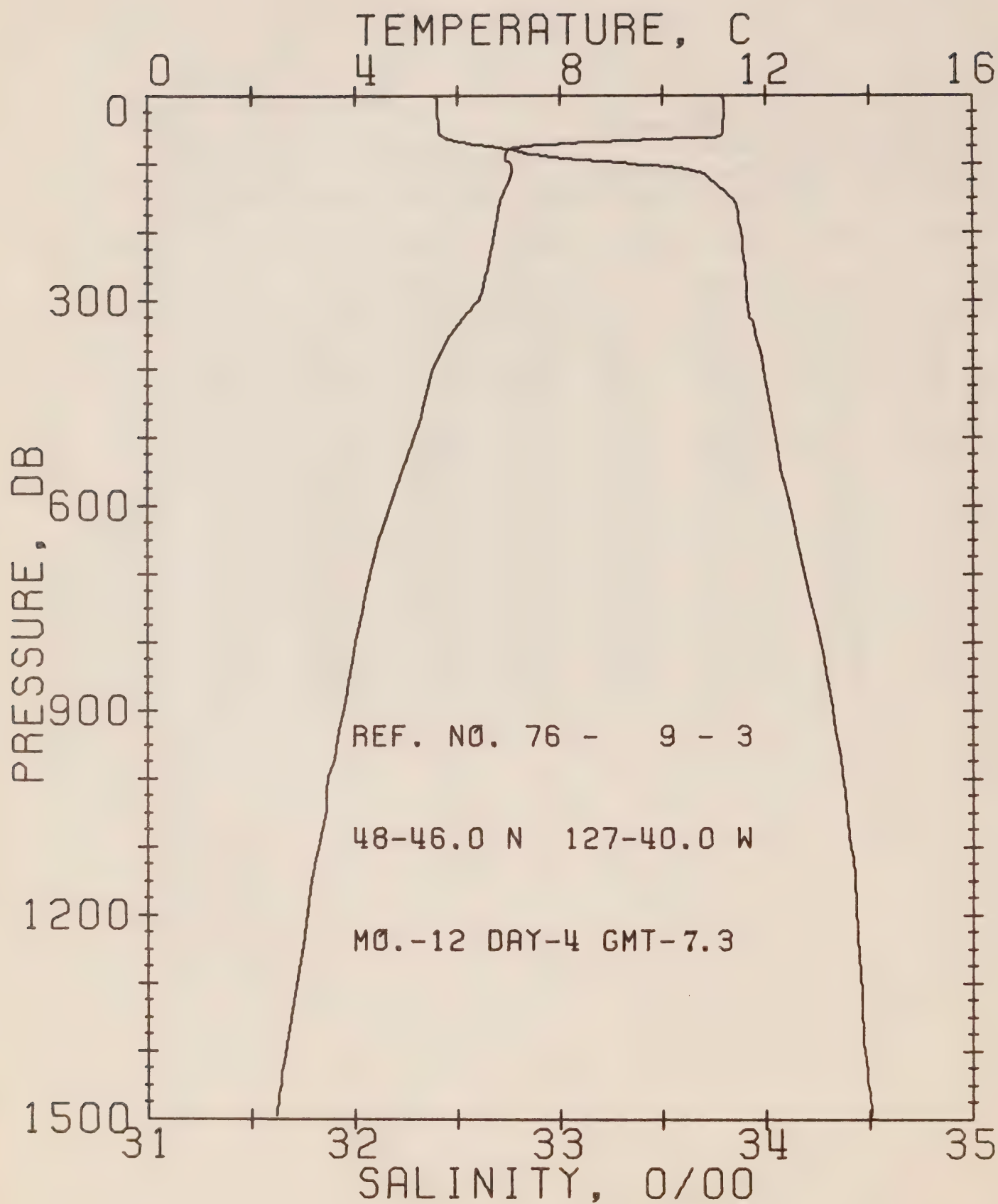
DATE 4/12/76

STATION 3

POSITION 48-42.0N, 126-40.0W SMT 3.8

RESULTS OF STP CAST 143 POINTS TAKEN FROM ANALOG TRACE

PRESS	TEMP	SAL	DEPTH	SIGMA T	SVA	DELTA D	POT. EN	SOUND
0	10.25	31.90	0	24.52	342.7	0.0	0.0	1437.
10	10.26	31.97	10	24.57	338.1	0.34	0.02	1438.
20	10.29	32.06	20	24.64	332.1	0.67	0.07	1438.
30	10.20	32.09	30	24.66	328.2	1.00	0.15	1438.
50	9.48	32.43	50	25.06	292.4	1.64	0.41	1450.
75	7.26	32.70	75	25.60	241.1	2.28	0.82	1475.
100	7.19	33.02	99	25.86	216.9	2.85	1.33	1479.
125	7.28	33.44	124	26.18	187.0	3.36	1.91	1480.
150	7.22	33.61	149	26.31	174.1	3.81	2.54	1481.
175	7.09	33.80	174	26.49	158.3	4.22	3.22	1481.
200	7.08	33.85	199	26.53	154.9	4.62	3.97	1481.
225	6.84	33.89	223	26.59	149.0	4.99	4.79	1481.
250	6.67	33.92	248	26.63	145.1	5.36	5.63	1480.
300	6.21	33.95	298	26.72	137.3	6.07	7.65	1479.
400	5.18	33.99	397	26.88	122.9	7.37	12.40	1477.
500	4.98	34.05	496	26.95	117.0	8.57	17.80	1478.
600	4.53	34.13	595	27.07	106.5	9.70	24.11	1478.
800	4.06	34.31	793	27.26	89.6	11.65	37.99	1479.
1000	3.59	34.40	991	27.38	79.4	13.33	53.33	1481.





## OFFSHORE OCEANOGRAPHY GROUP

REFERENCE NO. 76- 9- 3

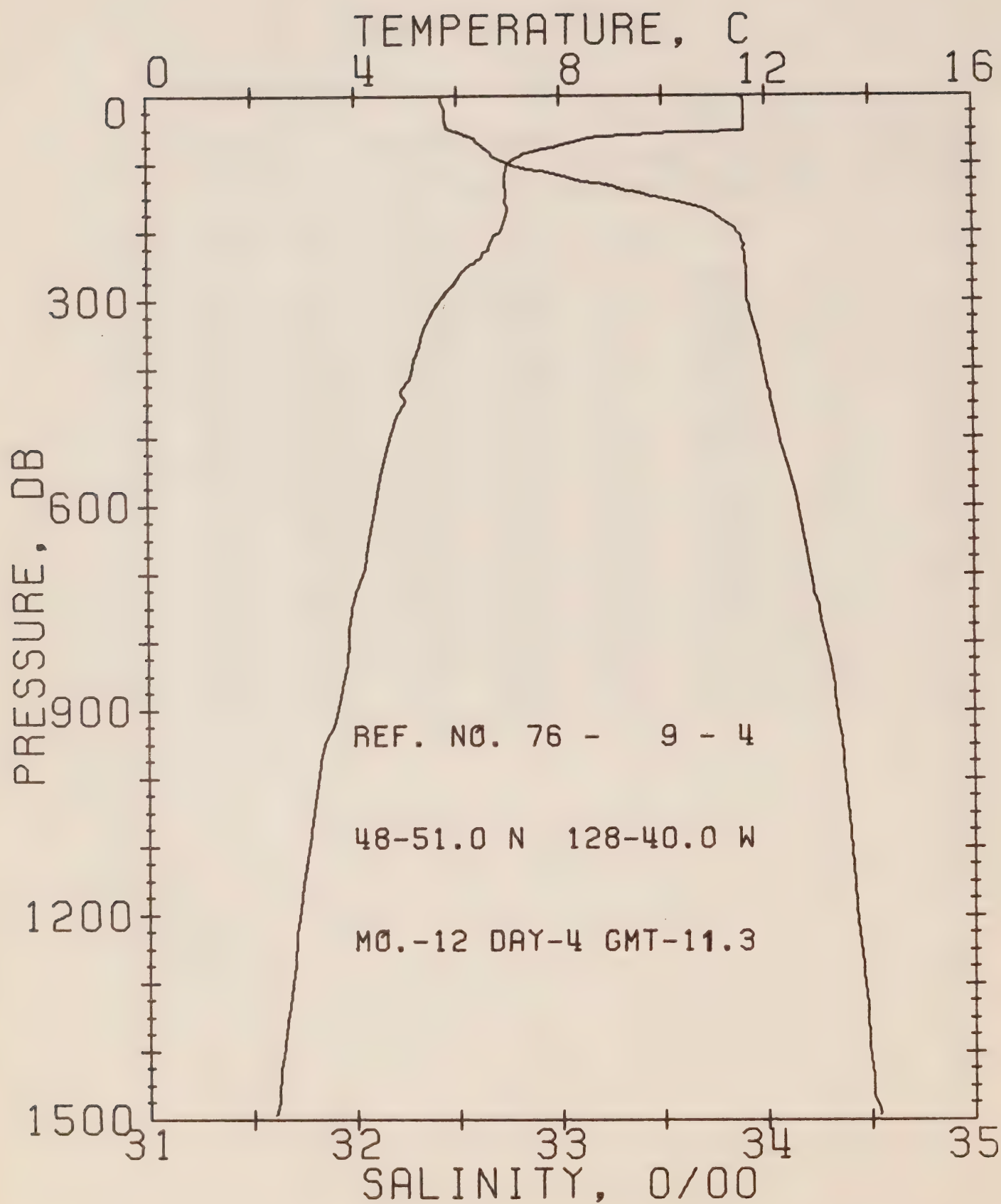
DATE 4/12/76

STATION 4

POSITION 48-46.0N, 127-40.0W GMT 7.3

RESULTS OF STP CAST 102 POINTS TAKEN FROM ANALOG TRACE

PRESS	TEMP	SAL	DEPTH	SIGMA T	SVA	DELTA D	PCT. EN	SOUND
0	11.16	32.39	0	24.74	321.4	0.0	0.0	1491.
10	11.19	32.40	10	24.74	321.5	0.32	0.02	1492.
20	11.19	32.40	20	24.74	321.8	0.64	0.07	1492.
30	11.19	32.40	30	24.75	321.8	0.97	0.15	1492.
50	11.18	32.41	50	24.75	321.5	1.61	0.41	1492.
75	7.33	32.65	75	25.55	245.7	2.35	0.88	1478.
100	7.02	33.32	99	26.12	191.7	2.90	1.37	1479.
125	6.99	33.74	124	26.45	160.8	3.33	1.35	1479.
150	6.84	33.83	149	26.55	152.2	3.72	2.40	1479.
175	6.78	33.87	174	26.58	149.2	4.09	3.02	1480.
200	6.72	33.88	199	26.60	147.7	4.46	3.73	1480.
225	6.66	33.89	223	26.62	145.6	4.83	4.53	1480.
250	6.60	33.90	248	26.63	145.5	5.20	5.41	1480.
300	6.40	33.91	293	26.67	142.7	5.92	7.43	1480.
400	5.49	33.99	397	26.84	126.8	7.26	12.20	1478.
500	5.13	34.05	496	26.93	119.1	8.49	17.84	1478.
600	4.68	34.11	595	27.03	109.8	9.64	24.26	1478.
800	4.00	34.26	793	27.22	92.8	11.65	38.60	1479.
1000	3.47	34.37	991	27.36	80.0	13.38	54.41	1480.
1200	3.06	34.44	1188	27.45	71.9	14.90	71.36	1482.



## OFFSHORE OCEANOGRAPHY GROUP

REFERENCE NO. 76- 9- 4

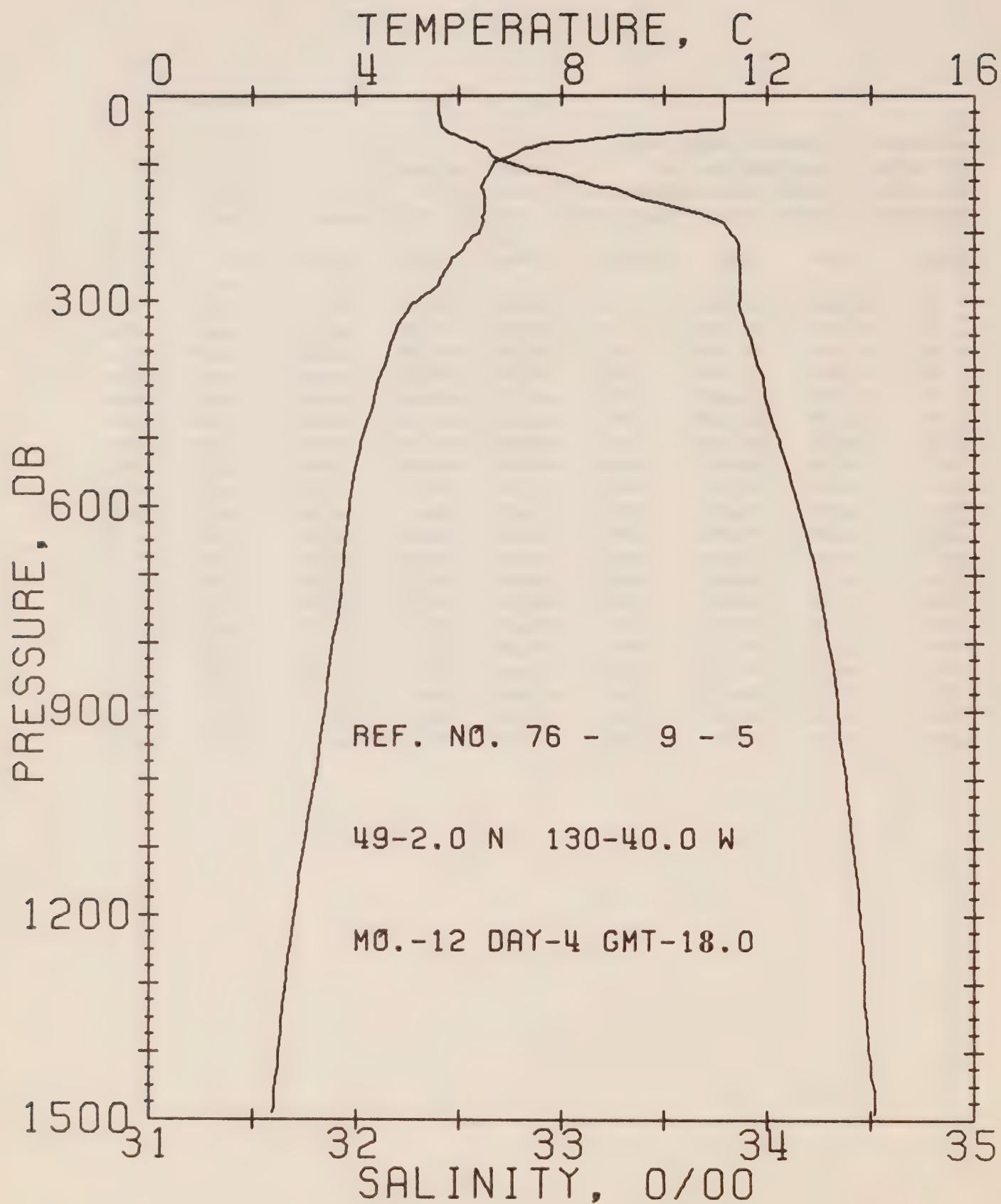
DATE 4/12/76

STATION 5

POSITION 48-51.0N, 128-40.0W GMT 11.3

RESULTS OF STP CAST 124 POINTS TAKEN FROM ANALOG TRACE

PRESS	TEMP	SAL	DEPTH	SIGMA T	SVA	DELTA D	POT. EN	SOUND
0	11.50	32.42	0	24.70	324.9	0.0	0.0	1492.
10	11.59	32.42	10	24.69	326.9	0.33	0.02	1493.
20	11.60	32.44	20	24.70	325.9	0.65	0.07	1493.
30	11.60	32.44	30	24.70	326.1	0.98	0.15	1493.
50	11.59	32.47	50	24.72	324.2	1.63	0.42	1494.
75	7.88	32.63	75	25.46	254.7	2.33	0.86	1481.
100	6.98	32.75	99	25.68	234.0	2.94	1.40	1478.
125	6.93	33.11	124	25.97	206.9	3.49	2.03	1478.
150	6.96	33.47	149	26.25	180.5	3.97	2.70	1479.
175	6.96	33.75	174	26.47	160.0	4.39	3.40	1480.
200	6.82	33.86	199	26.57	150.4	4.78	4.14	1430.
225	5.61	33.89	224	26.62	146.0	5.15	4.94	1430.
250	6.21	33.90	248	26.69	140.1	5.50	5.80	1479.
300	5.76	33.91	298	26.75	134.7	6.19	7.71	1478.
400	5.10	33.99	397	26.89	122.0	7.46	12.24	1477.
500	4.67	34.06	496	27.00	112.3	8.63	17.61	1477.
600	4.38	34.15	595	27.10	103.3	9.71	23.62	1477.
800	3.86	34.28	793	27.26	89.3	11.63	37.34	1478.
1000	3.26	34.38	991	27.39	77.3	13.30	52.55	1479.
1200	2.89	34.43	1188	27.47	70.2	14.77	69.06	1481.





## OFFSHORE OCEANOGRAPHY GROUP

REFERENCE NO. 76- 9- 5

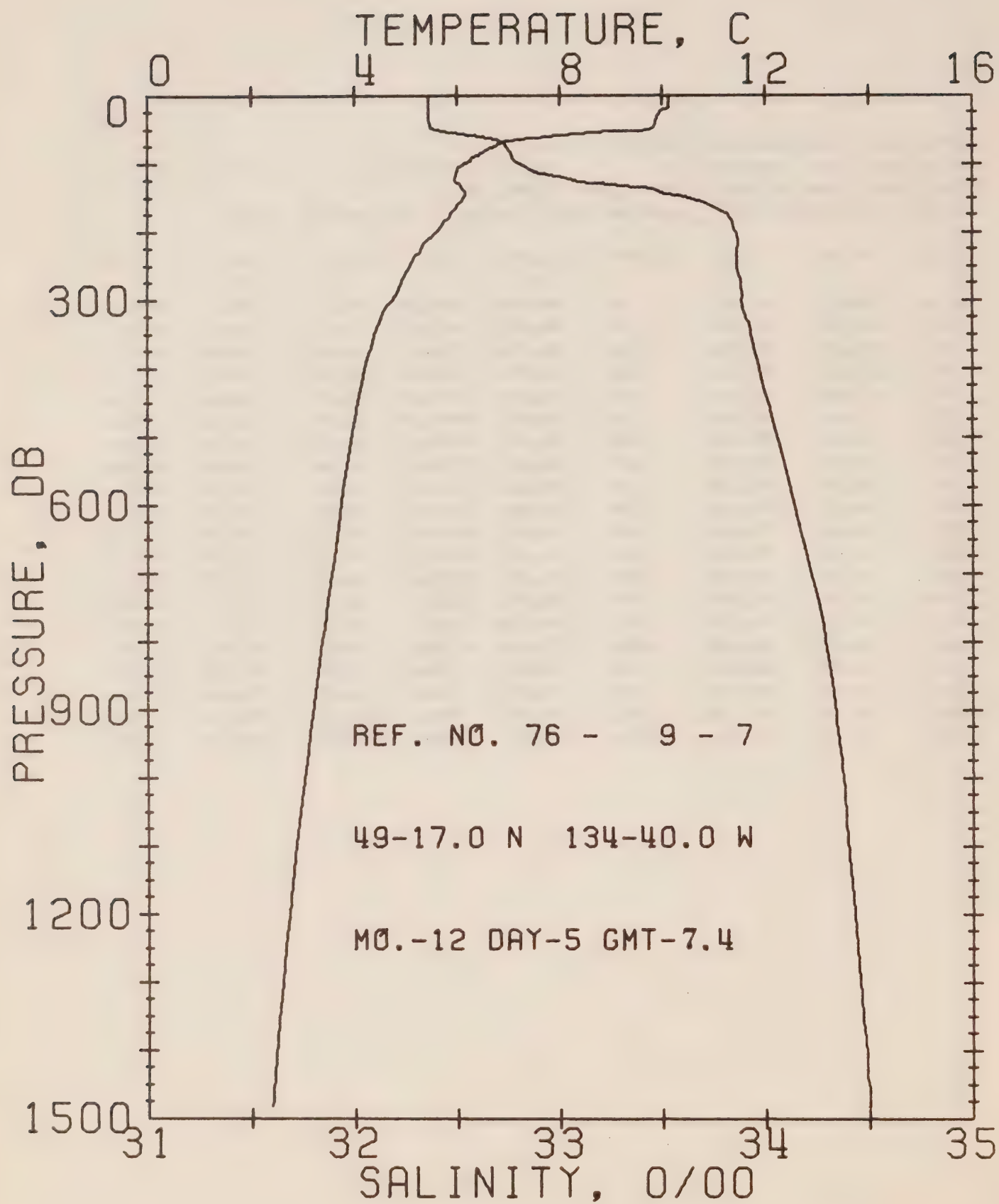
DATE 4/12/76

STATION 6

POSITION 49- 2.0N, 130-40.0W GMT 18.0

RESULTS OF STP CAST 131 POINTS TAKEN FROM ANALOG TRACE

PRESS	TEMP	SAL	DEPTH	SIGMA T	SVA	DELTA D	POT. EN	SOUND
0	11.17	32.40	0	24.75	320.8	0.0	0.0	1491.
10	11.17	32.40	10	24.75	321.2	0.32	0.02	1491.
20	11.17	32.40	20	24.75	321.4	0.64	0.07	1492.
30	11.17	32.40	30	24.75	321.3	0.96	0.15	1492.
50	11.04	32.43	50	24.79	317.8	1.61	0.41	1492.
75	7.40	32.62	75	25.52	248.9	2.30	0.85	1479.
100	6.66	32.76	99	25.72	229.4	2.90	1.38	1476.
125	6.48	33.08	124	26.00	203.3	3.44	2.00	1476.
150	6.50	33.37	149	26.23	132.3	3.92	2.67	1477.
175	6.47	33.69	174	26.48	158.2	4.35	3.38	1478.
200	6.39	33.82	199	26.60	148.0	4.73	4.10	1478.
225	6.04	33.86	223	26.67	140.9	5.09	4.88	1477.
250	5.76	33.87	248	26.71	137.2	5.43	5.72	1477.
300	5.18	33.87	298	26.78	130.7	6.11	7.61	1475.
400	4.50	33.96	397	26.93	117.2	7.34	12.01	1474.
500	4.12	34.05	496	27.04	107.1	8.47	17.16	1474.
600	3.87	34.15	595	27.15	98.0	9.49	22.89	1475.
800	3.54	34.29	793	27.30	85.0	11.32	35.85	1477.
1000	3.19	34.38	991	27.40	76.3	12.93	50.60	1479.
1200	2.79	34.45	1188	27.49	68.1	14.37	66.75	1481.



## OFFSHORE OCEANOGRAPHY GROUP

REFERENCE NO. 76- 9- 7

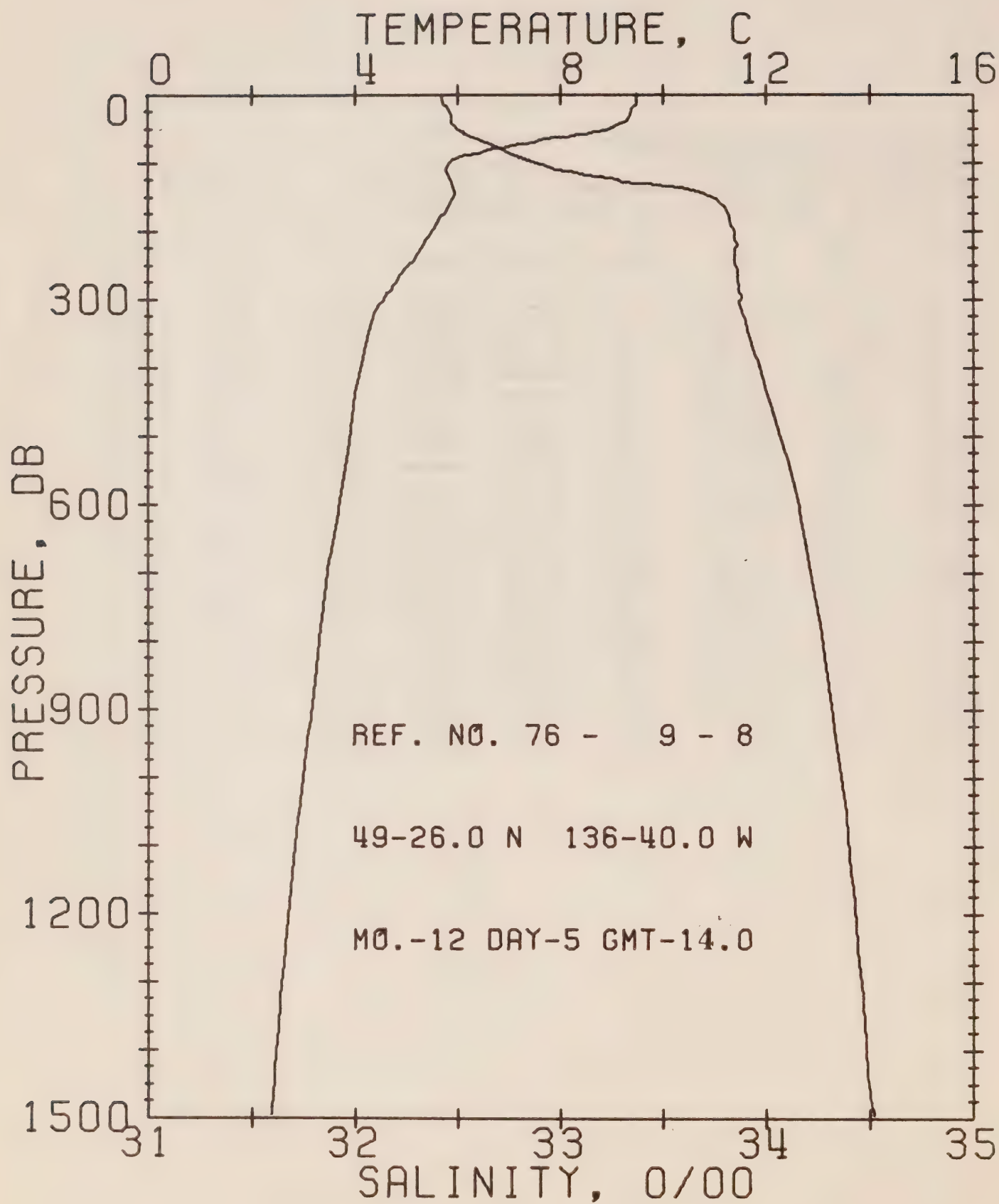
DATE 5/12/76

STATION 8

POSITION 49-17.0N, 134-40.0W GMT 7.4

RESULTS OF STP CAST 128 POINTS TAKEN FROM ANALOG TRACE

PRESS	TEMP	SAL	DEPTH	SIGMA T	SVA	DELTA D	POT. EN	SOUND
0	10.13	32.36	0	24.90	306.7	0.0	0.0	1487.
10	10.14	32.36	10	24.89	307.2	0.31	0.02	1488.
20	10.08	32.36	20	24.90	306.5	0.61	0.06	1488.
30	9.89	32.36	30	24.94	303.6	0.92	0.14	1487.
50	9.75	32.40	50	24.99	298.8	1.52	0.39	1487.
75	6.72	32.74	75	25.70	231.4	2.16	0.79	1476.
100	6.16	32.80	99	25.82	220.2	2.72	1.29	1474.
125	5.97	33.09	124	26.07	196.4	3.25	1.89	1474.
150	6.12	33.62	149	26.47	159.0	3.68	2.50	1475.
175	5.85	33.82	174	26.66	141.3	4.06	3.12	1475.
200	5.58	33.85	199	26.72	135.4	4.40	3.78	1475.
225	5.29	33.86	223	26.77	131.7	4.73	4.50	1474.
250	5.05	33.86	248	26.79	129.4	5.06	5.29	1474.
300	4.74	33.88	298	26.84	124.7	5.69	7.06	1473.
400	4.19	33.97	397	26.97	113.4	6.88	11.27	1473.
500	3.94	34.06	496	27.07	104.8	7.97	16.27	1474.
600	3.73	34.14	595	27.15	97.2	8.95	21.92	1474.
800	3.37	34.29	793	27.31	83.4	10.78	34.73	1475.
1000	3.02	34.37	990	27.41	74.8	12.36	49.17	1473.
1200	2.72	34.43	1188	27.48	68.6	13.80	65.27	1480.



## OFFSHORE OCEANOGRAPHY GROUP

REFERENCE NO. 76- 9- 8

DATE 5/12/76

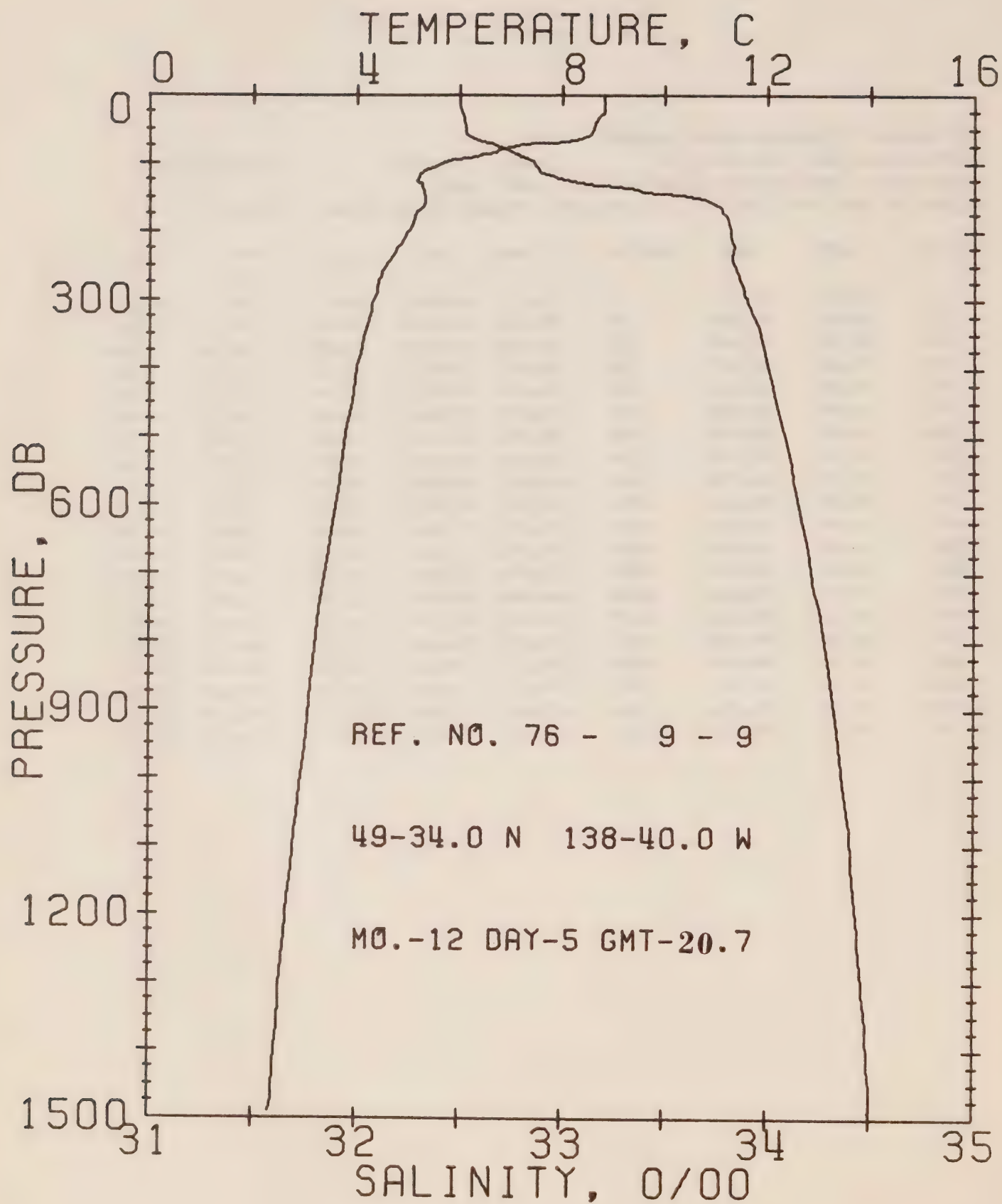
STATION 9

POSITION 49-26.0N, 136-40.0W GMT 14.00

RESULTS OF STP CAST 119 POINTS TAKEN FROM ANALOG TRACE

PRESS	TEMP	SAL	DEPTH	SIGMA T	SVA	DELTA D	POT. EN	SOUND
0	9.49	32.42	0	25.05	292.3	0.0	0.0	1485.
10	9.49	32.42	10	25.05	292.6	0.29	0.01	1485.
20	9.38	32.45	20	25.09	288.9	0.58	0.06	1485.
30	9.35	32.47	30	25.11	287.1	0.87	0.13	1485.
50	8.97	32.49	50	25.19	280.0	1.44	0.33	1484.
75	6.99	32.68	75	25.62	239.2	2.09	0.78	1477.
100	5.82	32.88	99	25.93	210.0	2.65	1.23	1473.
125	5.87	33.28	124	26.24	181.0	3.15	1.84	1474.
150	5.92	33.73	149	26.58	148.4	3.55	2.40	1476.
175	5.71	33.81	174	26.68	139.7	3.91	3.00	1475.
200	5.48	33.84	199	26.73	135.0	4.25	3.65	1475.
225	5.27	33.85	223	26.76	132.2	4.56	4.37	1474.
250	5.02	33.85	248	26.79	129.9	4.91	5.17	1474.
300	4.55	33.88	298	26.86	122.8	5.54	6.94	1473.
400	4.11	33.97	397	26.98	112.4	6.72	11.12	1472.
500	3.90	34.07	496	27.08	103.6	7.80	16.06	1473.
600	3.70	34.16	595	27.17	95.6	8.79	21.63	1474.
800	3.30	34.27	793	27.30	84.2	10.59	34.39	1476.
1000	2.99	34.36	990	27.40	75.5	12.16	48.98	1478.
1200	2.70	34.43	1188	27.48	68.4	13.61	65.00	1480.





## OFFSHORE OCEANOGRAPHY GROUP

REFERENCE NO. 76- 9- 9

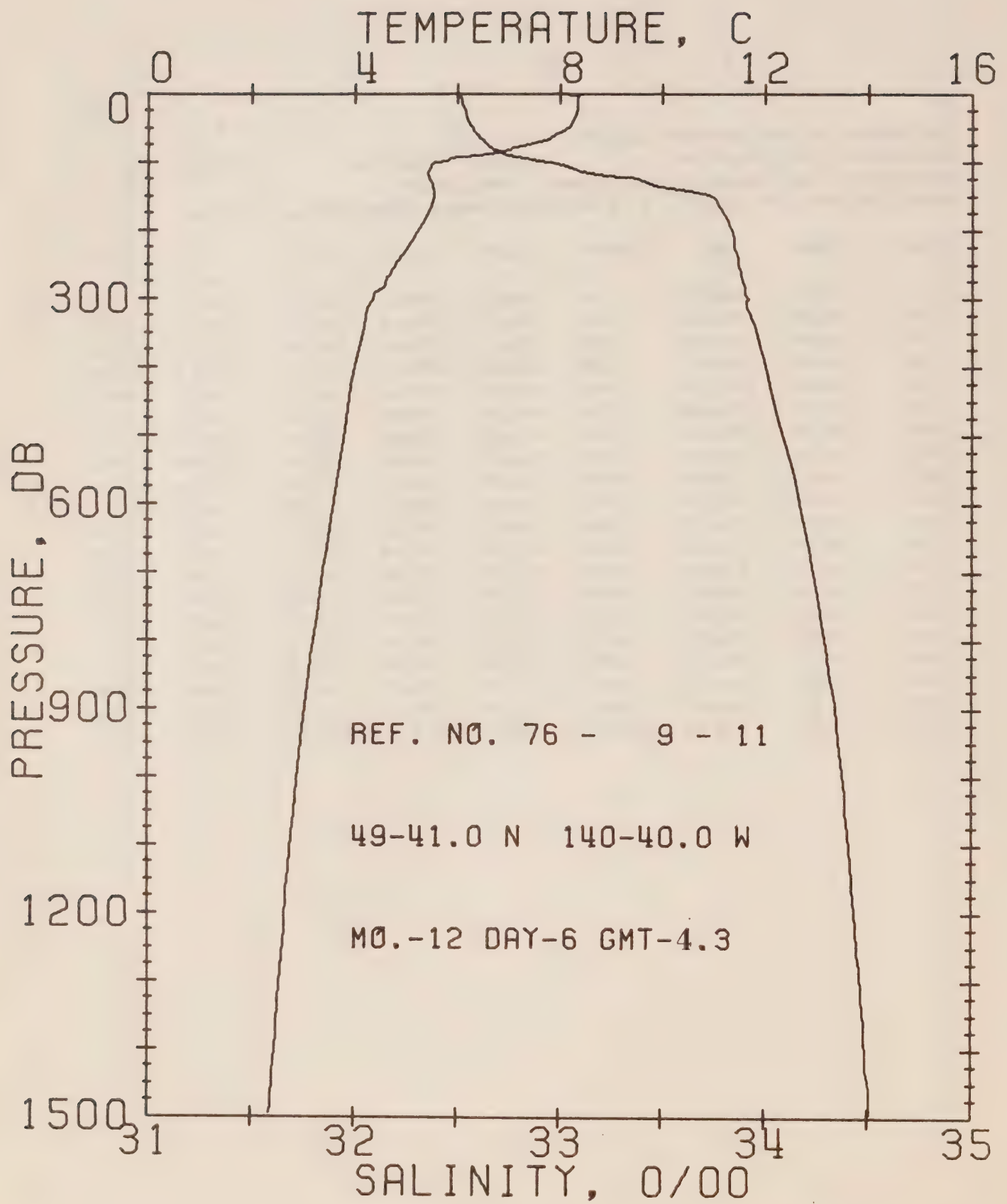
DATE 5/12/76

STATION 10

POSITION 49-34.0N, 138-40.0W GMT 20.7

RESULTS OF STP CAST 112 POINTS TAKEN FROM ANALOG TRACE

PRESS	TEMP	SAL	DEPTH	SIGMA T	SVA	DELTA D	POT. EN	SOUND
0	8.84	32.50	0	25.21	276.6	0.0	0.0	1483.
10	8.84	32.50	10	25.21	276.9	0.26	0.01	1483.
20	8.84	32.50	20	25.21	276.8	0.55	0.06	1483.
30	8.78	32.51	30	25.23	275.3	0.83	0.13	1483.
50	8.60	32.53	50	25.27	272.0	1.38	0.35	1483.
75	7.00	32.69	75	25.63	238.4	2.03	0.77	1477.
100	5.67	32.86	99	25.93	209.6	2.59	1.26	1473.
125	5.16	33.03	124	26.13	191.2	3.10	1.84	1471.
150	5.33	33.65	149	26.59	147.6	3.53	2.44	1473.
175	5.14	33.79	174	26.72	135.2	3.88	3.02	1473.
200	4.99	33.82	199	26.77	131.2	4.21	3.55	1473.
225	4.79	33.84	223	26.80	127.8	4.53	4.35	1472.
250	4.57	33.84	248	26.83	125.6	4.85	5.12	1472.
300	4.34	33.90	298	26.90	119.0	5.46	6.83	1472.
400	4.00	34.00	397	27.02	108.6	6.59	10.86	1472.
500	3.78	34.08	496	27.11	100.9	7.64	15.66	1473.
600	3.61	34.15	595	27.18	94.8	8.62	21.13	1474.
800	3.22	34.28	793	27.31	83.1	10.39	33.73	1476.
1000	2.93	34.37	990	27.41	74.4	11.96	48.09	1478.
1200	2.65	34.43	1188	27.49	67.9	13.37	63.94	1480.



## OFFSHORE OCEANOGRAPHY GROUP

REFERENCE NO. 76- 9- 11

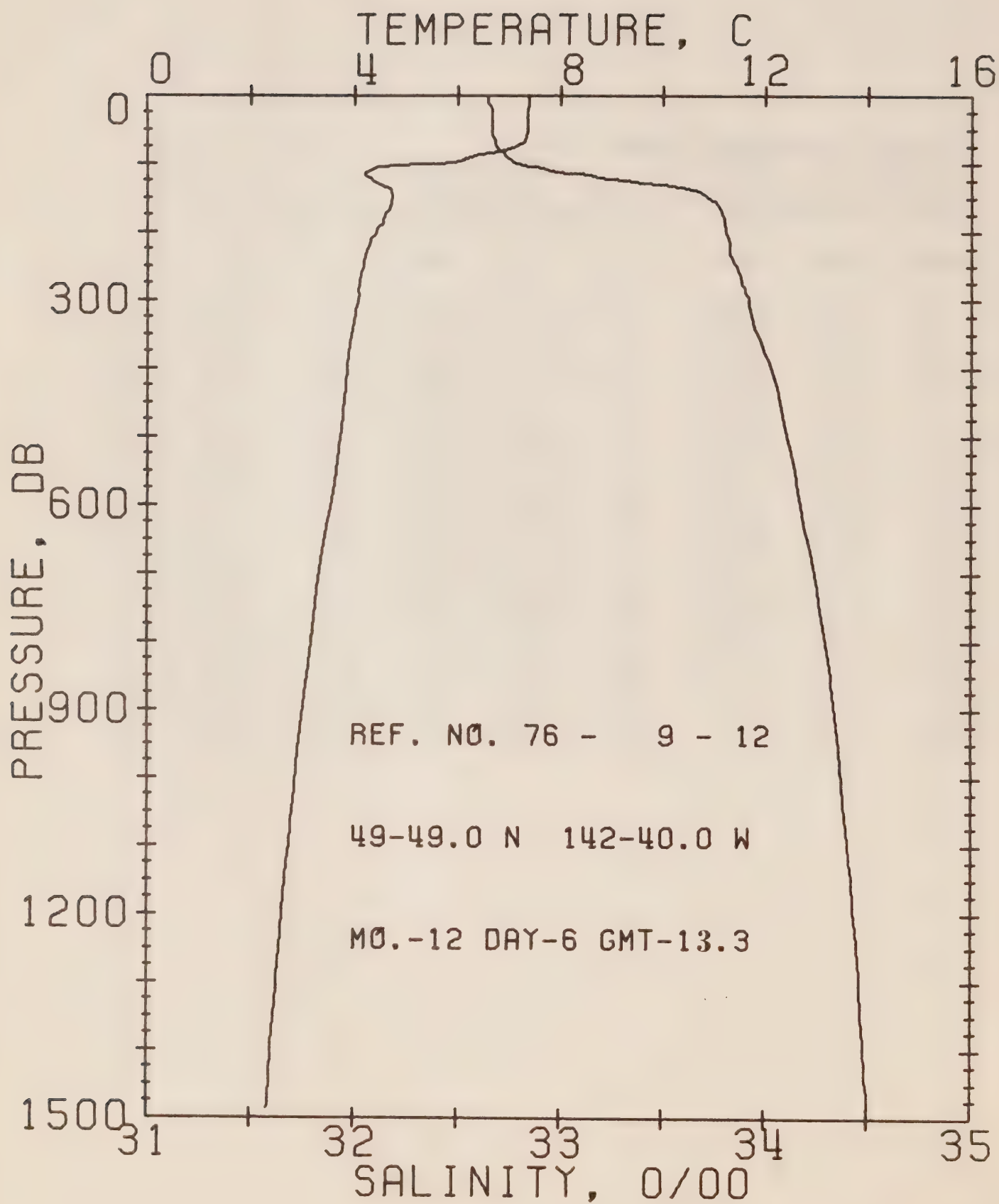
DATE 6/12/76

STATION 11

POSITION 49-41.0N, 140-40.0W GMT 4.3

RESULTS OF STP CAST 114 POINTS TAKEN FROM ANALOG TRACE

PRESS	TEMP	SAL	DEPTH	SIGMA T	SVA	DELTA D	POT. EN	SOUND
0	7.95	32.51	0	25.35	263.2	0.0	0.0	1479.
10	8.35	32.52	10	25.30	268.4	0.27	0.01	1481.
20	8.35	32.53	20	25.31	267.8	0.54	0.05	1481.
30	8.32	32.54	30	25.32	266.8	0.80	0.12	1481.
50	8.16	32.57	50	25.37	262.5	1.33	0.34	1481.
75	7.29	32.65	75	25.56	245.2	1.97	0.74	1478.
100	5.64	32.93	99	25.99	204.1	2.54	1.25	1473.
125	5.46	33.39	124	26.37	168.1	3.02	1.79	1473.
150	5.55	33.73	149	26.63	143.4	3.41	2.34	1474.
175	5.42	33.79	174	26.69	137.9	3.76	2.92	1474.
200	5.23	33.83	199	26.75	132.9	4.10	3.57	1474.
225	5.01	33.85	223	26.79	129.5	4.43	4.28	1473.
250	4.79	33.87	248	26.83	125.8	4.75	5.05	1473.
300	4.35	33.92	298	26.92	117.7	5.36	6.76	1472.
400	4.00	34.00	397	27.02	108.7	6.49	10.80	1472.
500	3.80	34.09	496	27.10	101.0	7.54	15.61	1473.
600	3.59	34.17	595	27.19	93.5	8.51	21.03	1474.
800	3.20	34.29	793	27.32	81.9	10.26	33.46	1476.
1000	2.89	34.38	990	27.42	73.1	11.80	47.59	1478.
1200	2.65	34.43	1188	27.49	67.5	13.21	63.32	1480.





## OFFSHORE OCEANOGRAPHY GROUP

REFERENCE NO. 76- 9- 12

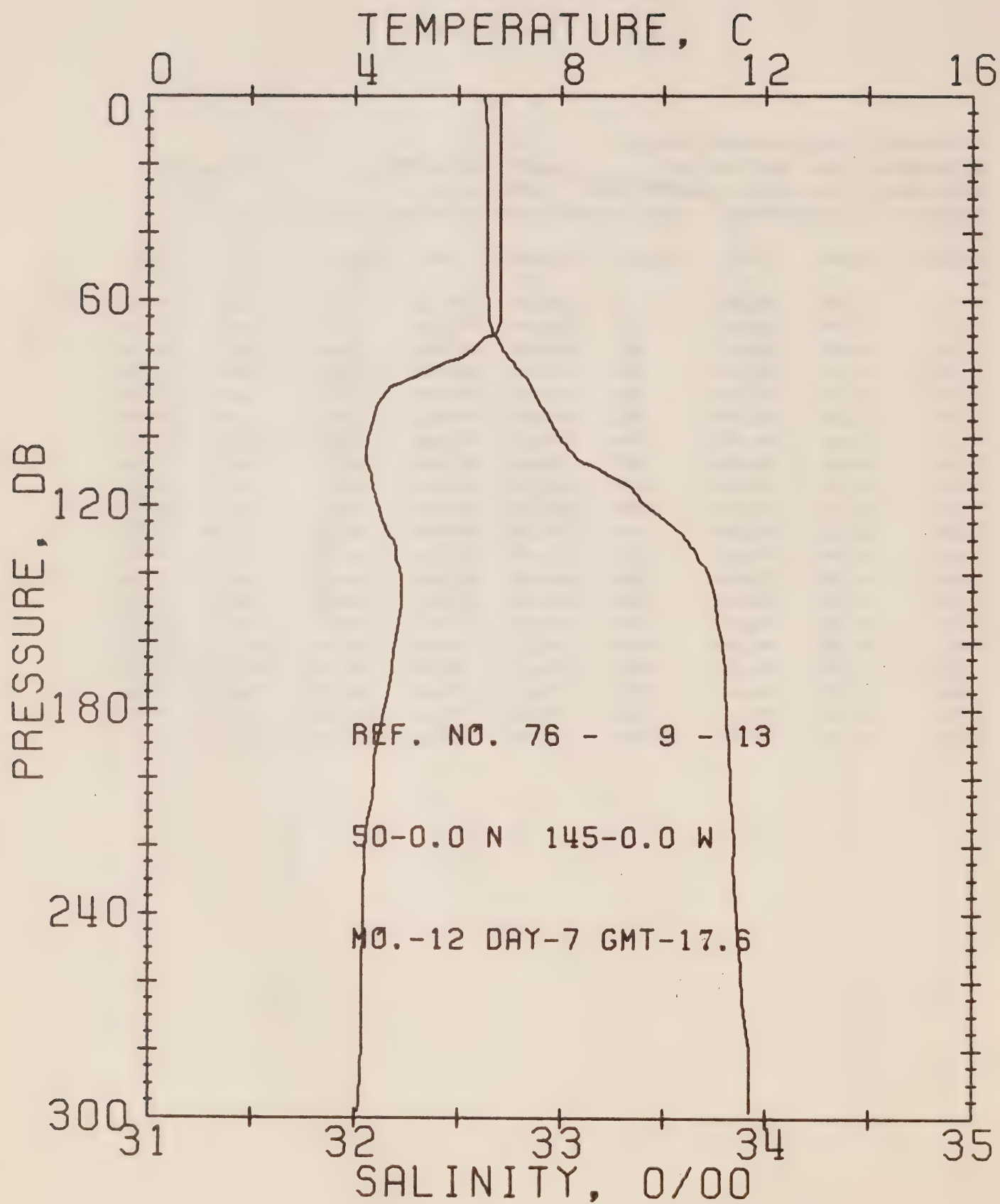
DATE 6/12/76

STATION 12

POSITION 49-49.0N, 142-40.0W GMT 13.3

RESULTS OF STP CAST 119 POINTS TAKEN FROM ANALOG TRACE

PRESS	TEMP	SAL	DEPTH	SIGMA T	SVA	DELTA D	PCT. EN	SOUND
0	7.38	32.65	0.	25.54	245.1	0.0	0.0	1477.
10	7.38	32.65	10	25.54	245.4	0.25	0.01	1478.
20	7.37	32.67	20	25.56	243.9	0.49	0.05	1478.
30	7.37	32.67	30	25.56	244.1	0.73	0.11	1478.
50	7.36	32.67	50	25.56	244.3	1.22	0.31	1478.
75	7.11	32.68	75	25.61	240.3	1.83	0.70	1478.
100	5.66	32.79	99	25.87	214.8	2.40	1.21	1472.
125	4.36	33.36	124	26.47	158.2	2.86	1.73	1468.
150	4.73	33.72	149	26.72	135.0	3.22	2.23	1471.
175	4.61	33.79	174	26.79	128.9	3.55	2.78	1471.
200	4.43	33.81	199	26.82	125.8	3.87	3.39	1470.
225	4.26	33.83	223	26.85	122.8	4.18	4.06	1470.
250	4.18	33.86	248	26.89	119.9	4.48	4.80	1470.
300	4.09	33.92	298	26.94	114.9	5.07	6.44	1471.
400	3.86	34.03	397	27.05	105.3	6.17	10.37	1471.
500	3.74	34.11	496	27.13	98.6	7.19	15.03	1473.
600	3.55	34.17	595	27.20	92.8	8.15	20.38	1474.
800	3.17	34.29	793	27.33	81.3	9.88	32.69	1475.
1000	2.86	34.37	990	27.42	73.2	11.42	46.76	1478.
1200	2.61	34.43	1188	27.49	67.3	12.82	62.50	1480.



## OFFSHORE OCEANOGRAPHY GROUP

REFERENCE NO. 76- 9- 13

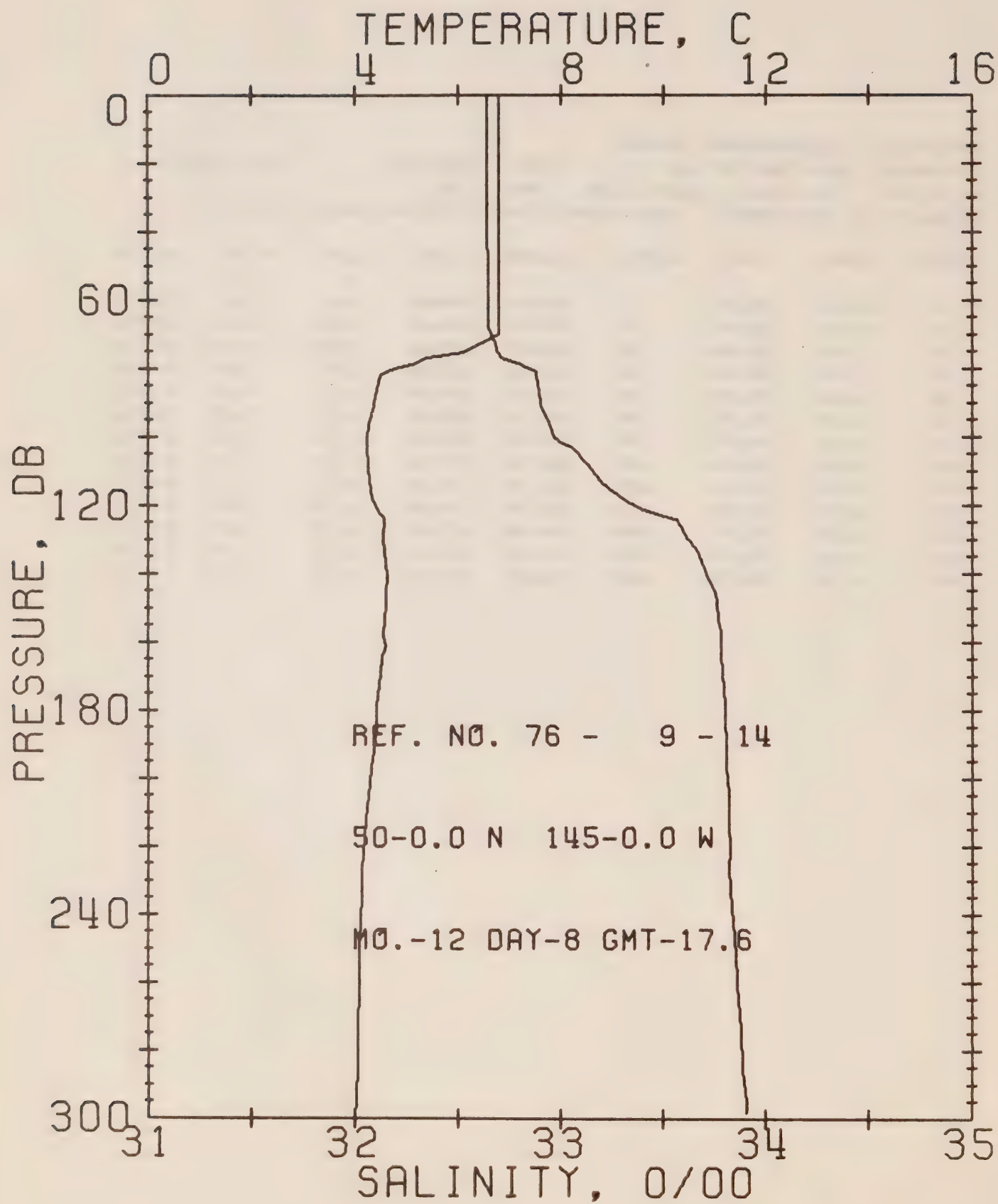
DATE 7/12/76

STATION P

POSITION 50- 0.0N. 145- 0.0W GMT 17.6

RESULTS OF STP CAST 76 POINTS TAKEN FROM ANALOG TRACE

PRESS	TEMP	SAL	DEPTH	SIGMA T	SVA	DLT TA D	POT. EN	SOUND
0	6.83	32.63	0	25.60	239.6	0.0	0.0	1475.
10	6.83	32.64	10	25.61	239.2	0.24	0.01	1475.
20	6.82	32.64	20	25.61	239.2	0.48	0.05	1476.
30	6.83	32.64	30	25.61	239.3	0.72	0.11	1476.
50	6.84	32.64	50	25.61	239.8	1.20	0.31	1476.
75	6.21	32.72	75	25.75	226.3	1.79	0.68	1474.
100	4.23	32.99	99	26.19	184.4	2.29	1.13	1467.
125	4.55	33.52	124	26.58	148.3	2.71	1.60	1469.
150	4.90	33.75	149	26.72	134.8	3.06	2.09	1471.
175	4.64	33.80	174	26.79	128.6	3.38	2.63	1471.
200	4.36	33.83	199	26.84	123.6	3.70	3.23	1470.
225	4.19	33.84	223	26.87	121.3	4.00	3.89	1470.
250	4.14	33.87	248	26.90	118.7	4.30	4.62	1470.



## OFFSHORE OCEANOGRAPHY GROUP

REFERENCE NO. 76- 9- 14

DATE 8/12/76

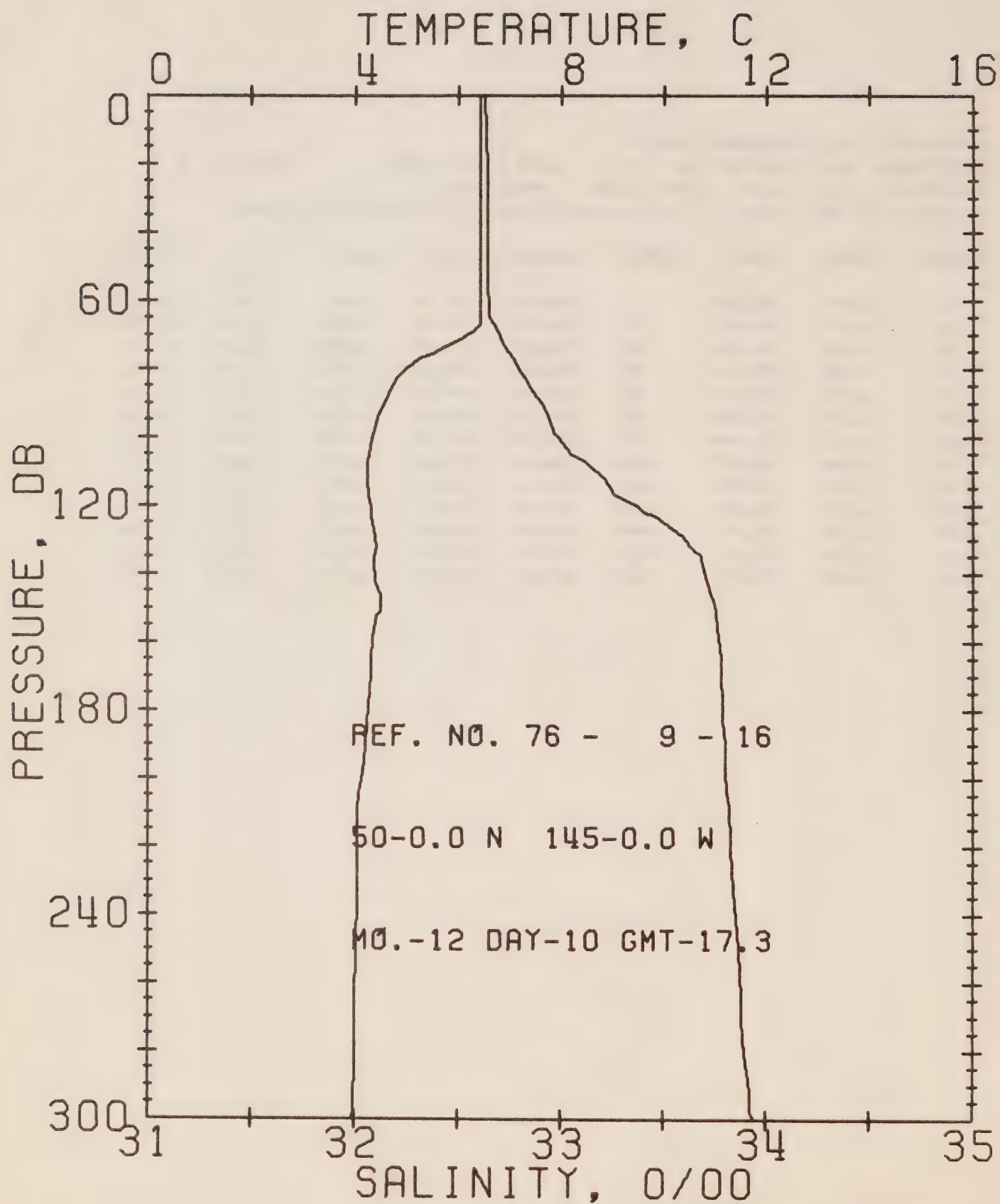
STATION P

POSITION 50- 0.0N, 145- 0.0W GMT 17.6

RESULTS OF STP CAST 65 POINTS TAKEN FROM ANALOG TRACE

PRESS	TEMP	SAL	DEPTH	SIGMA T	SVA	DELTA D	POT. EN	SOUND
0	6.80	32.64	0	25.61	238.4	0.0	0.0	1475.
10	6.80	32.64	10	25.61	238.7	0.24	0.01	1475.
20	6.80	32.64	20	25.61	238.8	0.48	0.05	1475.
30	6.80	32.64	30	25.61	239.1	0.72	0.11	1476.
50	6.81	32.65	50	25.62	238.8	1.19	0.30	1476.
75	6.11	32.69	75	25.74	227.3	1.79	0.68	1474.
100	4.25	32.96	99	26.17	186.9	2.28	1.12	1467.
125	4.58	33.57	124	26.61	144.6	2.70	1.60	1469.
150	4.60	33.76	149	26.76	130.7	3.04	2.08	1470.
175	4.46	33.80	174	26.81	126.9	3.36	2.61	1470.
200	4.30	33.81	199	26.84	124.2	3.68	3.21	1470.
225	4.14	33.82	223	26.86	122.1	3.99	3.88	1470.
250	4.08	33.85	248	26.89	119.5	4.29	4.61	1470.





## OFFSHORE OCEANOGRAPHY GROUP

REFERENCE NO. 76- 9- 16

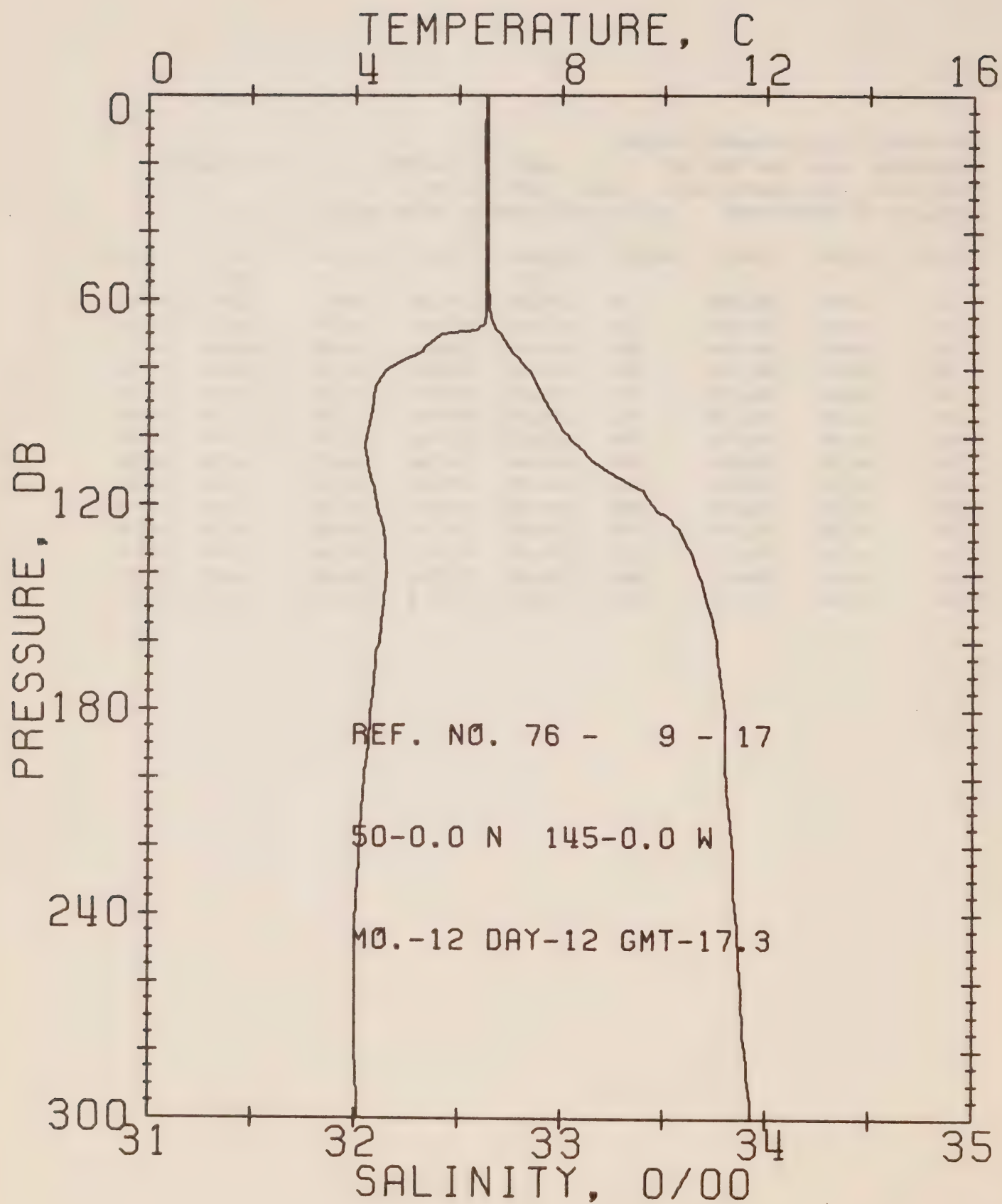
DATE 10/12/76

STATION P

POSITION 50- 0.0N, 145- 0.0W GMT 17.3

RESULTS OF STP CAST 62 POINTS TAKEN FROM ANALOG TRACE

PRESS	TEMP	SAL	DEPTH	SIGMA T	SVA	DELTA D	POT. EN	SOUND
0	6.43	32.63	0	25.65	234.6	0.0	0.0	1474.
10	6.43	32.63	10	25.66	234.6	0.23	0.01	1474.
20	6.43	32.64	20	25.66	234.4	0.47	0.05	1474.
30	6.43	32.64	30	25.66	234.4	0.70	0.11	1474.
50	6.43	32.64	50	25.66	234.7	1.17	0.30	1474.
75	5.54	32.74	75	25.85	217.0	1.75	0.67	1471.
100	4.31	32.98	99	26.17	186.0	2.25	1.11	1467.
125	4.35	33.50	124	26.58	147.8	2.67	1.59	1468.
150	4.51	33.75	149	26.76	131.0	3.01	2.06	1470.
175	4.28	33.79	174	26.82	125.9	3.33	2.59	1469.
200	4.13	33.80	199	26.85	123.2	3.64	3.19	1469.
225	4.05	33.83	223	26.88	120.3	3.94	3.84	1469.
250	4.02	33.87	248	26.91	117.5	4.24	4.56	1469.
300	3.96	33.94	298	26.97	112.1	4.82	6.19	1470.



## OFFSHORE OCEANOGRAPHY GROUP

REFERENCE NO. 76- 9- 17

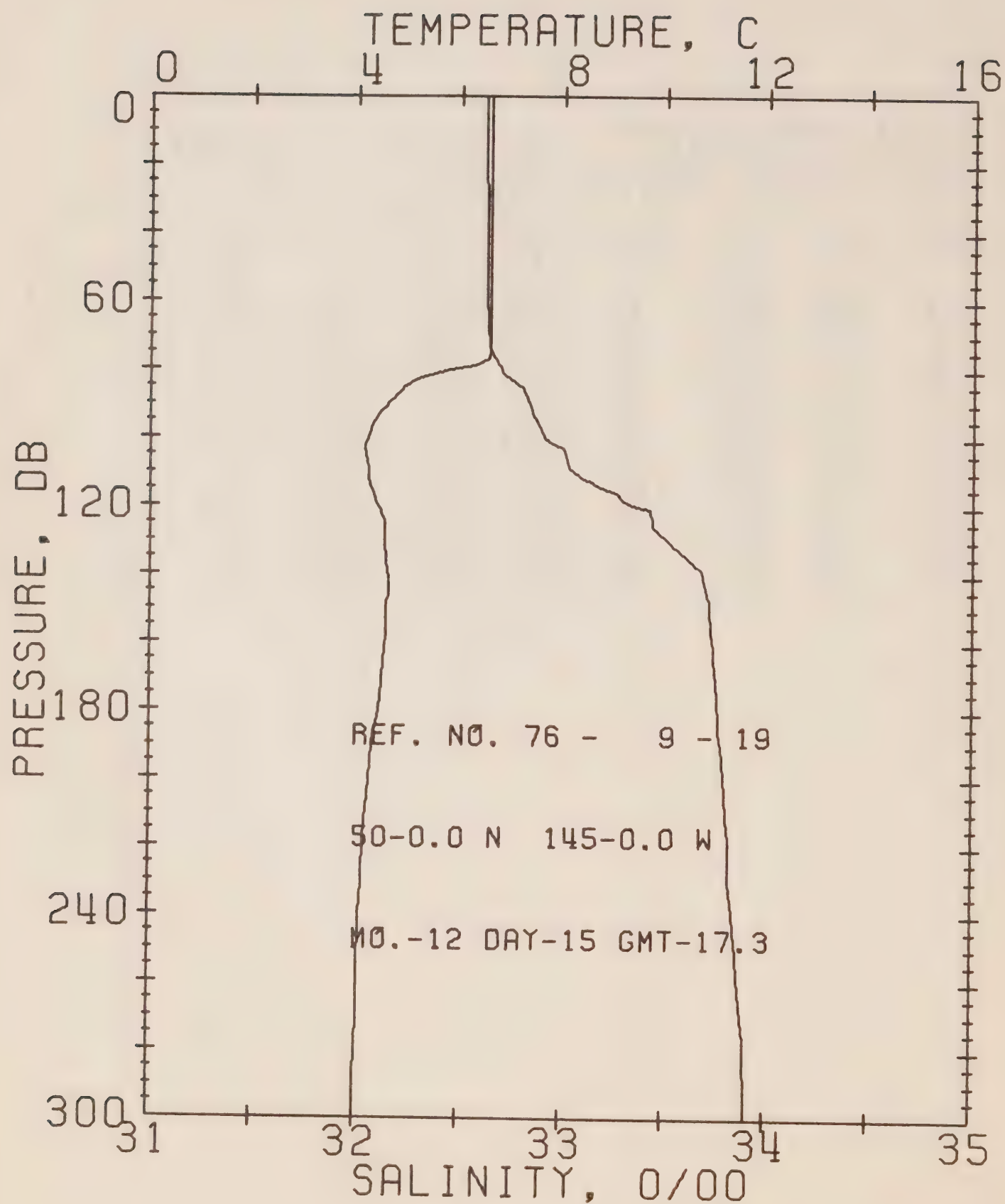
DATE 12/12/76

STATION P

POSITION 50- 0.0N, 145- 0.0W GMT 17.3

RESULTS OF STP CAST 69 POINTS TAKEN FROM ANALOG TRACE

PRESS	TEMP	SAL	DEPTH	SIGMA T	SVA	DELTA D	POT. EN	SOUND
0	6.53	32.64	0	25.65	235.0	0.0	0.0	1474.
10	6.52	32.64	10	25.65	235.3	0.24	0.01	1474.
20	6.53	32.64	20	25.65	235.5	0.47	0.05	1474.
30	6.53	32.64	30	25.65	235.6	0.71	0.11	1475.
50	6.53	32.64	50	25.65	235.8	1.18	0.30	1475.
75	5.27	32.75	75	25.89	213.2	1.75	0.67	1470.
100	4.21	33.03	99	26.22	181.3	2.24	1.10	1467.
125	4.52	33.54	124	26.60	146.3	2.65	1.56	1469.
150	4.55	33.72	149	26.74	133.3	3.00	2.05	1470.
175	4.34	33.79	174	26.81	126.2	3.32	2.59	1470.
200	4.18	33.81	199	26.84	123.6	3.63	3.13	1469.
225	4.07	33.84	223	26.88	120.0	3.94	3.84	1469.
250	3.99	33.87	248	26.91	117.5	4.23	4.56	1469.
300	4.04	33.93	298	26.96	113.7	4.81	6.18	1470.





## OFFSHORE OCEANOGRAPHY GROUP

REFERENCE NO. 76- 9- 19

DATE 15/12/76

STATION P

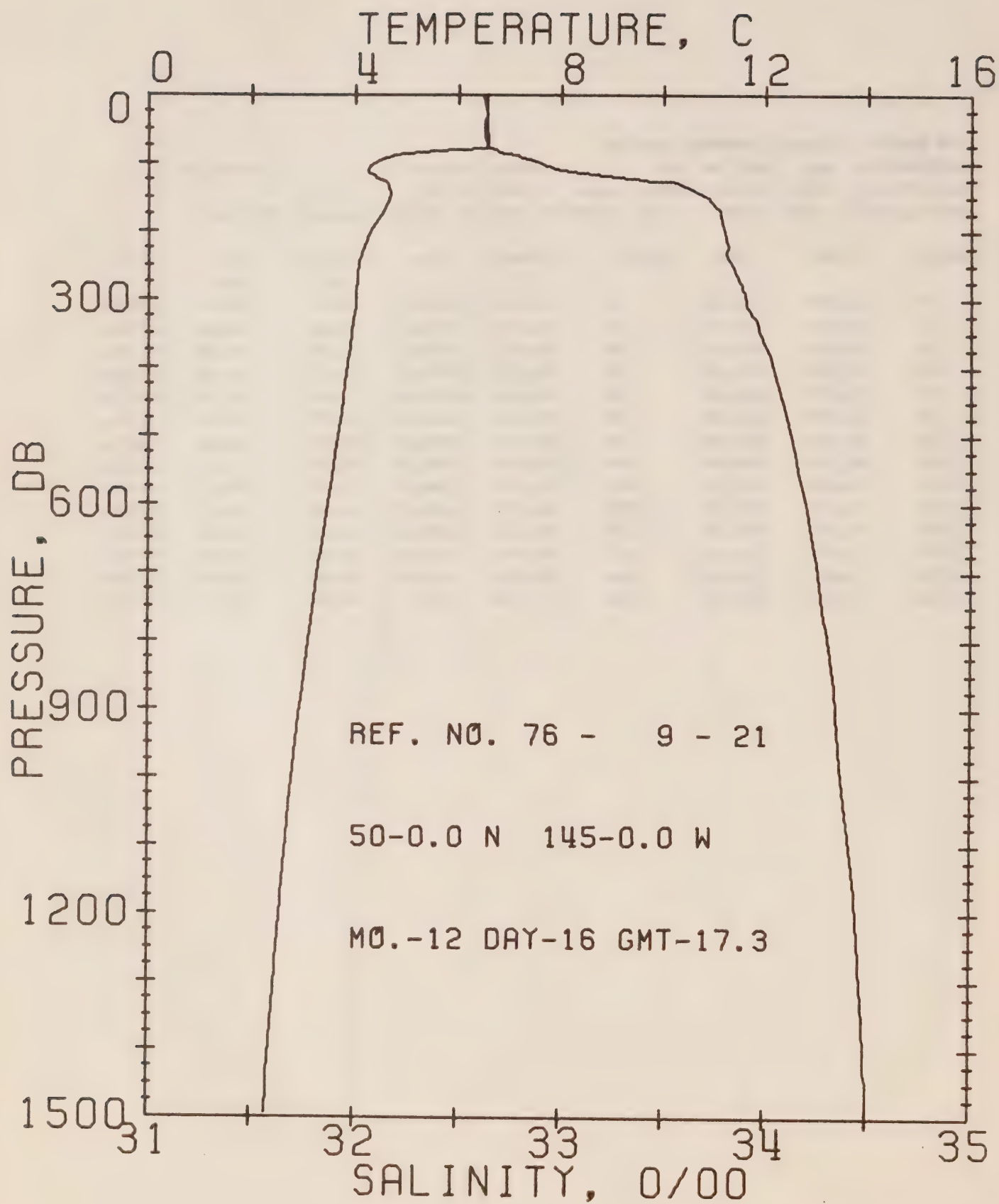
POSITION 50- 0.0N, 145- 0.0W

GMT 17.3

RESULTS OF STP CAST

71 POINTS TAKEN FROM ANALOG TRACE

PRESS	TEMP	SAL	DEPTH	SIGMA T	SVA	DELTA D	PDT. EN	SOUND
0	6.58	32.62	0	25.63	237.2	0.0	0.0	1474.
10	6.58	32.62	10	25.63	237.5	0.24	0.01	1474.
20	6.58	32.62	20	25.63	237.7	0.47	0.05	1475.
30	6.58	32.63	30	25.63	237.0	0.71	0.11	1475.
50	6.58	32.63	50	25.63	237.2	1.19	0.30	1475.
75	6.58	32.65	75	25.65	236.0	1.78	0.68	1476.
100	4.22	32.91	99	26.13	190.4	2.30	1.14	1467.
125	4.56	33.44	124	26.51	154.3	2.73	1.63	1469.
150	4.60	33.72	149	26.73	134.0	3.08	2.13	1470.
175	4.48	33.76	174	26.77	130.0	3.41	2.67	1470.
200	4.26	33.79	199	26.83	125.3	3.73	3.28	1470.
225	4.14	33.82	223	26.86	122.3	4.04	3.95	1470.
250	4.07	33.86	248	26.90	118.9	4.34	4.68	1470.
300	4.00	33.91	298	26.94	114.7	4.92	6.31	1470.



## OFFSHORE OCEANOGRAPHY GROUP

REFERENCE NO. 76- 9- 21

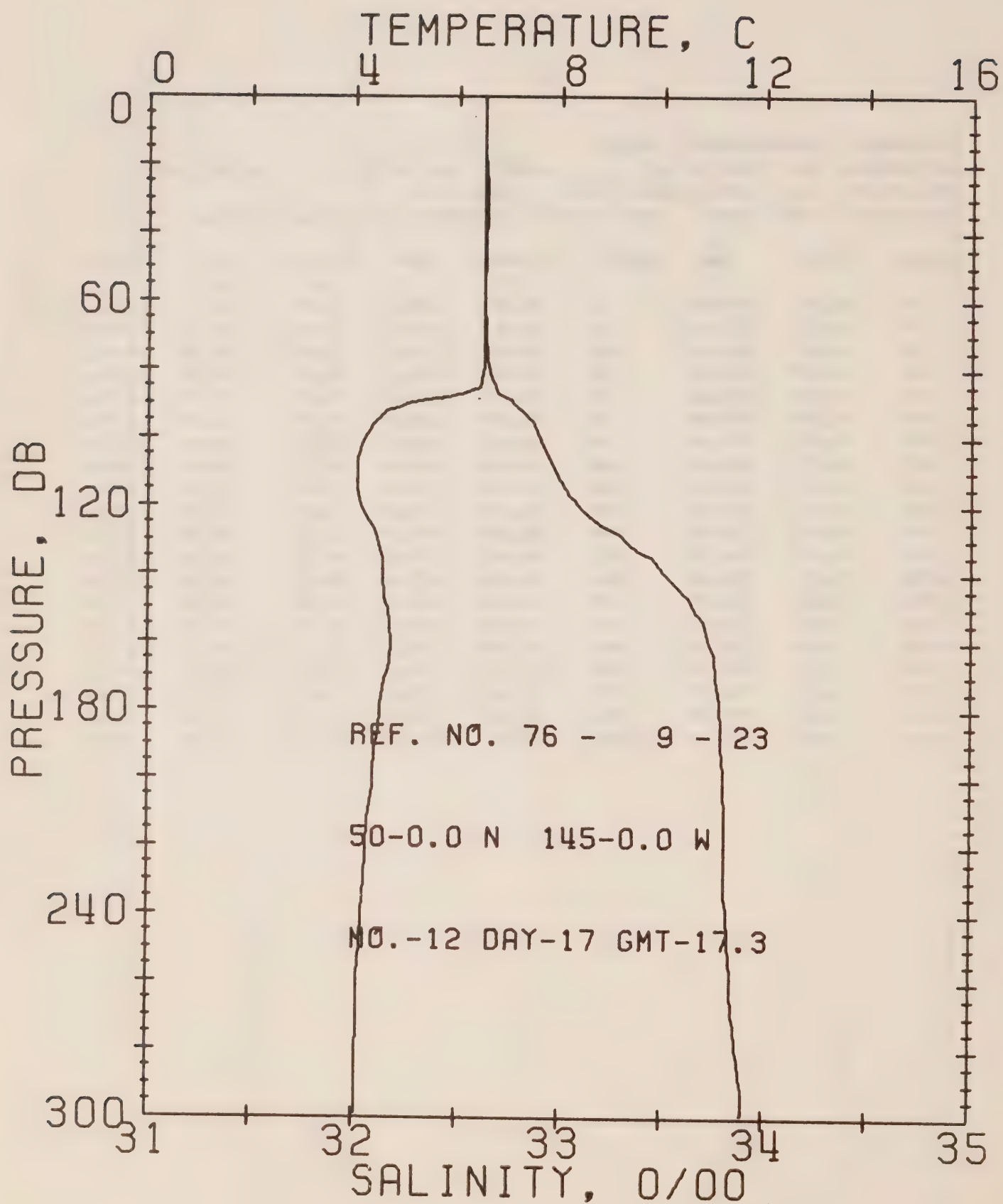
DATE 16/12/76

STATION P

POSITION 50- 0.0N, 145- 0.0W GMT 17.3

RESULTS OF STP CAST 101 POINTS TAKEN FROM ANALOG TRACE

PRESS	TEMP	SAL	DEPTH	SIGMA T	SVA	DELTA D	POT. EN	SOUND
0	6.57	32.62	0	25.63	237.0	0.0	0.0	1474.
10	6.57	32.63	10	25.63	236.8	0.24	0.01	1474.
20	6.57	32.63	20	25.64	236.5	0.47	0.05	1475.
30	6.57	32.64	30	25.64	236.1	0.71	0.11	1475.
50	6.57	32.63	50	25.64	237.1	1.18	0.30	1475.
75	6.56	32.64	75	25.64	236.7	1.78	0.68	1475.
100	4.38	32.90	99	26.10	192.9	2.31	1.15	1467.
125	4.53	33.44	124	26.52	153.9	2.75	1.66	1469.
150	4.68	33.71	149	26.72	135.3	3.11	2.15	1470.
175	4.52	33.78	174	26.79	128.8	3.43	2.70	1470.
200	4.31	33.80	199	26.82	125.4	3.75	3.30	1470.
225	4.18	33.82	223	26.85	122.8	4.06	3.98	1470.
250	4.08	33.84	248	26.88	120.6	4.37	4.71	1470.
300	4.03	33.91	298	26.94	115.0	4.96	6.35	1470.
400	3.86	34.04	397	27.06	104.4	6.05	10.26	1472.
500	3.69	34.13	496	27.15	96.6	7.06	14.86	1473.
600	3.50	34.20	595	27.23	90.1	7.99	20.09	1473.
800	3.13	34.31	793	27.35	79.6	9.68	32.13	1475.
1000	2.82	34.38	990	27.43	72.5	11.20	45.98	1477.
1200	2.56	34.44	1188	27.51	65.7	12.57	61.40	1480.



## OFFSHORE OCEANOGRAPHY GROUP

REFERENCE NO. 76- 9- 23

DATE 17/12/76

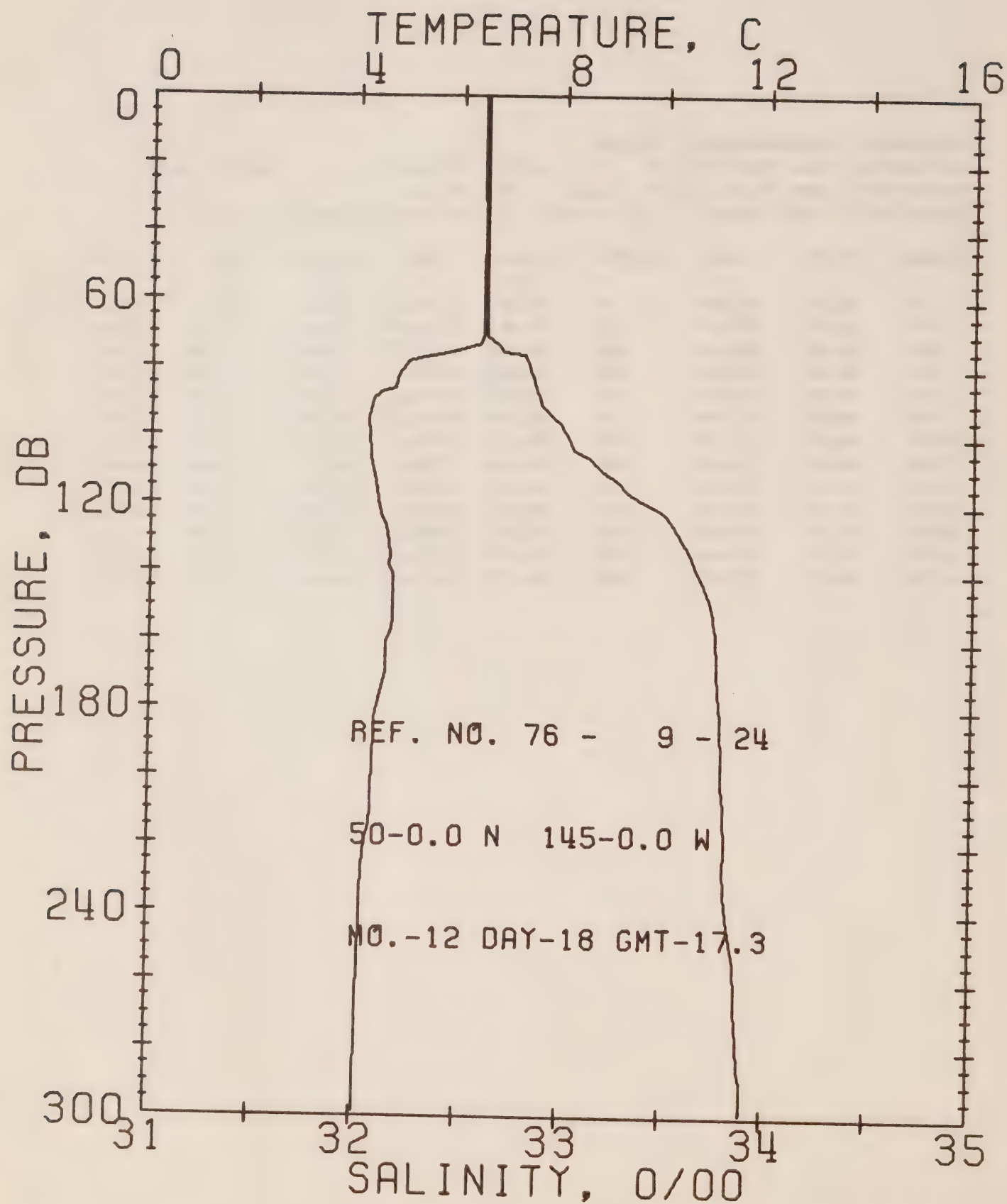
STATION P

POSITION 50- 0.0N, 145- 0.0W GMT 17.3

RESULTS OF STP CAST 71 POINTS TAKEN FROM ANALOG TRACE

PRESS	TEMP	SAL	DEPTH	SIGMA T	SVA	DELTA C	POT. EN	SOUND
0	6.51	32.63	0	25.64	235.6	0.0	0.0	1474.
10	6.51	32.63	10	25.64	235.9	0.24	0.01	1474.
20	6.51	32.63	20	25.65	235.7	0.47	0.05	1474.
30	6.51	32.64	30	25.65	235.4	0.71	0.11	1474.
50	6.52	32.63	50	25.64	236.2	1.18	0.30	1475.
75	6.52	32.64	75	25.65	236.1	1.77	0.68	1475.
100	4.19	32.89	99	26.12	191.3	2.31	1.16	1466.
125	4.32	33.18	124	26.34	170.9	2.77	1.68	1468.
150	4.66	33.65	149	26.67	139.9	3.15	2.21	1470.
175	4.54	33.77	174	26.78	129.7	3.49	2.77	1470.
200	4.37	33.80	199	26.82	125.9	3.81	3.38	1470.
225	4.22	33.81	223	26.84	123.8	4.12	4.05	1470.
250	4.12	33.83	248	26.87	121.4	4.42	4.80	1470.





## OFFSHORE OCEANOGRAPHY GROUP

REFERENCE NO. 76- 9- 24

DATE 18/12/76

STATION P

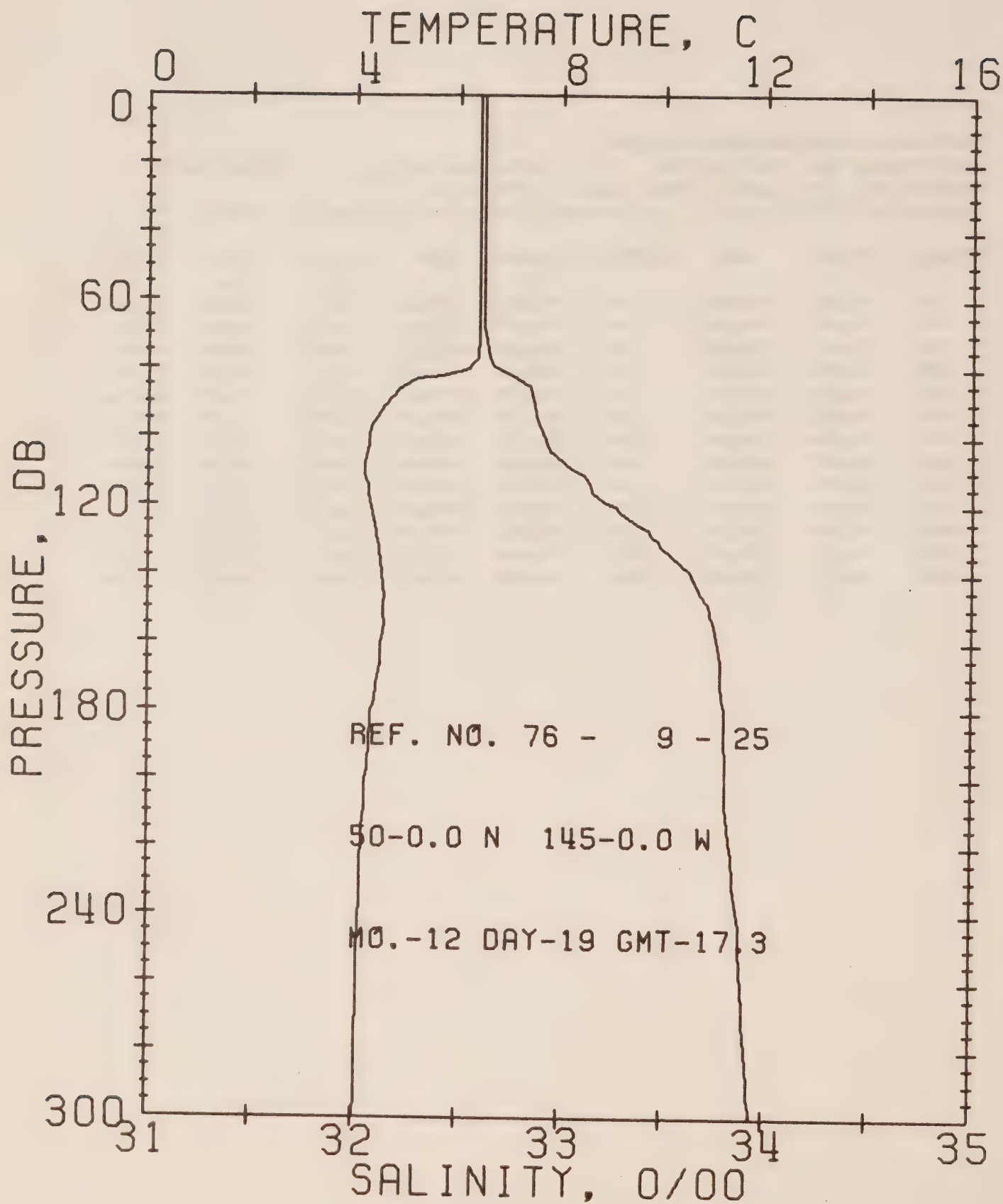
POSITION 50- 0.0N. 145- 0.0W

GMT 17.3

RESULTS OF STP CAST

69 POINTS TAKEN FROM ANALOG TRACE

PRESS	TEMP	SAL	DEPTH	SIGMA T	SVA	DELTA D	POT. EN	SOUND
0	6.43	32.62	0	25.65	235.3	0.0	0.0	1474.
10	6.43	32.62	10	25.65	235.6	0.24	0.01	1474.
20	6.43	32.62	20	25.65	235.7	0.47	0.05	1474.
30	6.44	32.62	30	25.64	236.0	0.71	0.11	1474.
50	6.44	32.62	50	25.64	236.3	1.18	0.30	1475.
75	5.81	32.70	75	25.79	223.1	1.77	0.68	1472.
100	4.24	33.02	99	26.21	182.3	2.26	1.11	1467.
125	4.55	33.53	124	26.58	147.6	2.67	1.58	1469.
150	4.73	33.73	149	26.72	134.8	3.02	2.08	1471.
175	4.47	33.77	174	26.78	129.0	3.35	2.62	1470.
200	4.34	33.79	199	26.81	126.4	3.67	3.23	1470.
225	4.17	33.80	223	26.84	123.8	3.98	3.91	1470.
250	4.11	33.85	248	26.88	120.1	4.29	4.65	1470.



## OFFSHORE OCEANOGRAPHY GROUP

REFERENCE NO. 76- 9- 25

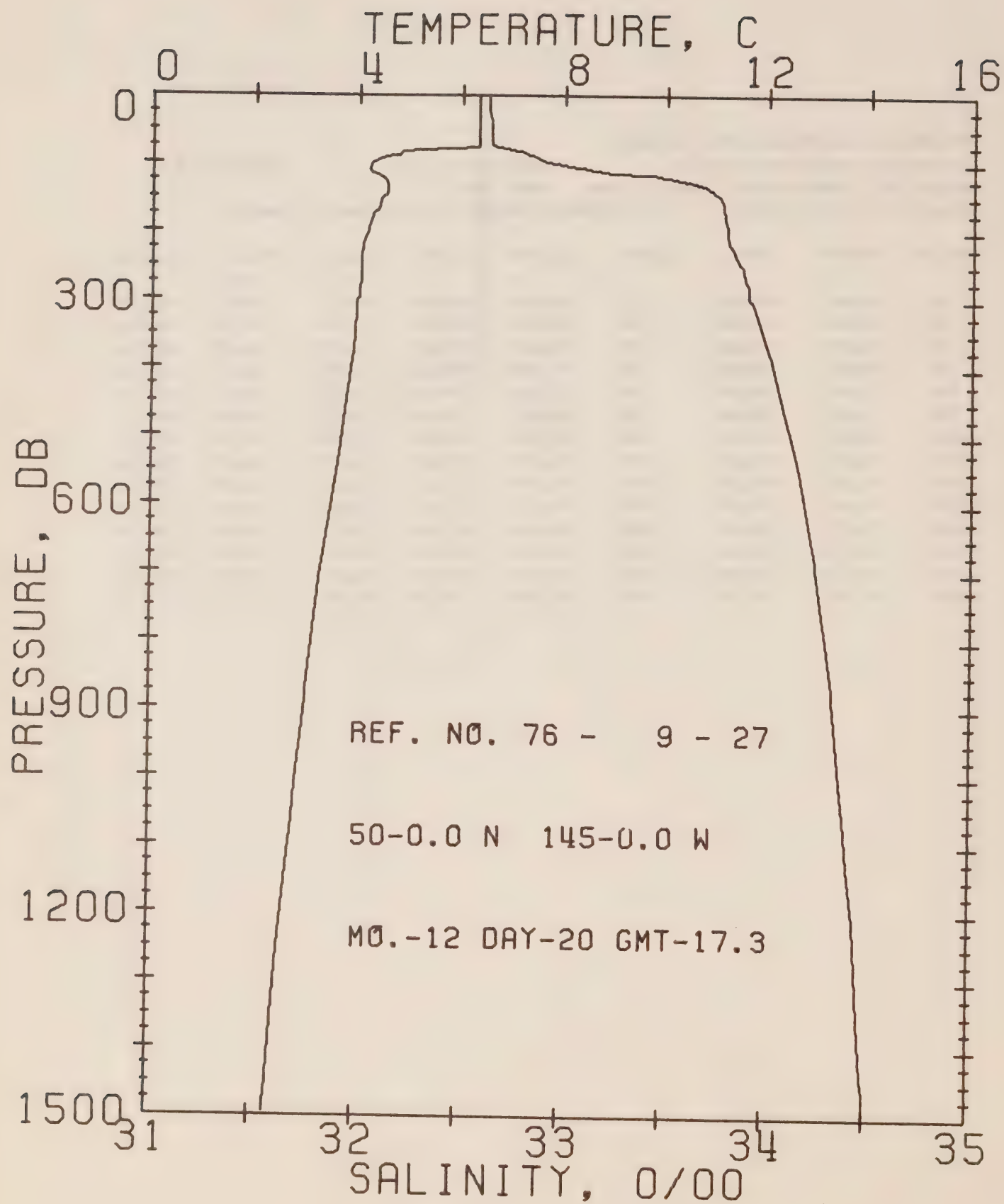
DATE 19/12/76

STATION P

POSITION 50- 0.0N, 145- 0.0W GMT 17.3

RESULTS OF STP CAST 71 POINTS TAKEN FROM ANALOG TRACE

PRESS	TEMP	SAL	DEPTH	SIGMA T	SVA	DELTA D	POT. EN	SOUND
0	6.41	32.62	0	25.65	235.1	0.0	0.0	1474.
10	6.41	32.62	10	25.65	235.4	0.24	0.01	1474.
20	6.40	32.62	20	25.65	235.5	0.47	0.05	1474.
30	6.40	32.62	30	25.65	235.5	0.71	0.11	1474.
50	6.41	32.62	50	25.65	235.9	1.18	0.30	1474.
75	6.39	32.64	75	25.67	234.0	1.77	0.63	1475.
100	4.27	32.92	99	26.13	190.3	2.28	1.13	1467.
125	4.39	33.37	124	26.48	157.6	2.72	1.64	1468.
150	4.57	33.72	149	26.74	133.3	3.08	2.14	1470.
175	4.41	33.79	174	26.80	127.2	3.41	2.68	1470.
200	4.21	33.81	199	26.84	123.5	3.72	3.27	1469.
225	4.13	33.84	223	26.88	120.5	4.03	3.94	1470.
250	4.09	33.88	248	26.91	117.5	4.32	4.66	1470.
300	4.03	33.94	298	26.97	112.7	4.90	6.27	1470.





## OFFSHORE OCEANOGRAPHY GROUP

REFERENCE NO. 76- 9- 27

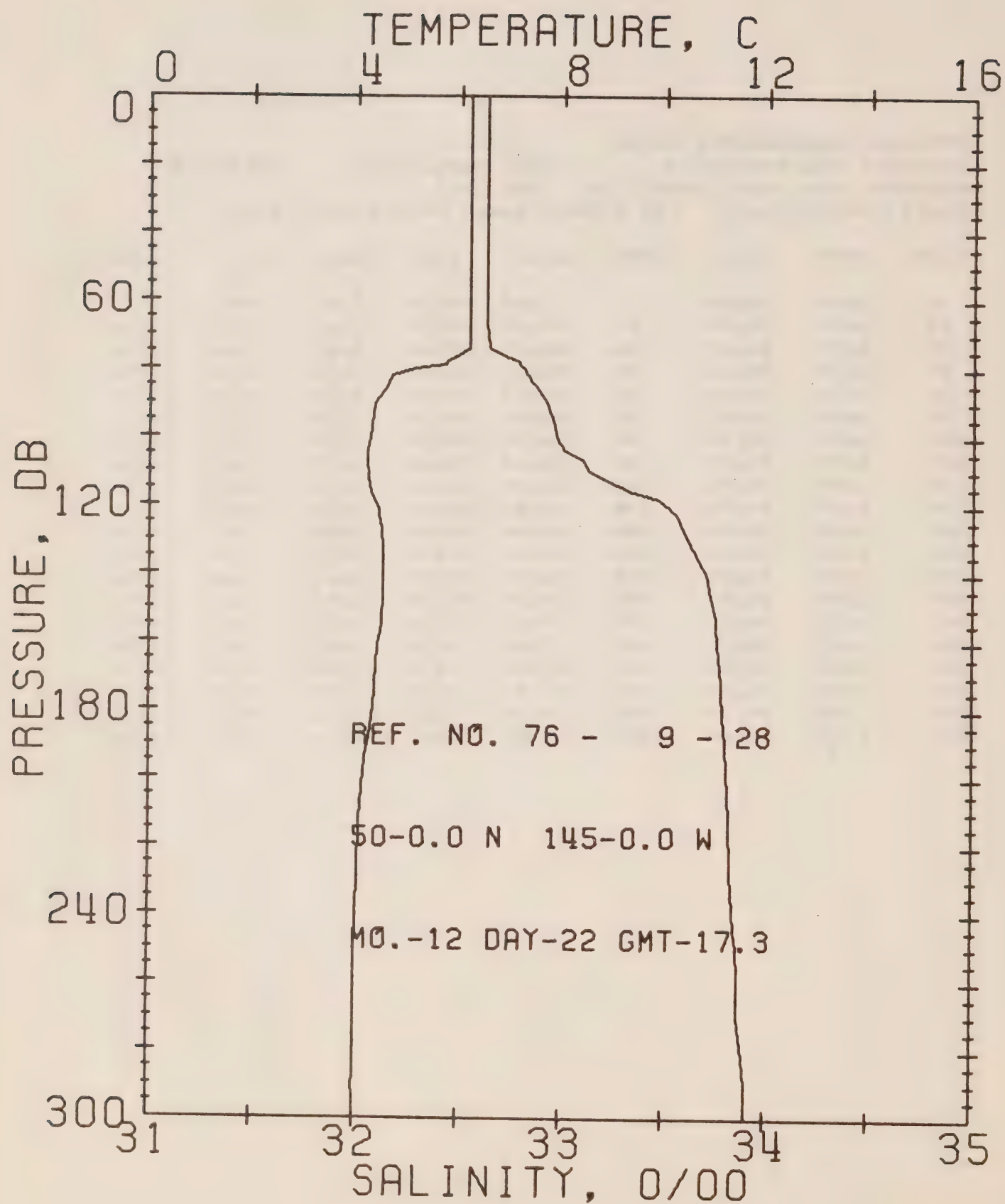
DATE 20/12/76

STATION P

POSITION 50- 0.0N, 145- 0.0W GMT 17.3

RESULTS OF STP CAST 85 POINTS TAKEN FROM ANALOG TRACE

PRESS	TEMP	SAL	DEPTH	SIGMA T	SVA	DELTA D	POT. EN	SJUND
0	6.33	32.63	0	25.67	233.4	0.0	0.0	1473.
10	6.33	32.63	10	25.67	233.7	0.23	0.01	1473.
20	6.33	32.63	20	25.67	233.8	0.47	0.05	1474.
30	6.33	32.63	30	25.67	233.7	0.70	0.11	1474.
50	6.33	32.64	50	25.67	233.5	1.17	0.30	1474.
75	6.31	32.67	75	25.70	231.2	1.75	0.67	1474.
100	4.24	32.94	99	26.15	188.1	2.26	1.12	1467.
125	4.52	33.59	124	26.64	142.6	2.68	1.60	1469.
150	4.47	33.76	149	26.78	129.2	3.01	2.07	1470.
175	4.27	33.79	174	26.82	125.5	3.33	2.59	1469.
200	4.18	33.80	199	26.84	124.0	3.64	3.19	1469.
225	4.07	33.83	223	26.87	121.0	3.95	3.85	1469.
250	4.05	33.87	248	26.91	117.5	4.25	4.58	1470.
300	3.98	33.92	298	26.95	113.8	4.83	6.20	1470.
400	3.87	34.03	397	27.05	105.1	5.92	10.09	1472.
500	3.69	34.12	496	27.14	97.3	6.93	14.72	1473.
600	3.50	34.19	595	27.22	91.0	7.87	19.99	1473.
800	3.16	34.29	793	27.33	81.0	9.59	32.17	1475.
1000	2.86	34.37	990	27.42	73.6	11.13	46.26	1478.
1200	2.61	34.44	1188	27.49	66.9	12.53	62.00	1480.



## OFFSHORE OCEANOGRAPHY GROUP

REFERENCE NO. 76- 9- 28

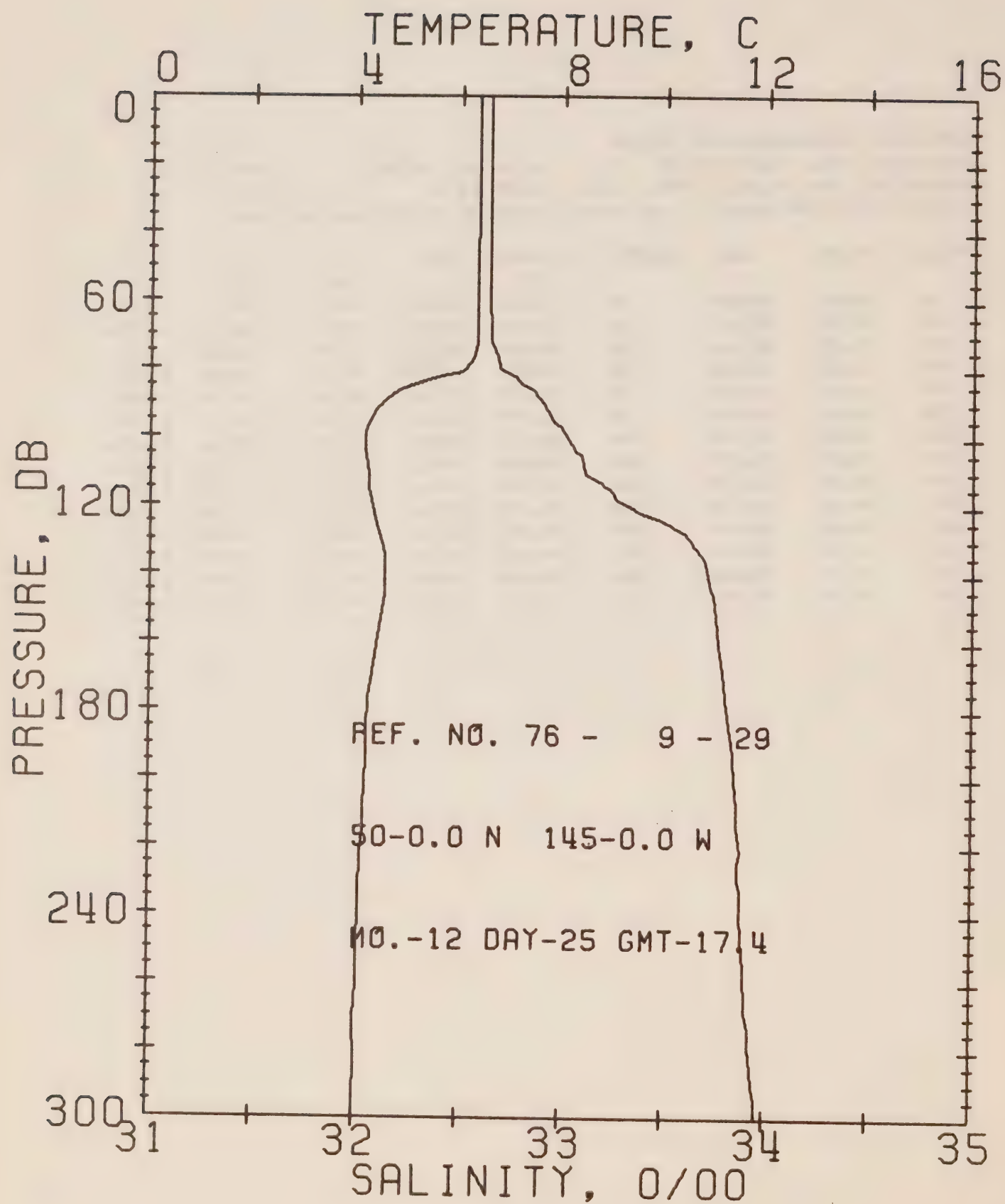
DATE 22/12/76

STATION P

POSITION 50- 0.0N, 145- 0.0W GMT 17.3

RESULTS OF STP CAST 63 POINTS TAKEN FROM ANALOG TRACE

PRESS	TEMP	SAL	DEPTH	SIGMA T	SVA	DELTA D	POT. EN	SOUND
0	6.20	32.63	0	25.68	231.8	0.0	0.0	1473.
10	6.20	32.63	10	25.68	232.2	0.23	0.01	1473.
20	6.20	32.63	20	25.68	232.3	0.46	0.05	1473.
30	6.20	32.63	30	25.68	232.4	0.70	0.11	1473.
50	6.20	32.63	50	25.68	232.6	1.16	0.30	1474.
75	6.09	32.67	75	25.73	228.6	1.74	0.57	1474.
100	4.27	32.97	99	26.17	186.4	2.24	1.11	1467.
125	4.48	33.57	124	26.63	143.3	2.65	1.58	1469.
150	4.52	33.74	149	26.75	131.6	2.99	2.06	1470.
175	4.36	33.78	174	26.80	127.1	3.32	2.59	1470.
200	4.16	33.81	199	26.85	122.9	3.63	3.19	1469.
225	4.06	33.83	223	26.87	120.8	3.93	3.85	1469.
250	4.01	33.86	248	26.90	118.2	4.23	4.57	1469.
300	4.00	33.91	298	26.94	114.7	4.61	6.20	1470.



## OFFSHORE OCEANOGRAPHY GROUP

REFERENCE NO. 76- 9- 29

DATE 25/12/76

STATION P

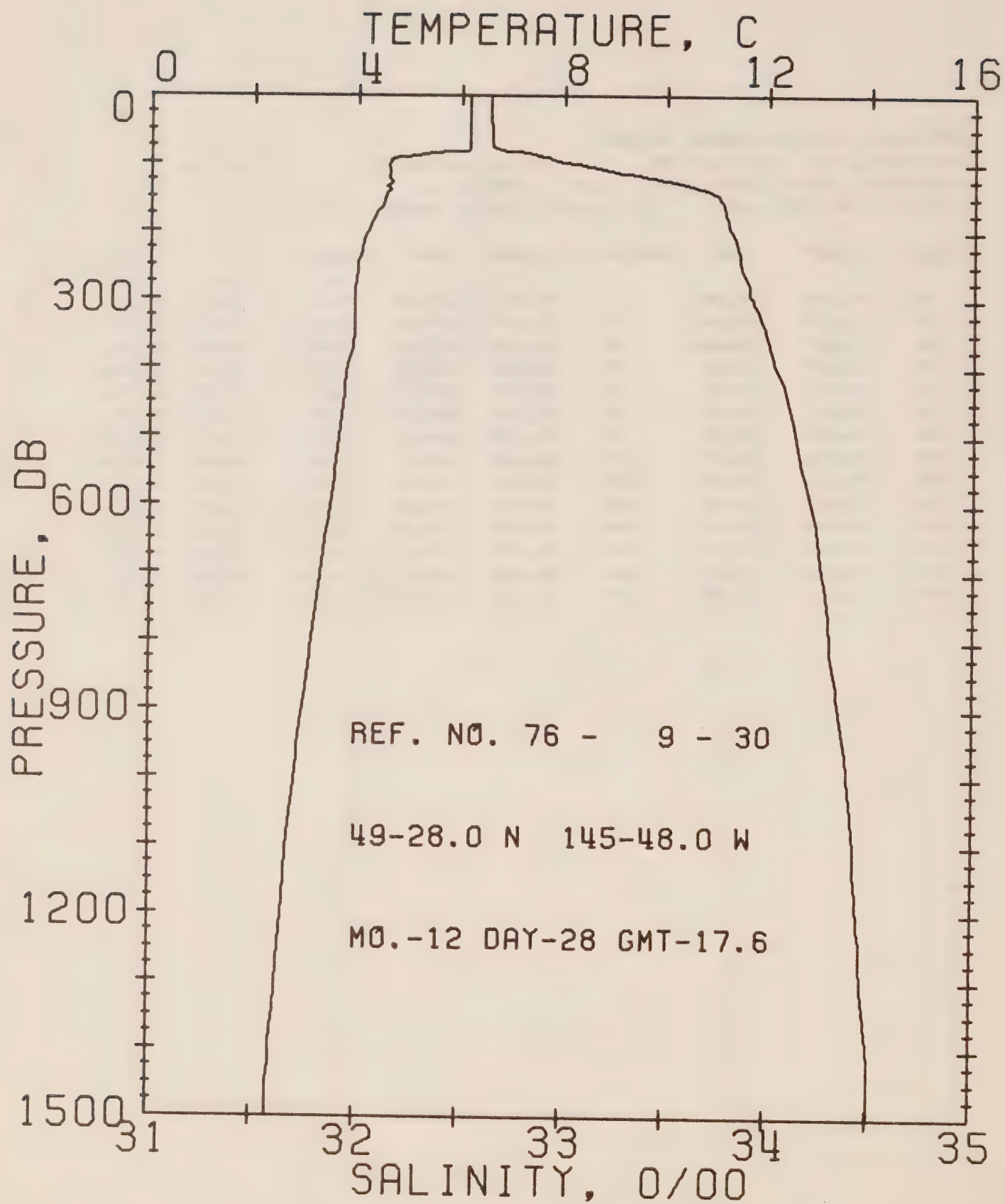
POSITION 50- 0.0N, 145- 0.0W

GMT 17.4

RESULTS OF STP CAST 71 POINTS TAKEN FROM ANALOG TRACE

PRESS	TEMP	SAL	DEPTH	SIGMA T	SVA	DELTA D	POT. EN	SOUND
0	6.35	32.64	0	25.67	232.8	0.0	0.0	1473.
10	6.35	32.64	10	25.67	233.2	0.23	0.01	1474.
20	6.35	32.64	20	25.67	233.3	0.47	0.05	1474.
30	6.35	32.64	30	25.67	233.4	0.70	0.11	1474.
50	6.33	32.64	50	25.67	233.5	1.17	0.30	1474.
75	6.27	32.67	75	25.70	230.8	1.75	0.67	1474.
100	4.16	33.02	99	26.22	181.5	2.26	1.12	1467.
125	4.39	33.51	124	26.59	147.3	2.68	1.60	1469.
150	4.52	33.75	149	26.76	131.1	3.02	2.08	1470.
175	4.26	33.80	174	26.83	124.7	3.34	2.61	1469.
200	4.20	33.85	199	26.87	120.5	3.65	3.19	1469.
225	4.10	33.87	223	26.90	118.1	3.94	3.84	1469.
250	4.06	33.89	248	26.92	116.2	4.24	4.55	1470.
300	4.00	33.96	298	26.98	110.9	4.81	6.14	1470.





## OFFSHORE OCEANOGRAPHY GROUP

REFERENCE NO. 76- 9- 30

DATE 28/12/76

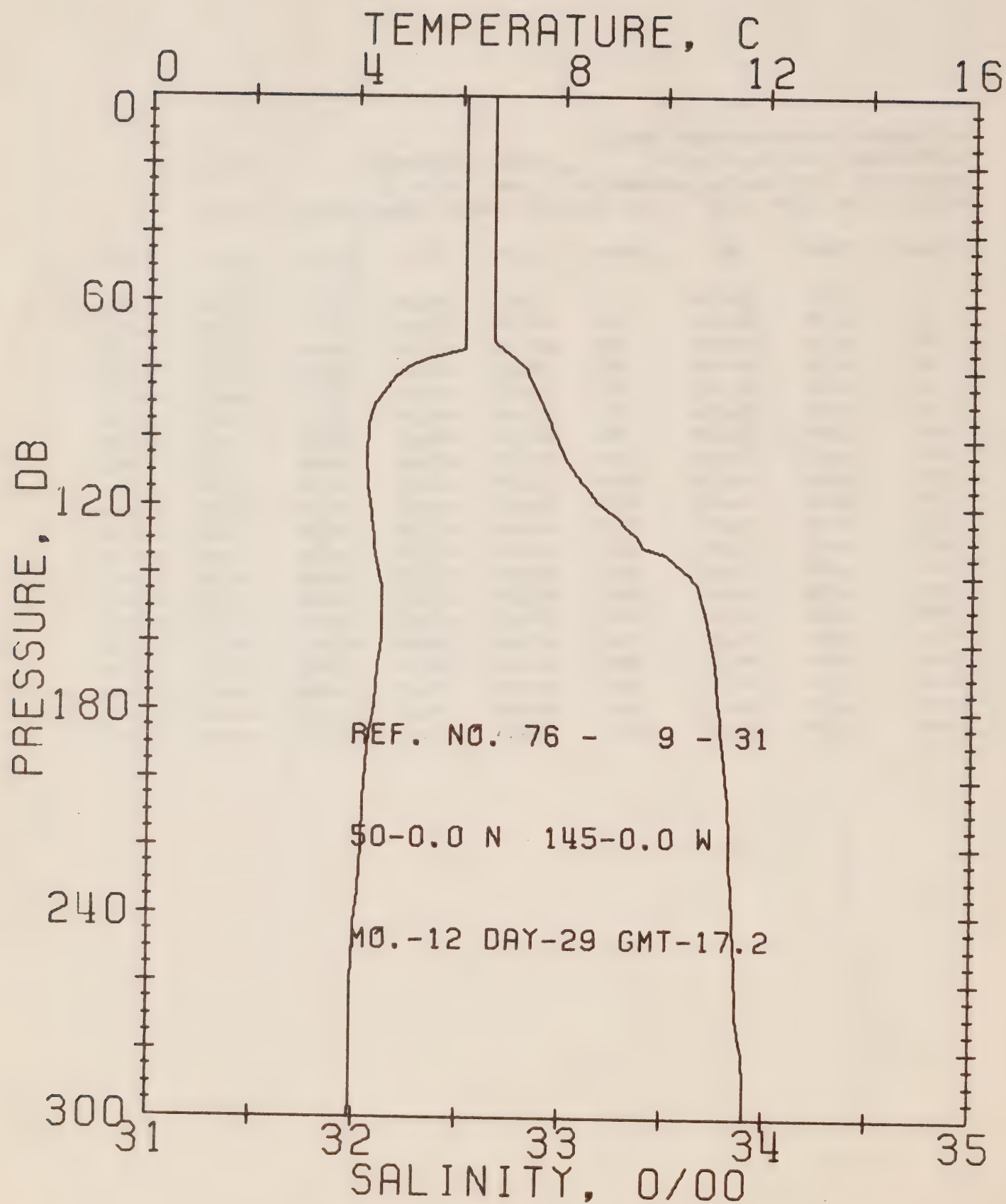
STATION P

POSITION 49-28.0N, 145-48.0W

GMT 17.6

RESULTS OF STP CAST 122 POINTS TAKEN FROM ANALOG TRACE

PRESS	TEMP	SAL	DEPTH	SIGMA T	SVA	DELTA D	POT. EN	SOUND
0	6.16	32.64	0	25.70	230.6	0.0	0.0	1473.
10	6.16	32.64	10	25.70	230.9	0.23	0.01	1473.
20	6.16	32.64	20	25.70	231.0	0.46	0.05	1473.
30	6.16	32.64	30	25.70	231.1	0.69	0.11	1473.
50	6.17	32.65	50	25.70	230.9	1.15	0.29	1473.
75	6.16	32.65	75	25.70	230.9	1.73	0.66	1474.
100	4.60	33.04	99	26.19	184.3	2.25	1.12	1468.
125	4.65	33.52	124	26.56	149.5	2.67	1.60	1470.
150	4.53	33.75	149	26.77	130.5	3.01	2.08	1470.
175	4.33	33.79	174	26.82	126.1	3.33	2.61	1469.
200	4.19	33.82	199	26.85	122.7	3.64	3.21	1469.
225	4.07	33.85	223	26.89	119.3	3.95	3.86	1469.
250	4.00	33.87	248	26.91	117.6	4.24	4.58	1469.
300	3.95	33.93	298	26.97	112.7	4.82	6.19	1470.
400	3.81	34.04	397	27.07	103.7	5.90	10.05	1471.
500	3.66	34.14	496	27.16	95.6	6.89	14.59	1472.
600	3.49	34.21	595	27.24	89.1	7.82	19.77	1473.
800	3.15	34.31	793	27.34	79.8	9.49	31.69	1475.
1000	2.82	34.40	990	27.44	71.1	11.00	45.48	1477.
1200	2.59	34.44	1188	27.50	66.0	12.37	60.76	1480.



## OFFSHORE OCEANOGRAPHY GROUP

REFERENCE NO. 76- 9- 31

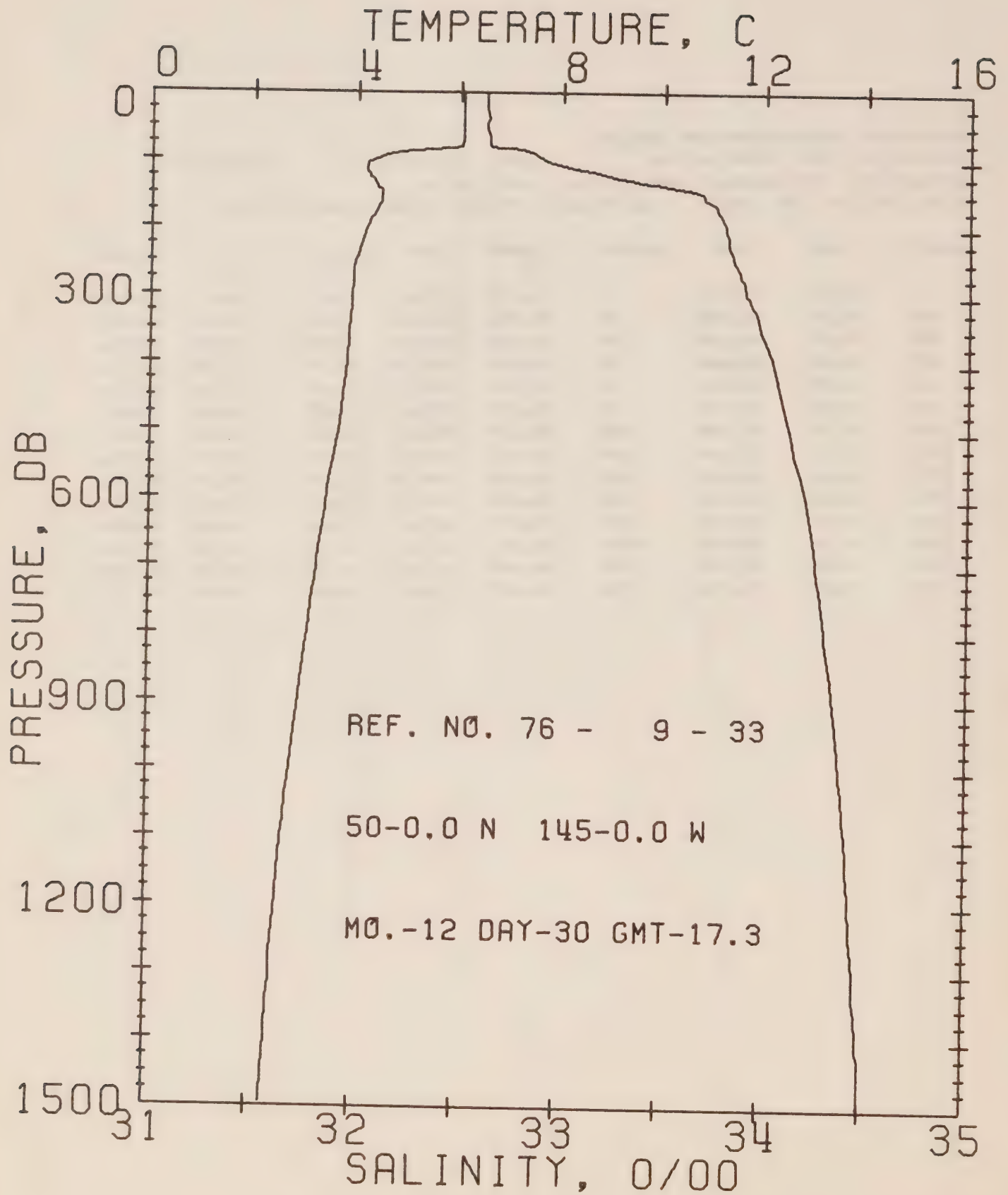
DATE 29/12/76

STATION P

POSITION 50- 0.0N, 145- 0.0W GMT 17.2

RESULTS OF STP CAST 60 POINTS TAKEN FROM ANALOG TRACE

PRESS	TEMP	SAL	DEPTH	SIGMA T	SVA	DELTA D	PCT. EN	SOUND
0	6.07	32.66	0	25.72	228.0	0.0	0.0	1472.
10	6.07	32.66	10	25.72	228.4	0.23	0.01	1472.
20	6.07	32.66	20	25.72	228.5	0.46	0.05	1473.
30	6.07	32.66	30	25.72	228.6	0.69	0.10	1473.
50	6.08	32.66	50	25.72	228.9	1.14	0.29	1473.
75	5.77	32.73	75	25.81	220.4	1.71	0.66	1472.
100	4.20	32.96	99	26.17	186.2	2.21	1.09	1467.
125	4.31	33.29	124	26.42	162.7	2.65	1.60	1468.
150	4.52	33.69	149	26.72	134.9	3.01	2.11	1470.
175	4.38	33.76	174	26.79	128.5	3.34	2.65	1470.
200	4.20	33.81	199	26.84	123.5	3.66	3.25	1469.
225	4.10	33.83	223	26.87	121.2	3.96	3.91	1469.
250	3.99	33.86	248	26.90	118.2	4.26	4.64	1469.
300	3.93	33.91	298	26.95	114.0	4.84	6.26	1470.





## OFFSHORE OCEANOGRAPHY GROUP

REFERENCE NO. 76- 9- 33

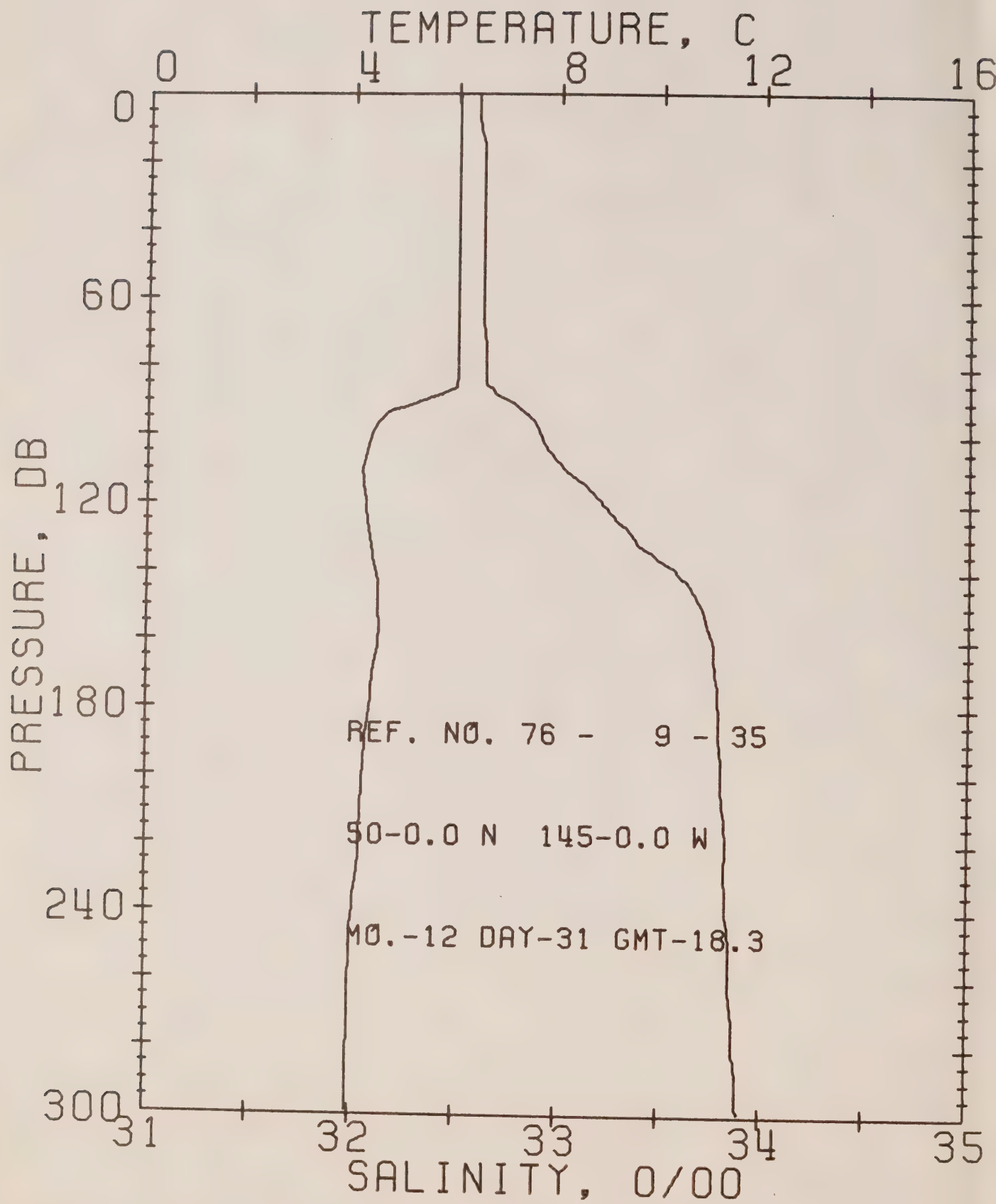
DATE 30/12/76

STATION P

POSITION 50- 0.0N, 145- 0.0W GMT 17.3

RESULTS OF STP CAST 130 POINTS TAKEN FROM ANALOG TRACE

PRESS	TEMP	SAL	DEPTH	SIGMA T	SVA	DELTA D	POT. EN	SOUND
0	6.05	32.63	0	25.70	230.0	0.0	0.0	1472.
10	6.05	32.63	10	25.70	230.4	0.23	0.01	1472.
20	6.05	32.63	20	25.70	230.5	0.46	0.05	1472.
30	6.05	32.63	30	25.70	230.3	0.69	0.11	1473.
50	6.04	32.63	50	25.70	230.7	1.15	0.29	1473.
75	6.03	32.64	75	25.71	230.2	1.73	0.66	1473.
100	4.32	32.91	99	26.12	191.2	2.25	1.12	1467.
125	4.27	33.28	124	26.42	163.2	2.70	1.63	1468.
150	4.48	33.69	149	26.72	134.7	3.07	2.15	1470.
175	4.38	33.77	174	26.79	128.2	3.39	2.69	1470.
200	4.20	33.81	199	26.84	123.4	3.71	3.29	1469.
225	4.09	33.82	223	26.86	121.8	4.01	3.96	1469.
250	3.98	33.85	248	26.90	118.6	4.31	4.68	1469.
300	3.93	33.92	298	26.96	113.2	4.89	6.30	1470.
400	3.82	34.05	397	27.07	103.5	5.97	10.15	1471.
500	3.68	34.13	496	27.15	96.5	6.98	14.74	1473.
600	3.45	34.21	595	27.24	88.9	7.90	19.93	1473.
800	3.11	34.31	793	27.35	79.3	9.58	31.86	1475.
1000	2.79	34.39	990	27.44	71.4	11.08	45.61	1477.
1200	2.54	34.44	1188	27.50	65.8	12.45	60.88	1480.



## OFFSHORE OCEANOGRAPHY GROUP

REFERENCE NO. 76- 9- 35

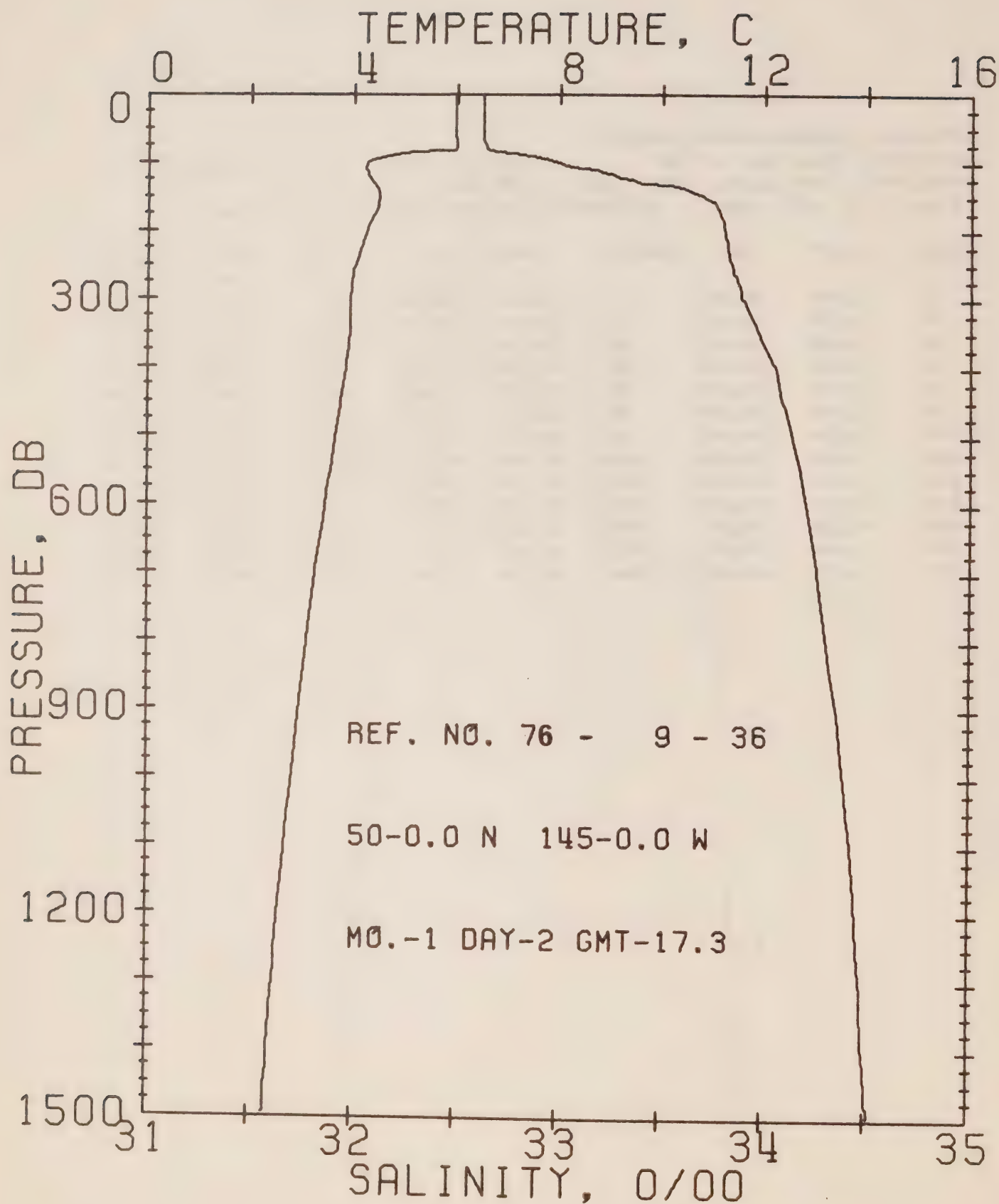
DATE 31/12/76

STATION P

POSITION 50- 0.0N, 145- 0.0W GMT 18.3

RESULTS OF STP CAST 83 POINTS TAKEN FROM ANALOG TRACE

PRESS	TEMP	SAL	DEPTH	SIGMA T	SVA	DELTA TD	POT. EN	SOUND
0	6.02	32.60	0	25.68	231.9	0.0	0.0	1472.
10	6.03	32.61	10	25.69	231.8	0.23	0.01	1472.
20	6.03	32.63	20	25.70	230.3	0.46	0.05	1472.
30	6.03	32.63	30	25.70	230.4	0.69	0.11	1473.
50	6.03	32.63	50	25.70	230.6	1.15	0.29	1473.
75	6.02	32.64	75	25.71	230.0	1.73	0.66	1473.
100	4.36	32.91	99	26.11	192.0	2.27	1.14	1467.
125	4.29	33.29	124	26.42	162.7	2.72	1.65	1468.
150	4.52	33.70	149	26.72	134.6	3.08	2.16	1470.
175	4.37	33.78	174	26.80	127.2	3.41	2.70	1470.
200	4.23	33.80	199	26.83	124.4	3.72	3.30	1469.
225	4.14	33.82	223	26.86	121.9	4.03	3.97	1470.
250	3.99	33.85	248	26.90	118.9	4.33	4.70	1469.



## OFFSHORE OCEANOGRAPHY GROUP

REFERENCE NO. 76- 9- 36

DATE 2/ 1/77

STATION P

POSITION 50- 0.0N, 145- 0.0W

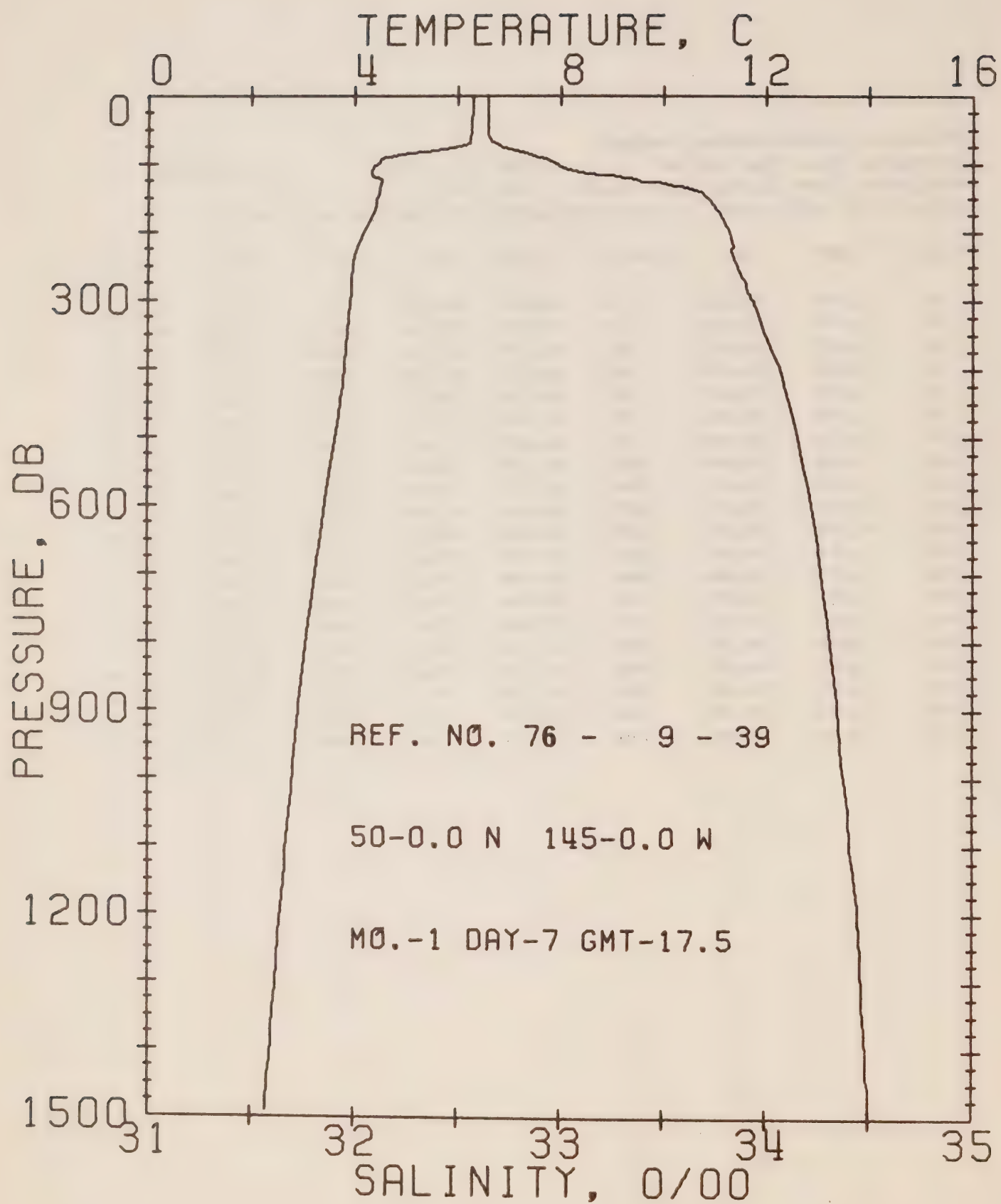
GMT 17.3

RESULTS OF STP CAST

114 POINTS TAKEN FROM ANALOG TRACE

PRESS	TEMP	SAL	DEPTH	SIGMA T	SVA	DELTA D	PCT. EN	SOUND
0	5.97	32.63	0	25.71	229.1	0.0	0.0	1472.
10	5.97	32.63	10	25.71	229.4	0.23	0.01	1472.
20	5.97	32.63	20	25.71	229.6	0.40	0.05	1472.
30	5.98	32.63	30	25.71	229.8	0.69	0.11	1472.
50	5.98	32.63	50	25.71	230.0	1.15	0.29	1473.
75	5.99	32.64	75	25.71	229.9	1.72	0.66	1473.
100	4.26	32.98	99	26.18	135.2	2.25	1.12	1457.
125	4.34	33.36	124	26.47	158.0	2.67	1.51	1459.
150	4.51	33.71	149	26.73	133.7	3.03	2.11	1470.
175	4.40	33.78	174	26.80	127.5	3.35	2.65	1470.
200	4.25	33.80	199	26.84	124.3	3.67	3.25	1470.
225	4.14	33.82	223	26.86	122.3	3.98	3.92	1470.
250	4.04	33.84	248	26.88	120.0	4.28	4.65	1470.
300	3.95	33.90	298	26.94	114.9	4.87	6.29	1470.
400	3.86	34.06	397	27.08	103.1	5.96	10.19	1472.
500	3.67	34.14	496	27.16	95.8	6.95	14.74	1472.
600	3.47	34.21	595	27.24	89.1	7.88	19.91	1473.
800	3.12	34.31	793	27.34	79.6	9.56	31.88	1475.
1000	2.83	34.39	990	27.44	71.5	11.07	45.65	1477.
1200	2.58	34.45	1188	27.51	65.3	12.45	60.93	1430.





## OFFSHORE OCEANOGRAPHY GROUP

REFERENCE NO. 76- 9- 39

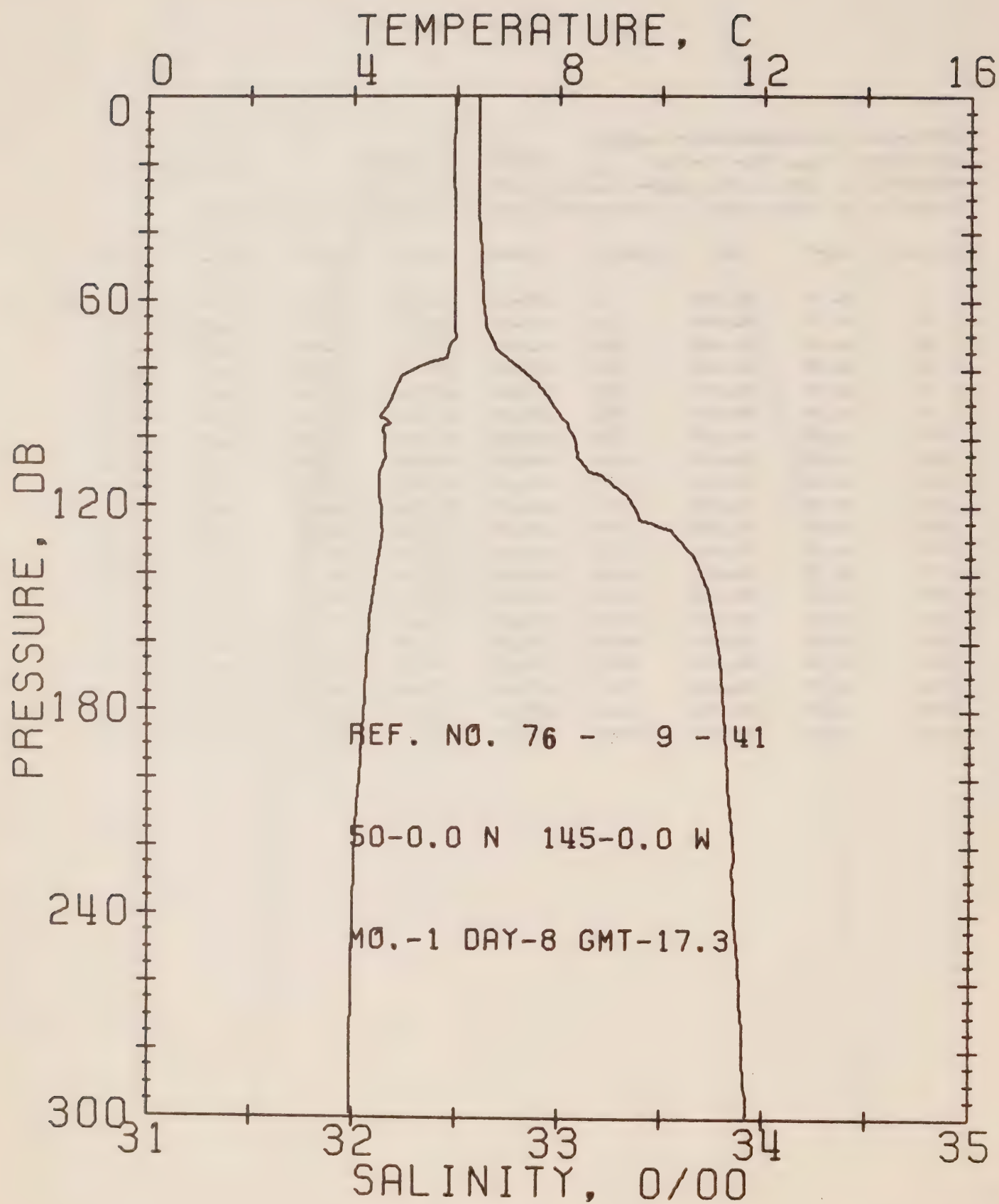
DATE 7/ 1/77

STATION P

POSITION 50- 0.0N, 145- 0.0W GMT 17.5

RESULTS OF STP CAST 112 POINTS TAKEN FROM ANALOG TRACE

PRESS	TEMP	SAL	DEPTH	SIGMA T	SVA	DELTA D	POT. EN	SOUND
0	6.29	32.65	0	25.69	231.4	0.0	0.0	1473.
10	6.29	32.65	10	25.69	231.7	0.23	0.01	1473.
20	6.29	32.65	20	25.69	231.8	0.46	0.05	1473.
30	6.28	32.65	30	25.69	231.9	0.70	0.11	1474.
50	6.27	32.65	50	25.69	232.0	1.16	0.30	1474.
75	5.96	32.71	75	25.78	223.6	1.74	0.66	1473.
100	4.45	32.98	99	26.16	187.5	2.24	1.11	1468.
125	4.52	33.38	124	26.47	158.0	2.63	1.61	1469.
150	4.45	33.71	149	26.74	133.0	3.03	2.10	1469.
175	4.35	33.78	174	26.80	127.3	3.35	2.64	1470.
200	4.18	33.82	199	26.86	122.4	3.67	3.24	1469.
225	4.02	33.83	223	26.88	120.1	3.97	3.89	1469.
250	3.97	33.86	248	26.91	118.0	4.27	4.61	1469.
300	3.92	33.94	298	26.98	111.7	4.84	6.22	1470.
400	3.81	34.07	397	27.09	101.8	5.91	10.04	1471.
500	3.64	34.16	496	27.18	94.1	6.89	14.52	1472.
600	3.44	34.22	595	27.25	87.9	7.80	19.61	1473.
800	3.08	34.31	793	27.35	78.9	9.47	31.45	1475.
1000	2.81	34.38	990	27.43	72.0	10.97	45.22	1477.
1200	2.58	34.45	1188	27.51	65.5	12.35	60.64	1480.



## OFFSHORE OCEANOGRAPHY GROUP

REFERENCE NO. 76- 9- 41

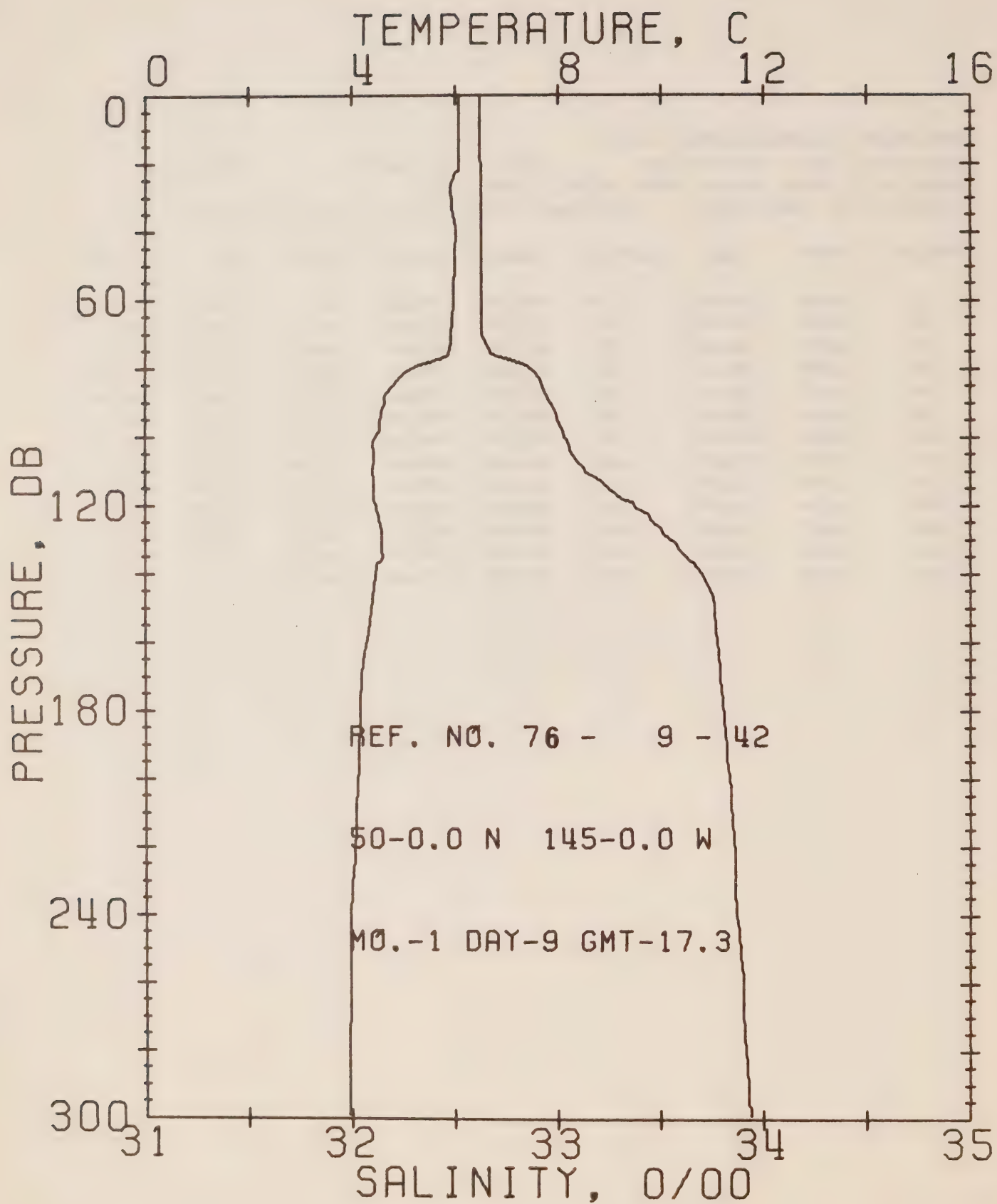
DATE 8/ 1/77

STATION P

POSITION 50- 0.0N. 145- 0.0W GMT 17.3

RESULTS OF STP CAST 74 POINTS TAKEN FROM ANALOG TRACE

PRESS	TEMP	SAL	DEPTH	SIGMA T	SVA	DELTA D	POT. EN	SOUND
0	5.97	32.61	0	25.69	230.6	0.0	0.0	1472.
10	5.97	32.61	10	25.70	230.9	0.23	0.01	1472.
20	5.96	32.61	20	25.70	230.9	0.46	0.03	1472.
30	5.97	32.61	30	25.70	231.1	0.69	0.11	1472.
50	5.97	32.62	50	25.70	230.5	1.15	0.29	1473.
75	5.84	32.71	75	25.79	222.9	1.73	0.66	1473.
100	4.61	33.07	99	26.21	182.6	2.22	1.10	1468.
125	4.56	33.46	124	26.53	152.8	2.64	1.58	1469.
150	4.35	33.74	149	26.78	129.5	2.99	2.06	1469.
175	4.24	33.80	174	26.83	124.5	3.30	2.58	1469.
200	4.13	33.83	199	26.87	121.2	3.61	3.17	1469.
225	4.03	33.86	223	26.90	118.3	3.91	3.82	1469.
250	3.99	33.87	248	26.92	117.0	4.20	4.53	1469.





## OFFSHORE OCEANOGRAPHY GROUP

REFERENCE NO. 76- 9- 42

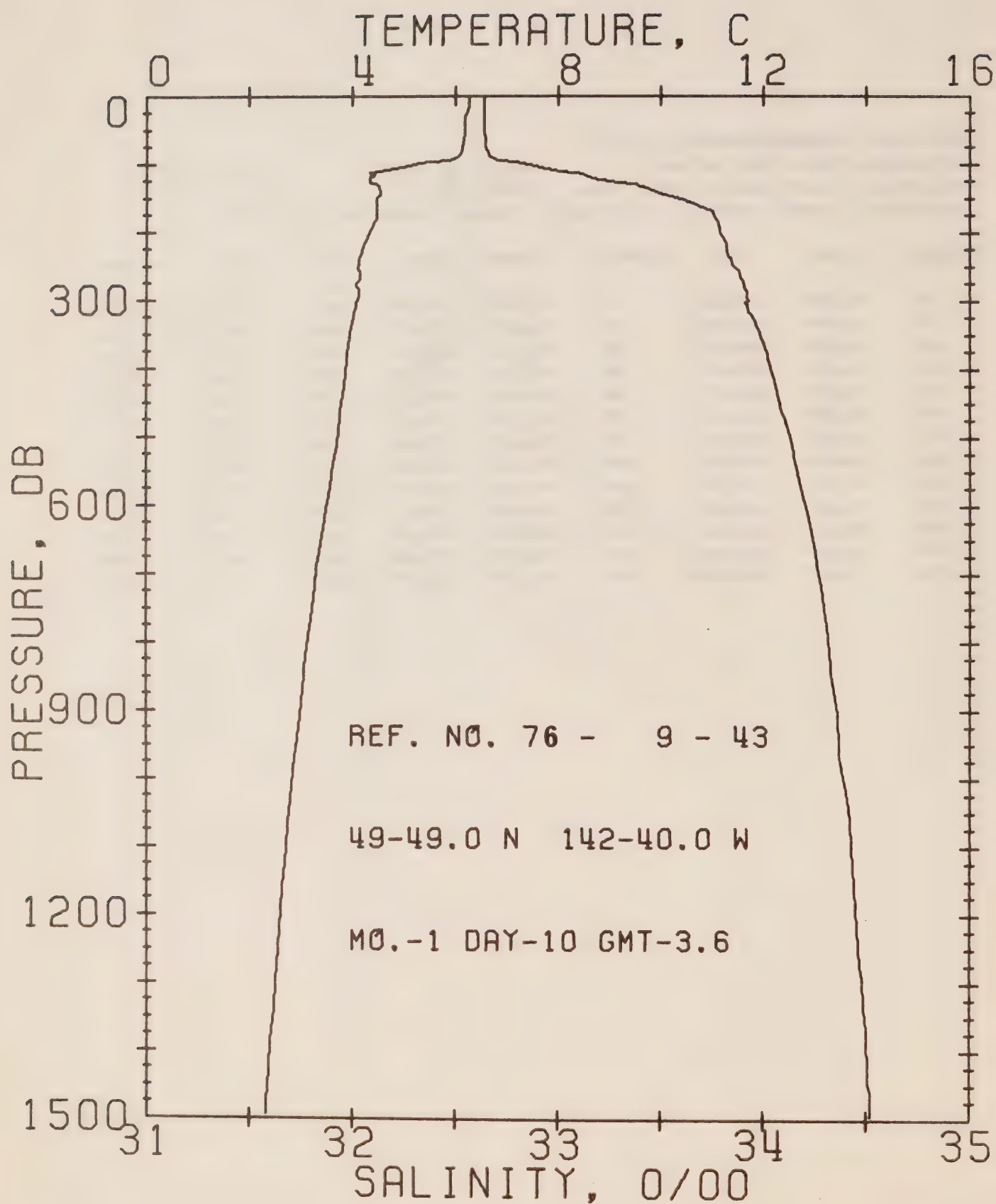
DATE 9/ 1/77

STATION P

POSITION 50- 0.0N. 145- 0.0W GMT 17.3

RESULTS OF STP CAST 89 POINTS TAKEN FROM ANALOG TRACE

PRESS	TEMP	SAL	DEPTH	SIGMA T	SVA	DELTA D	POT. EN	SOUND
0	6.09	32.62	0	25.69	231.3	0.0	0.0	1472.
10	6.09	32.62	10	25.69	231.5	0.23	0.01	1472.
20	6.08	32.62	20	25.69	231.2	0.46	0.05	1473.
30	5.94	32.63	30	25.71	229.3	0.69	0.11	1472.
50	6.00	32.63	50	25.71	230.3	1.15	0.29	1473.
75	5.88	32.67	75	25.75	226.1	1.73	0.66	1473.
100	4.42	33.03	99	26.20	183.4	2.22	1.03	1464.
125	4.55	33.47	124	26.53	152.2	2.64	1.58	1469.
150	4.37	33.76	149	26.79	128.5	2.99	2.06	1469.
175	4.18	33.80	174	26.84	124.0	3.30	2.59	1469.
200	4.11	33.83	199	26.87	120.7	3.61	3.17	1469.
225	4.03	33.86	223	26.90	118.1	3.91	3.82	1469.
250	3.97	33.89	248	26.93	115.7	4.20	4.52	1469.



## OFFSHORE OCEANOGRAPHY GROUP

REFERENCE NO. 76- 9- 43

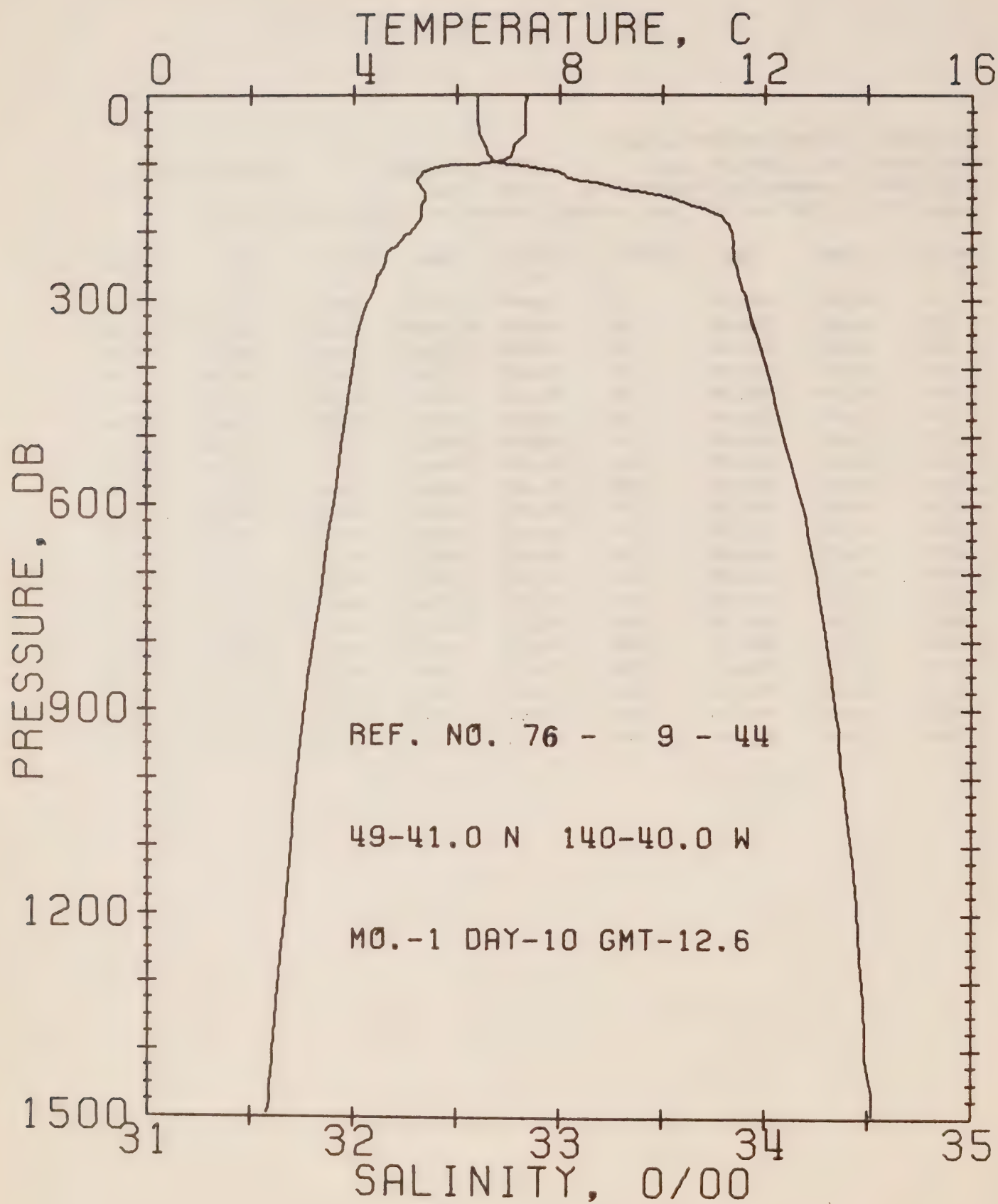
DATE 10/ 1/77

STATION 12

POSITION 49-49.0N, 142-40.0W GMT 3.6

RESULTS OF STP CAST 132 POINTS TAKEN FROM ANALOG TRACE

PRESS	TEMP	SAL	DEPTH	SIGMA T	SVA	DELTA D	POT. EN	SOUND
0	6.28	32.64	0	25.68	232.0	0.0	0.0	1473.
10	6.28	32.64	10	25.68	232.4	0.23	0.01	1473.
20	6.25	32.64	20	25.68	232.1	0.46	0.05	1473.
30	6.20	32.64	30	25.69	231.6	0.70	0.11	1473.
50	6.19	32.64	50	25.69	231.7	1.16	0.30	1474.
75	6.13	32.65	75	25.71	230.6	1.74	0.66	1474.
100	5.24	32.84	99	25.96	206.6	2.30	1.16	1471.
125	4.35	33.28	124	26.41	164.1	2.76	1.69	1468.
150	4.48	33.58	149	26.64	142.8	3.14	2.22	1469.
175	4.47	33.76	174	26.78	129.8	3.48	2.78	1470.
200	4.33	33.79	199	26.82	126.3	3.80	3.39	1470.
225	4.19	33.82	223	26.85	122.7	4.11	4.06	1470.
250	4.11	33.86	248	26.90	119.0	4.41	4.80	1470.
300	4.11	33.93	298	26.95	114.3	4.99	6.43	1471.
400	3.87	34.04	397	27.06	104.7	6.09	10.32	1472.
500	3.72	34.13	496	27.15	96.4	7.10	14.94	1473.
600	3.50	34.21	595	27.23	89.7	8.03	20.17	1473.
800	3.13	34.32	793	27.35	78.9	9.71	32.10	1475.
1000	2.84	34.39	990	27.44	71.7	11.22	45.90	1475.
1200	2.60	34.45	1188	27.51	65.7	12.58	61.18	1480.



## OFFSHORE OCEANOGRAPHY GROUP

REFERENCE NO. 78- 9- 44

DATE 10/ 1/77

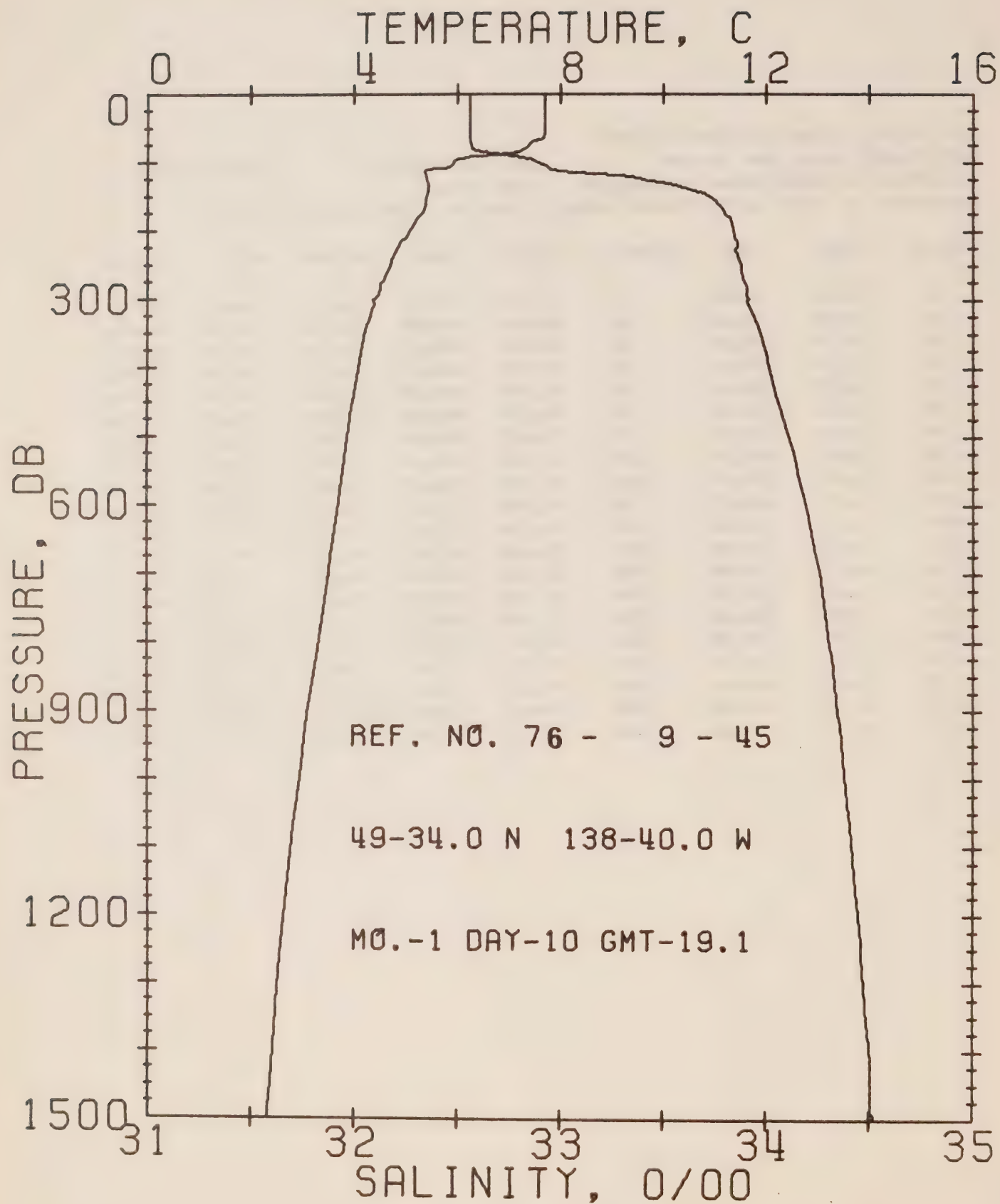
STATION 11

POSITION 49-41.0N, 140-40.0W GMT 12.6

RESULTS OF STP CAST 131 POINTS TAKEN FROM ANALOG TRACE

PRESS	TEMP	SAL	DEPTH	SIGMA T	SVA	DELTA D	POT. EN	SOUND
0	7.35	32.60	0	25.51	248.4	0.0	0.0	1477.
10	7.35	32.60	10	25.51	248.7	0.25	0.01	1477.
20	7.33	32.60	20	25.51	248.7	0.50	0.05	1478.
30	7.33	32.60	30	25.51	248.9	0.75	0.11	1478.
50	7.34	32.61	50	25.51	248.7	1.24	0.32	1478.
75	7.10	32.63	75	25.57	243.8	1.86	0.71	1478.
100	6.54	32.71	99	25.70	231.4	2.40	1.25	1476.
125	5.21	33.10	124	26.17	186.7	2.97	1.82	1471.
150	5.39	33.53	149	26.49	156.9	3.40	2.43	1473.
175	5.31	33.77	174	26.69	138.6	3.77	3.04	1473.
200	5.11	33.84	199	26.76	131.4	4.10	3.68	1473.
225	4.75	33.84	223	26.81	127.2	4.43	4.38	1472.
250	4.59	33.86	248	26.84	124.5	4.74	5.13	1472.
300	4.30	33.91	298	26.91	117.9	5.35	6.83	1472.
400	3.98	34.01	397	27.02	108.0	6.48	10.85	1472.
500	3.80	34.09	496	27.11	100.9	7.52	15.63	1473.
600	3.62	34.18	595	27.20	92.7	8.49	21.05	1474.
800	3.24	34.30	793	27.33	81.3	10.23	33.41	1476.
1000	2.91	34.38	990	27.42	73.3	11.76	47.48	1478.
1200	2.68	34.45	1188	27.50	66.6	13.16	63.10	1480.





## OFFSHORE OCEANOGRAPHY GROUP

REFERENCE NO. 76- 9- 45

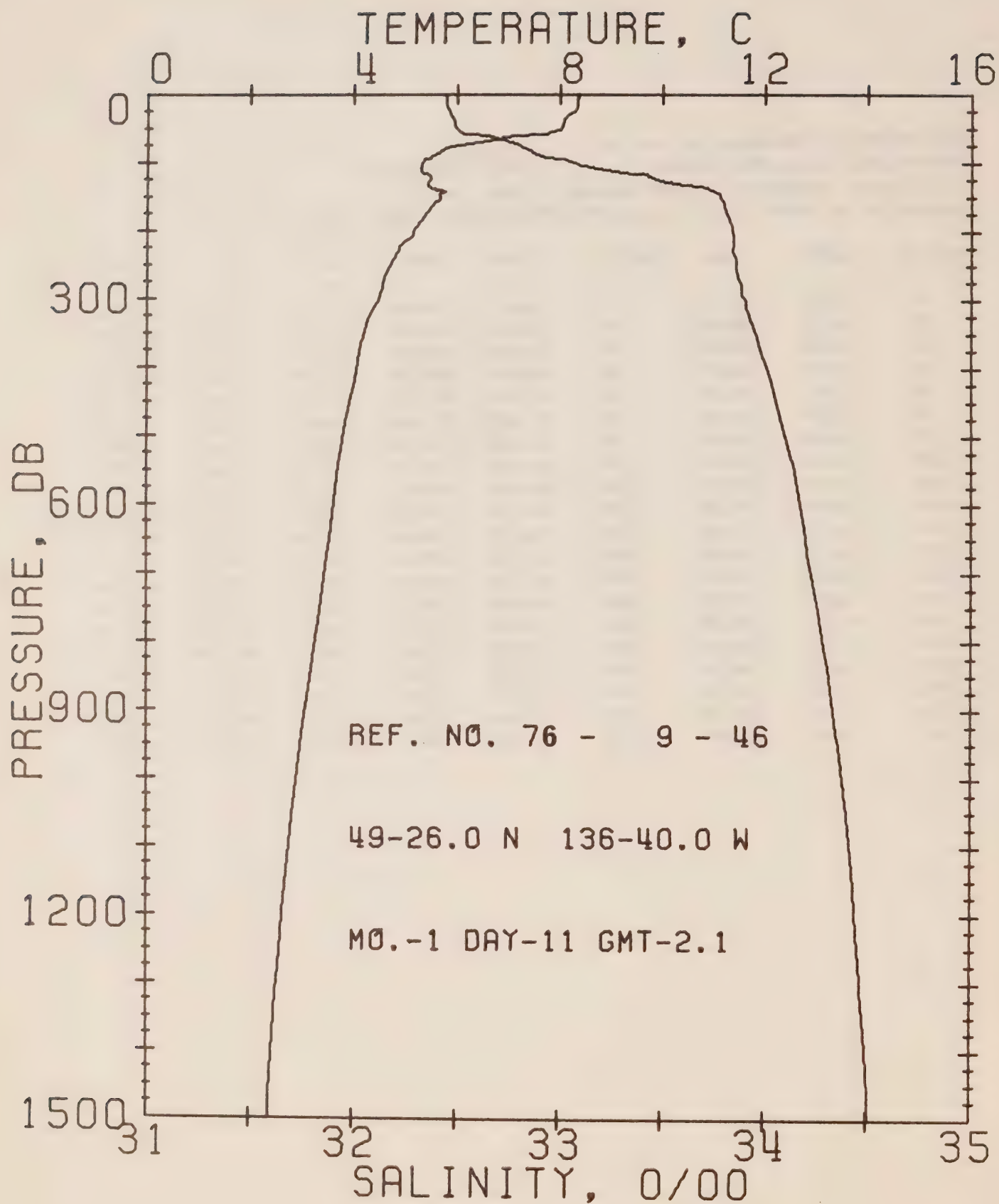
DATE 10/ 1/77

STATION 10

POSITION 49-34.0N, 138-40.0W GMT 19.1

RESULTS OF STP CAST 111 POINTS TAKEN FROM ANALOG TRACE

PRESS	TEMP	SAL	DEPTH	SIGMA T	SVA	DELTA D	PCT. EN	SOUND
0	7.72	32.56	0	25.42	256.3	0.0	0.0	1479.
10	7.72	32.56	10	25.42	256.7	0.26	0.01	1479.
20	7.72	32.56	20	25.42	256.8	0.51	0.05	1479.
30	7.72	32.56	30	25.42	257.0	0.77	0.12	1479.
50	7.71	32.56	50	25.43	257.2	1.28	0.33	1479.
75	7.37	32.57	75	25.48	252.5	1.92	0.73	1479.
100	5.92	32.89	99	25.92	210.4	2.51	1.25	1474.
125	5.41	33.41	124	26.40	165.5	2.99	1.80	1473.
150	5.41	33.73	149	26.64	142.3	3.37	2.33	1473.
175	5.28	33.81	174	26.72	134.9	3.71	2.90	1473.
200	5.06	33.84	199	26.77	130.4	4.04	3.53	1473.
225	4.82	33.86	223	26.82	126.8	4.36	4.23	1472.
250	4.69	33.88	248	26.85	124.0	4.68	4.99	1472.
300	4.39	33.91	298	26.91	118.5	5.28	6.69	1472.
400	4.08	34.02	397	27.02	108.3	6.41	10.71	1472.
500	3.87	34.11	496	27.12	100.0	7.46	15.48	1473.
600	3.69	34.19	595	27.20	92.7	8.42	20.87	1474.
800	3.31	34.31	793	27.33	81.7	10.16	33.21	1476.
1000	2.94	34.38	990	27.42	73.5	11.70	47.33	1478.
1200	2.64	34.45	1188	27.50	66.4	13.09	62.94	1480.



## OFFSHORE OCEANOGRAPHY GROUP

REFERENCE NO. 76- 9- 46

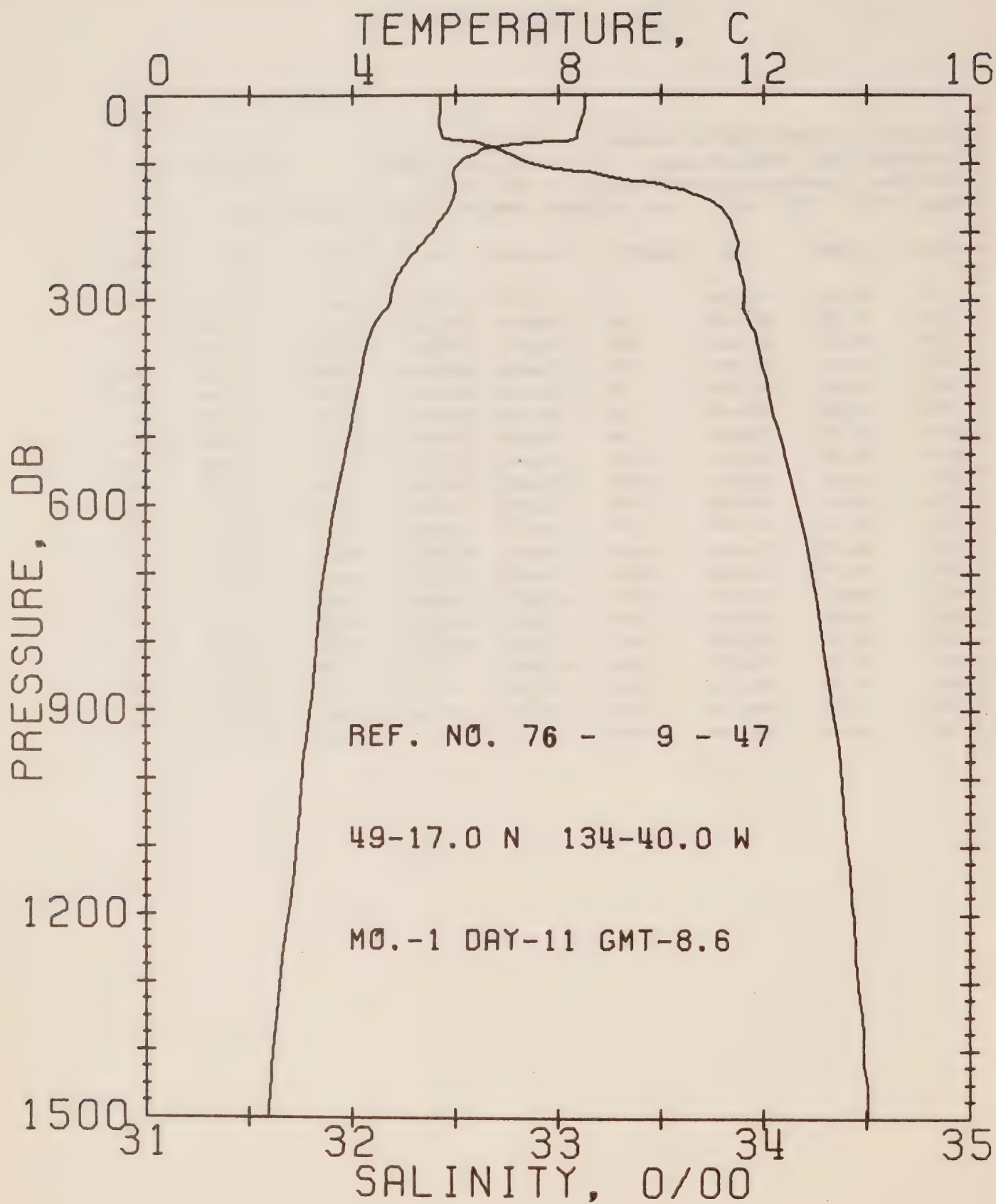
DATE 11/ 1/77

STATION 9

POSITION 49-26.0N, 136-40.0W GMT 2.1

RESULTS OF STP CAST 123 POINTS TAKEN FROM ANALOG TRACE

PRESS	TEMP	SAL	DEPTH	SIGMA T	SVA	DELTA D	POT. EN	SOUND
0	8.36	32.44	0	25.24	274.1	0.0	0.0	1481.
10	8.35	32.45	10	25.25	273.6	0.27	0.01	1481.
20	8.33	32.45	20	25.25	273.3	0.55	0.06	1481.
30	8.17	32.47	30	25.29	269.9	0.82	0.12	1481.
50	8.01	32.49	50	25.33	266.1	1.35	0.34	1481.
75	5.98	32.80	75	25.85	217.2	1.96	0.73	1473.
100	5.32	33.06	99	26.13	190.9	2.47	1.18	1471.
125	5.48	33.48	124	26.44	161.3	2.91	1.68	1473.
150	5.68	33.78	149	26.65	141.6	3.28	2.20	1475.
175	5.38	33.81	174	26.72	135.8	3.63	2.77	1474.
200	5.16	33.84	199	26.76	131.6	3.96	3.41	1473.
225	4.88	33.85	223	26.80	128.3	4.29	4.11	1473.
250	4.70	33.86	248	26.83	125.5	4.60	4.88	1472.
300	4.48	33.90	298	26.89	120.5	5.22	6.61	1472.
400	4.06	34.01	397	27.02	108.7	6.36	10.87	1472.
500	3.80	34.10	496	27.12	100.1	7.40	15.44	1473.
600	3.62	34.17	595	27.19	93.5	8.37	20.83	1474.
800	3.27	34.29	793	27.31	82.8	10.13	33.38	1476.
1000	2.91	34.38	990	27.42	73.3	11.69	47.61	1478.
1200	2.64	34.44	1188	27.50	66.9	13.08	63.21	1480.





## OFFSHORE OCEANOGRAPHY GROUP

REFERENCE NO. 76- 9- 47

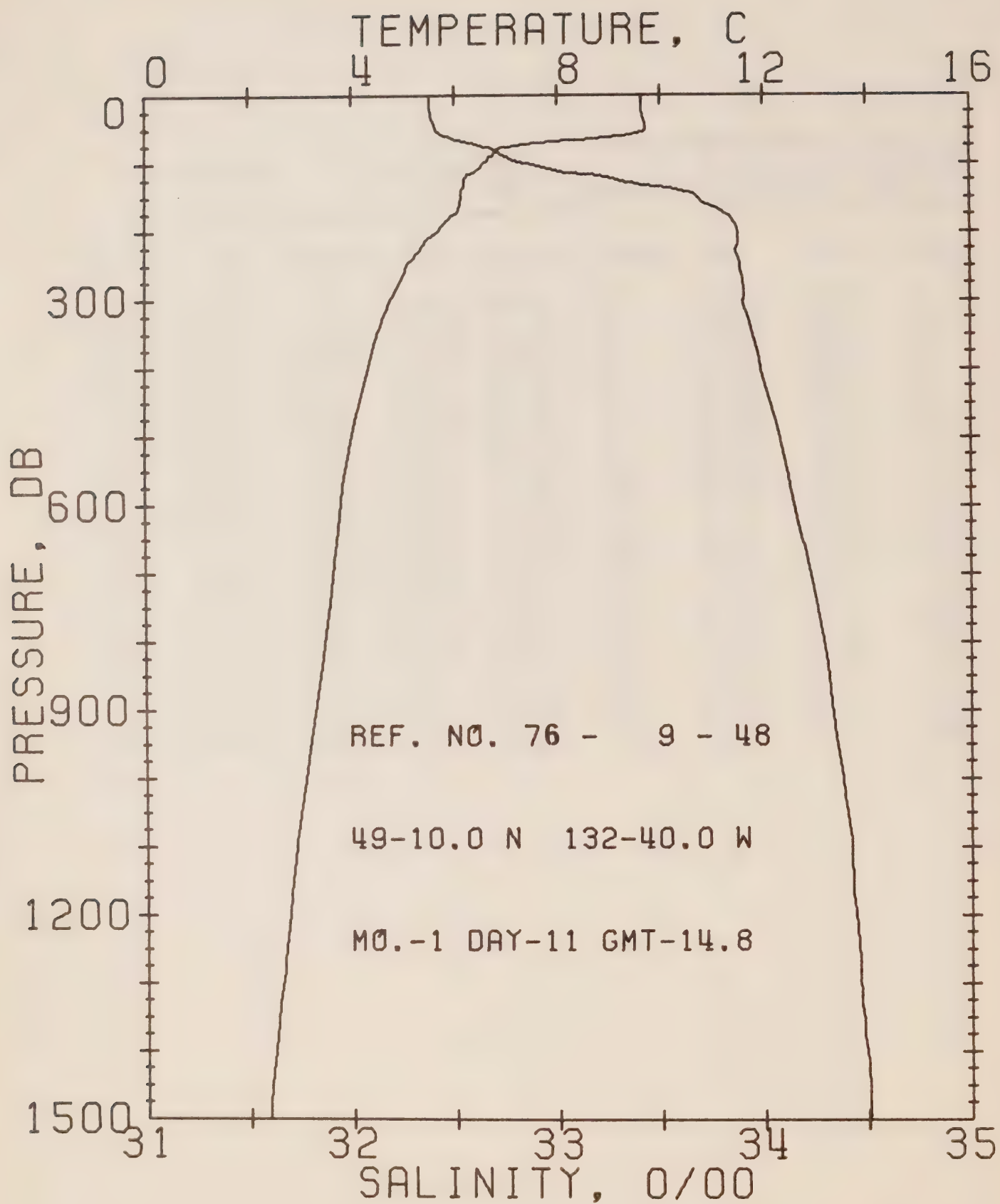
DATE 11/ 1/77

STATION 8

POSITION 49-17.0N, 134-40.0W GMT 8.6

RESULTS OF STP CAST 114 POINTS TAKEN FROM ANALOG TRACE

PRESS	TEMP	SAL	DEPTH	SIGMA T	SVA	DELTA D	PCT. EN	SOUND
0	8.53	32.43	0	25.20	277.3	0.0	0.0	1482.
10	8.53	32.43	10	25.20	277.7	0.28	0.01	1482.
20	8.53	32.43	20	25.20	277.7	0.56	0.06	1482.
30	8.50	32.43	30	25.21	277.8	0.83	0.13	1482.
50	8.40	32.42	50	25.22	276.9	1.39	0.35	1482.
75	6.79	32.68	75	25.65	236.5	2.06	0.78	1476.
100	6.04	32.86	99	25.88	214.1	2.62	1.28	1474.
125	5.99	33.34	124	26.27	177.7	3.11	1.84	1475.
150	5.96	33.70	149	26.55	151.3	3.51	2.40	1476.
175	5.78	33.81	174	26.67	140.6	3.87	3.00	1475.
200	5.55	33.86	199	26.73	134.9	4.22	3.66	1475.
225	5.25	33.88	223	26.78	130.3	4.55	4.37	1474.
250	4.98	33.88	248	26.81	127.1	4.87	5.15	1474.
300	4.75	33.92	298	26.87	122.1	5.49	6.89	1473.
400	4.19	34.00	397	27.00	111.0	6.65	11.03	1473.
500	3.94	34.08	496	27.09	102.8	7.72	15.93	1474.
600	3.67	34.16	595	27.18	94.8	8.71	21.46	1474.
800	3.32	34.29	793	27.31	83.2	10.48	34.01	1476.
1000	3.03	34.38	990	27.41	74.5	12.05	48.40	1478.
1200	2.77	34.44	1188	27.48	68.6	13.48	64.46	1481.



## OFFSHORE OCEANOGRAPHY GROUP

REFERENCE NO. 76- 9- 48

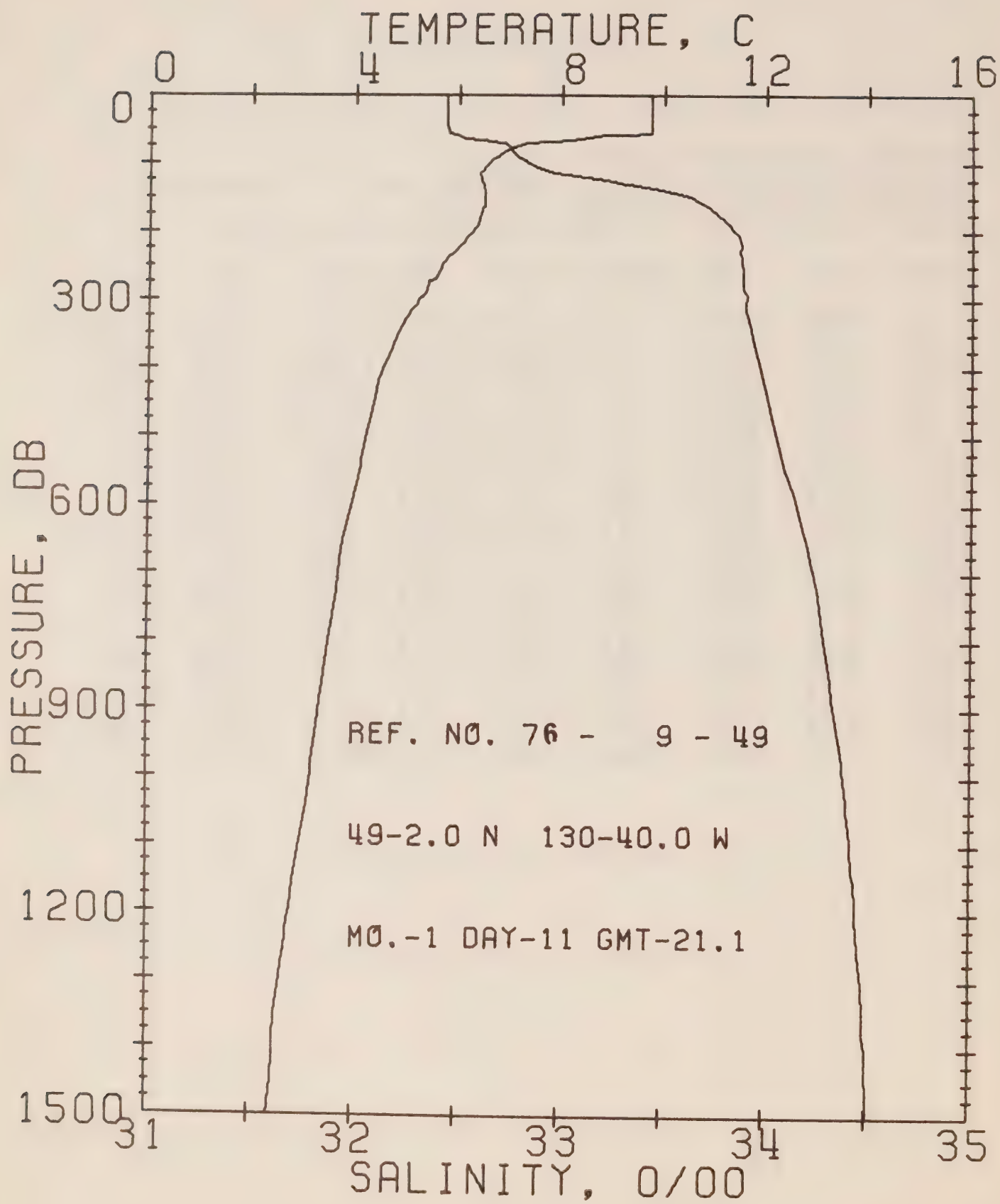
DATE 11/ 1/77

STATION 7

POSITION 49-10.0N, 132-40.0W GMT 14.8

RESULTS OF STP CAST 112 POINTS TAKEN FROM ANALOG TRACE

PRESS	TEMP	SAL	DEPTH	SIGMA T	SVA	DELTA D	POT. EN	SOUND
0	9.65	32.38	0	24.99	297.6	0.0	0.0	1486.
10	9.65	32.38	10	24.99	298.0	0.30	0.02	1486.
20	9.65	32.38	20	24.99	298.2	0.60	0.06	1486.
30	9.68	32.39	30	24.99	298.3	0.89	0.14	1486.
50	9.73	32.41	50	25.00	298.0	1.49	0.38	1487.
75	7.01	32.64	75	25.59	242.3	2.18	0.82	1477.
100	6.56	32.84	99	25.80	221.9	2.76	1.33	1476.
125	6.20	33.30	124	26.21	183.2	3.27	1.92	1476.
150	6.11	33.68	149	26.52	154.1	3.69	2.50	1476.
175	5.99	33.82	174	26.65	142.4	4.06	3.11	1476.
200	5.65	33.88	199	26.73	134.5	4.41	3.77	1475.
225	5.33	33.87	223	26.77	131.6	4.74	4.49	1475.
250	5.06	33.89	248	26.81	127.4	5.06	5.27	1474.
300	4.76	33.91	298	26.86	122.9	5.69	7.02	1473.
400	4.30	33.99	397	26.97	113.1	6.86	11.22	1473.
500	3.99	34.08	496	27.08	103.6	7.95	15.18	1474.
600	3.78	34.15	595	27.16	96.9	8.95	21.79	1475.
800	3.47	34.29	793	27.30	84.7	10.76	34.68	1477.
1000	3.09	34.38	990	27.41	75.1	12.36	49.32	1479.
1200	2.76	34.44	1188	27.48	68.2	13.79	65.27	1481.



## OFFSHORE OCEANOGRAPHY GROUP

REFERENCE NO. 76- 9- 49

DATE 11/ 1/77

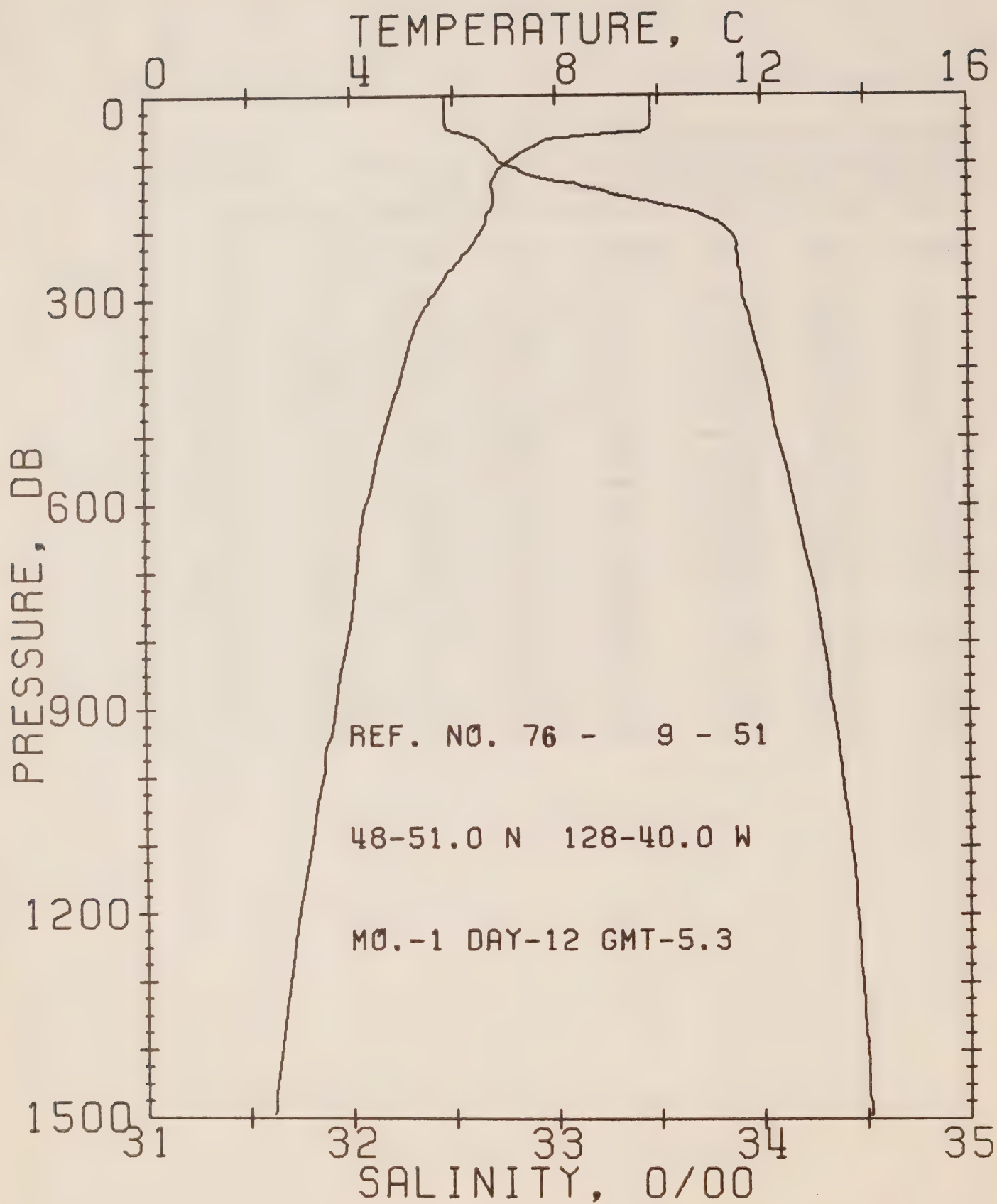
STATION 6

POSITION 49- 2.0N, 130-40.0W GMT 21.1

RESULTS OF STP CAST 116 POINTS TAKEN FROM ANALOG TRACE

PRESS	TEMP	SAL	DEPTH	SIGMA T	SVA	DELTA D	PCT. LV	SOUND
0	9.75	32.44	0	25.02	294.8	0.0	0.0	1486.
10	9.75	32.44	10	25.02	295.2	0.29	0.02	1486.
20	9.75	32.44	20	25.02	295.4	0.59	0.00	1487.
30	9.75	32.44	30	25.02	295.6	0.89	0.14	1487.
50	9.75	32.45	50	25.03	295.5	1.48	0.35	1487.
75	7.13	32.74	75	25.64	236.6	2.15	0.80	1478.
100	6.57	32.84	99	25.80	222.2	2.73	1.31	1476.
125	6.44	33.22	124	26.11	192.5	3.25	1.91	1477.
150	6.51	33.63	149	26.43	163.1	3.69	2.53	1478.
175	6.43	33.77	174	26.55	151.9	4.08	3.16	1478.
200	6.26	33.85	199	26.64	144.1	4.45	3.83	1476.
225	5.97	33.88	223	26.70	138.7	4.81	4.65	1477.
250	5.67	33.88	248	26.74	135.0	5.15	5.48	1476.
300	5.23	33.91	298	26.81	128.5	5.81	7.33	1475.
400	4.55	33.98	397	26.94	116.6	7.04	11.70	1474.
500	4.24	34.05	496	27.03	108.2	8.16	16.84	1475.
600	3.95	34.15	595	27.14	98.4	9.20	22.64	1475.
800	3.52	34.29	793	27.29	85.2	11.02	35.59	1477.
1000	3.18	34.38	991	27.40	75.9	12.62	50.29	1479.
1200	2.77	34.45	1188	27.49	67.7	14.06	66.32	1451.





## OFFSHORE OCEANOGRAPHY GROUP

REFERENCE NO. 76- 9- 51

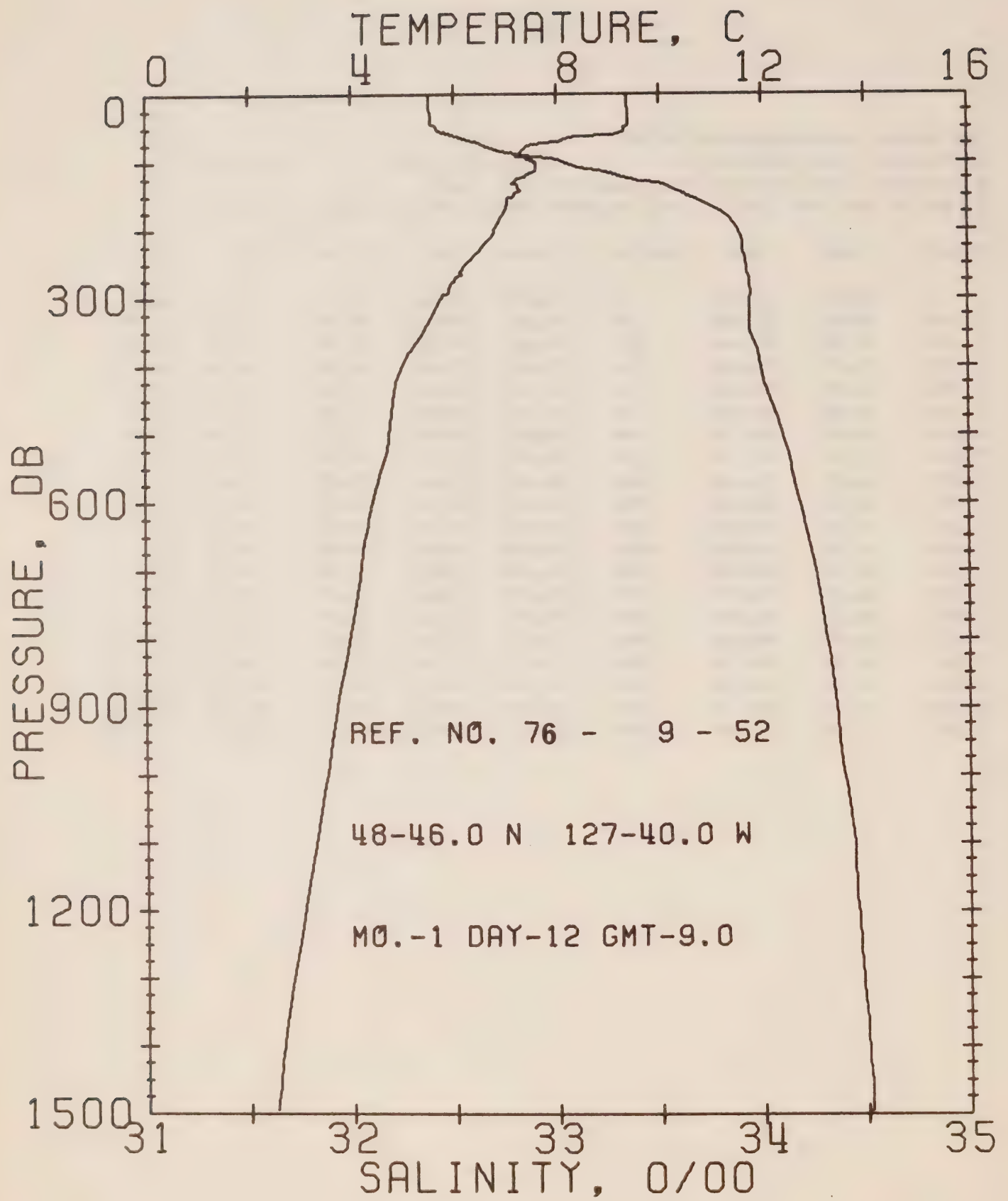
DATE 12/ 1/77

STATION 5

POSITION 48-51.0N, 128-40.0W GMT 5.3

RESULTS OF STP CAST 132 POINTS TAKEN FROM ANALOG TRACE

PRESS	TEMP	SAL	DEPTH	SIGMA T	SVA	DELTA C	POT. EN	SOUND
0	9.87	32.46	0	25.02	295.2	0.0	0.0	1487.
10	9.87	32.46	10	25.02	295.6	0.30	0.02	1487.
20	9.87	32.46	20	25.02	295.7	0.59	0.06	1487.
30	9.87	32.46	30	25.02	295.8	0.89	0.14	1487.
50	9.82	32.47	50	25.03	294.8	1.48	0.32	1487.
75	7.58	32.66	75	25.52	248.1	2.14	0.80	1479.
100	7.03	32.74	99	25.66	235.5	2.75	1.34	1478.
125	6.76	33.01	124	25.91	212.1	3.31	1.98	1478.
150	6.80	33.34	149	26.17	188.2	3.81	2.68	1479.
175	6.65	33.70	174	26.47	159.7	4.24	3.39	1479.
200	6.53	33.85	199	26.60	147.9	4.62	4.12	1479.
225	6.31	33.88	223	26.66	142.5	4.98	4.90	1479.
250	6.02	33.89	248	26.70	138.8	5.34	5.75	1478.
300	5.53	33.91	298	26.78	131.7	6.01	7.64	1477.
400	5.00	34.01	397	26.91	119.6	7.26	12.09	1476.
500	4.60	34.08	496	27.01	110.7	8.41	17.37	1476.
600	4.26	34.16	595	27.11	101.9	9.47	23.31	1477.
800	3.90	34.29	793	27.26	89.3	11.38	36.86	1479.
1000	3.43	34.38	991	27.38	78.6	13.05	52.18	1480.
1200	2.96	34.45	1188	27.48	69.4	14.52	68.67	1481.



## OFFSHORE OCEANOGRAPHY GROUP

REFERENCE NO. 76- 9- 52

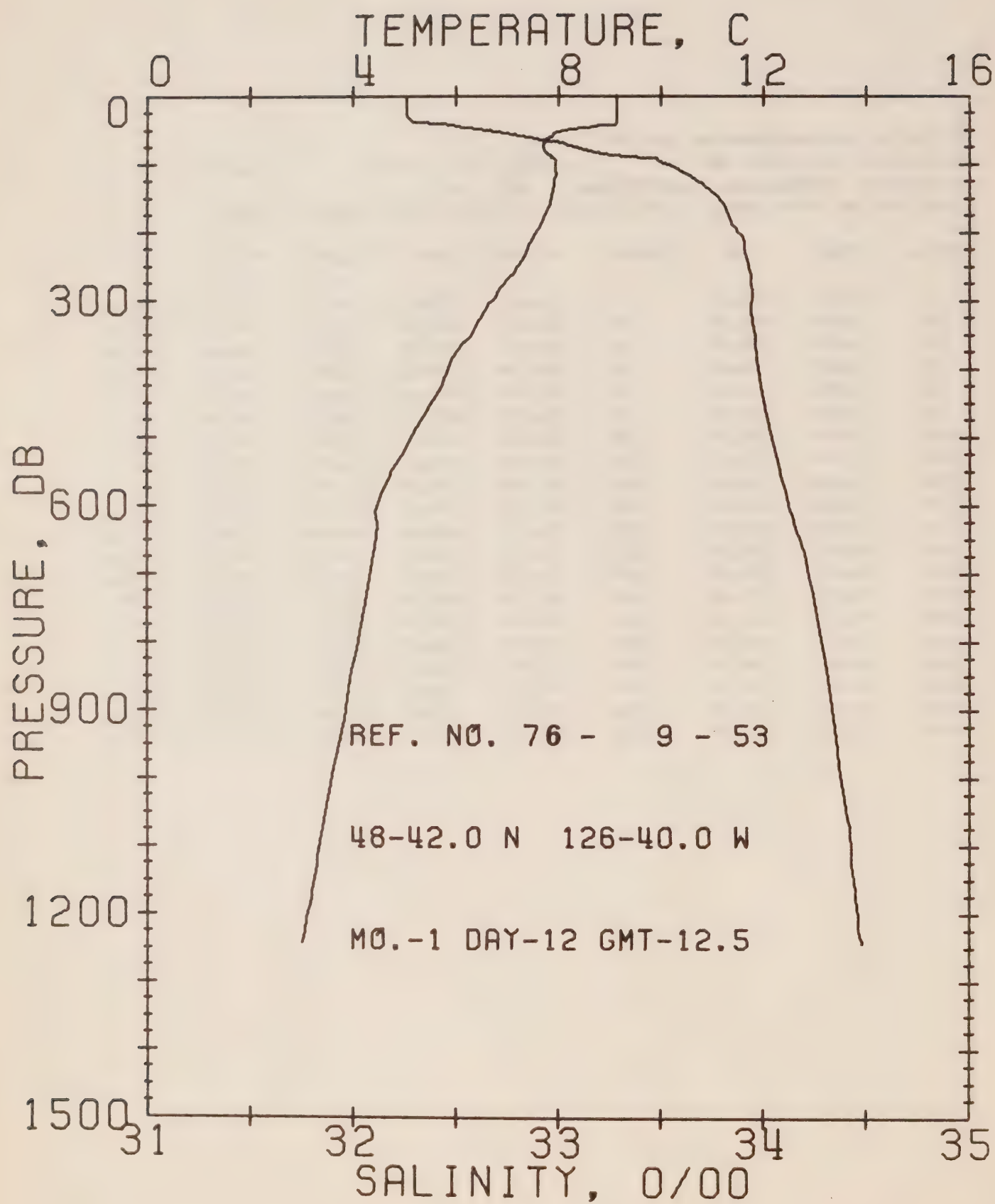
DATE 12/ 1/77

STATION 4

POSITION 48-46.0N, 127-40.0W GMT 9.0

RESULTS OF STP CAST 133 POINTS TAKEN FROM ANALOG TRACE

PRESS	TEMP	SAL	DEPTH	SIGMA T	SVA	DELTA D	POT. EN	SOUND
0	9.39	32.38	0	25.03	293.7	0.0	0.0	1435.
10	9.38	32.38	10	25.03	293.9	0.29	0.01	1435.
20	9.40	32.38	20	25.03	294.4	0.59	0.06	1435.
30	9.40	32.39	30	25.04	294.1	0.88	0.13	1435.
50	9.34	32.41	50	25.07	291.6	1.47	0.37	1485.
75	7.51	32.64	75	25.51	249.2	2.15	0.81	1479.
100	7.60	33.03	99	25.81	221.4	2.74	1.33	1480.
125	7.19	33.38	124	26.14	190.2	3.26	1.93	1480.
150	7.16	33.64	149	26.35	170.8	3.71	2.35	1480.
175	6.95	33.81	174	26.51	155.5	4.11	3.22	1480.
200	6.78	33.88	199	26.59	148.4	4.49	3.95	1480.
225	6.52	33.91	223	26.65	143.4	4.86	4.74	1479.
250	6.22	33.92	248	26.70	139.1	5.21	5.59	1479.
300	5.75	33.95	298	26.78	131.8	5.85	7.48	1478.
400	4.96	34.00	397	26.91	119.9	7.16	12.00	1476.
500	4.73	34.10	496	27.01	110.7	8.31	17.28	1477.
600	4.40	34.18	595	27.12	101.6	9.37	23.22	1477.
800	3.96	34.31	793	27.27	88.8	11.26	36.68	1479.
1000	3.51	34.39	991	27.38	79.1	12.93	51.97	1480.
1200	3.05	34.46	1188	27.47	70.3	14.42	68.57	1482.





## OFFSHORE OCEANOGRAPHY GROUP

REFERENCE NO. 76- 9- 53

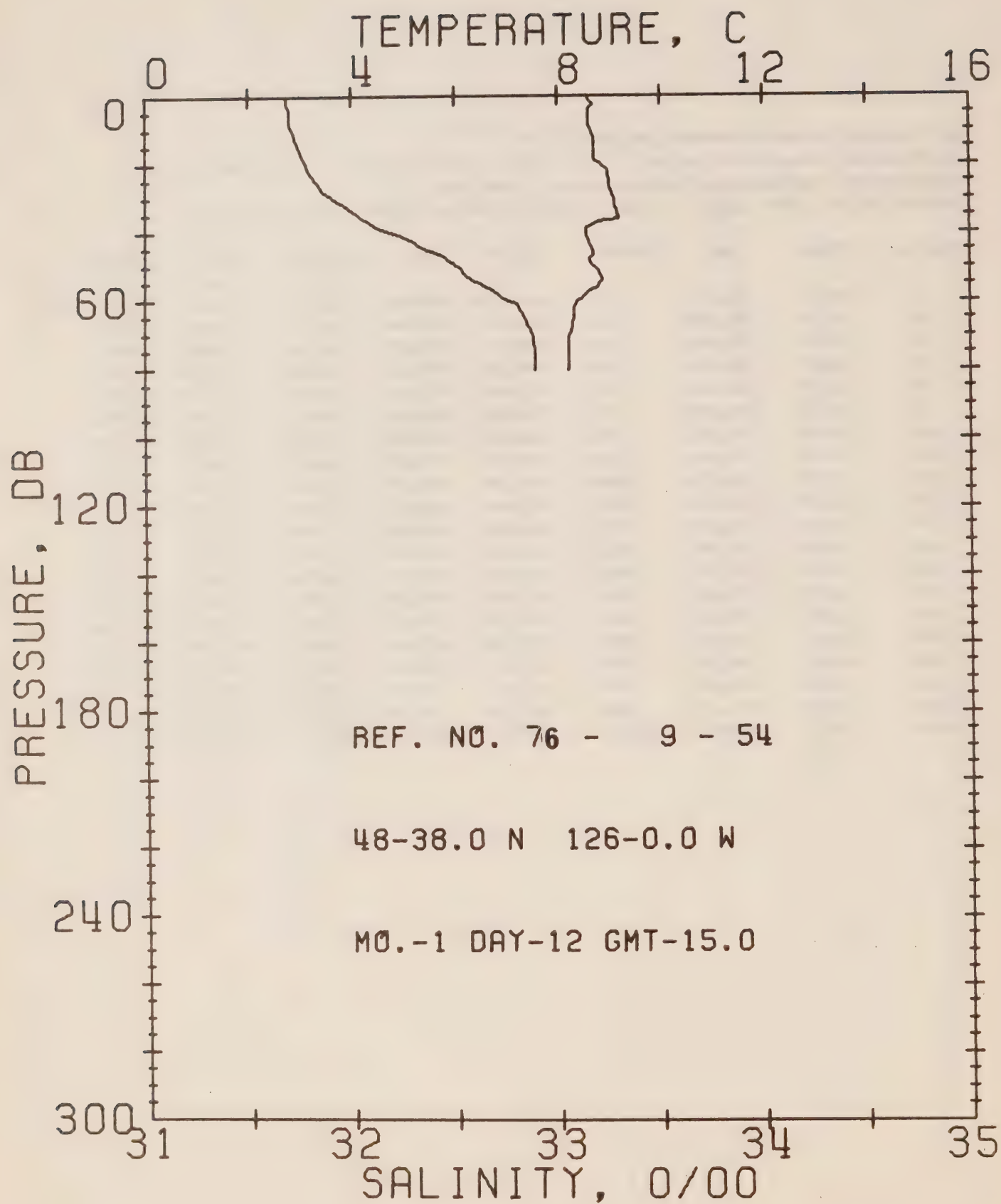
DATE 12/ 1/77

STATION 3

POSITION 48-42.0N, 126-40.0W GMT 12.5

RESULTS OF STP CAST 106 POINTS TAKEN FROM ANALOG TRACE

PRESS	TEMP	SAL	DEPTH	SIGMA T	SVA	DELTA D	POT. EN	SOUND
0	9.15	32.26	0	24.98	299.0	0.0	0.0	1484.
10	9.15	32.26	10	24.98	299.4	0.30	0.02	1484.
20	9.15	32.26	20	24.98	299.5	0.60	0.06	1484.
30	9.14	32.26	30	24.98	299.5	0.90	0.14	1484.
50	8.07	32.65	50	25.44	255.4	1.47	0.37	1481.
75	7.71	33.09	75	25.84	218.2	2.06	0.74	1481.
100	7.95	33.52	99	26.15	189.5	2.56	1.19	1482.
125	7.92	33.69	124	26.28	177.4	3.02	1.72	1483.
150	7.85	33.78	149	26.36	169.7	3.45	2.32	1483.
175	7.74	33.83	174	26.42	165.1	3.87	3.01	1483.
200	7.55	33.88	199	26.49	158.8	4.28	3.79	1483.
225	7.37	33.91	223	26.53	154.7	4.67	4.63	1483.
250	7.19	33.93	248	26.57	151.1	5.05	5.56	1482.
300	6.70	33.95	298	26.66	143.8	5.79	7.62	1481.
400	5.82	33.98	397	26.79	131.7	7.17	12.53	1480.
500	5.11	34.04	496	26.93	119.2	8.43	18.30	1478.
600	4.47	34.12	595	27.07	106.5	9.55	24.60	1477.
800	4.09	34.28	793	27.23	92.1	11.53	38.69	1479.
1000	3.58	34.38	991	27.36	80.8	13.26	54.50	1481.
1200	3.11	34.46	1188	27.47	70.9	14.77	71.42	1482.



## OFFSHORE OCEANOGRAPHY GROUP

REFERENCE NO. 76- 9- 54

DATE 12/ 1/77

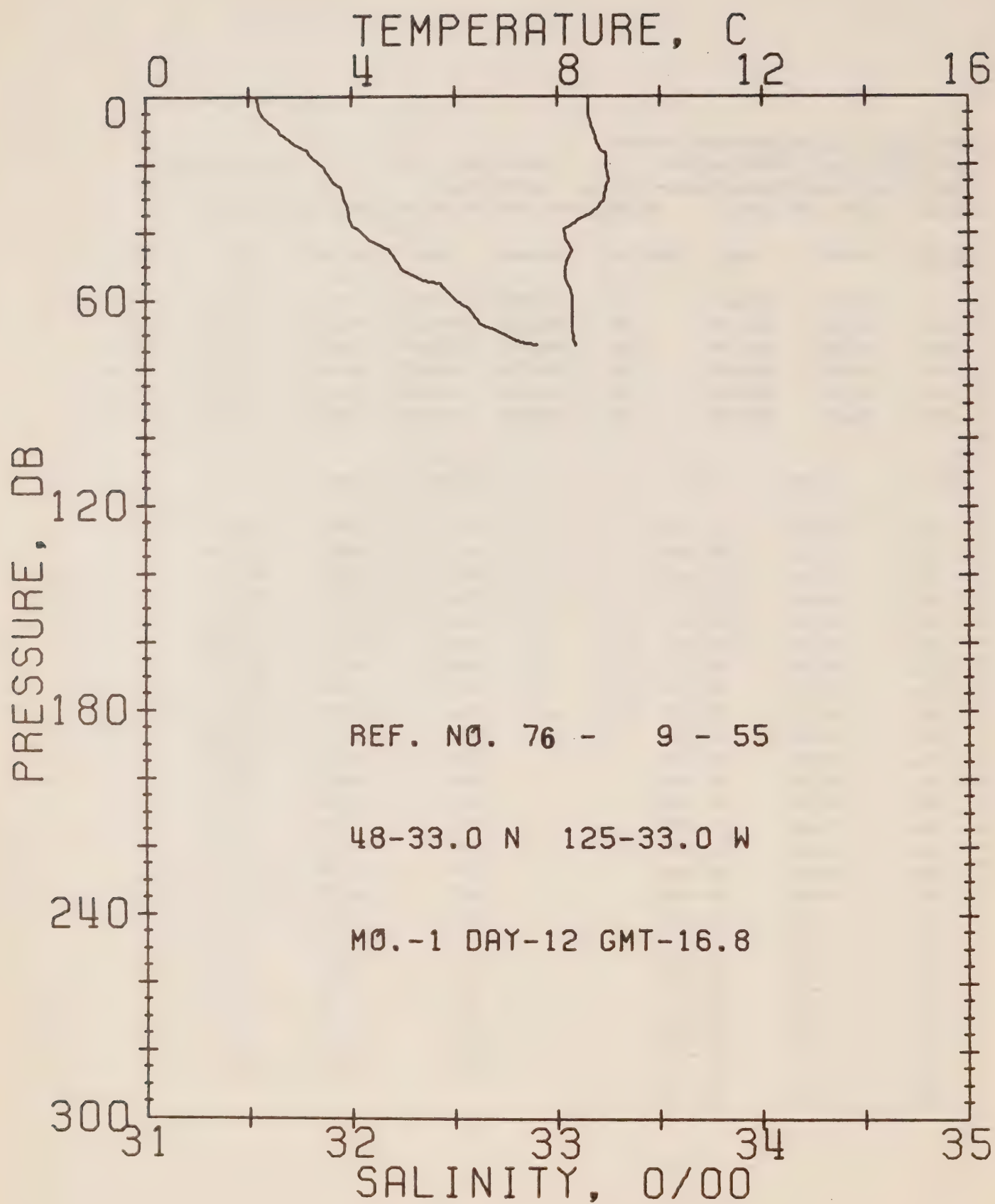
STATION 2

POSITION 48-38.0N, 126- 0.0W GMT 15.0

RESULTS OF STP CAST 51 POINTS TAKEN FROM ANALOG TRACE

PRESS	TEMP	SAL	DEPTH	SIGMA T	SVA	DELTA D	POT. EN	SOUND
0	8.58	31.69	0	24.62	333.0	0.0	0.0	1481.
10	8.64	31.71	10	24.63	332.8	0.33	0.02	1431.
20	8.85	31.78	20	24.65	330.7	0.66	0.07	1482.
30	9.09	31.90	30	24.71	325.2	0.99	0.15	1484.
50	8.70	32.51	50	25.24	274.9	1.59	0.39	1483.
75	8.21	32.89	75	25.61	240.0	2.25	0.79	1432.

DEPTH	TEMP	SAL	DEPTH	TEMP	SAL
0.	8.58	31.69	45.	8.69	32.37
2.	8.65	31.69	47.	8.70	32.44
3.	8.68	31.69	48.	8.60	32.46
4.	8.61	31.70	49.	8.64	32.49
9.	8.61	31.70	51.	8.77	32.53
11.	8.67	31.72	52.	8.82	32.54
13.	8.73	31.73	54.	8.87	32.58
15.	8.72	31.74	55.	8.82	32.62
19.	8.71	31.77	56.	8.79	32.65
20.	8.85	31.78	57.	8.65	32.68
22.	8.99	31.79	58.	8.55	32.71
27.	9.02	31.85	59.	8.52	32.72
28.	9.05	31.86	60.	8.41	32.76
29.	9.06	31.88	61.	8.36	32.80
31.	9.12	31.93	62.	8.33	32.81
32.	9.12	31.96	65.	8.31	32.84
33.	9.12	31.98	67.	8.30	32.85
34.	9.17	32.01	68.	8.28	32.86
35.	9.18	32.03	69.	8.27	32.87
36.	9.20	32.05	71.	8.22	32.88
37.	8.79	32.08	72.	8.22	32.88
38.	8.65	32.11	75.	8.21	32.89
39.	8.55	32.13	76.	8.21	32.89
41.	8.57	32.23	78.	8.21	32.89
43.	8.61	32.30	80.	8.21	32.89
44.	8.64	32.32			



## OFFSHORE OCEANOGRAPHY GROUP

REFERENCE NO. 76- 9- 55

DATE 12/ 1/77

STATION 1

POSITION 48-33.0N, 125-33.0W GMT 16.8

RESULTS OF STP CAST 34 POINTS TAKEN FROM ANALOG TRACE

PRESS	TEMP	SAL	DEPTH	SIGMA T	SVA	DELTA D	POT. EN	SOUND
0	8.62	31.54	0	24.50	344.7	0.0	0.0	1481.
10	8.69	31.64	10	24.56	338.8	0.34	0.02	1481.
20	8.97	31.84	20	24.68	327.8	0.68	0.07	1483.
30	8.92	31.96	30	24.78	318.6	1.00	0.15	1483.
50	8.17	32.23	50	25.10	288.0	1.60	0.40	1481.

DEPTH	TEMP	SAL	DEPTH	TEMP	SAL
0.	8.62	31.54	39.	8.13	32.03
4.	8.62	31.55	42.	8.15	32.08
6.	8.62	31.57	45.	8.28	32.18
10.	8.69	31.64	49.	8.18	32.22
11.	8.71	31.65	51.	8.16	32.24
14.	8.78	31.72	54.	8.15	32.34
16.	8.89	31.78	55.	8.19	32.43
17.	8.96	31.79	56.	8.23	32.44
21.	8.97	31.86	59.	8.30	32.49
23.	8.98	31.88	60.	8.29	32.51
25.	9.01	31.91	62.	8.29	32.56
27.	8.96	31.95	65.	8.28	32.60
30.	8.92	31.96	67.	8.28	32.62
33.	8.80	31.98	69.	8.29	32.71
35.	8.62	31.99	71.	8.32	32.77
36.	8.42	31.99	72.	8.33	32.82
38.	8.26	32.00	73.	8.37	32.90





**Surface Salinity and Temperature Observations**

**(P-76-9)**

SURFACE SALINITY AND TEMPERATURE OBSERVATIONS  
CRUISE REFERENCE NUMBER 76- 9

DATE/TIME				SALINITY	TEMP	LONGITUDE
YR	MO	DAY	GMT	O/00	C	WEST
76	12	3	2300	32.044	9.4	125-33
76	12	4	140	31.526	8.5	126- 0
76	12	4	345	31.833	10.0	126-40
76	12	4	720	32.360	11.1	127-40
76	12	4	1115	32.424	11.6	128-40
76	12	4	1455	32.327		129-40
76	12	4	1755	32.400	11.1	130-40
76	12	4	2140	32.394		131-40
76	12	5	30	32.325	10.9	132-40
76	12	5	520	32.352		133-40
76	12	5	720	32.362	10.1	134-40
76	12	5	1105	32.358	10.1	135-40
76	12	5	1400	32.424	9.5	136-40
76	12	5	1745	32.511		137-40
76	12	5	2040	32.500	8.8	138-40
76	12	6	130	32.479		139-40
76	12	6	420	32.523	8.4	140-40
76	12	6	810	32.554		141-40
76	12	6	1315	32.657	7.3	142-40
76	12	8	0	32.635	6.6	ON STATION
76	12	9	0	32.633	6.6	ON STATION
76	12	10	0	32.626	6.9	ON STATION
76	12	11	0	32.640	6.4	ON STATION
76	12	12	0	32.619	6.6	ON STATION
76	12	13	0	32.637	6.4	ON STATION
76	12	14	0	32.639	6.6	ON STATION
76	12	15	0	32.631	6.5	ON STATION
76	12	16	0	32.634	6.5	ON STATION
76	12	17	0	32.643	6.4	ON STATION
76	12	18	0	32.634	6.4	ON STATION
76	12	19	0	32.629	6.3	ON STATION
76	12	20	0	32.632	6.3	ON STATION
76	12	21	0	32.629	6.4	ON STATION
76	12	22	0	32.634	6.4	ON STATION
76	12	23	0	32.631	6.2	ON STATION
76	12	24	0	32.625	6.4	ON STATION
76	12	25	0	32.605	6.1	ON STATION
76	12	26	0	32.630	6.1	ON STATION
76	12	27	0	32.633	6.6	ON STATION
76	12	28	0	32.637	6.5	ON STATION
76	12	29	0	32.639	6.0	ON STATION
76	12	30	0	32.639	6.0	ON STATION
76	12	31	0	32.638	6.0	ON STATION
77	1	1	0	32.581	6.0	ON STATION

SURFACE SALINITY AND TEMPERATURE OBSERVATIONS  
CRUISE REFERENCE NUMBER 76- 9

DATE/TIME				SALINITY	TEMP	LONGITUDE
YR	MO	DAY	GMT	0/00	C	WEST
77	1	2	0	32.621	6.0	ON STATION
77	1	3	0	32.626	6.0	ON STATION
77	1	4	0	32.614	6.1	ON STATION
77	1	5	0	32.623	6.1	ON STATION
77	1	6	0	32.610	5.9	ON STATION
77	1	7	0	32.622	6.0	ON STATION
77	1	9	0	32.589	5.8	ON STATION
77	1	9	2315	32.627		143-40
77	1	10	330	32.631	6.2	142-40
77	1	10	630	32.597		141-40
77	1	10	1230	32.593	7.4	140-40
77	1	10	1625	32.536		139-40
77	1	10	1900	32.546	7.6	138-40
77	1	10	2250	32.533		137-40
77	1	11	200	32.429	8.3	136-40
77	1	11	535	32.421		135-40
77	1	11	835	32.420	8.5	134-40
77	1	11	1135	32.342		133-40
77	1	11	1445	32.377	9.5	132-40
77	1	11	2105	32.416	9.6	130-40
77	1	12	215	32.494		129-40
77	1	12	515	32.440	9.7	128-40
77	1	12	900	32.357	9.4	127-40
77	1	12	1230	32.255	9.0	126-40
77	1	12	1500	31.849	8.4	126- 0
77	1	12	1645	31.536	8.5	125-33

b DENOTES SALINITY SAMPLE TAKEN FROM A  
BUCKET. ALL OTHER SAMPLES TAKEN FROM  
THE SEAWATER LOOP









CAI

LEP 321

-77R08

# THE USE OF EXTRUDED PLASTIC FAIRING FOR A SUBSURFACE MOORING

by  
W.H. BELL



INSTITUTE OF OCEAN SCIENCES, PATRICIA BAY  
Victoria, B.C.

For additional copies or further information please write to:

Department of Fisheries and the Environment

Institute of Ocean Sciences, Patricia Bay

512 - 1230 Government Street

Victoria, B.C.

V8W 1Y4

THE USE OF EXTRUDED PLASTIC FAIRING  
FOR A SUBSURFACE MOORING

by

W.H. Bell

Institute of Ocean Sciences, Patricia Bay  
Victoria, B.C.

May 1977



This is a manuscript which has received only limited circulation. On citing this report in a bibliography, the title should be followed by the words "UNPUBLISHED MANUSCRIPT" which is in accordance with accepted bibliographic custom.

ABSTRACT

Vertical excursions of instruments suspended beneath a subsurface buoy, resulting from hydrodynamic drag forces on the cable, cause problems in oceanographic data acquisition and analysis. In an effort to alleviate the problem, a plastic cable fairing was evaluated in a field experiment. An empirical value for the fairing drag coefficient was obtained using a mathematical simulation of the mooring. Then, again using the mooring model, comparisons were made of instrument excursions resulting from the use of unfaired cable, faired cable and additional system buoyancy.



TABLE OF CONTENTS

	<u>Page</u>
Abstract	i
Table of Contents	ii
List of Figures	iii
List of Tables	iii
Introduction	1
Field Program	1
Sensor Data	3
The Mooring Model	6
Fairing Drag Coefficient	7
Effect of Faired Cable	10
Effect of Increased Buoyancy	10
Conclusion	12
Acknowledgements	12
References	13

LIST OF FIGURES

		<u>Page</u>
Fig. 1	Vertical excursion of a current meter.	2
Fig. 2	Vertical deflection from rest position for the top instrument in a moored array.	11

LIST OF TABLES

Table I	Mooring Component Dimensions	4
Table II	Data Obtained From Current Meter Sensors	5
Table III	Sensor Data Converted To Ft-Lb-Sec System	6
Table IV	Mooring Component Rest Position Distances	7
Table V	Model Input Parameters	8
Table VI	Data Pertaining to Check on $C_{D_F}$ Estimate	9
Table VII	Predicted Instrument Excursions at Several Current Speeds Using Faired and Unfaired Cable	10
Table VIII	Predicted Instrument Excursions at Several Current Speeds Using Two Buoys and Unfaired Cable	12



## Introduction

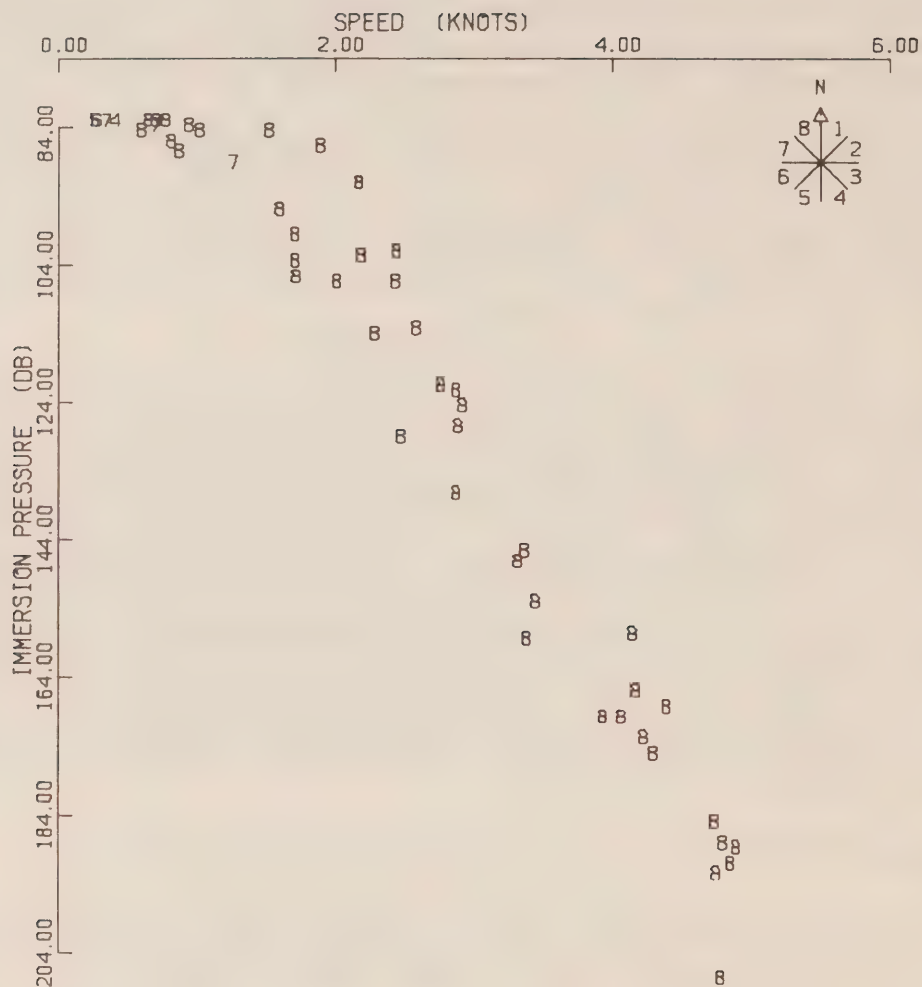
Hydrodynamic drag forces on cables used for mooring an array of current meters or other instruments, where the array is supported by a subsurface buoy, result in excursions of the instruments over some interval of depth as the current varies in strength. These excursions are undesirable inasmuch as they prevent measurements from being obtained at the desired vertical positions at all times and they make the task of correlating measurements from different stations more difficult. Figure 1 shows such a case, where sequential samples from current meter sensors show the vertical position *vs* the current speed at that position over a period of about 2 hours. In this particular case, the current meter was suspended 60 m below a spherical buoy whose rest position was at a depth of 40 m. Total length of  $\frac{1}{4}$ -inch diameter wire rope mooring line was 275 m. Note that the maximum vertical displacement shown is equivalent to about 120 m in depth as the current speed approached 5 knots. The numbers used to denote the data points in Figure 1 refer to direction octants.

One means of reducing the effect of the cable drag is to increase the buoyancy of the system. Another possibility for improving the situation is to reduce the actual drag by fairing the cable to produce a more streamlined profile. An extruded plastic fairing for  $\frac{1}{4}$ -inch diameter cable is made by Fathom Oceanology Limited of Port Credit, Ontario, marketed under the trade name of "Rigstream" fairing. It was decided to try a field experiment to evaluate this product in actual use. A contract was let to Dobrocky Seatech Ltd. of Victoria, B.C. to deploy and retrieve a test mooring utilizing three current meters on a faired cable and, subsequently, to provide the Institute of Ocean Sciences, Patricia Bay with the resulting data tapes for analysis, together with a report describing the mooring activities (Dobrocky Seatech Ltd., 1977). The drag coefficient for the fairing was unknown, but was to be estimated by using the data in conjunction with a numerical computer model (Bell, 1977).

## Field Program

The site chosen for the test mooring was in Haro Strait at the position 48°35.6'N, 123°15.5'W. Prior experience suggested that the velocity profile at this location was quite uniform in both amplitude and direction, especially during periods of large tidal range. The condition of uniformity over depth facilitates subsequent analysis. The water depth at the site is approximately 720 ft.

The mooring was deployed on October 22, 1976 and remained in position until November 1, when it was retrieved. Because of some handling difficulties during installation of the system, the exact amount of fairing applied to the cable was not recorded. The fairing segments were each 2 feet long and it was known that a few segments were left off so that the personnel involved could grip the cable more easily to restrain its motion during deployment. It was also noticed, as the cable moved overboard, that a few segments of fairing were improperly installed. It is suspected that these fell off the cable shortly thereafter. Upon retrieval, the remaining length of fairing was obtained and corresponded to approximately 93% of the total wire rope length.



SCATTER DIAGRAM - PRESSURE VS. VELOCITY

Figure 1. Vertical excursion of a current meter. System buoyancy - 800 lb, length of line between current meter and anchor - 215 m, sample interval - 10 min, tidal range - 2.5 m.

The current meters used in the moored array were Aanderaa Model RCM-4's, equipped with pressure sensors. The pressure sensor accuracy is quoted as being better than 1% of the range. The sensor in the uppermost meter of the array had a range of 0-200 psi, with an accuracy equivalent to  $\pm 4.5$  ft of saline water. The sensors in the other two instruments had a range of 0-500 psi, with a correspondingly reduced accuracy. A further consideration is the resolution provided by one data bit in the data logger, which is equivalent to 0.5 ft of water. Thus, an uncertainty of one bit in each pressure reading could result in an error of  $\pm 1$  ft in determining depth differences. A value for the hysteresis error of the pressure sensors is not given but, for small changes in depth, it could result in a substantial percentage error in depth differences. The accuracy of directions obtained from the magnetic compass is given as  $\pm 5^\circ$  by the manufacturer. The direction and pressure data are obtained as instantaneous values, whereas the speed is integrated over the sample period. The sampling interval used in the present instance was 2 minutes.

A spherical steel buoy with a diameter of approximately 3 ft and a weight in air of 322 lb was used as a subsurface float for the array. It was planned for installation at a height above bottom of about 520 ft, using  $\frac{1}{2}$ -inch diameter 6x19 steel cable to connect it to an anchor clump of 3 railway wheels and an 80 lb Danforth anchor. The three current meters were to be positioned at 100 ft, 300 ft and 500 ft above bottom in quiescent water, i.e. a spacing of 200 ft between instruments. The actual separations, as obtained by measurement of the components involved and allowing for some cable stretch, were slightly different and are given in Table I. The current meters are actually installed in the cable by means of a spindle and gimbal arrangement, with the cable fastening to the ends of the spindle. The pressure sensor location is about 1 ft below the upper end of the spindle, whose total length is about 2.4 ft. This is reflected in the entries of the table.

### Sensor Data

The data records obtained from the test mooring were carefully examined to obtain a good sample set for subsequent processing. Unfortunately, the instrument in the middle position had an intermittent malfunction which narrowed the choice of samples considerably. The chosen data set is presented in Table II. There is good correspondence of the velocities. The directions are slightly different at the bottom sensor, but not enough to be of much consequence. For subsequent use in the mathematical mooring model, the mean of 10 samples is used. This is an aid in smoothing out irregularities in the data arising from the previously mentioned difference in sampling technique between speed and pressure or direction, or from nonuniformities in the velocity profile between measurement stations. It should also be pointed out that, while oceanographic variables are normally reported in the metric system as in Table II, they will here be converted to engineering units (ft-lb-sec) for use in the mooring model. These units are used in the model because of the present utility of the force unit in connection with mooring systems (as anyone who tries to purchase a cable with a breaking strength of X newtons will soon find out). Table III presents some pertinent data thus converted.

TABLE I. Mooring Component Dimensions

<u>Component</u>	<u>Length (ft)</u>	<u>Distance between Major Components (ft)</u>
Anchor clump	2.0	
Unstretched cable	96.5	
Cable extension	0.1	
Swivel & shackles	1.0	
Lower spindle end (LSE) to bottom pressure sensor	1.4	
		101.0
Bottom pressure sensor to upper spindle end (USE)	1.0	
Unstretched cable	198.7	
Cable extension	0.3	
LSE to middle pressure sensor	1.4	
		201.4
Middle pressure sensor to USE	1.0	
Swivel & shackles	1.0	
Unstretched cable	199.0	
Cable extension	0.3	
LSE to top pressure sensor	1.4	
		202.7
Top pressure sensor to USE	1.0	
Swivel & shackles	1.0	
Cable	21.3	
		23.3



TABLE II. Data Obtained From Current Meter Sensors

Record No.	Instrument No.					
	2199			2326		
	Pressure (m)*	Direction (OT)	Speed (cm/sec)	Pressure (m)*	Direction (OT)	Speed (cm/sec)
251	75.7	153	151	138.2	159	158
252	76.0	153	151	138.6	159	139
253	75.7	153	146	138.6	153	146
254	75.1	152	144	138.6	154	140
255	74.7	153	146	137.9	160	139
256	74.7	158	141	137.9	162	139
257	74.8	159	146	137.9	164	139
258	74.5	157	144	137.9	162	137
259	74.7	160	140	137.9	157	151
260	75.7	158	141	138.6	155	175
Mean Value	75.2	155.6	145.0	138.2	158.5	146.3
Rest Position	66.3			129.9		
				194.9	138.7	146.4
				192.4		

Mean value of all speed samples = 146 cm/sec

Mean value of all direction samples = 151<sup>OT</sup>

\* Pressure unit is meters of fresh water



TABLE III. Sensor Data Converted To Ft-Lb-Sec System

	Instrument No.		
	2199	2326	2194
Mean Depth (ft)*	240.9	442.8	624.4
Rest Position (ft)*	212.4	416.2	616.4
Change in depth (ft)	28.5	26.6	8.0

Mean speed = 4.8 ft/sec

Mean direction = 151°T

\* Depth is obtained from the pressure reading and includes the effect due to the water column being saline (specific gravity = 1.024).

### The Mooring Model

Mathematical simulation of the mooring system is accomplished by writing the appropriate static force balance equations for the buoy, the cable and the instruments, and solving them simultaneously using a numerical integration procedure. Boundary conditions are established by the buoy at the upper end of the cable and the integration proceeds from there, in discrete steps, to the anchor end of the cable. Here, the anchor and the bottom must coincide (within a specified limit) or an iteration is necessary. Because of the step-wise integration, the cable consists of an integral number of segment lengths and instruments can only be inserted between segments. As a result, the model dimensions must be altered slightly from those of the real system it is intended to simulate. The effect of this is shown in Table IV for the present case. The next requirement is one of setting out the remaining model input parameters with reasonable accuracy, as presented in Table V.

A value for the drag coefficient of the fairing is assumed and the model predictions obtained for the change in depth of the sensors under the influence of the given current. When this is done for two or three different values of drag coefficient, an interpolation can be made for that coefficient which corresponds to the measured depth excursions. Mention should be made of the fact that only the normal drag force is considered here, consisting principally of form drag, but including a small additive skin friction term. Longitudinal drag is neglected as an unnecessary complication (although provision for calculating it is included in the model). Thus, if the cable is at an angle to the flow, the drag is taken basically as the product of the square of the sine of the angle and the drag which would occur normal to the flow. So long as the angles involved are reasonably close to 90°, the error

due to the omission of frictional drag in the axial direction is small.

TABLE IV. Mooring Component Rest Position Distances (ft above bottom)

Component	Distance			
	Planned	Measured	Pressure*	Model
Bottom sensor	100	101.0	101.1	100
Middle sensor	300	302.4	301.3	300
Top sensor	500	505.1	505.1	506
Buoy	520	528.4	528.4	528

Model cable segment length = 2 ft

No. of segments = 264

\* Derived from pressure sensor data assuming a water depth of 717.5 ft so that the top sensor position coincides with the measured value.

### Fairing Drag Coefficient

Two model simulations were made, using  $C_{DF}$  values of 0.45 and 0.55.

These resulted in predicted depth excursions which bracketed the actual excursions of the upper two current meters. A linear interpolation was then made, indicating coincidence of the measured and predicted excursions at a value of  $C_{DF} = 0.50$  for the upper instrument,  $C_{DF} = 0.52$  for the middle

instrument, and  $C_{DF} = 0.28$  for the lower one. This latter value is suspect in

light of the agreement in results for the top two meters. Also the bottom sensor underwent a relatively small excursion with a possibility of a relatively large hysteresis error. Much more confidence is placed in the result obtained from the top sensor, since it is the most accurate of the three used and it experienced the largest excursion in depth. Thus, the value used henceforth for the drag coefficient of the fairing (based on frontal area) is:

$$C_{DF} = 0.50$$

for sub-critical flow. The uncertainty in this value due to the data logger accuracy of  $\pm 1$  bit is only  $\pm 0.02$ . More uncertainty resides in the lack of complete knowledge of the velocity profile, but a number cannot readily be assigned to this.

TABLE V - Model Input Parameters

## 1. Velocity Profile:

Uniform, 4.8 ft/sec

## 2. Buoy:

Radius = 1.542 ft

Reynolds No. =  $9.9 \times 10^5$  (super-critical)

$C_{DB} = 0.2$

Buoyancy = 984 lb (for specific weight of water = 64 lb/ft<sup>3</sup>)

Weight = 322 lb

Weight, including the weight in water of swivels and shackles = 356 lb.

## 3. Cable:

## (a) Wire Rope:

Diameter = 0.021 ft

Reynolds No. =  $6.7 \times 10^3$  (sub-critical)

$C_{DR} = 1.4$

Weight = 10.0 lb/100 ft

Buoyancy = 2.2 lb/100 ft

Unstretched length = 515.5 ft (excluding swivels and current meter spindles)

## (b) Fathom Rigstream Fairing:

Width (frontal aspect) = 0.030 ft

Chord = 0.125 ft

Reynolds No. =  $4.0 \times 10^4$  (based on chord)

$C_{DF} =$  To be determined

Weight = 10.2 lbs/100 ft

Buoyancy = 7.5 lbs/100 ft

Length = 478 ft

## (c) Fairing - Wire Rope Combination:

Width = 0.030 ft

Weight = 20.2 lbs/100 ft

Buoyancy = 9.7 lbs/100 ft

## 4. Instruments (Aanderaa current meters):

Diameter = 0.42 ft

Reynolds number =  $1.3 \times 10^5$  (sub-critical)

$C_{DI} = 1.1$

Weight = 54 lb

Buoyancy = 17 lb

Frontal area = 0.5 ft<sup>2</sup>

Instrument locations = 24, 228, 428 ft from buoy

At first glance, the estimated drag coefficient value seems high for a reasonably streamlined shape. However, it should be emphasized that the flow regime is sub-critical, i.e. the boundary layer has not yet become turbulent with a consequent rearward movement of the flow separation points. (Also, we have usually had much more exposure to examples of super-critical drag coefficients for streamlined bodies.) Hoerner (1958, p. 13-19) shows a fairing having a cross-section almost identical to that of the Rigstream fairing, except that the trailing edge is less blunt. He gives a sub-critical drag coefficient of 0.73 for that fairing, and a super-critical coefficient of 0.16. Almost always, the cable of any normal mooring system will experience only sub-critical flow; towed systems may be subjected to super-critical flow.

As a check on the validity of the estimate for  $C_{DF}$ , the derived value is used for a prediction of instrument excursion corresponding to another point in the empirical data set. At this point, the data is not constant over more than 2 or 3 samples, but it is smoothly varying so we can, with some confidence, use specific records for a spot check, dispensing with averages as used previously. For this case, the converted data is given in Table VI. The velocity profile is obviously not uniform but does appear to be almost linear. Therefore, a least-mean-squares fit was used to obtain coefficients for a profile of the form  $V = a + bz$ , where  $V$  is the velocity and  $z$  is the depth. The predicted instrument excursions are also shown in Table VI. It is seen that the uppermost two instruments were actually displaced downwards more than the distance predicted by the model, with the disagreement being of the order of 10%. The indication is either that the estimated drag coefficient for the fairing is too small or, more likely, that the velocity between instrument positions was higher than assumed.

TABLE VI. Data Pertaining to Check on  $C_{DF}$  Estimate

	Instrument No.		
	2199	2326	2194
Current Speed (ft/sec)	6.2	5.4	4.2
Current Direction (°T)	150	157	144
Recorded Instrument Depth (ft)	269.5	463.6	631.2
Rest Position (ft)	212.4	416.2	616.4
Actual change in depth (ft)	57.1	47.4	14.8
Predicted change in depth (ft)	51.3	43.2	19.6



### Effect of Faired Cable

Now that an estimate of fairing drag has been obtained, the reduction effected in the magnitude of instrument excursions due to use of the fairing can be determined by having the mooring model simulate both faired and unfaired cables at various current speeds. Since the test mooring was typical of a normal data-gathering array, it will continue to be used as an example.

Table VII presents the results of several such simulations. An examination of this data indicates that a substantial reduction in vertical excursion depth is obtained by using the fairing, with the largest percentage reduction occurring at the lower velocities.

TABLE VII. Predicted Instrument Excursions at Several Current Speeds Using Faired and Unfaired Cable (All values are in feet).

Instrument Position	V = 4 ft/sec		V = 6 ft/sec		V = 8 ft/sec	
	Faired	Unfaired	Faired	Unfaired	Faired	Unfaired
Top	14	30	55	102	120	186
Middle	12	28	49	89	101	154
Bottom	6	14	24	41	45	64

### Effect of Increased Buoyancy

It is instructive to examine the reduction in excursion depth which results from an increase in the buoyant force at the upper end of the cable. The most practical way of adding buoyancy is to do it in modules corresponding to the available buoys, i.e. install additional buoys in the system. In practice, this may require the use of a heavier anchor as well. If carried to extremes, a stronger (and thicker) cable would be necessary, leading to some additional drag, and this might well invoke the law of diminishing returns. For the present example, the provision of two identical buoys in the system does not require any increase in cable strength. The predicted excursions in such a case are given in Table VIII. The results there can be compared with the two situations presented in Table VII, where it will be seen that a much greater reduction in excursion depth is obtained through the addition of an extra buoy as compared to the addition of cable fairing. This is more clearly seen, perhaps, in Figure 2, where the data pertaining to the top instrument of the moored array is plotted for each of the three situations discussed above.



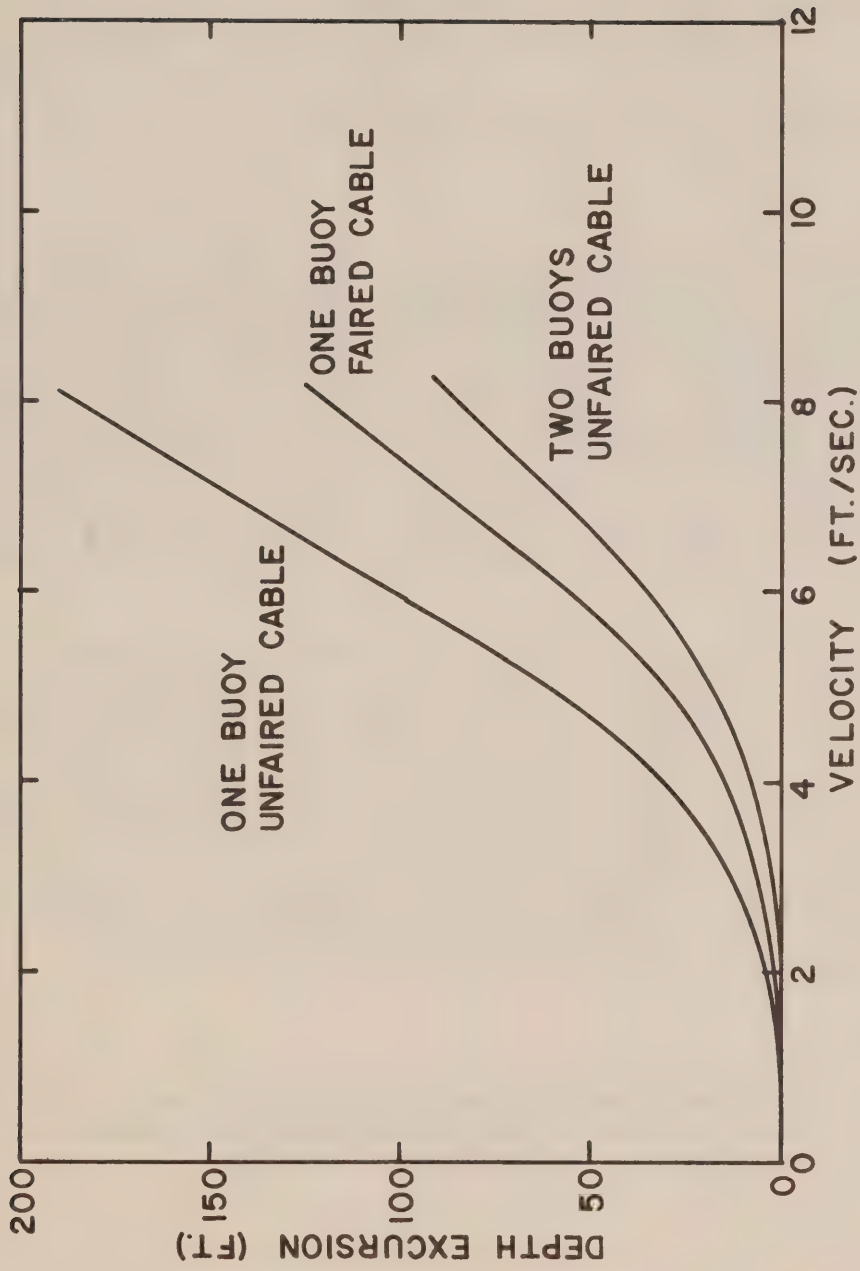


Figure 2. Vertical deflection from rest position for the top instrument in a moored array.

TABLE VIII. Predicted Instrument Excursions at Several Current Speeds Using Two Buoys and Unfaired Cable (All values are in feet).

Instrument Position	V = 4 ft/sec	V = 6 ft/sec	V = 8 ft/sec
Top	8	35	85
Middle	7	31	72
Bottom	3	14	32

### Conclusion

The preceding considerations show that a cable fairing can be used to reduce cable drag and, thereby, the vertical excursions undergone by instruments on the cable when the current speed increases. However, a more effective way of reducing the excursions is to double the buoyant force at the upper end of the cable. In all likelihood, it will be easier to cope with an extra buoy during the installation of an array than it will be to handle a cable covered with plastic fairing. Some consideration must be given, though, to the increased anchor weight required by the use of an additional buoy, and to the possibility that a heavier cable might also be required if the extra buoyancy increases the cable load beyond the normal working range.

Another point, not yet discussed, concerns the "strumming" behaviour of a cable. Strumming, or vibration, results when vortices are shed from an object at a frequency close to the natural frequency of the object. This is apparently a common occurrence with wire rope and may result in a substantial increase in drag. Vortex shedding is inhibited by the use of a splitter plate or fairing, so this may well be a consideration in favour of the plastic fairing. There is an easier-to-use alternative here as well, in the form of the so-called "haired" fairing. This consists of a multitude of flexible plastic threads or ribbons fastened permanently to a cable in such a fashion as to trail downstream from the cable, acting as splitter plates to inhibit vortex shedding.

### Acknowledgements

Grateful acknowledgement is made to the expert work of Dobrocky Seatech personnel, especially Brian Lea, in arranging and installing the test mooring, and to A. Stickland for assisting at all stages.

References

- Bell, W.H. 1977. Static Analysis of Single-Point Moorings. (In Preparation.)
- Dobrocky Seatech Ltd. 1977. Experimental Mooring of Current Meters and Test Fairing in Haro Straits, British Columbia. Victoria, B.C.
- Hoerner, S.F. 1958. Fluid Dynamic Drag. Published by the author. Brick Town, N.J.







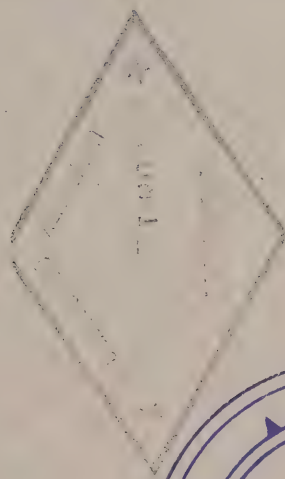


CAI EP 321

-77R09

**A STUDY OF ANOMALOUS SALINITY AND OXYGEN  
VALUES IN THE DEEP WATER AT OCEAN STATION P  
FROM 1960-1976**

**Margaret MacNeill**



**INSTITUTE OF OCEAN SCIENCES, PATRICIA BAY  
Victoria, B.C.**

For additional copies or further information please write to:

Department of Fisheries and the Environment  
Institute of Ocean Sciences, Patricia Bay  
512 - 1230 Government Street  
Victoria, B.C.  
V8W 1Y4

A STUDY OF ANOMALOUS SALINITY AND  
OXYGEN VALUES IN THE DEEP WATER AT OCEAN STATION P  
FROM 1960-1976

by

Margaret MacNeill

Institute of Ocean Sciences, Patricia Bay  
Victoria, B.C.

May 1977

This is a manuscript which has received only limited circulation. On citing this report in a bibliography, the title should be followed by the words "UNPUBLISHED MANUSCRIPT" which is in accordance with accepted bibliographic custom.



## ABSTRACT

Anomalous oxygen and salinity data from the deep water at Ocean Station P (50°N, 145°W) from 1960 to 1977 that were either intentionally omitted from publication or were published anyway, fall into two main categories - samples exhibiting both low oxygen and low salinity (determined by comparison to the average values at that depth or by reversal in the sign of the gradient); and samples with low oxygen and 'normal' salinity. The low oxygen-low salinity anomalies are attributed to leaking or mistripped sampling bottles; the low oxygen-normal salinity anomalies appear to be caused by technical problems although no satisfactory explanation is found to support this.

A decline in quality control may be partially responsible for the increase in the number of unexplained anomalous oxygen values in recent years.

I suggest that only very obviously spurious data be deleted from publication and that all other suspected bad data be published, but marked in some way as suspect.



## TABLE OF CONTENTS

	<u>Page</u>
ABSTRACT .....	i
INTRODUCTION .....	1
THE DEEP WATERS OF THE NORTH PACIFIC OCEAN .....	2
ANALYSIS OF THE DATA .....	4
1. Original Measurements and Computations .....	4
2. Omission of Data from Publication .....	4
3. Significance of the Irregular Data .....	7
4. Paired Bottles .....	12
DISCUSSION .....	16
CONCLUSIONS .....	19
ACKNOWLEDGEMENTS .....	20
REFERENCES .....	21
LIST OF TABLES .....	23
LIST OF FIGURES .....	24



## INTRODUCTION

Oceanographic data have been collected at Ocean Station P in the North Pacific ( $50^{\circ}\text{N}$ ,  $145^{\circ}\text{W}$ , depth 4200 m) on a regular basis since 1956. Observations at depths greater than 2000 m began in 1960; prior to 1960, lack of a suitable winch limited observations to above 2000 m. The data were initially published by the Fisheries Research Board of Canada for the period 1965 to 1969, [except for 1967 and 1968 when they were published by the Canadian Oceanographic Data Centre (now called the Marine Environmental Data Service)], first as the Manuscript Report Series, then as the Data Record Series; and were published by the Institute of Ocean Sciences, Patricia Bay<sup>1</sup> in its Pacific Marine Science Report series. Examination of the data published for the period of deep water casts, 1976, showed occasional deletion of dissolved oxygen content (hereafter termed oxygen) and salinity values - presumably because the data was suspect for some reason. The increase in the incidence of deleted data by almost 100% in 1973 drew attention to the increase in the number of irregular values of oxygen and salinity occurring, especially in the deep water. Because no clear set of criteria had been established for eliminating data before publication, we considered it useful to review the original data logs in order to re-examine the causes for the frequent data omissions, and at the same time, to study any other anomalies present in the data. The object of the present study is to determine the reason for the irregular oxygen and salinity data in the deep water at Ocean Station P and to suggest a set of criteria for omitting data in the future.

<sup>1</sup> Formerly known as the Marine Sciences Branch and then the Marine Sciences Directorate.



## THE DEEP WATERS OF THE NORTH PACIFIC OCEAN

The main features of the water column at Ocean Station P can be observed in the curves in Figure 1, showing temperature-depth, salinity-depth, oxygen-depth and sigma-t-depth for October 9, 1971 - cruise 6, cast 32 (P-71-6-32). These curves are typical for the time of year. Tabata (1961, 1965) described the water column as three layered - the upper, seasonal zone (0-100 m); the principal halocline (100-200 m); and a lower zone beneath the halocline. These layers can be identified in Figure 1. Beneath the upper 30 m of isothermal water at  $10.5^{\circ}\text{C}$ , a thermocline is situated between 30 and 100 m in the seasonal zone. Throughout the seasonal zone, the oxygen and salinity are uniform at about 7.5 ml/l and  $32.7\text{‰}$ . In the principal halocline, the temperature is fairly constant although oxygen decreases rapidly with depth. Below the halocline, the temperature decreases gradually with depth to a minimum of  $1.5^{\circ}\text{C}$  at 4000 m. At 600-900 m, the oxygen reaches a minimum of less than 1 ml/l due to biological decay, after which it increases steadily to about 3.3 ml/l at 4000 m. Salinity increases gradually from the halocline to approximately  $34.690\text{‰}$  at 4000 m. The present study is concerned only with the characteristics of the deep and bottom water below 3000 m.

The water below 2500 m at Ocean Station P is part of the Pacific Deep and Bottom Water called Oceanic Common Water by Montgomery (1958). Its flow northward from the Antarctic Circumpolar current was inferred by Knauss (1962) from the distribution of water properties and further studied by Reed (1969), but the circulation has been difficult to determine because of the small variation in horizontal water properties, and is probably far more complicated at smaller spatial scales. Fofonoff and Tabata (1966), for example, detected a relatively narrow "tongue" of high salinity water extending from the north in the deep water at Ocean Station P.

Reed (1969) studied average values of water properties in the North Pacific at 3000 m, 4000 m, and 5000 m based on United States Coast and Geodetic Survey Cruises from 1961-1966, between  $20^{\circ}\text{N}$  and  $60^{\circ}\text{N}$ , and  $150^{\circ}\text{W}$  and  $170^{\circ}\text{W}$ . At 4000 m, the range of salinity over the whole region was  $34.675\text{‰}$  to  $34.700\text{‰}$  and the range of oxygen was 3.30 ml/l to 3.60 ml/l. At the reoccupied sites, Reed found that 95% of the salinity values deviated less than  $0.008\text{‰}$  from the mean salinity over 5 years; and that 95% of the oxygen values deviated less than 0.12 ml/l from the mean oxygen value. During this particular 5 year period then, the variation in deep water properties over the entire region was small. At Ocean Station P itself, Rupp (1969) found the average properties at 4200 m near the bottom from 1961-1965 to be  $1.50^{\circ}\text{C}$ ,  $34.69\text{‰}$ , and 3.30 ml/l and their respective standard deviations to be  $0.02^{\circ}\text{C}$ ,  $0.012\text{‰}$  and 0.10 ml/l.

Figures 2a and 2b show six T-S and T- $\text{O}_2$  curves that are fairly typical of the water from 3000 to 4200 m at Station P. In general, as the temperature decreases with depth, both oxygen and salinity increase. Occasionally, there are small decreases in salinity (as in P-62-3-13 by  $0.005\text{‰}$ , Figure 2a), or in oxygen, but this is not unusual considering the small gradients at 4200 m and the limits of the errors ( $\pm 0.003\text{‰}$  and  $\pm 0.03$  ml/l) defined by the methods of analysis described in the next section.

There are also increases in temperature of up to  $0.03^{\circ}\text{C}$  with depth near the bottom as seen in Figures 2a and 2b - eg.  $0.02^{\circ}\text{C}$  in P-60-2-19.

## ANALYSIS OF THE DATA

1. Original Measurements and Computations

All temperatures given in the present study are observed temperatures. Since 1969, they were recorded using a pair of Richter & Wiese reversing thermometers on each sampling bottle. The thermometers yield an accuracy of  $\pm 0.02^{\circ}\text{C}$  in routine use, and the accuracy based on readings from two thermometers should be greater.

Salinities were measured using an inductive salinometer--ashore from 1960-1962, and in the ships' laboratory from 1962 to date. The two models presently in use are an Auto-Lab Model 601 MK III and a Plessey Model 6220. Both salinometers are calibrated with Copenhagen water approximately every 20 samples. The accuracy using duplicate determinations is estimated to be  $\pm 0.003\text{‰}$  in a shore laboratory and  $\pm 0.004\text{‰}$  in a ship's laboratory at sea (Strickland, 1958).

The dissolved oxygen content was measured using the Winkler or modified Winkler method with an estimated error of  $\pm 0.03\text{ ml/l}$  (Strickland and Parsons, 1968).

Two types of sampling bottles were used to collect the water samples - Nansen bottles from 1960 to 1972 and Niskin bottles from 1972 to 1976. The practice in drawing both salinity and oxygen samples is to first rinse the bottles and caps twice; then a standard method is used to draw each sample although individual techniques may vary.

2. Omission of Data from Publication

First, all omitted data points were checked against the original data logs and when found, recorded; then an attempt was made to determine the approximate guideline used to eliminate this data. The oxygen values deleted fell into two categories - either the absolute value of the oxygen was too high (or low) compared to the average value for that depth (eg. greater than  $3.6\text{ ml/l}$  or less than  $2.6\text{ ml/l}$  at  $4200\text{ m}$ ) or there was a reversal in the vertical gradient of oxygen, causing an apparent decrease in oxygen with depth. In most cases, the oxygen had to decrease at least  $0.1\text{ ml/l}$  from one sampling bottle to the next deeper one for the value to be omitted (although there were cases of oxygen values being omitted when the difference was as low as  $0.07\text{ ml/l}$ ). Salinity values were omitted when a decrease in salinity of greater than  $0.02\text{‰}$  between successive sampling bottles occurred.

Table I shows the number of oxygen and salinity values omitted each year from the deep water data for unexplained irregularities. The total number of deep casts taken each year is recorded in Column 1. Column 6 shows that from 1967 to 1973, 25 oxygen values were omitted for no apparent reason, and Column 7 shows that 26 oxygen values and 35 salinity values were omitted for documented technical reasons during the same period. Technical reasons included:

- 1) bad oxygen reagents - 5 cases,
- 2) overtitration of oxygen sample - 3 cases,

Table I. A Table of Oxygen and Salinity Values Omitted From Publication  
From 1960-1976

Year	No. of Deep Casts	No. of Irregular O <sub>2</sub> Values Published	No. of Irregular S‰ Values Published	No. of Irregular O <sub>2</sub> Values Omitted	No. of Irregular S‰ Values Omitted	No. of Values Omitted For No Apparent Reason	No. of Values Omitted For Technical Reasons
1960	16	1	-	-	-	O <sub>2</sub> S‰	O <sub>2</sub> S‰
1961	17	2	-	-	-	-	-
1962	18	3	1	-	-	-	-
1963	13	5	-	-	5	-	-
1964	12	1	1	-	1	-	2/-
1965	11	1	-	-	2	-	/4
1966	11	-	1	-	1	-	/1
1967	16	2	2	-	-	4/-	-
1968	16	-	1	7	5	2/-	/5
1969	31	-	-	11	5	8/-	/1
1970	29	1	1	3	1	2/-	2/5
1971	39	2	2	10	5	2/-	4/3
1972	40	4	2	13	13	-/-	8/3
1973	22	2	-	6	9	4/-	5/4
1974	24	2	2	12	13	-/-	-/4
1975	33	11	9	20	15	-/-	1/5
1976	24	5	6	25	21	-/-	4/1

Column #: 1

2

3

4

5

6

7



- 3) bottom sediment in sampling bottle - 1 case,
- 4) leaking sampling bottle - 10 cases,
- 5) drift in salinometer - 15 cases,
- 6) nonrepeatability of a salinity value - i.e. duplicate samples more than 0.01‰ apart - 7 cases,
- 7) Others - 9.

Next, the published data was examined for irregular data points that had not been omitted. Columns 2 and 3 show the number of irregular oxygen and salinity values that had been published. The criteria for selecting these values as irregular were as follows:

- 1) oxygen decreasing with depth by greater than 0.01 ml/l between sampling bottles,
- 2) salinity decreasing with depth by greater than 0.012‰ between sampling bottles,
- 3) an oxygen value that was at least 0.3 ml/l higher than the average value for that depth.

Although the data has a published accuracy of  $\pm 0.04$ ‰ for duplicate samples of salinity run at sea and 0.03 ml/l for oxygen, it is felt that the above uncertainties ( $\pm 0.05$  ml/l and  $\pm 0.006$ ‰) are more realistic as error limits for testing irregular data. For example, the published errors do not take into account the variations in drawing the samples before the determinations of oxygen and salinity are made and the possible errors introduced at that time. The published errors assume the samples are run by highly trained technicians which may not always be the case.

Rupp (1969) showed that in the deep water at Station P from 1960-1966 the actual uncertainties encountered were 0.012‰ and 0.10 ml/l. The study by Reed (1969) for the same period at several other North Pacific Stations showed a deviation from the mean of less than 0.008‰ for salinity and 0.12 ml/l for oxygen in more than 95% of the cases out of 85 samples. Corritt and Carpenter (1966) showed that random and systematic errors in oxygen data using Winkler titrations may be as great as 0.1 ml/l and that for saturated samples and very small values the errors could be much greater. Strickland and Parsons (1968, page 21), in their description of the Winkler method, state that the precision they predict; 0.03 n ml/l, where n is the number of samples run, is "the highest precision considered likely for work in a shorebase laboratory under near ideal conditions, using thiosulphate standardized by the mean of at least five titrations" and that "under routine conditions at sea, the uncertainty range will be appreciably greater, perhaps doubled".

A recent, unpublished study of the well mixed surface layer at Ocean Station P by S. Tabata shows that from 1969 to 1976 the mean standard deviations of the water properties in the well mixed surface layer were as follows:

	<u>October-March</u>	<u>April-September</u>
Temperature	$\pm 0.02^{\circ}\text{C}$	$\pm 0.03^{\circ}\text{C}$
Salinity	$\pm 0.003$ ‰	$\pm 0.003$ ‰
Oxygen	$\pm 0.04$ ml/l	$\pm 0.04$ ml/l



The above statistics are drawn from well over 100 observations. They show the mean standard deviation of salinity values to be the same as the predicted error of  $\pm 0.003\text{‰}$  and the mean standard deviation of the oxygen values to be slightly larger than the published error of  $\pm 0.03 \text{ ml/l}$ . The mean standard deviation in the temperatures is slightly larger in the period April to September than the period October to March, probably due to the direct heating effect of the sun.

The number of published, irregular oxygen and salinity values recorded in Table I demonstrates the arbitrariness of data omissions. For example, in 1975, an extreme case, 17 irregular oxygen values were omitted from publication but 10 irregular oxygen values were not omitted. For most years (Table I), there are a few irregular oxygen and salinity values not omitted, even though they appear to fit the estimated criteria previously used. There are also several blocks of data which appear suspect but which have been published anyway. The three examples are:

- 1) P-76-1: all the temperatures from 3500 m-4200 m are  $0.03$  to  $0.06^{\circ}\text{C}$  higher than normal for those depths. This has been attributed by C. de Jong, chief technician for Ocean Station P cruises (personal communication) to uncalibrated thermometers,
- 2) P-61-5: Casts 8 and 13 - low salinities encountered in all the deep samples; eg.  $34.653\text{‰}$  and  $34.664\text{‰}$  at 4200 m,
- 3) P-76-6: low salinities in all samples from 3000-4200 - eg.  $34.662\text{‰}$  at 4200 m.

The following is a list of data that could not be found with the appropriate original log sheets. Either the data were misfiled, mislaid or were never computed.

- 1) P-63-1: Cast 12; oxygen values not published and original data sheet not found.
- 2) P-65-2: Cast 11; oxygen values not published and original data not found.
- 3) P-70-4: Casts 3 to 9, no deep oxygens calculated.
- 4) P-70-5: Cast 46; the computations were not completed.

Finally, it should be mentioned that there are many anomalous salinity values omitted from the 1976 data reports and replaced with interpolated values but are not marked as interpolated in these reports. Also, some of the published salinity values are the 'better' value of two duplicate samples run from the same sampling bottle, even though the two values are separated by more than  $0.01\text{‰}$ . The usual practice is to run duplicate salinity samples from each depth, then to average the two values obtained to arrive at the published salinity value. If the difference between the two values is greater than  $0.01\text{‰}$  then the values should be discarded and an interpolated value inserted.

### 3. Significance of the Irregular Data

When large amounts of data are collected over a period of years such as at Ocean Station P, there are certain to be spurious data points, even with strict quality control. Over the 17 years under study, 50 different people have taken observations at Station P, some with no previous deep sea experience and little training in the observational and analytical procedures

used to obtain oceanographic data aboard ship. Therefore, it is not unexpected to find a few anomalous oxygen or salinity values in the data. After 1967 though, the number of irregular oxygen and salinity values increases so markedly that it is apparent these errors are not merely random. Table II lists the total number of irregular oxygen and salinity values each year as defined by the criteria on page 6. It also lists the number of anomalous oxygen and salinity values per deep cast each year. Note the increase through the years. Up until 1968, except for 1963, there were fewer than 1 anomalous oxygen or salinity value for every 5 casts. In 1963, 3 of the irregular oxygen values were high values associated with one particular cast. From 1968 to 1974, the average number of irregular oxygens increased to 1 every 3 casts; the average number of irregular salinities also increased to 1 every 3 casts. By 1975-76, there was more than one irregular oxygen value per cast and about one irregular salinity value per cast.

The most common recurring anomaly is combined low oxygen-low salinity. Prior to 1968, this event never occurred. Another, less common anomaly is a low oxygen value accompanied by a 'normal'<sup>1</sup> salinity value. Except for a few cases, the temperature readings encountered are not anomalous. The following is a summary of low oxygen-low salinity; and low oxygen-'normal' salinity occurrences from 1968 to 1976.

- 1968 P-68-1 - every deep cast had low oxygen, low salinity in the 4200 m bottle.
- 1969 - irregularities sporadic
- 1970 - irregularities sporadic
- 1971 P-71-1 - 3 low oxygen-low salinity out of 5 casts (one documented as Teaking).  
P-71-3 - every deep cast exhibited low oxygen-low salinity in the 4000 m (next to bottom) bottle although two of these cases were within limit of error.
- 1972 P-72-3 - low oxygen in the bottom bottle for two out of three casts.  
P-72-7 - three of five deep casts had low oxygen-low salinity in the bottom bottle, 2 out of five deep casts had low oxygen-low salinity in the 3000 m bottle.  
P-72-9 - every deep cast (4) had low salinity-low oxygen in the bottom bottle.

Starting in 1973, the 4200 m bottle was replaced with 2 bottles 10 m apart. This was done specifically to investigate the already increasing irregularities observed in the deep water.

- 1973 P-73-9 - in every one of 5 casts, at least one of the bottom bottles had low oxygen-low salinity.
- 1974 P-74-7 - low oxygen-low salinity for casts 717, 721, 730 - twice in a 3000 m bottle.

---

<sup>1</sup> positive gradient with increasing depth, and within 0.012‰ of the average salinity for that depth

Table II. Shows the Total Number of Unexplained Irregular Salinity and Oxygen Values Per Cast From 1960-1976 and The Number of Unexplained Irregular Values Per Cast If The Simultaneous Low Oxygen-Low Salinity Can Be Explained As a Leaking Sampling Bottle.

Year	No. of Deep Casts	Total No. of Irregular O <sub>2</sub> Values	Total No. of S <sub>00</sub> Values Irregular	Ratio = COL2/COL1	S <sub>00</sub> & O <sub>2</sub> Irregular Simultaneously	COL2-COL5 COL1	Ratio COL3/COL2	COL3-COL5 COL1
1960	16	1	-	0.06	-	0.06	0.06	0.06
1961	17	2	-	0.13	-	0.13	0.12	0.12
1962	18	3	1	0.16	-	0.16	0.17	0.17
1963	13	5	5	0.38	-	0.38	0.38	0.38
1964	12	1	2	0.08	-	0.08	0.17	0.17
1965	11	1	2	0.09	-	0.09	0.18	0.18
1966	11	-	2	0	-	-	0.18	0.18
1967	16	2	3	0.12	-	0.12	0.12	0.12
1968	16	7	6	0.42	5	0.12	0.38	0.06
1969	31	11	5	0.33	-	0.33	0.16	0.16
1970	29	4	2	0.14	1	0.1	0.07	0.03
1971	39	12	7	0.30	6	0.15	0.18	0.03
1972	40	16	15	0.40	10	0.15	0.40	0.12
1973	22	8	9	0.36	5	0.14	0.41	0.18
1974	24	14	15	0.60	8	0.30	0.63	0.29
1975	33	31	24	0.95	17	0.45	0.73	0.21
1976	24	30	26	1.25	20	0.40	1.1	0.25
Column No.: 1	2	3	4	5	6	7	8	



- P-74-9 - casts 923, 911, 917, 930 - low oxygen-low salinity in top bottle at 4200 m.
- 1975 P-75-1 - casts 109, 120, 127, 133, 134 - low oxygen-low salinity in one or both bottom bottles in each cast.
- P-75-3 - casts 309, 320, 323 of 6 casts - low oxygen-low salinity in bottom bottle.
- P-75-4 - no irregularities.
- P-75-5 - no consistent irregularities.
- P-75-7 - low oxygen-low salinity in four of six casts  
low oxygen only in two of six casts
- P-75-9 - low oxygen-low salinity in 3 out of 6 casts
- 1976 P-76-1 - very low oxygen values (1.4-2.4 ml/l) and low salinity (33.8‰-34.5‰) at 4000 m for all four casts.
- P-76-2 - relatively low oxygen values in six out of six casts in bottom 4200 m bottle (2.8-32. ml/l).
- P-76-4 - 5 cases of very low oxygen-low salinity in bottom 4200 m bottle; 4 other cases of low oxygen-low salinity occurred.
- P-76-6 - 6 deep casts; 2 cases of low oxygen-low salinity in both bottom bottles; 4 cases of low oxygen-low salinity in only one bottom bottle.

This summary shows a marked increase in 1975 in the number of cruises where irregular values occur consistently. It also shows, that looking at the whole period from 1968-1976, the occurrence of cruises recording recurring low salinity-low oxygen is really quite sporadic and does not seem to show any kind of a pattern. Most of the odd values are found in one of the bottom two bottles (at 4200 m). From 1968 to 1976; of the 70 cases of low salinity-low oxygen, 51 or 70% were found in one of the bottom bottles. In P-72-3 and in P-76-2, the anomalies were low oxygen accompanied by "normal" salinity.

The family of T-S and T-O<sub>2</sub> curves in Figures 3a and b and 5a and b illustrates the two anomalous situations encountered. Figures 3a and b show consistently low dissolved oxygen in the lower 4200 meter bottle during cruise P-76-2. There is no consistent irregularity in the accompanying salinity although in several casts (particularly noticeable in cast 2-5) the salinity decreases slightly in the bottom bottle. (The T-S curve and the T-O<sub>2</sub> curve in Figures 4 and 4b respectively are drawn from the mean temperature, salinity and dissolved oxygen values for each bottle from six casts and make the general trends of the curves clearer.) The mean T-O<sub>2</sub> curve of Figure 4 exhibits the same general pattern as the 'typical' T-O<sub>2</sub> curves in Figure 2b except that by oxygen in the bottom bottle decreases by approximately 0.3 ml/l from the bottle 10 m above. The corresponding T-S curve in Figure 4a exhibits relatively low salinity in the bottom bottle compared to Figure 2a - 34.675‰ compared to 34.680‰ but shows no appreciable reversal in the salinity gradient. One unusual factor of the large reversal in vertical oxygen gradient is that it occurs only between the bottom two bottles which are 10 m apart; even though the range of depth of the bottom bottles is 3925

to 4183 m - a range of over 250 m (the published error in depth is  $\pm 5$  m).

Figures 5a and 5b, P-71-3, illustrate the situation of low salinity-low oxygen. Again, the mean curves produced in Figures 6a and b show the trends more clearly. The unique feature is the decrease in dissolved oxygen (0.2 ml/l), temperature (0.02°C), and salinity (0.09‰) in the second to bottom bottle at 4100 m (here, the last three bottles are each separated by 100 m). During this cast, the second to bottom bottle ranged over a depth from 3895 to 4090 m; the bottom bottle actually sampled within this depth range during cruise P-71-3 but recorded "normal" salinity and oxygen. The decrease in salinity at 4000 m makes the water column unstable at this depth. Sigma-t decreases as much as 0.015 over 100 m, eg. 27.772 to 27.657.

There are two possible reasons for the recurring anomalies - either they are caused by a real phenomenon or by a recurring technical problem. One technical problem that is occasionally referred to in the log sheets, and could be responsible for the low oxygen-low salinity situations, is a leaking sampling bottle. Between 1970 and 1974 there were 10 recorded cases of leaking bottles; none were recorded before 1970 and none in 1975 and 1976. C. de Jong (private communication), states that Niskin sampling bottles are susceptible to leakage if the top and bottom lids are not seated properly upon snapping shut, especially if this occurs with an open air vent. Sometimes, if Niskin bottles are left cocked for extended periods, a nick can form in the O-ring which could contribute to leakage. de Jong also states that a leaking bottle might not be noticed by an observer, because even perfectly functioning sampling bottles drip a lot of sea water under normal conditions.

The characteristic properties of a leaking sampling bottle seem to be low salinity and low dissolved oxygen in varying degrees (although recorded cases don't always exhibit low oxygen). Table II lists the number of cases of low salinity-low oxygen occurring each year. The number increases quite considerably in 1972, the year the sampling bottles were changed from Nansen to Niskin. It is possible that Niskin bottles are more susceptible to leakage. If it is assumed that the low salinity-low oxygen cases are explained by this technical failure, then the remaining number of unexplained anomalous oxygen values per case each year are reduced to the ratios in Column 6, Table II. Except for 1963 (previously discussed), and 1975 and 1976, most of the ratios for the other years are low enough that the remaining anomalies are probably random. In 1975, half (6) of the remaining irregular oxygen values after the 'leaking bottle' cases are removed, are high values scattered throughout the cruises. The rest are low oxygen values, 3 of which are found in the bottom bottle of 3 casts during P-75-7 and P-75-9. In 1976, five of the remaining 11 irregular oxygens occur in the lower 4200 m bottle during P-76-2. The oxygen values range from 2.7 ml/l to 3.1 ml/l; the oxygens decrease 0.2 to 0.5 ml/l from the bottle 10 m above. Thorough examination of the original data reveals no computation errors to account for this consistent decrease in oxygen at 4200 m. As shown in Column 8, the number of anomalous salinities per cast is also much lower after those low salinities occurring with low oxygens are removed. Even in 1975 and 1976, the number of irregularities per cast is not excessive.



#### 4. Paired Bottles

Starting in 1973, another sample bottle was placed 10 m above the bottom bottle at the 4200 m depth for every deep cast. The yearly statistics for these paired bottles are shown in Table III. The number of cases of irregular values is far greater in 1975 and 1976.

Columns 2 and 5, Table III, show the mean oxygen ( $\bar{O}_2$ ) and salinity ( $\bar{S}\text{‰}$ ) values for both upper and lower bottles at 4200 m for each year. If the average of the two  $\bar{O}_2$  values is calculated for each year, and the yearly averages compared for the four year period, a yearly decrease in the average  $\bar{O}_2$  is observed: from 3.28 ml/l in 1973 to 3.12 ml/l in 1976. This compares with 3.3 ml/l observed by Rupp (1969) as the average deep water oxygen from 1961-1965. Over this same period, the average temperature rose from 1.50°C (Rupp, 1969) to about 1.52°C (average temperature for 1973-1976). Another noticeable change is the increase in the difference between the upper bottle  $\bar{O}_2$  and the lower bottle  $\bar{O}_2$  from 0.05 ml/l in 1973 to 0.25 ml/l in 1976. This can also be seen in Figures 7a and 7b, time plots of the individual differences in salinity (a) and oxygen (b) between the upper and lower bottles from 1973 to 1976. The dashed lines show the published error in salinity and oxygen values (0.006‰ and 0.06 ml/l) that are increased slightly to include the error in drawing the samples (to 0.012 and 0.1 ml/l). A positive difference indicates a higher salinity or oxygen in the bottom bottle and vice versa. The most outstanding feature is the increased number of " $\Delta O_2$ " values outside the dashed error lines in 1975 and 1976 compared to 1973 and 1974. The larger " $\Delta O_2$ " are more prominent during certain months such as December 1974, January to April 1975 and February to August in 1976. Salinity differences, " $\Delta S\text{‰}$ ", are also large for May, June, July and August of 1976. Another period of high " $\Delta S\text{‰}$ " is August 1974 to January 1975.

The yearly standard deviation of the means in Table III includes systematic and random errors as well as real yearly variations. The standard deviations of the mean oxygen values range from 0.14 to 0.35 ml/l. Reed (1969) found that the range of dissolved oxygen in the deep water of the North Pacific was 0.40 ml/l, so in comparison, considering this horizontal range of properties, the standard deviations are not entirely unreasonable, although 0.35 ml/l seems a high yearly standard deviation for 4200 m, especially considering that the bottle only 10 m above had a standard deviation of only 0.13 ml/l for the same period. The standard deviations of the mean salinities range from 0.005‰ to 0.06‰. Again, the large differences between the standard deviations of the upper and lower bottles seem anomalous. The range of salinity found by Reed (1969) in the study mentioned was only 0.02‰, much smaller than the yearly standard deviations calculated for 1973, 0.06‰ and 0.05‰.

Column 6 shows the 95% confidence limits of difference between the pairs of  $\bar{S}\text{‰}$  and  $\bar{O}_2$  values. In general, zero lies between the confidence limits indicated except for the salinity in 1974 and the salinity and oxygen in 1976. This implies that in 1976, there was a 95% probability that in 1976 both the oxygen and the salinity were actually higher in the upper bottle.

Table III. Yearly Statistics For The Two Sampling Bottles 10 m Apart At 4200 m, Showing The Mean Temperature, Oxygen and Salinity For Each Bottle and Their Standard Deviations (The Standard Deviation of All The Mean Temperatures is Less Than .01 C°). The Last Four Columns Show The Number of Anomalous Oxygen and Salinity Values For Each Bottle Per Year.

Year	Bottle (4200 m)	No. of Values	$\bar{O}_2$	$\sigma O_2$	$\bar{S}_{\text{‰}}$	$\sigma S_{\text{‰}}$	95% Confidence Limits of $O_2$ Lower - $O_2$ Upper	95% Confidence Limits of $S_{\text{‰}}$ Lower - $S_{\text{‰}}$ Upper
1973	Upper Lower Simultaneous Average	17 17 17	3.26 3.31 3.28	0.32 0.23	34.66 34.67 34.665	0.06 0.05	0.05±0.15	0.01±0.04
1974	Upper Lower Simultaneous Average	18 18 18	3.24 3.31 3.27	0.21 0.18	34.66 34.69 34.675	0.030 0.005	0.07±0.12	0.03±0.14
1975	Upper Lower Simultaneous Average	34 34 34	3.30 3.21 3.25	0.14 0.17	34.67 34.68 34.675	0.03 0.02	0.09±0.1	0.01±0.012
1976	Upper Lower Simultaneous Average	21 21 21	3.25 3.00 3.12	0.13 0.35	34.68 34.66 34.67	0.01 0.04	0.32±0.2	0.02±0.02
Column No.:		1	2	3	4	5	6	7

Table III (Cont'd.)

Year	Bottle (4200 m)	No. of S‰ Values Low Alone	No. of O <sub>2</sub> Values Low Alone	No. of O <sub>2</sub> & S‰ Values Low Simultaneously	No. of O <sub>2</sub> Values High	$\bar{T}^{\circ}\text{C}$
1973	Upper Lower Simultaneous Average	5 3 1	3 2 1	3 1 -	- - -	1.54 1.53 1.53
1974	Upper Lower Simultaneous Average	7 - -	7 - 1	6 - -	- - -	1.53 1.52 1.52
1975	Upper Lower Simultaneous Average	12 10 6	9 13 6	9 10 6	- 1 -	1.52 1.51 1.51
1976	Upper Lower Simultaneous Average	6 12 3	7 15 3	4 10 3	- 1 -	1.52 1.52 1.52
Column No.:						8      9      10      11      12

There are cases of duplicated anomalies. In each of the years 1973 and 1974 there was one case of low oxygen in both the upper and lower bottle. In both bottles, the oxygen values were within 0.03 ml/l of each other (2.84, 2.85 ml/l and 2.61, 2.64 ml/l) - well within the published error. In 1975, three out of six of the simultaneous cases of low oxygen-low salinity were within 0.008‰ and 0.05 ml/l of each other. In one of the cases of low salinity in both bottom bottles in 1976, the low values of salinity were identical (34.662‰); and in one of the cases of low oxygen-low salinity in both bottom bottles, the salinity values were identical although the oxygen values were different by 0.2 ml/l.



## DISCUSSION

Many of the anomalous oxygen and salinity values in the deep water at Station P appear to be caused by leaking sampling bottles. The suspected cases of leaking sampling bottles exhibit the same low oxygen-low salinity combination found in the few recorded cases which display water properties characteristic of shallower water. The range of salinity, 34.5‰ to 34.7‰ (excluding salinity values below 34.0‰), and of oxygen, 1.4 ml/l to 3.2 ml/l, in these anomalous cases seems too large for them to be indicators of a single real phenomenon. The low oxygen-low salinity cases each year are usually concentrated in certain cruises rather than scattered throughout the year, but the frequency of cases and date of these cruises vary from one year to the next - for example, in 1971, there was only one cruise in April-May with this anomaly recurring at 4200 m; in 1972, there were two cruises - one in October and one in December; in 1973, there was only one cruise in December exhibiting low salinity and oxygen at 4200 m; in 1974, there were two cruises - one in October and one in November; in 1975, low oxygen and salinity occurred repeatedly in 3 cruises - at 4200 m in January, at 4000 m in October and at 4000 m in December; and finally, in 1976, up to November, low oxygen and low salinity occurred consistently at 4200 m in two cruises, one in May-June and one in August-September. Again, the cruises with anomalous values seem to occur too sporadically to attribute the anomalous salinity and oxygen values to a single phenomenon.

There are many speculations about the circulation of deep water in the North Pacific inferred from the distribution of water properties. Knauss, (1962) for example, predicted that the deep water moves up the Pacific Basin from the south with a net speed of 0.05 to 0.1 cm/sec and is gradually warmed by mixing with water above and from heating from the earth's interior. The mixing also gradually decreases its salinity. He believed that the deep water moved more readily up the western side and there were indications of an eastward flow at the equator. Reed (1969), on the other hand, suggested an eastward transport of water along 50°N, south of the Aleutians and northward transport at 5000 m south of 40°N. Because of the small variations in horizontal properties, deep circulation is difficult to infer. Direct current measurements in the deep Pacific have proved thus far unreliable because of the limit of the current meters used in resolving water speeds down to 1 mm/sec from 0-5 cm/sec (Collins, 1969) and the fluctuating barotropic flows of 1 cm/sec or more (Barbee, 1965) and deep tidal currents at least this great, which make resolution of small (order of 1 mm/sec) net velocities difficult (Knauss, 1962). The measurements taken by Collins (1969) using a Geodyne Current Meter model 102 with a Savonius rotor on the bottom (4250 m) at Ocean Station P recorded mean current speeds of 1.54 cm/sec and 0.47 cm/sec on two separate days. The net transport velocities are generally considered small. It is impossible to explain the extremely low oxygens and low salinities and large variations in the time scale of days by such slow advection, especially considering the small range of properties at 4000 m over the whole North Pacific from 1961-1966 found by Reed, i.e. 0.3 ml/l and 0.025‰. It is improbable that the instability caused by a large decrease in salinity with depth at constant temperature would be present at 4000 m for any length of time.



Three other factors suggest that the anomalous values are due to leaking sampling bottles: first, the low oxygen-low salinity samples usually come from a particular bottle on each cruise rather than a particular depth, which implies that some bottles are more susceptible to leaking than others; second, in the 44 cases of low salinity-low oxygen in paired bottles at 4200 m, from 1973-1976, only 9 occur simultaneously in both bottles and in only one case are both the salinity and oxygen of the two depths within 0.012‰ and 0.1 ml/l of each other. If the anomalies are caused by such a localized phenomenon that only one of two bottles 10 m apart can detect it, it seems unlikely that the anomalous characteristics would be sampled so repeatedly in the same bottle. Third, the temperatures which are measured at depth by reversing thermometers show no unusual deviations from the average values for the deep water in these low salinity-low oxygen samples. If the samples are indicative of a different water mass, it is probable that the characteristic temperature would also be different.

It is possible that some of the low oxygen-low salinity samples are due to sampling bottles that do not shut when originally hit by the messenger but trip on the way up to the surface due to a sudden jerk on the wire. B. de Lange Boom (personal communication), an observer aboard the weathership in January, 1976 states that the present messengers are poorly suited to the Niskin bottles and occasionally fail to trip a bottle. Examination of the cases of the deep water low salinity-low oxygen samples from 1971-1976 shows that in 1976, 7 out of 20 of these samples exhibited oxygen and salinity corresponding to a specific shallower depth - usually the shallower depth is 3000-3500 m; in 1975, 8 out of 17 low oxygen-low salinity samples are from a specific shallower depth; in 1974, 2 out of 8 cases fall into this category; in 1973 - none; in 1972 - 1 out of 10; and in 1971 - 3 out of 6. These cases could result from mistripped bottles.

If leakage or mistripping is the technical difficulty causing the low oxygen-low salinity irregularity, one unsolved characteristic of the problem remains: why do the anomalies occur so often in the bottom bottle? Looking at the water column above 800 m, where salinity is increasing and oxygen is decreasing with depth, there are seven cases of low salinity and high oxygen recorded in 1975 and 1976, which would be characteristic of a leaking sampling bottle at these depths. The leaking bottles are not exclusive to 4200 m then, but do occur there much more often than at other depths. Also, in the few cases of duplication of irregular values in the two 4200 m bottles, it is hard to explain the anomalies by two sampling bottles leaking in exactly the same way or mistripping at exactly the same depth.

If the low salinity-low oxygen samples are caused by leaking sampling bottles, the only remaining unexplained anomalies are the low oxygen-normal salinity samples found in the 4000-4200 m bottles during P-72-3, P-75-7, and P-76-2. The low oxygens occur in only 2 out of 3 casts in P-72-3. In P-75-7 and P-75-9, the 3 low oxygen-normal salinity samples are found in the bottom bottle of 3 casts interspersed between 6 other casts exhibiting low oxygen and low salinity in the bottom bottle. These anomalies in themselves do not appear significant. But in P-76-2, every bottom bottle exhibits low oxygen (from 0.2 to 0.5 ml/l lower than normal) although two of these samples also exhibit low salinity as well. These low oxygens appear to

be caused by some technical problem: first, because they always occur in the same bottle during P-76-2; second because the low oxygen values are not reproduced in the sample from 10 m shallower, even though the difference in oxygen in the two bottles is as much as 0.5 ml/l and the range of depth of the paired bottles is 250 m. Unfortunately, there is no obvious explanation for the anomalous oxygen values.

Although oxygen is usually considered a conservative property in the deep water, it can be changed by biological influences. Sedimentary respiration affects the oxygen only a few centimeters above the bottom, and would not likely be detected at the depths nor to the degree of the recorded oxygen anomalies (Dr. Grant Gardner, Institute of Ocean Sciences, Patricia Bay, personal communication). A strong density gradient might trap organic material, causing a depletion of oxygen, but there are no such gradients associated with these low oxygens. Since 1962, no nutrient analysis has been performed on deep water samples so it is not possible to use them as indicators of biological activity. Observations of nutrients in 1960 show silicate increasing from the surface to the bottom with the highest values (app. 162  $\mu\text{g.a./l}$ ) from 1000 to 4000 m; the limited number of phosphate observations in 1960 show phosphate decreasing from 3  $\mu\text{g.at./l}$  at 1500 m to 2  $\mu\text{g.at./l}$  at 4000 m.

It should be noted that the anomalous oxygen values are not entirely limited to the deep water; for example, cruise P-76-2 recorded high (by at least 0.25 ml/l) oxygen values in the 800 m bottle in the oxygen minimum layer in every cast.

The low oxygen values in the deep water at Ocean Station P that are not accompanied by low salinity in 1975 and 1976 defy explanation as either a technical problem or a real phenomenon. If the low oxygen is a real phenomenon, the many cases of low oxygen-low salinity caused by leaking sampling bottles would tend to mask any low oxygens that were real. Sporadic cases of high oxygen-normal salinity, non-duplicated salinity, and low salinity-normal oxygen which occur in 1975-76 also make interpretation of the low oxygen cases difficult.

## CONCLUSIONS

1. Samples taken from the deep water that have both low oxygen and low salinity are attributed to leaking sampling bottles or mistripped bottles.
2. The samples taken from the deep water with low oxygen and normal salinity during P-76-2 are essentially inexplicable but are probably also caused by sampling or analytical technique.
3. A firm set of criteria should be set down for eliminating data from publication. Probably only recorded technical failures and extremely irregular values (especially in the case of samples exhibiting low oxygen, low salinity and normal temperature which indicate a leaking sampling bottle) should be omitted, with other suspected data being published but marked in some way to show they are suspect. The most recent reports are beginning to use this procedure, noting both interpolated and suspected values. When determining whether values are irregular, the published error should be slightly increased to include error in drawing the samples, so that two samples are considered significantly different if they are separated by 0.01 to 0.012‰ for 0.08 to 0.1 ml/l, for example. Suspected values should be those a) that show reversal in vertical gradient by at least the above amounts; or b) oxygen or salinity values that differ by more than 0.3 ml/l or 0.02‰ from the average values for that depth (especially if a whole cast exhibits anomalous values). All interpolated values should be marked, including those inserted to replace omitted original data.
4. The increase in the number of unexplained anomalous oxygens, the increase in difference between the oxygen values in the two 10 m bottles at 4200 m, and the increase in the number of cases of non-duplicated salinities in recent years seem to indicate that a higher degree of quality control in data collection and reduction should be exercised in the future. More care should be taken in recording all technical failures.



## ACKNOWLEDGEMENTS

I wish to acknowledge those who have assisted in the production of this report; especially Dr. S. Tabata who suggested and supervised the study, and Patricia Kimber who prepared the illustrations. I also wish to thank C. de Jong and B. Minkley who provided technical suggestions.

## REFERENCES

- Canada, Department of Energy, Mines and Resources, Ottawa, Data Record Series, 1967-1968. Ocean Weather Station P, North Pacific Ocean.
- Canada, Fisheries Research Board. Manuscript Report Series (Oceanographic and Limnological), 1960-1969: Data Record for Ocean Weather Station P.
- Carritt, D.E. and J.H. Carpenter, 1966. Comparison and evaluation of currently employed modifications of the Winkler Method for determining dissolved oxygen in seawater; a NASCO report. J. Mar. Res., 24, 286-318.
- Fofonoff, N.P. and S. Tabata, 1966. Variability of oceanographic conditions between Ocean Station P and Swiftsure Bank off the Pacific coast of Canada. J. Fish. Res. Bd. Canada, 23(6), 825-868.
- Institute of Ocean Sciences, Patricia Bay, Marine Sciences Report Series, 1973-1977. Oceanographic Observations at Ocean Station P.
- Knauss, J.A., 1962. On some aspects of the deep circulation of the Pacific. J. Geophys. Res., 67, 3943-54.
- Marine Sciences Branch, Marine Sciences Report Series, 1969-1972. Oceanographic Observations at Ocean Station P.
- Marine Sciences Directorate, Marine Sciences Report Series, 1972-1973. Oceanographic Observations at Ocean Station P.
- Montgomery, R.B., 1958. Water characteristics of Atlantic Ocean and of World Ocean. Deep-Sea Res., 5, 134-48.
- Reed, R.K., 1969. Deep water properties and flow of the central North Pacific. J. Mar. Res., 27, 24-31.
- Rupp, S.M., 1969. Temporal variations of the deep water at Ocean Station P. Chesapeake Bay Institute Technical Report 57, Reference 69-10.
- Tabata, S., 1961. Temporal changes of salinity, temperature and dissolved oxygen content of the water at Station P in the Northeast Pacific Ocean and some of their determining factors. J. Fish. Res. Bd. Canada, 18, 1073-124.
- \_\_\_\_\_, 1965. Variability of oceanographic conditions at Ocean Station P in the Northwest Pacific Ocean. Trans. Roy. Soc. Canada, Vol. III, Series IV., 367-418.
- Strickland, J.D.H., 1958. Standard methods of seawater analysis. Vol. II. Fish. Res. Bd. Canada, MS. Rept. (Oceanog. and Limnol.), No. 19, 78 pp.



- Strickland, J.D.H. and T.R. Parsons, 1968. A manual of seawater analysis. Fish. Res. Bd. Canada, Bull. No. 125, 185 pp.
- Sverdrup, H.U., Johnson, M.J., and R.H. Fleming, 1942. The Oceans, their Physics, Chemistry and general biology. Prentic-Hall, New York.

## LIST OF TABLES

	<u>Page</u>
TABLE I: A Table of Oxygen and Salinity Values Omitted From Publication From 1960-1976 .....	5
TABLE II: Shows the Total Number of Unexplained Irregular Salinity and Oxygen Values Per Cast From 1960-1976 and The Number of Unexplained Irregular Values Per Cast If The Simultaneous Low Oxygen-Low Salinity Can Be Explained As a Leaking Sampling Bottle .....	9
TABLE III: Yearly Statistics For the Two Sampling Bottles 10 m Apart At 4200 m, Showing The Mean Temperature, Oxygen And Salinity For Each Bottle and Their Standard Deviations (The Standard Deviation of All The Mean Temperatures is Less Than 0.01 C°). The Last Four Columns Show The Number of Anomalous Oxygen And Salinity Values For Each Bottle Per Year .....	13

## LIST OF FIGURES

- Figure 1: T-Z,  $\sigma_t$ -Z, S‰-Z, O<sub>2</sub>-Z plots for Ocean Station P, October 9, 1971.
- Figure 2a: Six typical T-S curves for Ocean Station P, 1960-1976.
- 2b: The T-O<sub>2</sub> curves corresponding to Fig. 2a.
- Figure 3a: T-S curves for cruise P-76-2 at Ocean Station P showing low oxygen in the 4200 m bottle.
- 3b: T-O<sub>2</sub> curves for P-76-2 corresponding to Fig. 3a.
- Figure 4a: Mean T-S curve for P-76-2 from Fig. 3a.
- 4b: Mean T-O<sub>2</sub> curve for P-76-2 from Fig. 3b.
- Figure 5a: T-S curves for cruise P-71-3 at Ocean Station P showing low salinity and low oxygen in the 4000 m bottle.
- 5b: T-O<sub>2</sub> curves corresponding to Fig. 5a for P-71-3.
- Figure 6a: Mean T-S curve for P-71-3 from Fig. 5a.
- 6b: Mean T-O<sub>2</sub> curve for P-71-3 from Fig. 5b.
- Figure 7a: The difference ( $\Delta S‰$ ) between the salinity in the upper and lower bottles separated by 10 m at 4200 m at Ocean Station P from 1973-1976. The dashed lines designate 0.012‰, the published error limit of the measurements with 0.004‰ added to include errors in drawing the samples.
- 7b: The difference ( $\Delta O_2$ ) between oxygen in the upper and lower bottles at 4200 m at Ocean Station P from 1973-1976. The dashed line denotes 0.1 ml/l, the published error limit of the measurements which has been increased to include errors in drawing the sample.

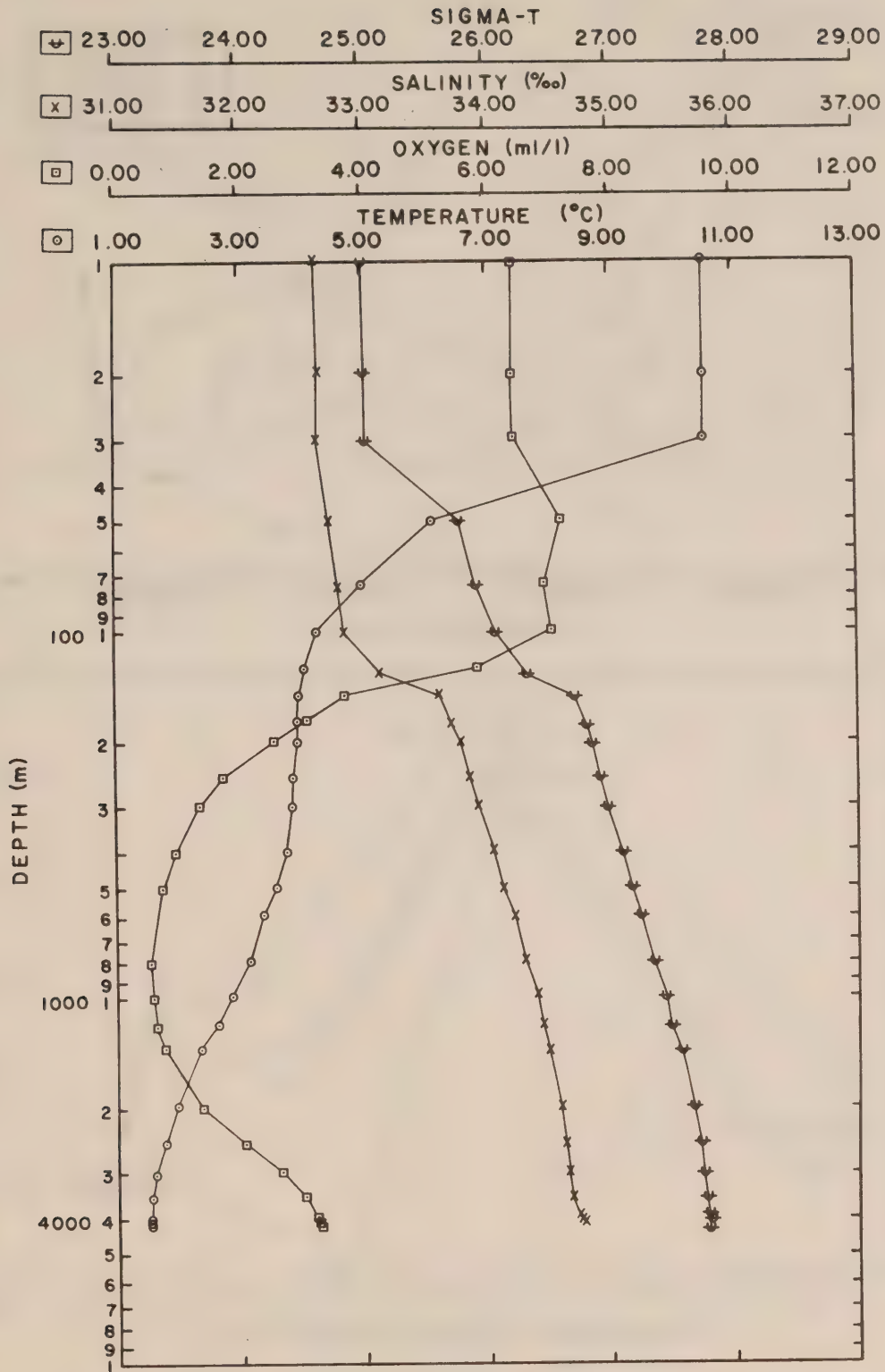


Figure 1: T-Z,  $\sigma_t$ -Z,  $S_{00}$ -Z,  $O_2$ -Z plots for Ocean Station P, October 9, 1971.

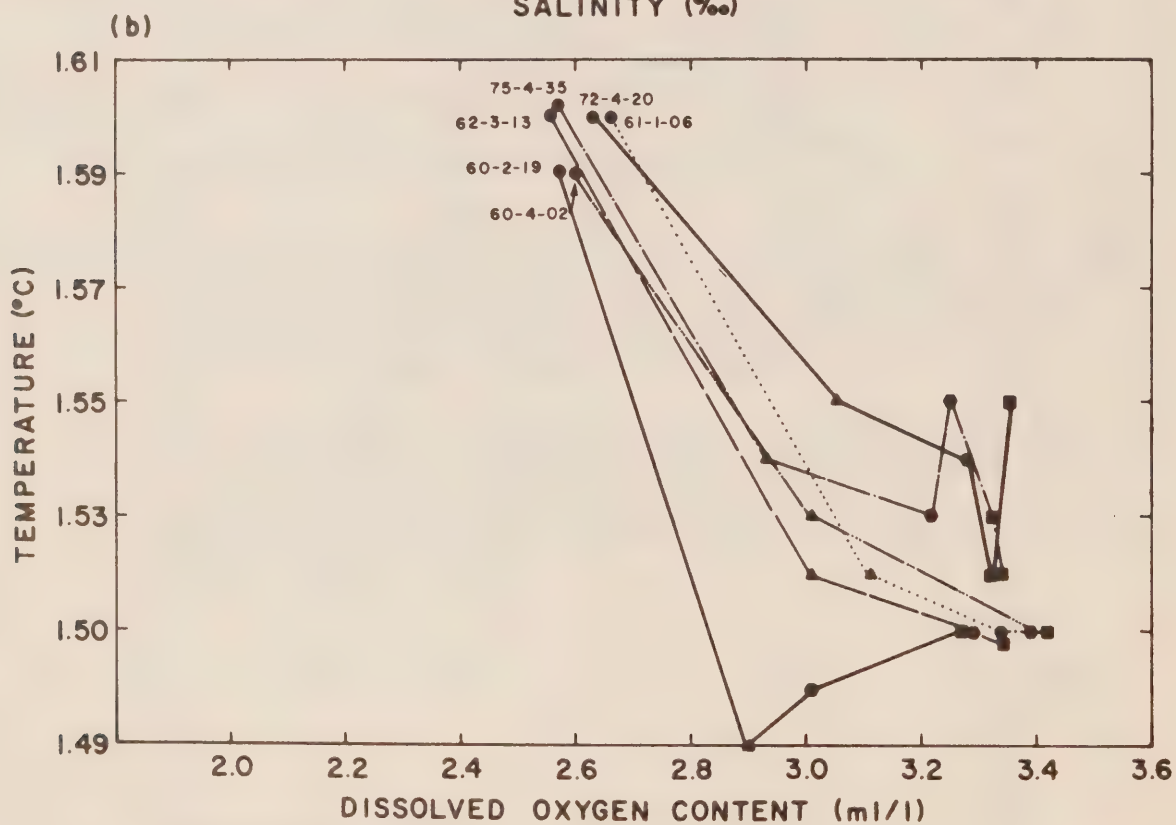
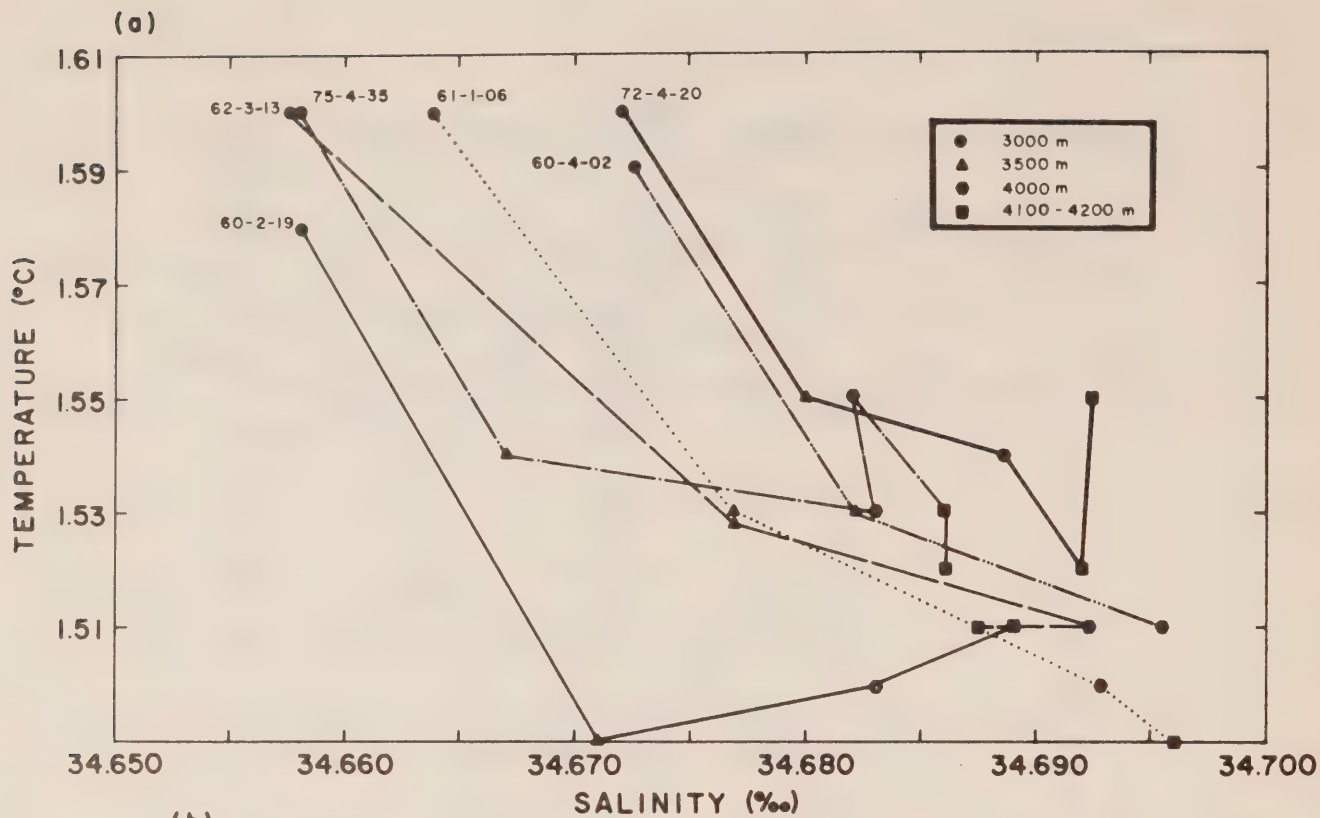


Figure 2a: Six typical T-S curves for Ocean Station P, 1960-1976.

2b: The T-O<sub>2</sub> curves corresponding to Fig. 2a.



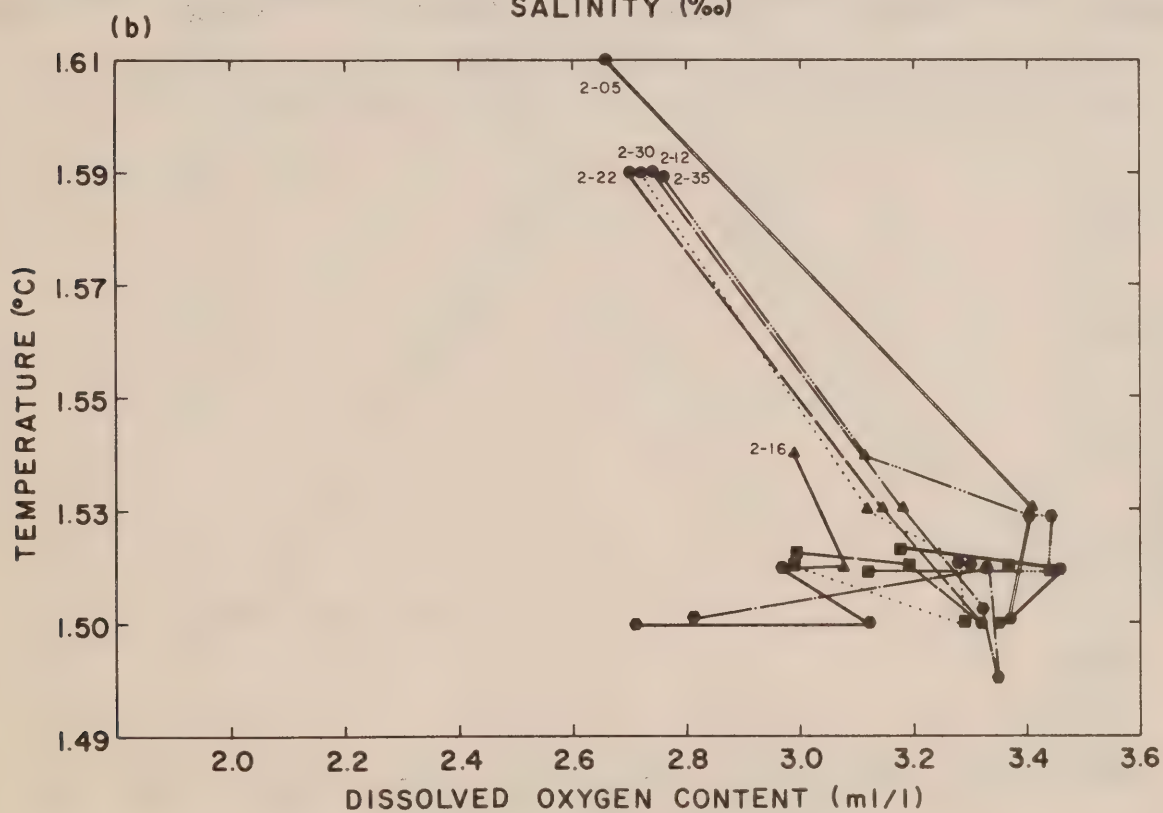
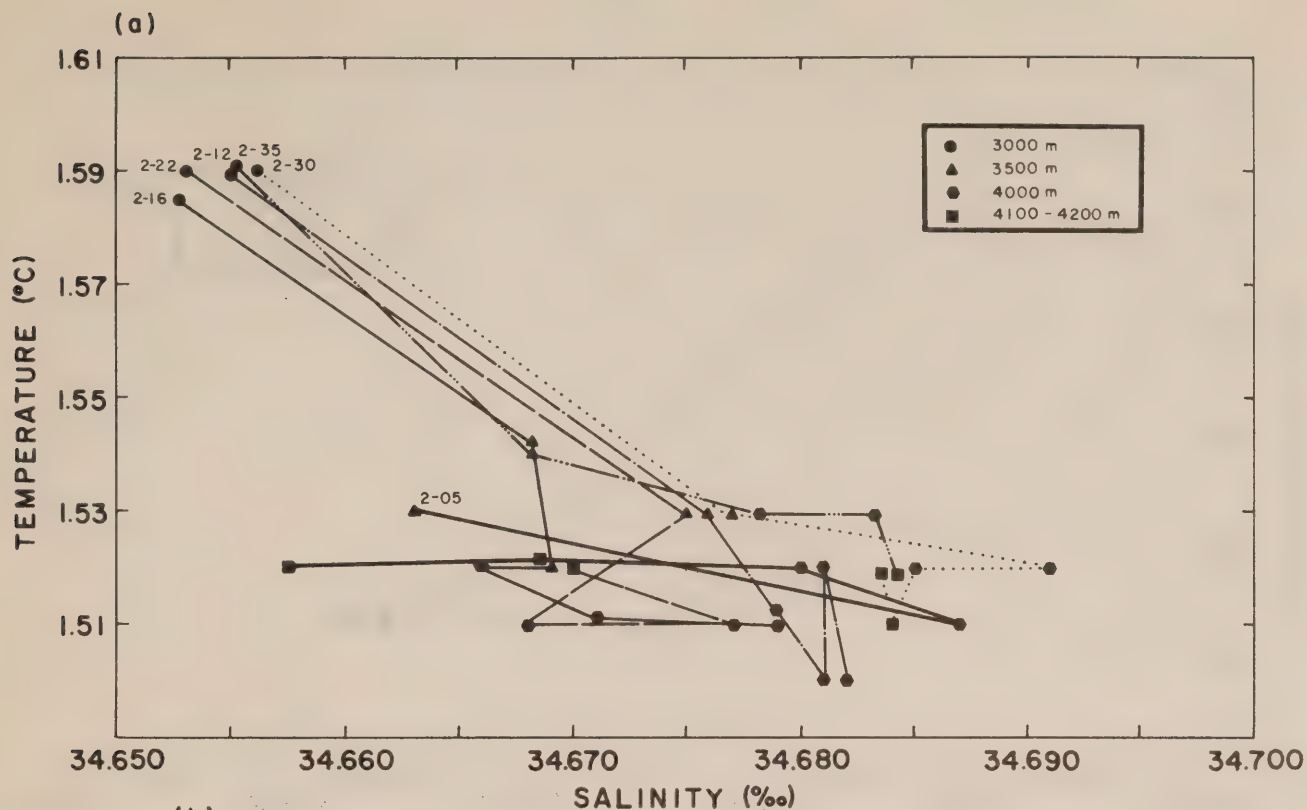


Figure 3a: T-S curves for cruise P-76-2 at Ocean Station P showing low oxygen in the 4200 m bottle.

3b: T-O<sub>2</sub> curves for P-76-2 corresponding to Fig. 3a.

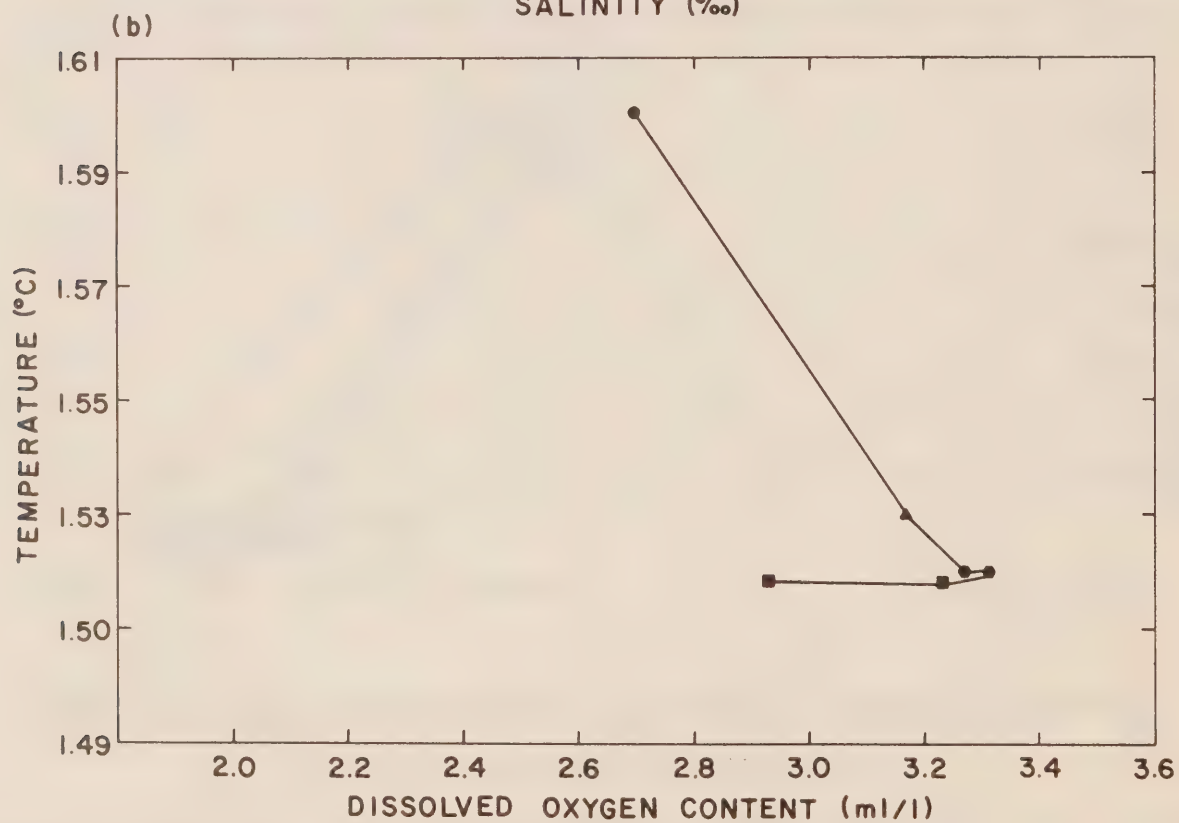
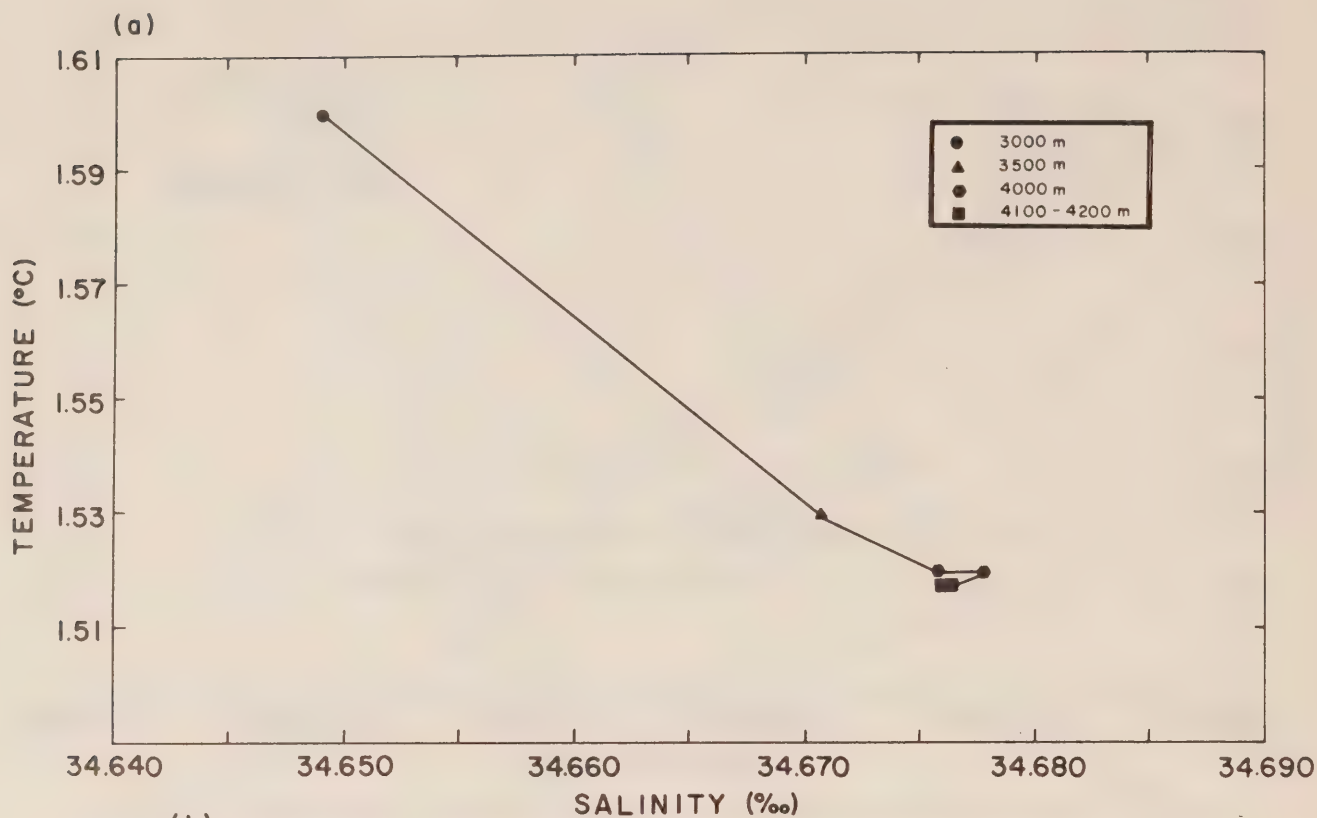


Figure 4a: Mean T-S curve for P-76-2 from Fig. 3a.

4b: Mean T-O<sub>2</sub> curve for P-76-2 from Fig. 3b.

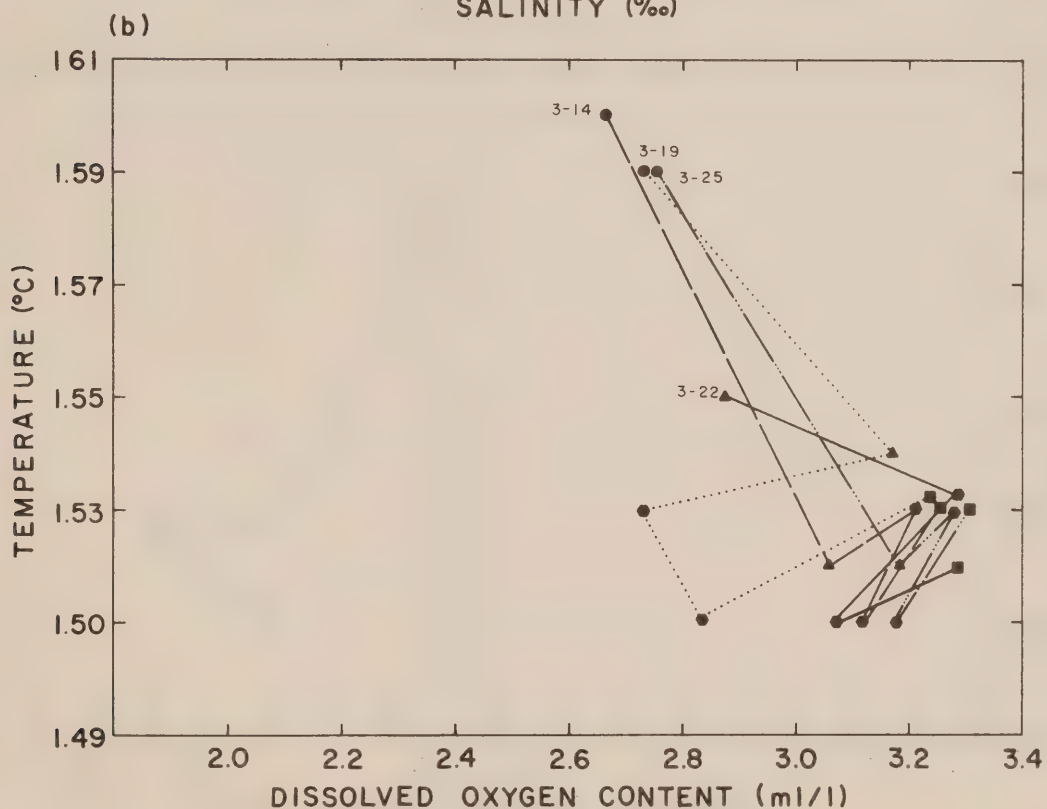
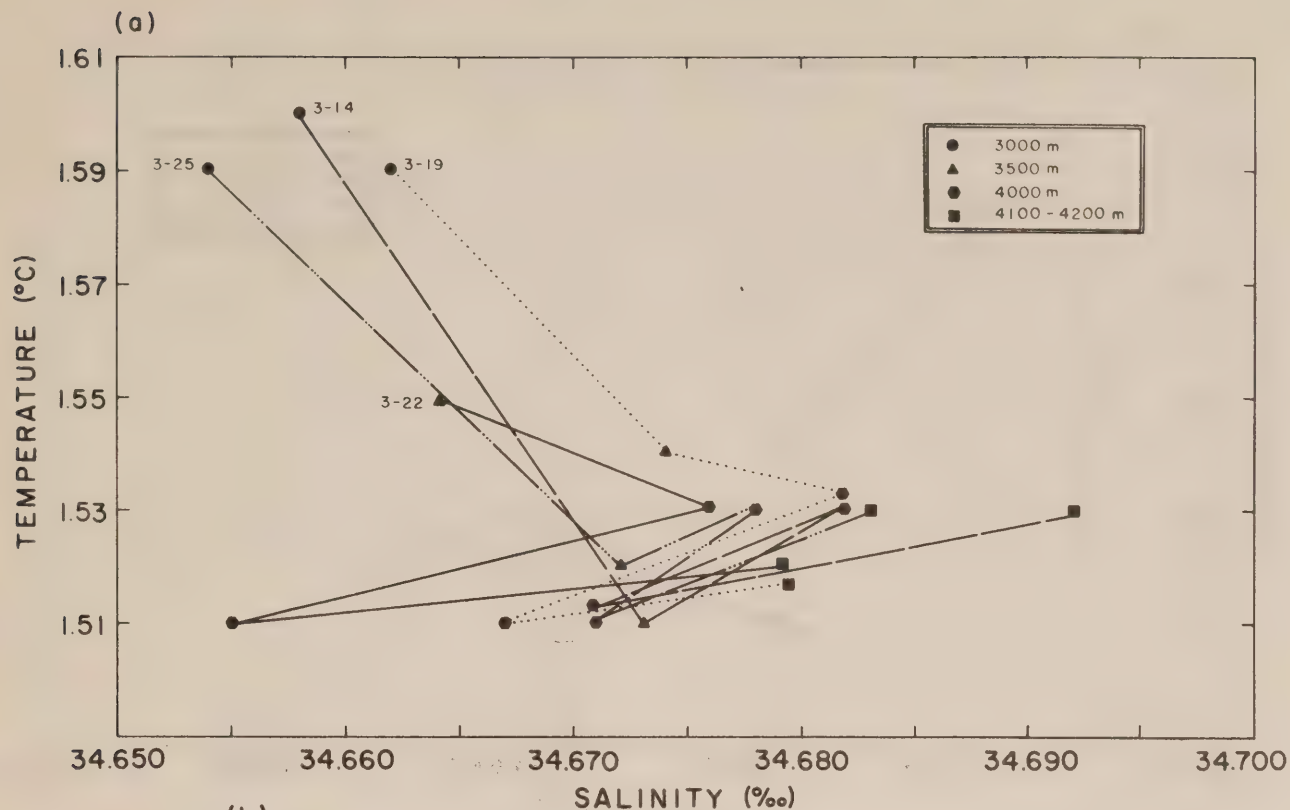


Figure 5a: T-S curves for cruise P-71-3 at Ocean Station P showing low salinity and low oxygen in the 4000 m bottle.

5b: T-O<sub>2</sub> curves corresponding to Fig. 5a for P-71-3.

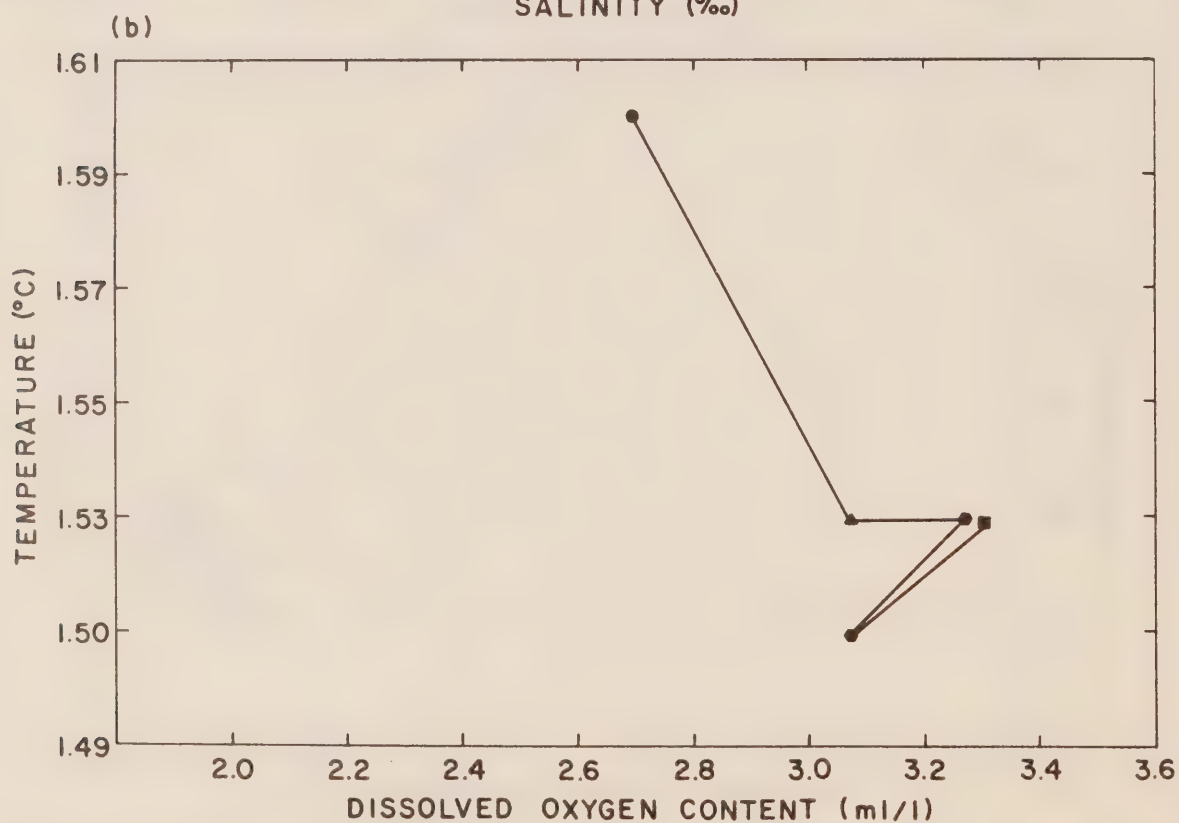
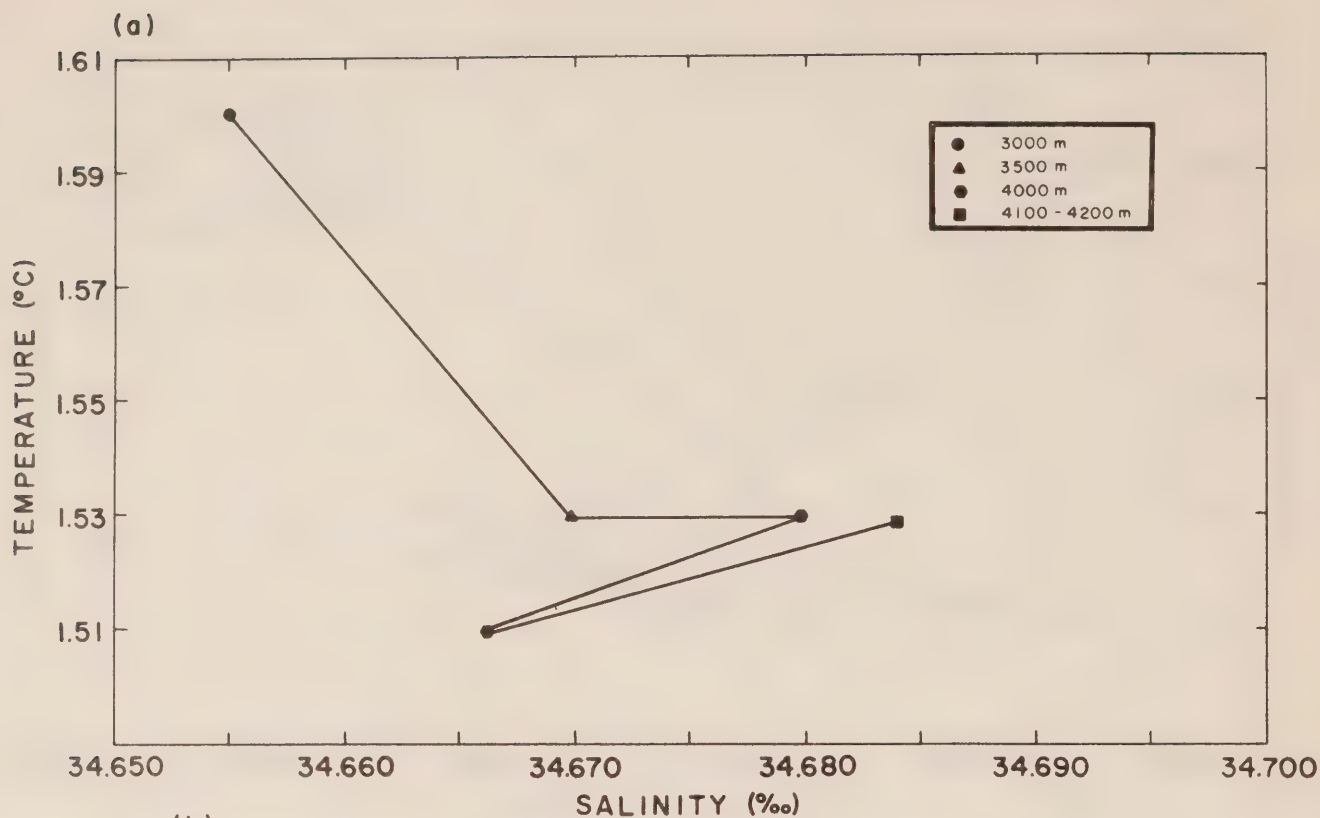


Figure 6a: Mean T-S curve for P-71-3 from Fig. 5a.

6b: Mean T-O<sub>2</sub> curve for P-71-3 from Fig. 5b.

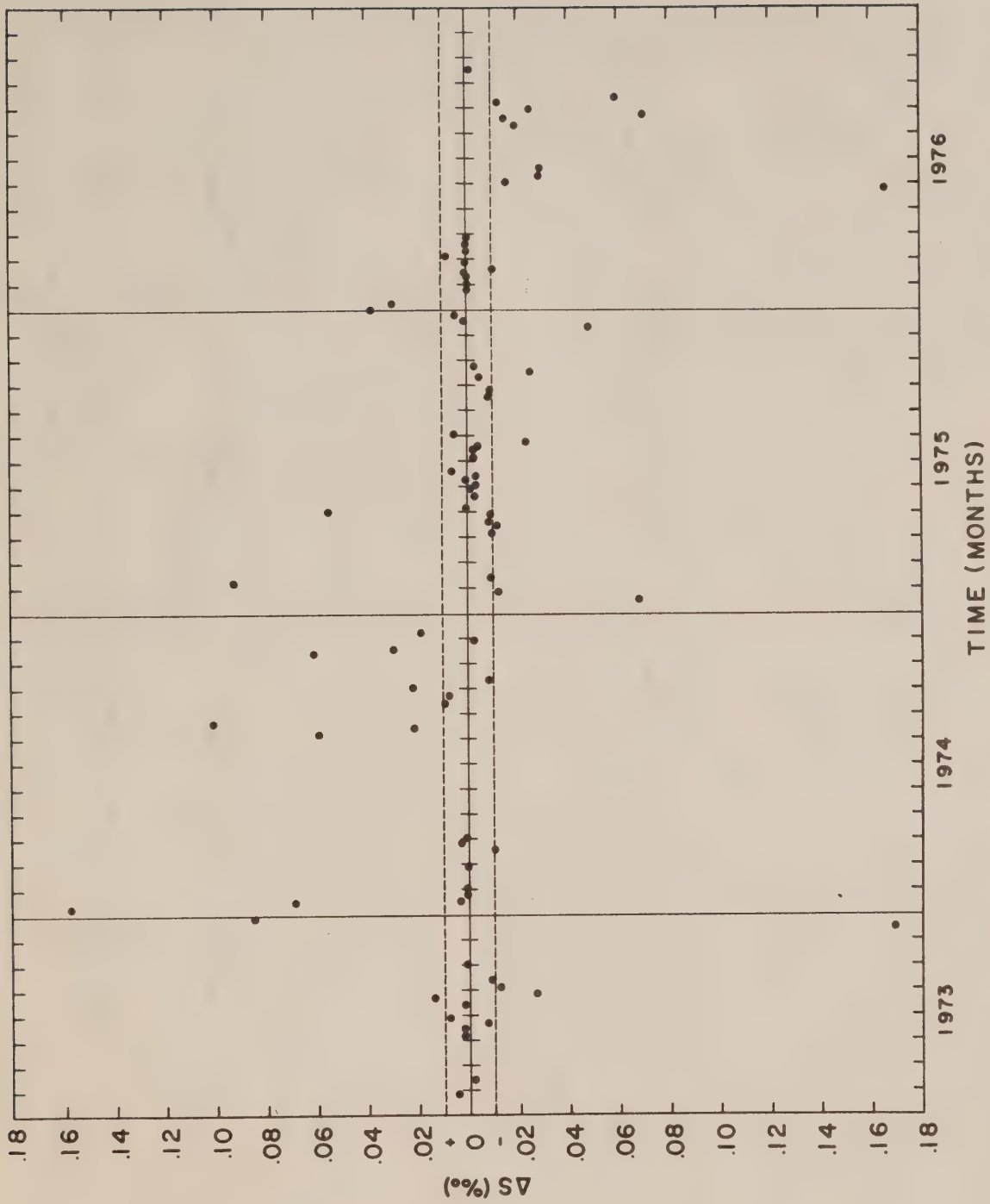


Figure 7a: The difference ( $\Delta S$ ‰) between the salinity in the upper and lower bottles separated by 10 m at 4200 m at Ocean Station P from 1973-1976. The dashed lines designate 0.012‰, the published error limit of the measurements with 0.004‰ added to include errors in drawing the samples.



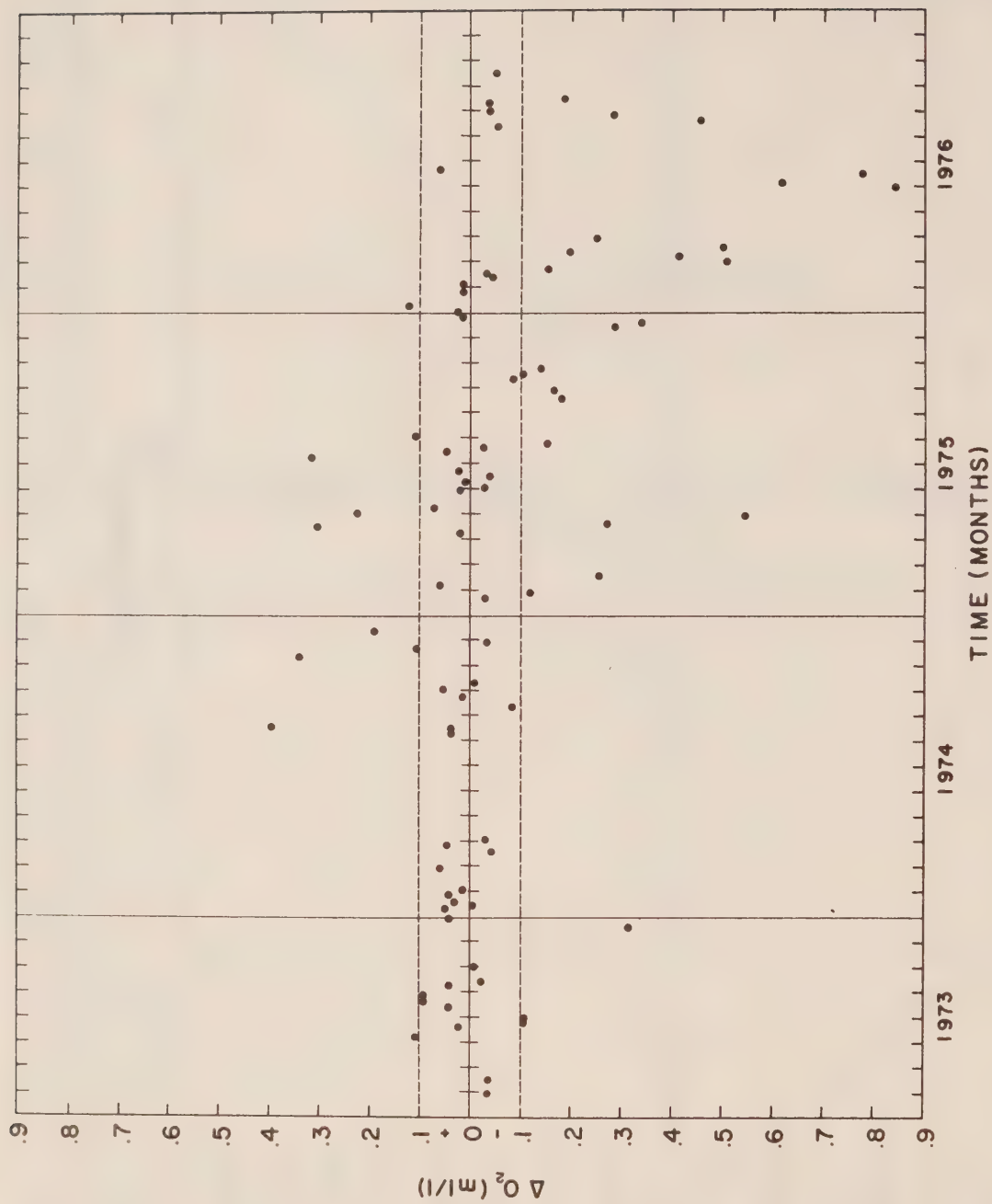


Figure 7b: The difference ( $\Delta O_2$ ) between oxygen in the upper and lower bottles at 4200 m at Ocean Station P from 1973-1976. The dashed line denotes 0.1 ml/l, the published error limit of the measurements which has been increased to include errors in drawing the sample.





**Manual for Tidal Heights  
Analysis and Prediction**



**M.G.G. Foreman**

**INSTITUTE OF OCEAN SCIENCES, PATRICIA BAY  
Victoria, B.C.**



For additional copies or further information please write to:

Department of Fisheries and the Environment

Institute of Ocean Sciences, Patricia Bay

512 - 1230 Government Street

Victoria, B.C.

V8W 1Y5



MANUAL FOR TIDAL  
HEIGHTS ANALYSIS AND PREDICTION

by

M.G.G. Foreman

Institute of Ocean Sciences, Patricia Bay  
Victoria, B.C.

July 1977

This is a manuscript which has received only limited circulation. On citing this report in a bibliography, the title should be followed by the words "UNPUBLISHED MANUSCRIPT" which is in accordance with accepted bibliographic custom.

## Table of Contents

	page
Preface	iii
Acknowledgements	iv
 1. Use of the Tidal Heights Analysis Computer Program	
1.1 General Description	1
1.2 Routines Required	1
1.3 Data Input	2
1.4 Output	7
1.5 Program Conversion, Modifications, Storage and Dimension Guidelines	9
 2. Tidal Heights Analysis Program Details	
2.1 The Constituent Data Package	
2.1.1 The Astronomical Variables	14
2.1.2 Choice of constituents and Rayleigh Comparison Pairs	16
2.1.3 Satellite Constituents and Nodal Modulation	24
2.1.4 Shallow Water Constituents	26
2.2 The Least Squares Method of Analysis	
2.2.1 Formulation of the Problem	29
2.2.2 Solution of the Matrix Equation, the Condition Number, and Statistical Properties	34
2.3 Modifications to the Least Squares Analysis Results	
2.3.1 Astronomical Argument and Greenwich Phase Lag	40
2.3.2 Nodal Corrections	42
2.3.3 Final Amplitude and Phase Results	46
2.3.4 Inferred Constituents	46

3. Use of the Tidal Heights Prediction Computer Program	
3.1 General Description	50
3.2 Routines Required	50
3.3 Data Input	50
3.4 Output	54
3.5 Program Conversion, Modifications, Storage and Dimension Guidelines	55
4. Tidal Heights Prediction Program Details	
4.1 Problem Formulation and the Equally Spaced Predictions Method	58
4.2 The High and Low Tide Prediction Method	61
5. Consistency of the Analysis and Prediction Programs	68
6. Appendices	
1 Standard Constituent Input Data for the Tidal Heights Analysis Computer Program	70
2 Sample Tidal Station Input Data for the Analysis Program	80
3 Final Analysis Results Arising from the Input Data of Appendices 1 and 2	84
4 Sample Input for the Tidal Heights Prediction Program	86
5 Tidal Heights Prediction Results Arising from the Input Data of Appendix 4	93
7. References	97

## Preface

This report is intended to serve as a user's manual to G. Godin's tidal heights analysis and prediction programs, revised along lines suggested by Godin. In addition to describing input and output of these programs, the report gives an outline of the methods used; a full presentation of which can be found in Godin [1972] and Godin and Taylor [1973].

Users who wish to receive updates of these programs and manual should send their names, addresses and type of computer used for implementation to the author.



ACKNOWLEDGEMENTS

The writer wishes to thank Dr. G. Godin for his guidance during the computer program revisions, Mr. J. Taylor and Dr. R.F. Henry for their helpful suggestions, Mrs. C. Wallace for assisting in the preparation of the diagrams, and Ms. E. Peirson and Mrs. S. McKenzie for typing the report.

## 1. USE OF THE TIDAL HEIGHTS ANALYSIS COMPUTER PROGRAM

### 1.1 General Description

This program analyzes the hourly height tide gauge data for a given period of time. Amplitudes and Greenwich phase lags are calculated via a least squares fit method coupled with nodal modulation for only those constituents that can be resolved over the length of record. Unless specified otherwise, a standard data package of 69 constituents will be considered for inclusion in the analysis, however, up to 77 additional shallow water constituents can be requested. If the record length is such that certain important constituents are not included directly in the analysis, provision is made for the inference of the amplitude and phase of these constituents from others. Gaps within the tidal record are permitted.

### 1.2 Routines Required

- 1) MAIN..... reads in some of data, controls most of the output and calls other routines.
- 2) INPUT..... reads in the hourly height data for the desired time period and checks for errors.
- 3) UCON..... chooses the constituents to be included in the analysis via the Rayleigh criterion.
- 4) SCFIT2..... finds the least squares fit to an equally spaced time series using sines and cosines of specified frequencies as fitting functions.

- 5) VUF..... reads required information and calculates the nodal corrections for all constituents.
- 6) INFER..... reads required information and calculates the amplitude and phase of inferred constituents, as well as adjusting the amplitude and phase of the constituent used for the inference.
- 7) CHLSKY..... solves the symmetric positive definite matrix equation resulting from a linear least squares fit.
- 8) CDAY..... returns the consecutive day number from a specific origin for any given date in the range 1901 to 1999, and vice versa.
- 9) SETTAB..... sorts results in preparation for 'J' card output.
- 10) DGM388..... produces 'J' card output and lists the constituents in species by increasing frequency.

### 1.3 Data Input

For a computer run of the tidal heights analysis program, two logical units are used for data input. Logical unit number 8 contains the tidal constituent information while logical unit 4 contains the hourly heights and information relating to the type of analysis and output required. A listing of the standard constituent information for logical unit 8 and a sample set of input for logical unit 4 are given in Appendices 1 and 2 respectively.

Logical unit 8 expects four types of data:

- i) One card each for all the possible constituents, KONTAB, to be included in the analysis along with their frequencies, FREQ, in cycles/hour and the constituent with which they should be compared under the Rayleigh criterion, KMPR. The format used is (4X,A5,3X,F13.10,4X,A5). Unless

KONTAB is specifically designated on logical unit 4 for inclusion, a blank data field for KMPR results in the constituent not being included in the analysis. A blank card terminates this data type.

- ii) Two cards specifying values for the astronomical arguments S0,H0,P0,ENPO, PPO,DS,DH,DP,DNP,DPP in the format (5F13.10).

S0 = mean longitude of the moon (cycles) at the reference time origin.

H0 = mean longitude of the sun (cycles) at the reference time origin.

P0 = mean longitude of the lunar perigee (cycles) at the reference time origin.

ENPO = negative of the mean longitude of the ascending node (cycles) at the reference time origin.

PPO = mean longitude of the solar perigee (perihelion) at the reference time origin.

DS,DH,DP,DNP,DPP are their respective rates of change over a 365 day period at the reference time origin.

- iii) At least one card for all the main tidal constituents specifying their Doodson numbers and phase shift along with as many cards as are necessary for the satellite constituents. The first card for each such constituent is in the format (6X,A5,1X,6I3,F5.2,I4) and contains the following information:

KON = constituent name,

II,JJ,KK,LL,MM,NN = the six Doodson numbers for KON,

SEMI = the phase correction for KON,

NJ = the number of satellite constituents.

A blank card terminates this data type.

If  $NJ > 0$ , information on the satellite constituents follows, three satellites per card, in the format (11X,3(3I3,F4.2,F7.4,1X,1I,1X)).

For each satellite the values read are:

LDEL,MDEL,NDEL = the last three Doodson numbers of the main constituent subtracted from the last three Doodson numbers of the satellite constituent;

PH = the phase correction of the satellite constituent relative to the phase of the main constituent;

EE = the amplitude ratio of the satellite tidal potential to that of the main constituent;

IR = 1 if the amplitude ratio has to be multiplied by the latitude correction factor for diurnal constituents,  
 = 2 if the amplitude ratio has to be multiplied by the latitude correction factor for semidiurnal constituents,  
 = otherwise if no correction is required to the amplitude ratio.

iv) One card specifying each of the shallow water constituents and the main constituents from which they are derived. The format is

(6X,A5,1I,2X,4(F5.2,A5,5X)) and the respective values read are:

KON = the name of the shallow water constituent,

NJ = the number of main constituents from which it is derived,

COEF,KONCO = combination number and name of these main constituents.

The end of these shallow water constituents is denoted by a blank card.



Logical unit 4 contains six types of data.

- i) One card for the variables IOUT1, RAYOPT, ZOFF, ICHK in the format (I2, 2X, F4.2, 2X, F10.0, I2).

IOUT1	= 6 if the only output desired is a line printer listing of results,
	= 2 if both analysis card output and listing are desired.
RAYOPT	= Rayleigh criterion constant value if different from 1.0.
ZOFF	= constant to be subtracted from all the hourly heights.
ICLK	= 0 if the hourly height input data is to be checked for format errors,
	= otherwise if this checking to be waived.

- ii) One card for each possible inference pair. The format is (2(4X, A5, E16.10), 2F10.3) and the respective values read are:

KONAN & SIGAN	= the name and frequency of the analyzed constituent to be used for the inference,
KONIN & SIGIN	= the name and frequency of the inferred constituent,
R	= amplitude ratio of KONIN to KONAN,
ZETA	= the Greenwich phase lag of the inferred constituent subtracted from the Greenwich phase lag of the analyzed constituent.

These are terminated by one blank card.

- iii) One card for each shallow water constituent, other than those in the standard 69 constituent data package, to be considered for inclusion in the analysis. The Rayleigh comparison constituent is also required and the additional shallow water constituent must be found in data type i)

of logical unit 8 but have a blank data field where the Rayleigh comparison constituent is expected. The format is (6X,A5,4X,A5) and a blank card is required at the end.

- iv) One card in the format (I1,1X,4I2,2X,4I2) specifying the following information on the period of the analysis:

INDY                      = 8 indicates an analysis is desired for the  
                              upcoming period;  
                              = 0 indicates no further analyses are required;  
1HH1,1DD1,1MM1,1YY1= hour, day, month and year of the beginning of the  
                              analysis (measured in time ITZONE of input data v));  
1HHL,1DDL,1MML,1YYL= hour, day, month and year of the end of the analysis.

- v) One card in the format (I1,4X,A5,3A6,A4,A3,1X,2I2,I3,I2,5X,A5) containing the following information on the tidal station:

INDIC                      = 1 if J card output is desired (see 1.4),  
                              = otherwise if not;  
KSTN                        = tidal station number;  
(NA(J),J=1,4)            = tidal station name (22 characters maximum length);  
ITZONE                     = time zone of the hourly observations;  
LAD,LAM                   = station latitude in degrees and minutes;  
LOD,LOM                   = station longitude in degrees and minutes;  
IREF                       = reference station number.

- vi) The hourly height data cards contain the following information in the format (I1,1X,I5,7X,3I2,12A4).

KOLI                       = 1 or 2 indicates whether this specific card is the  
                              first or second one for that day,  
                              = otherwise indicates a non-data card which is ignored.

JSTN = tidal station number.

ID,IM,IY = day, month and year of the heights on this card.

(KARD(J),J=1,12) = the hourly heights in integer form. The final constituent amplitudes are in units 1/100 of those for the hourly height. Missing values should be specified as a blank field or 9999.

When KOLI=1 the first hourly height on the data card is assumed to be at 0100 hr and when KOLI=2 it is assumed to be at 1300 hr. Although it is not necessary, for reasons outlined in 2.3.1, it is recommended that these observations be recorded in Greenwich mean time.

After the initial analysis of a computer run is completed, control returns to input iv). Successive cards are read then until either a 0 or 8 value is found for INDY.

The hourly height data cards need not begin and end so as to include exactly the analysis period. The program ignores data outside this range. However if more than one analysis is desired from a single job submission and hourly height data cards do extend beyond the first analysis period, care should be taken to ensure that one of these cards does not have KOLI=0 or blank, otherwise the job will be terminated. This is because all successive cards after the one containing the last hour of the desired analysis period are read in input iv) format.

## 1.4 Output

Four logical units are used for the output of results from the tidal heights analysis program. Device number 6 is the line printer; 2 and 7 are files used for analysis punched card, and alphatext or flexowriter J punched card outputs respectively; and 9 is a temporary disc file used for storing preliminary punch output and program termination. 6 and 9 are

required for all program runs whereas the use of 2 and 7 is controlled by the input variables IOUT1 and INDIC which are read from device 4.

When IOUT1 is 6, INDIC is other than 1, and there are no inferred constituents, the only output is two pages on the line printer. The first of these lists the constituents included in the least squares fit, their frequencies in cycles per hour (although eight decimal places are given, depending on computer accuracy, less than this number may be significant), the C and S coefficient values (see 2.2.1) measured in units 1/100 of those for the hourly heights, and their respective standard deviation estimates. It also specifies the number of hourly height observations (excluding gaps) within the analysis period, the average and standard deviation of the original observations, the root mean square residual error, and the matrix condition number. In the columns titled AL, GL, A, and G, the second page respectively lists the amplitudes and phases (degrees) obtained for each constituent from the C and S coefficient values, and the same amplitudes and phases after nodal modulation and astronomical argument adjustments. The initial and final hour of the analysis are also specified along with the Rayleigh criterion constant ('separation'), the midpoint of the analysis period, the total number of possible hourly observations in the analysis period, and the total number of possible observations used in the analysis. This last value includes gaps in the record and is the largest odd number less than or equal to the total number of possible hourly observations (if the total number of possible hourly observations is an even number, the last hour is ignored). If there is at least one inferred constituent, page 2 results are repeated with the inclusion of inferred constituents and appropriate adjustments to the constituents from which the inferences were made. Appendix 3 lists the final page of results obtained from the input values of Appendix 2.



The only effect of changing the value of IOUT1 to 2 (regardless of INDIC's value) is to store on file 2, the same information as the second (and third) page(s) of the line printer. The list of constituent names, amplitudes and Greenwich phase lags begins on line 5 of this file and is in the correct format for input to the tidal heights prediction program, namely (5X,A5,28X,F8.4,F7.2).

When INDIC is 1, J card output for the alphetext or flexowriter is produced on logical units 6 and 7. This should not be required by the general user as it is simply a reorganization of the results in a manner so that they can be used for further processing, such as lunital computations and the production of tide tables. On the line printer these results are given on two pages following the standard output. The first of these lists the phase and amplitude results in a specific constituent order while the second page rearranges them according to increasing frequency and prints them in a format similar to that of device 7. Blank lines separate different constituent groups, and on the card punch, these groups are padded if necessary by a blank J card to give them an even number of elements.

### 1.5 Program Conversion, Modifications, Storage, and Dimension Guidelines

The source program and constituent data package described in this manual were tested on the IBM 370-168 computer installation at the University of British Columbia and the UNIVAC 1106 at Institute of Ocean Sciences, Patricia Bay. Although as much of the program as possible was written in basic ASCII FORTRAN, some changes will have to be made before the program and data package can be used on other installations. These may include:



- i) converting the character code from EBCDIC to BCD,
- ii) switching the numeric-character to integer conversion technique in subroutine INPUT from DECODE to the local equivalent.
- iii) deleting some or all REAL\*8 declaration statements. These are used either to permit alphanumeric strings longer than 4 characters (which is the ASCII FORTRAN single precision word length) to be read (e.g. constituent names are read in A5 format), or to gain computational precision in the average, standard deviation, and sine/cosine iteration formula calculations of subroutine SCFIT2. CDC installations should not require double precision variables for either of these cases because their single precision is about 1.5 that of IBM and UNIVAC, and because there are no alphanumeric strings longer than 6 characters (which is the CDC word length) in the program.
- iv) altering the variable list structure for ENTRY statements and reference to them.
- v) changing some or all of the logical unit (file reference) numbers from their present values (namely 2,4,6,7,8,9) in order to conform with local machine restrictions.
- vi) deleting, or changing the form of, the END FILE statement in subroutine DGM388 which writes an end of file mark before rewinding device 9.

The program in its present form requires approximately 5000, and 52000 UNIVAC words, for the storage of its instructions, and arrays respectively. A large part of this is due to AS, the 170 by 170 matrix resulting from the least squares fit for constituent amplitudes and phases (see 2.2.1). If memory requirements are restrictive on a particular installation, array storage can be cut to approximately 38000 words by storing only the upper triangle of this matrix in a one dimensional array. A program version that does this is available upon request, however it will have somewhat slower processing times than the one described in this manual (see 2.2.2 for details).

Changing the number or type of constituents in the standard data package may require some alterations to the analysis program. The arrays NAME and ARRAY in subroutines SETTAB and DGM388 respectively, are used for producing J card output, and their contents to have been designed specifically for the present data package. If J card output is desired, appropriate changes to these arrays should accompany any to the data package. If constituents are added to the standard data package, the dimensions of several arrays may have to be altered. Restrictions on the minimum dimension of such arrays are now given.

Let

MTOT be the total number of possible constituents contained in the data package (presently 146),

M be the number of constituents considered for inclusion in the analysis (presently 69 + the number of shallow water constituents specifically designated for inclusion),

MCON be the number of main constituents in the standard data package (presently 45),

MSAT be the sum of the total number of satellites for these main constituents and the number of main constituents with no satellites (presently 162+8),

and MSHAL be the sum for all shallow water constituents, of the number of main constituents from which each is derived (presently 251).

Then in the main program, arrays KONTAB, FREQ, and KMPR should have minimum dimension MTOT; arrays KON,C,S,SIG,ERC,ERS,A,EPS,KO,AA and GD should have minimum dimension M; array AS should have minimum dimension 2M-1 by 2M-1; array NKON should have dimension at least as large as the number of extra shallow water constituents specifically designated for analysis inclusion (its present maximum is 15); and array Z should be large enough to contain the hourly heights (and gaps) in the analysis period (its present maximum is 375 days).

In subroutine INPUT, because arrays Z,AS,A, and EPS are in a common block, they should be dimensioned the same as in the main program.

In subroutine VUF, arrays KON,VU,F and NJ should have minimum dimension MTOT; arrays II,JJ,KK,LL,MM,NN, and SEMI should have minimum dimension MCON; arrays EE,LDEL,MDEL, NDEL, IR, and PH should have minimum dimension MSAT; and KONCO, COEFF should have minimum dimension MSHAL.

In subroutine INFER, arrays KONAN,KONIN,SIGAN,SIGIN,R, and ZETA can presently accommodate a maximum of 10 inferred constituents.

In subroutine SETTAB, arrays KO,AA,GD and NKON should be dimensioned as in the main program, while NAME should have minimum dimension M.

In subroutine DGM388,ARRAY should have minimum dimension M; and arrays IZONE,CT,DATAN,NUM,JJ,STATNO,G, and H should have minimum dimensions  $M+1$ .

In subroutine SCFIT2, arrays X,A,AM, and EPM are in COMMON with Z,AS,A, and EPS of the main program and hence should have the same dimensions. Arrays CW,SW,RHSC, and RHSS should have minimum dimension M, and array RHS should have minimum dimension  $2M-1$ . AC and AS should have the same first dimension as A and care should be taken that through their equivalence relationships, neither AC and AS, nor RHSC and RHSS overlap.

Finally, in subroutine CHLSKY, arrays A and F should have minimum dimensions  $2M-1$  by  $2M-1$ , and  $2M-1$  respectively.



## 2. TIDAL HEIGHTS ANALYSIS PROGRAM DETAILS

### 2.1 The Constituent Data Package

#### 2.1.1 The astronomical variables

The astronomical variables required by the tidal analysis program were used by Doodson [1921] in his development of the tidal potential. From them one can calculate the position of the sun or moon, and hence the tide generating forces, at any time. These variables are:

$S(t)$  = mean longitude of the moon,

$H(t)$  = mean longitude of the sun,

$P(t)$  = mean longitude of the lunar perigee,

$N'(t)$  = negative of the longitude of the mean ascending node,

and  $P'(t)$  = mean longitude of the solar perigee (perihelion).

For  $H$ ,  $N'$  and  $P'$  these longitudes are measured along the ecliptic eastward from the mean vernal equinox position at time  $t$ ; while for  $S$  and  $P$  they are measured in the ecliptic eastward from the mean vernal equinox position at time  $t$  to the mean ascending node of the lunar orbit, and then along this orbit. Together with the rates of change of these variables,  $\tau$  the local mean lunar time, and the Doodson numbers for each tidal constituent, one can calculate the constituent frequencies, their astronomical argument phase angles  $V$ , and their nodal modulation phase,  $u$ , and amplitude,  $f$ , corrections.

The values of the astronomical variables in the constituent data package were calculated from power series expansion formulae in the Explanatory Supplement to the Astronomical Ephemeris and the American Ephemeris and Nautical Almanac [1961], and the Astronomical Ephemeris [1974]. These formulae were derived from Newcomb's Tables of the Sun and a revision of Brown's lunar theory (used in the development of his Tables of Motion of the Moon) so that it is in



accord with Newcomb's. Calculations were done in double precision on an IBM computer and have approximately 14 significant digits accuracy.

In the program, the astronomical variables used in the calculation of  $V(t)$ ,  $u(t)$  and  $f(t)$ , are evaluated to the first term in their Taylor expansion; e.g.  $S(t) = S(t_0) + (t-t_0) \frac{dS(t_0)}{dt}$ . Provided they are consistent with other time dependent calculations,  $t$  and  $t_0$  can be chosen arbitrarily. However, in order to facilitate computations (see 2.2.1),  $t$  is chosen to be the central hour of the desired analysis, and in order to gain precision  $t_0$ , the reference time origin, is taken to be 000 ET<sup>1</sup> January 1, 1976. This latter date, it was felt, would be closer to the analysis period of most records than the previous choice of 000 ET January 1, 1901, and hence would yield more accurate results via the linear approximation.

In keeping with the choice of reference time origin and astronomical variable specifications,  $t$  should be measured in Ephemeris time. However, the correction from Universal time is irregular and in most cases small, so it has been assumed for computational purposes that all observations are recorded in E.T.

The frequencies specified for all constituents have been calculated from the rates of change of the astronomical variables and the respective Doodson numbers. This means that they too are calculated at the time origin January 1, 1976; although there would be very little change were they taken at January 1, 1901 instead.

---

<sup>1</sup>Ephemeris Time (ET) is the uniform measure of time defined by the laws of dynamics and determined in principle from the orbital motion of the Earth as represented by Newcomb's Tables of the Sun. Universal or Greenwich Mean Time is defined by the rotational motion of the Earth and is not rigorously uniform.

### 2.1.2 Choice of constituents and Rayleigh comparison pairs

There is a maximum of 146 possible tidal constituents that can be included in the tidal analysis, 45 of these are astronomical in origin (main constituents) while the remaining 101 are shallow water constituents.<sup>(1)</sup> Because computation time (and cost) of the computer program increases approximately as the square of the number of constituents included in the analysis, and because for many tidal stations, most of the shallow water constituents are insignificant, a smaller standard package was seen as adequate for general use. Based on the suggestions of G. Godin, it was decided that this package contain all the main constituents and 24 of the shallow water. However, provision was made so that other shallow water constituents among the 77 remaining could be included if desired.

The Rayleigh comparison constituent is used for the purpose of deciding whether or not a specific constituent should be included in the analysis. If  $F_0$  is the frequency of such a constituent,  $F_1$  is the frequency of its Rayleigh comparison constituent and  $T$  is the time span of the proposed record to be analyzed, then the constituent will be included in the analysis only if  $|F_0 - F_1| T \geq \text{RAY}$ . RAY is commonly given the value 1 although it can be specified differently in the program.

---

<sup>(1)</sup> The criterion for selecting these main constituents was to include all the diurnal and semidiurnal constituents with Cartwright [1973] tidal potential amplitudes greater than 0.00250, along with M3 and the most important low frequency constituents. Section 2.1.3 gives the analogous shallow water constituent criterion.

In order to determine the set of Rayleigh comparison pairs, it is important to consider, within a given constituent group (e.g. diurnal or semi-diurnal), the order of constituent inclusion in the analysis as  $T$  (the time span of the record to be analyzed) increases. Assuming this point of view, the specific objectives used when constructing the set listed in Appendix 1 were:

- i) within each constituent group, when possible, have the order of constituent selection correspond with decreasing magnitude of tidal potential amplitude (as calculated by Cartwright [1973]),
- ii) when possible, compare a candidate constituent with whichever of the neighbouring, already selected constituents, that is nearest in frequency,
- iii) when there are two neighbouring constituents of relatively equal tidal potential amplitude, rather than waiting until the record length is sufficient to permit the selection of both at the same time (i.e. by comparing them to each other), choose a representative of the pair whose inclusion will be as early as possible. This will give information sooner about that frequency range, and via inference, still enable some information to be obtained on both constituents.

The Rayleigh comparison pairs chosen for the low frequency, diurnal, semi-diurnal and terdiurnal constituent groups are given in Tables 1, 2, 3 and 4 respectively. Figures given for the length of record required for constituent inclusion assume a Rayleigh criterion constant value (input variable RAYOPT) of 1.0.

2Q1 and SIG1 provide an example of objective iii). Because 2Q1 has a greater frequency separation from Q1 and hence would appear in an analysis of shorter record length than SIG1, it was chosen as the representative.

However, it can be seen in several cases, that it was not possible or feasible to adhere to all the objectives just outlined. Choosing a Rayleigh comparison constituent from the list of those constituents already included in the analysis proved to be difficult near the frequency edges of constituent groups. Upward arrows indicate failure to uphold this objective. 001 is such a case. For it, the potential comparison pairs were S01, K1 and J1. The first of these would result in both S01 and 001 appearing at the same later time than had J1 or K1 been chosen. Hence, information about 001 would be unnecessarily delayed. Although, due to the tidal potential amplitude of J1, objective i) is violated with both the second and third choices, it was felt that the third was a better compromise. With it, 001 only appears 11 hours sooner than J1.



Table I

Order of Slower than Diurnal Constituent Selection in Accordance with the Rayleigh Criterion

← Link Rayleigh Comparison Pairs

( ) Tidal Potential Amplitudes for Main Constituents

Length of Record (hr) Required for Constituent Inclusion	Frequency Differences (cycles/hr) $\times 10^3$ Between Neighbouring Constituents						
	ZO	SA	SSA	MSM	MM	MSF	MF
13		0.11407	0.11408	1.08162	0.20237	1.30978	0.222816
355	ZO					(1369) MSF	
764					(8254) MM		
4383			(7281) SSA				(15647) MF
4942				(1579) MSM			
8766		(1156) SA					



Order of Diurnal Constituent	Selection in Accordance with the Rayleigh Criterion
←	Link Rayleigh Comparison Pairs
( )	Tidal Potential Amplitudes for Main Constituents

Length of Record (hr) Required for Constituent Inclusion	Frequency Differences (cycles/hr) × 10 <sup>3</sup>	Between Neighbouring Constituents
24	ALPI 2QI SIGI QI RHOI OI TAU I BET I NOI CH I I P I I P I S I K I PS I I PH I I THE I J I SO I OO I UPS I	
328	(37694)	O I
651	(1624)	OO I
662	(955) (7217)	2Q I ← Q I
764	(278)	ALP I
4383	(1152)	SIG I
4942	(1371)	RHO I
8767		

Table 3

Order of Semi Diurnal Constituent Selection in Accordance with the Rayleigh Criterion

← Link Rayleigh Comparison Pairs

( ) Tidal Potential Amplitudes for Main Constituents

Length of Record (hr) Required for Constituent Inclusion	Frequency Differences (cycles / hr) × 10 <sup>3</sup>	Between Neighbouring Constituents																	
	QQ2	EPS2	2N2	MU2	N2	NU2	GAM2	HI	M2	H2	MKS2	LDA2	L2	T2	S2	R2	K2	MSN2	ETA2
13									(90809) M2										
355															(42248) S2				
662					(17386) N2														(643) ETA2
764																			
4383																			
4942																			
8767																			
11326																			

Diagram illustrating the selection of semi-diurnal constituents based on the Rayleigh Criterion. The constituents are linked by arrows indicating the selection process, and their tidal potential amplitudes are provided in parentheses.

Key links and amplitudes shown in the diagram:

- M2 (90809) links to S2 (42248), H2 (277), HI (313), and GAM2 (273).
- S2 (42248) links to R2 (355), T2 (2476), L2 (2597), and MKS2.
- H2 (277) links to H2 (277).
- HI (313) links to HI (313).
- GAM2 (273) links to GAM2 (273).
- N2 (17386) links to N2 (17386).
- NU2 (3302) links to NU2 (3302).
- MU2 (2776) links to MU2 (2776).
- 2N2 (2301) links to 2N2 (2301).
- EPS2 (671) links to EPS2 (671).
- QQ2 (259) links to QQ2 (259).
- L2 (2597) links to L2 (2597).
- MKS2 links to MKS2.
- LDA2 (670) links to LDA2 (670).
- T2 (2476) links to T2 (2476).
- R2 (355) links to R2 (355).
- K2 (11498) links to K2 (11498).
- MSN2 (11498) links to MSN2 (11498).
- ETA2 (643) links to ETA2 (643).

Table 4

Order of Terdiurnal Constituent Selection in Accordance with the Rayleigh Criterion

← Link Rayleigh Comparison Pairs

( ) Tidal Potential Amplitude for Main Constituent

Length of Record (hr) Required for Constituent Inclusion	Frequency Differences (cycles/hr) $\times 10^3$ Between Neighbouring Constituents				
	M03	M3	S03	MK3	SK3
25		(1188) M3			
355					
656	M03			MK3	SK3
4383			S03		

1.52505  
1.29689  
0.22816  
2.82193

Table 5

Shallow Water Constituents in the Standard Data Package

Shallow Water Constituent	Length of Record (hr) Required for Constituent Inclusion	Component Main Constituents and Lengths (hr) of Record Required for Their Inclusion in the Analysis					
S O 1	4383	S 2	355	O 1	328		
M K S 2	4383	M 2	13	K 2	4383	S 2	356
M S N 2	4383	M 2	13	S 2	355	N 2	662
M O 3	656	M 2	13	O 1	328		
S O 3	4383	S 2	355	O 1	328		
M K 3	656	M 2	13	K 1	24		
S K 3	355	S 2	355	K 1	24		
M N 4	662	M 2	13	N 2	662		
M 4	25	M 2	13				
S N 4	764	S 2	355	N 2	662		
M S 4	355	M 2	13	S 2	355		
M K 4	4383	M 2	13	K 2	4383		
S 4	355	S 2	355				
S K 4	4383	S 2	355	K 2	4383		
2 M K 5	24	M 2	13	K 1	24		
2 S K 5	178	S 2	355	K 1	24		
2 M N 6	662	M 2	13	N 2	662		
M 6	26	M 2	13				
2 M S 6	355	M 2	13	S 2	355		
2 M K 6	4383	M 2	13	K 2	4383		
2 S M 6	355	S 2	355	M 2	13		
2 S K 6	4383	M 2	13	S 2	355	K 2	4383
3 M K 7	24	M 2	13	K 1	24		
M 8	26	M 2	13				



K2 is an example of an unavoidable violation of objective i). Because it is so close in frequency to S2, its importance as a major semidiurnal constituent does not insure it an early inclusion in the analysis package.

Because shallow water constituents do not have a tidal potential amplitude, objective i) does not apply to them. However, based on his experience, Godin was able to suggest a hierarchy of their relative importance. A further criteria used when selecting comparison pairs for them was that no shallow water constituent should appear in an analysis before all the main constituents, from which it is derived, have also been selected. Table 5 shows that this has been upheld for all the shallow water constituents in the standard 69 constituent data package.

I suggest that the objectives outlined here be employed when choosing the Rayleigh comparison constituent for any additions to the list of possible constituents to be included in the analysis.

### 2.1.3 Satellite constituents and nodal modulation

Doodson's [1921] development of the tidal potential contains a very large number of constituents. Due to the great length of record required for their separation, several of these can be considered, for all intents and purposes, unanalysable. The standard approach to this problem is to form clusters consisting of all constituents with the same first three Doodson numbers. The major contributor in terms of tidal potential amplitude lends its name to the cluster and the lesser constituents are called satellites.

The method of analysis uses this main and satellite constituent approach in the following manner. The Rayleigh criteria is applied to the main constituent frequencies to determine whether or not they are to be included in the analysis.



For each of those so chosen, we analyse at its frequency and obtain an apparent amplitude and phase. However, because these results are actually due to the cumulative effect of all the constituents in that cluster, an adjustment is made so that only the contribution due to the main constituent is found. This adjustment is called the nodal modulation.

In order to make the nodal modulation correction to the amplitude and phase of a main constituent, it is necessary to know the relative amplitudes and phases of the satellites. As is commonly done, it is assumed in this program that the same relationship as is found with the equilibrium tide (tidal potential), holds with the actual tide. That is, the tidal potential amplitude ratio of a satellite to its main constituent is assumed to be equal to the corresponding tidal heights amplitude ratio, and the difference in tidal potential phase equals the difference in tidal height phase.

The source of the tidal potential amplitude ratio, as found in the constituent data package of Appendix 1, is Cartwright [1971,1973]. Using new computation methods and the latest values for the astronomical constants, he obtains more accurate results than those from the previously used Doodson computations. It should be noted that in several cases (whenever the satellite arises via a third order term), this version of the constituent data package requires that the amplitude ratio be multiplied by a latitude correction factor. This represents a refinement of the previous version where a latitude of 50°N was assumed and the multiplication factor was incorporated directly into the ratio.

Phase differences between satellites and main constituents arise when the tidal potential development yields different trigonometric terms for these constituents. The common convention is to express all terms in cosine form and

so an extra  $-\frac{1}{4}$  cycle phase shift is introduced if the term was originally a sine. Satellites requiring such a shift are called third order. A further  $\frac{1}{2}$  cycle change is also introduced when all negative amplitudes are made positive.

Because several test analyses indicate less consistent results when third order satellites are included in the N2 and L2 nodal modulation, Godin has decided to delete these from the present standard constituent data package. Instead he suggests that the results of analyses with this package should be compared with those of previous analyses in order to find the most suitable adjustment for these constituents.

The only other main constituents that do not have all their satellites included for nodal modulation are the slow frequency constituents. For them, no satellites are specified. Because low frequency noise may be as much as an order of magnitude greater than the satellite contributions, and Mm, MSf and Mf when they are detectable are often of shallow water origin, the effect of making corrections for the expected satellites would be to obscure further, rather than clarify the actual low frequency periodic signal.

Section 2.3.2 gives further details on the nodal modulation correction.

#### 2.1.4 Shallow water constituents

Shallow water tidal constituents arise from the distortion of main constituent tidal oscillations in shallow water. Because the speed of propagation of a progressive wave is approximately proportional to the square root of the depth of water in which it is travelling, shallow water has the effect of retarding the trough of a wave more than the crest. This distorts the original sinusoidal wave shape and introduces harmonic signals that are not predicted in tidal potential development. The frequencies of these derived harmonics can

be found by calculating the effect of non-linear terms in the hydrodynamic equations of motion on a signal due to one or more main constituents (see Godin, [1972] pages 154-164 for further details).

The shallow water constituents chosen for inclusion in the standard 69 constituent data package were suggested by G. Godin. They are listed in Table 5 and are derived only from the largest main constituents, namely M2, S2, N2, K2, K1 and O1, using the lowest types of possible interaction. The 77 additional shallow water constituents that can be included in the analysis if so desired are derived from lesser main constituents and higher types of interaction. In the constituent data package listing of Appendix 1, they can be spotted by their lack of a Rayleigh comparison constituent.

When shallow water effects are noticeable, main constituents, if they are close in frequency, may coexist or be masked by constituents of non-linear origin. The resultant nodal modulation will be due to the pair and thus will not coincide to the calculated modulation of the main constituent. In suspected cases, the effectiveness of nodal corrections in a series of successive analyses will indicate the presence of pairs or emphasize the predominance of one constituent over the other. The following table (taken from unpublished notes of Godin) lists compound constituents which may coexist with or mask constituents of direct astronomical origin. In all cases except S01 and M03, the main rather than the compound constituent is included in the standard constituent data package.

TABLE 6

Shallow Water Constituents that may Mask Main Constituents

Main Constituent	Compound Constituent which may coexist at or near its frequency
Q1	NK1
O1	MK1 *
TAU1	MP1 *
N01 (with M1 as a satellite)	N01 *
P1	SK1 *
K1	M01
J1	MQ1
S01	S01
OQ2	OQ2 *
EPS2	MNS2
2N2	O2 *
MU2	2MS2
N2	KQ2 *
GAM2	OP2 *
M2	KO2 *
L2	2MN2 *
S2	KP2
K2	K2
M03	M03 *
M3	NK3 *

\* The modulation or frequency of the compound constituent is sufficiently different that the pair could be separated if a long enough record of high precision were available.



## 2.2 The Least Squares Method of Analysis

### 2.2.1 Formulation of the problem

The first stage in the actual analysis of tidal records is the least squares fit for constituent amplitude and phase. If the tidal record is of minimum length 13 hours, the present program and data package insure that the constant constituent Z0 is always included in the analysis. If  $\sigma_j$  for  $j = 1, M$  are the frequencies (cycles/hr) of the other tidal constituents chosen for inclusion in the analysis by the Rayleigh criterion, then the problem is to find the amplitudes  $A_j$  and phases  $\phi_j$  of the function  $C_0 + \sum_{j=1}^M A_j \cos(2\pi(\sigma_j t_i - \phi_j))$  that best fit the series of observations  $y(t_i)$ ,  $i = 1, N$ <sup>(1)</sup>. Assuming  $N > 2M + 1$  we see that it is impossible to solve the system  $y(t_i) = C_0 + \sum_{j=1}^M A_j \cos(2\pi(\sigma_j t_i - \phi_j))$  exactly because it is over-determined. Hence, it is necessary to adopt a criterion which will enable unique optimum values for the parameters  $A_j$  and  $\phi_j$  to be found. The most common optimization criterion used, and the one chosen here, is the least squares technique.

Re-expressing  $\sum_{j=1}^M A_j \cos(2\pi(\sigma_j t_i - \phi_j))$  as

$$\sum_{j=1}^M (C_j \cos(2\pi\sigma_j t_i) + S_j \sin(2\pi\sigma_j t_i)),$$

where  $A_j = \sqrt{C_j^2 + S_j^2}$  and  $\phi_j = \arctan S_j/C_j$ , so that the fitting function is linear in the parameters  $S_j$  and  $C_j$  and hence more easily solved; and rewriting  $y(t_i)$  as  $y_i$ ; the objective of the least squares technique is to minimize

---

(1) In order to minimize the loss of accuracy due to round off, the average of the hourly heights observations is subtracted from all original values. The  $y(t_i)$  values mentioned in all computations henceforth are actually the resultant deviations. At the end of all calculations,  $C_0$  is adjusted by this mean value.



$$T = \sum_{i=1}^N (y_i - C_0 - \sum_{j=1}^M (C_j \cos 2\pi\sigma_j t_i + S_j \sin 2\pi\sigma_j t_i))^2,$$

for  $C_0$  and all  $C_j, S_j \quad j=1, M$ .

This is done by solving the following  $2M + 1$  simultaneous equations for  $j=1, M$ :

$$0 = \frac{\partial T}{\partial C_0} = 2 \sum_{i=1}^N (y_i - C_0 - \sum_{j=1}^M C_j \cos 2\pi\sigma_j t_i - \sum_{j=1}^M S_j \sin 2\pi\sigma_j t_i) (-1);$$

$$0 = \frac{\partial T}{\partial C_j} = 2 \sum_{i=1}^N (y_i - C_0 - \sum_{j=1}^M C_j \cos 2\pi\sigma_j t_i - \sum_{j=1}^M S_j \sin 2\pi\sigma_j t_i) (-\cos 2\pi\sigma_j t_i);$$

$$0 = \frac{\partial T}{\partial S_j} = 2 \sum_{i=1}^N (y_i - C_0 - \sum_{j=1}^M C_j \cos 2\pi\sigma_j t_i - \sum_{j=1}^M S_j \sin 2\pi\sigma_j t_i) (-\sin 2\pi\sigma_j t_i).$$

This results in the matrix equation  $B\underline{x} = \underline{y}$  of Figure 1 (page 33).

Gaps in the data record (i.e. missing hourly observations) are easily handled by the least squares method because it is not necessary that the observation times  $t_i \quad i = 1, N$  be evenly spaced. For example, if the analysis covers the total time period of 100 hr but hours 50 to 74 inclusive are missing, then  $t_{50}$  will correspond to the 75th hour. However, because the following identities which simplify the summations require that the observation times be evenly spaced, it is necessary that each of the matrix terms be calculated as the sum of contributions over the data periods that contain no gaps. Assuming that  $[n_0, n_1]$  is the hour range of a section of record containing no gaps, we can substitute  $t_k = k$  in the matrix coefficients expressions since the times are at successive hours.

Using the relationships

$$\cos a \cos b = \frac{1}{2}(\cos(a+b) + \cos(a-b))$$

$$\sin a \sin b = \frac{1}{2}(\cos(a-b) - \cos(a+b))$$

$$\sin a \cos b = \frac{1}{2}(\sin(a+b) + \sin(a-b)),$$

the formula for the sum of a geometric series, namely

$$a + ar + \dots + ar^n = a(r^{n+1} - 1)/(r - 1),$$

and expressing  $\cos x$  and  $\sin x$  as the real and imaginary parts of  $e^{ix}$ , we obtain the identities:

$$\sum_{k=n_0}^{n_1} \cos kx = \sin \left( \frac{(n_1 - n_0 + 1)x}{2} \right) \cos \left( \frac{(n_1 + n_0)x}{2} \right) / \sin (x/2),$$

$$\text{and } \sum_{k=n_0}^{n_1} \sin kx = \sin \left( \frac{(n_1 - n_0 + 1)x}{2} \right) \sin \left( \frac{(n_1 + n_0)x}{2} \right) / \sin (x/2)$$

Hence, the summation expressions in the least squares matrix can be simplified (with regard to computer execution time) as follows.

$$\sum_{k=n_0}^{n_1} \cos (2\pi\sigma_1 k) \cos (2\pi\sigma_2 k) = 1/2 \sum_{k=n_0}^{n_1} \left[ \cos (2\pi k(\sigma_1 + \sigma_2)) + \cos (2\pi k(\sigma_1 - \sigma_2)) \right]$$

$$= 1/2 \left( \sin ((n_1 - n_0 + 1)\pi (\sigma_1 + \sigma_2)) \cos ((n_1 + n_0)\pi (\sigma_1 + \sigma_2)) / \sin \pi (\sigma_1 + \sigma_2) \right.$$

$$\left. + \sin ((n_1 - n_0 + 1)\pi (\sigma_1 - \sigma_2)) \cos ((n_1 + n_0)\pi (\sigma_1 - \sigma_2)) / \sin \pi (\sigma_1 - \sigma_2) \right)$$

$$\sum_{k=n_0}^{n_1} \sin (2\pi\sigma_1 k) \sin (2\pi\sigma_2 k) = 1/2 \sum_{k=n_0}^{n_1} \left[ \cos (2\pi k(\sigma_1 - \sigma_2)) - \cos (2\pi k(\sigma_2 + \sigma_1)) \right]$$

$$= 1/2 \left( \sin ((n_1 - n_0 + 1)\pi (\sigma_1 - \sigma_2)) \cos ((n_1 + n_0)\pi (\sigma_1 - \sigma_2)) / \sin \pi (\sigma_1 - \sigma_2) \right.$$

$$\left. - \sin ((n_1 - n_0 + 1)\pi (\sigma_1 + \sigma_2)) \cos ((n_1 + n_0)\pi (\sigma_1 + \sigma_2)) / \sin \pi (\sigma_1 + \sigma_2) \right).$$

$$\sum_{k=n_0}^{n_1} \sin(2\pi\sigma_1 k) \cos (2\pi\sigma_2 k) = 1/2 \sum_{k=n_0}^{n_1} \left[ \sin (2\pi k(\sigma_1 + \sigma_2)) + \sin (2\pi k(\sigma_1 - \sigma_2)) \right]$$

$$= 1/2 \left( (\sin ((n_1 - n_0 + 1)\pi (\sigma_1 + \sigma_2)) \sin ((n_1 + n_0)\pi (\sigma_1 + \sigma_2)) / \sin \pi (\sigma_1 + \sigma_2) \right.$$

$$\left. + \sin ((n_1 - n_0 + 1)\pi (\sigma_1 - \sigma_2)) \sin ((n_1 + n_0)\pi (\sigma_1 - \sigma_2)) / \sin \pi (\sigma_1 - \sigma_2) \right).$$

With these substitutions made in Fig. 1 we have the least squares matrix equation  $B\underline{x} = \underline{y}$  generated in subroutine SCFIT2.

Because  $B$  is symmetric it is sufficient to store only its upper triangle consisting of  $2M^2 + 3M + 1$  elements instead of the entire matrix of  $(2M + 1)^2$  elements. However this saving does not come without its price as the complicated subscripting scheme required to keep track of these elements when stored in a one dimensional array significantly affects the solution computation time (see 2.2.2 for details). Assuming that this program will not have storage problems on most computer installations, it was decided to waive the storage saving in favour of improved computational time.

Partitioning the matrix equation  $B\underline{x} = \underline{y}$  into the form

$$\begin{pmatrix} B_{11} & B_{12} \\ B_{21} & B_{22} \end{pmatrix} \begin{pmatrix} \underline{c} \\ \underline{s} \end{pmatrix} = \begin{pmatrix} \underline{y}_C \\ \underline{y}_S \end{pmatrix},$$

where  $B_{11}$ ,  $B_{12}$ ,  $B_{21}$ ,  $B_{22}$ ,  $\underline{c}$ ,  $\underline{s}$ ,  $\underline{y}_C$ ,  $\underline{y}_S$  have dimensions  $(M+1) \times (M+1)$ ,  $(M+1) \times M$ ,  $M \times (M+1)$ ,  $M \times M$ ,  $(M+1) \times 1$ ,  $M \times 1$ ,  $(M+1) \times 1$ ,  $M \times 1$  respectively, it is easily seen when  $n_0 = -n_1$ , that  $B_{12}$  and  $B_{21}$  become zero matrices and two smaller matrix equations,  $B_{11}\underline{c} = \underline{y}_C$  and  $B_{22}\underline{s} = \underline{y}_S$  result. The combined computation time to solve these equations is less than that of the original (see 2.2.2) so it is desirable to attain this condition when possible. Since the time origin of the hourly observations is arbitrary provided it is consistent with that of the astronomical argument  $V$ , we can attain the desired condition for a record with no gaps by choosing the central hour of the record as the origin. (This requires that the total number of observations be odd and is satisfied by ignoring the last observation, if the total is even). Although there is generally no corresponding matrix simplification in the case of a record with gaps, for consistency with the foregoing choice, it is convenient to choose the central hour of the record universally as the time origin.

FIGURE 1

The Matrix Equation  $\underline{Bx} = \underline{y}$  Resulting from the  
Least Squares Fit for Constituent Amplitudes and Phases

$$C_k = \sum_{i=1}^N \cos 2\pi\sigma_k t_i$$

$$S_k = \sum_{i=1}^N \sin 2\pi\sigma_k t_i$$

$$CC_{kj} = \sum_{i=1}^N (\cos 2\pi\sigma_k t_i) (\cos 2\pi\sigma_j t_i) = CC_{jk}$$

$$SS_{kj} = \sum_{i=1}^N (\sin 2\pi\sigma_k t_i) (\sin 2\pi\sigma_j t_i) = SS_{jk}$$

$$CS_{kj} = \sum_{i=1}^N (\cos 2\pi\sigma_k t_i) (\sin 2\pi\sigma_j t_i) = SC_{jk}$$

N	$C_1$	$C_2$	.....	$C_M$	$S_1$	$S_2$	.....	$S_M$	$C_0$	$\sum_{i=1}^N y_i$
$C_1$	$CC_{11}$	$CC_{12}$	.....	$CC_{1M}$	$CS_{11}$	$CS_{12}$	.....	$CS_{1M}$	$C_1$	$\sum_{i=1}^N y_i \cos 2\pi\sigma_1 t_i$
$C_2$	$CC_{21}$	$CC_{22}$	.....	$CC_{2M}$	$CS_{21}$	$CS_{22}$	.....	$CS_{2M}$	$C_2$	$\sum_{i=1}^N y_i \cos 2\pi\sigma_2 t_i$
$C_M$	$CC_{M1}$	$CC_{M2}$	.....	$CC_{MM}$	$CS_{M1}$	$CS_{M2}$	.....	$CS_{MM}$	$C_M$	$\sum_{i=1}^N y_i \cos 2\pi\sigma_M t_i$
$S_1$	$SC_{11}$	$SC_{12}$	.....	$SC_{1M}$	$SS_{11}$	$SS_{12}$	.....	$SS_{1M}$	$S_1$	$\sum_{i=1}^N y_i \sin 2\pi\sigma_1 t_i$
$S_M$	$SC_{M1}$	$SC_{M2}$	.....	$SC_{MM}$	$SS_{M1}$	$SS_{M2}$	.....	$SS_{MM}$	$S_M$	$\sum_{i=1}^N y_i \sin 2\pi\sigma_M t_i$



### 2.2.2 Solution of the matrix equation, the condition number, and statistical properties

Most of the discussion and development of the Cholesky factorization algorithm introduced in this section is taken directly from Forsythe and Moler [1967]. Although all results and discussion are now stated only for the matrix  $B$  and the equation  $Bx = y$ , they apply as well for the partitioned systems  $B_{11}, B_{11}C = Y_C$  and  $B_{22}, B_{22}S = Y_S$ .

In addition to symmetry, a useful property of the matrix  $B$  in Fig. 1, is that it qualifies the matrix equation for a simpler solution than were it a general matrix, is its positive definiteness. This property requires that for all  $(2M+1) \times 1$  dimensional vectors  $\underline{x} \neq 0$ ,  $\underline{x}^T B \underline{x} > 0$ .

The positive definiteness of  $B$  can be demonstrated by considering the overdetermined matrix equation  $\underline{y} = A\underline{x} + \underline{e}$  resulting from the system of equations  $y(t_i) = C_0 + \sum_{j=1}^M (C_j \cos 2\pi\sigma_j t_i + S_j \sin 2\pi\sigma_j t_i) + e_i$  for  $i = 1, N$  where the vector  $\underline{x}^T = (C_0, C_1, C_2, \dots, C_M, S_1, S_2, \dots, S_M)$ ,  $\underline{y}^T = (y(t_1), \dots, y(t_N))$  and  $\underline{e}$  is the vector of residuals. It is easily seen that  $A^T A = B$ , and so for any  $\underline{x} \neq 0$ ,

$$\underline{x}^T B \underline{x} = \underline{x}^T A^T A \underline{x} = \underline{z}^T \underline{z} = \sum_{i=1}^N z_i^2, \text{ where } \underline{x}^T A^T = \underline{z}^T = (z_1, \dots, z_N).$$

It is worth mentioning that the overdetermined system  $\underline{y} = A\underline{x} + \underline{e}$  can be solved in many ways, depending on the criterion chosen for minimizing  $\underline{e}$ . For our purposes, those methods which solve the system without changing the form of the matrix are impractical from a storage, processing time and rounding error point of view because the first dimension of  $A$  (= the number of hourly observations) is commonly 9000. However, minimizing  $\underline{e}^T \underline{e}$  is equivalent to the least squares criterion adopted here.



An important result for any positive definite symmetric matrix  $B$  is that it can be uniquely decomposed in the form  $B = GG^T$ , where  $G$  is a lower triangular matrix with positive diagonal elements (1). Expanding this relationship leads to the matrix element equalities:

$$b_{jj} = \sum_{k=1}^j g_{jk}^2,$$

$$b_{ij} = \sum_{k=1}^j g_{ik}g_{jk} \quad \text{for all } i > j.$$

The algorithm resulting from using these equations in the proper order to find the elements of  $G$  is known as Cholesky's square root method for factoring a positive definite matrix (also attributed to Banachiewicz; see Faddeev and Faddeeva [1963]). Unlike other matrix decomposition methods such as Gaussian elimination, it does not have to search for and divide by pivots. Such techniques must insure that the reduced matrix elements are not too large so that rounding errors and loss of accuracy do not occur. In Cholesky's method however, we can see that  $|g_{ij}| \leq \sqrt{b_{ii}}$  for all  $i, j$  and so upper bounds for the elements of  $G$  always exist.

Prior to revision of SCFIT2 the constituent  $Z_0$  was treated like all others in the sense that both  $C_0$  and  $S_0$  were found. In order to insure that  $Z_0$ 's phase was zero,  $S_0$  was forced to zero by setting the corresponding diagonal element of  $B$  to a very large number. Although this did not affect the symmetry or positive definiteness of the matrix, there was a loss of accuracy (which is more evident on computers, such as IBM, with a smaller number of single precision significant digits) due to the corresponding

---

(1) If  $B$  is symmetric but not positive definite a similar decomposition exists. However some elements of  $G$  may be complex or, in the degenerate case, zero along the diagonal.

large element in the reduced matrix. For this reason and the slightly reduced array storage required, in the revised subroutine, only  $C_0$  is now sought in the least squares fit.

Once  $B$  has been decomposed into the upper and lower triangular matrices, it is a relatively easy matter to solve the matrix solution. This is done by breaking down the equation  $GG^T \underline{x} = \underline{y}$  into  $G\underline{b} = \underline{y}$  and  $G^T \underline{x} = \underline{b}$ . Because of the triangular nature of  $G$ , these equations can be solved by forward and backward substitution for  $\underline{b}$  and  $\underline{x}$  respectively.

The amount of arithmetic in a matrix algorithm is usually measured by the number of multiplicative operations (i.e. multiplications and divisions) used, since there are normally approximately the same number of additive operations. For a matrix of dimension  $n \times n$ , the Cholesky factorization algorithm requires  $n$  square roots and approximately  $1/6 n^3$  multiplications. This compares favourably with the  $1/3 n^3$  multiplications required by Gaussian elimination (Wilkinson [1967]) to produce a triangular matrix.

Wilkinson [1967] suggests a factorization of  $B$  into  $LDL^T$ , where  $L$  is a lower triangular matrix and  $D$  is a positive diagonal matrix, that involves no more multiplications than Cholesky and avoids the square roots. However, assuming that the time ratio of a square root operation to a multiplication is 15:1 (approximate ratio for IBM 370-168) and that all 69 constituents in the data package are included in the analysis (i.e.  $n = 137$ ) the time saved by eliminating the square roots is only 0.5%. Furthermore some of this gain would be replaced by time required for storing and retrieving information from the additional matrix  $D$ , and for the  $n$  additional division operations each time a solution is calculated by forward and backward substitution. Hence, the factorization was not adopted in the present program.

Because the time required for the factorization of B varies as the cube of the number of unknowns, an approximate four-fold time reduction should result when the tidal record has no gaps and the partitioned rather than the original matrix equations are solved. However as the following table of execution times for sections of subroutine SCFIT2 demonstrates, significant improvements can also be expected in the time required for matrix generation, and error calculation. The values shown were obtained on an IBM 370-168 computer with a 34 constituent analysis of a 38 day tidal record.

TABLE 7  
Comparison of Processing Times between the Partitioned  
and Non-partitioned Matrix Equation Solutions

	Partitioned matrix system times (sec.)	Non-partitioned matrix system (sec.)
Parameter initializations & right hand generation	.347	.346
Matrix generation	.059	.178
Matrix factorization	.049	.146
Solution	.010	.018
Error calculations	.128	.403

The advantage of storing the lower triangle of B in a two dimensional array and thus avoiding the complicated subscripting scheme required for one dimensional storage is illustrated in TABLE 3. The values shown were obtained from solving a matrix equation of order 110 resulting from a yearly tidal analysis. For comparison, the times required when using the Forsythe and Moler technique (Gaussian elimination with partial pivoting, forward and backward substitution) with two dimensional matrix storage are also included.

TABLE 8

Comparison of Processing Times for the Cholesky and Forsythe & Moler Methods of Solving the Least Squares Matrix Equation

	PROCESSING TIMES (SEC.)		
	Cholesky method with two dimensional array storage	Cholesky method with one dimensional array storage	Forsythe and Moler method with two dimensional array storage
Matrix factorization	.753	1.299	2.313
Solution	.053	.059	.047

A rough indication of the roundoff difficulties associated with solving the equation  $Bx = y$  is given by the matrix condition number. Although several different definitions for a condition number exist, an appropriate one for our purposes, in the sense that it pertains to least squares matrices and is easily calculated, is specified by Davis and Rabinowitz [1961]. Its development is as follows.

If  $\{\underline{b}_1, \dots, \underline{b}_n\}$  are  $n$ -dimensional vectors such that the matrix

$$B = \begin{pmatrix} \underline{b}_1 & \dots & \underline{b}_n \end{pmatrix} = \begin{pmatrix} \underline{b}_1 \cdot \underline{b}_1 & \dots & \underline{b}_1 \cdot \underline{b}_n \\ \vdots & & \vdots \\ \underline{b}_n \cdot \underline{b}_1 & \dots & \underline{b}_n \cdot \underline{b}_n \end{pmatrix},$$

then it can be shown that  $0 \leq \det(B) \leq \|\underline{b}_1\| \|\underline{b}_2\| \dots \|\underline{b}_n\|$  where if  $\underline{b}_j = (b_{j1}, \dots, b_{jn})$ , the norm  $\|\underline{b}_j\| = \sqrt{\sum_{i=1}^n b_{ji}^2}$ . Furthermore  $\det(B) = 0$

if and only if the vectors are linearly dependent, and  $\det(B) = \|\underline{b}_1\| \dots \|\underline{b}_n\|$  if and only if they are orthogonal (i.e.  $\underline{b}_i \cdot \underline{b}_j = 0$  for  $i \neq j$ ). This determinant is known as the Gram determinant of the system  $\{\underline{b}_1, \dots, \underline{b}_n\}$  and is the square of the  $n$ -dimensional volume of the parallelepiped whose edges are these vectors.



Since it can be shown that all least squares matrices can be expressed in this manner, this result can be applied to our situation. In particular when the vectors are normalized so that  $\|\underline{b}_i\| = 1$ , the actual value of  $\det(B)$  will always be bounded and provide a measure of the linear independence of the system, and hence roundoff difficulties encountered in solving the equation. A value close to 1 will mean near orthogonality, a virtually diagonal matrix for  $B$ , and thus an easy solution. On the other hand, a value close to 0 will mean that at least two rows are near scalar multiples of one another, and thus greater accuracy problems will occur when their difference is calculated during the equation solution.

For our particular case observe that  $\det(B) = \det(GG^T) = (\det G)^2 = \prod_{i=1}^n g_{ii}^2$ , and that  $B$  can be written as

$$GG^T = \begin{bmatrix} \underline{g}_1 \cdot \underline{g}_1 & \dots & \underline{g}_1 \cdot \underline{g}_n \\ \vdots & \ddots & \vdots \\ \underline{g}_n \cdot \underline{g}_1 & \dots & \underline{g}_n \cdot \underline{g}_n \end{bmatrix},$$

$$\text{where } G^T = \begin{bmatrix} g_{11} & g_{21} & \dots & g_{n1} \\ 0 & g_{22} & \dots & g_{n2} \\ \vdots & \vdots & \ddots & \vdots \\ 0 & \dots & 0 & g_{nn} \end{bmatrix} = (\underline{g}_1, \underline{g}_2, \dots, \underline{g}_n).$$

Since  $b_{jj} = \sum_{k=1}^j g_{jk}^2$ ,  $\|\underline{g}_j\| = \sqrt{b_{jj}}$  and the determinant of the matrix resulting from normalizing the  $\underline{g}_j$  vectors is  $\prod_{i=1}^n (g_{ii}^2/b_{ii})$ . The square root of this value is the volume of the  $n$ -dimensional parallelepiped whose edges are these normalized vectors and is the quantity calculated as the condition number of the matrix  $B$ .



The statistical properties of the least squares fit solution can be found in any analysis of variance or regression model text. They are outlined briefly as follows.

Reverting to the overdetermined problem statement, the least squares objective can be stated as finding the vector  $\underline{x}$  in  $\underline{y} = A\underline{x} + \underline{\bar{e}}$  such that  $\underline{\bar{e}}^T \underline{\bar{e}}$  is minimized. This yields the solution  $\hat{\underline{x}} = (A^T A)^{-1} A^T \underline{y}$ .

The total sum of squares is  $\underline{y}^T \underline{y}$  and the sum of squares due to regression is  $\hat{\underline{x}}^T A^T \underline{y}$ . Their difference is the residual error sum of squares and this difference divided by the degrees of freedom in the fit is the residual mean square error (MSE). 'Degrees of freedom' is the difference between the number of hourly observations (excluding gaps) and A the number of parameters fit in the analysis. If there were M constituents including Z0 chosen for the analysis, the degrees of freedom would be  $N - 2M + 1$ .

If it is assumed, as is commonly done, that the vector  $\underline{\bar{e}}$  is distributed normally with 0 standard deviation and  $\sigma^2 I$  variance, where I is the unit diagonal matrix, then the variance of  $\hat{\underline{x}}$  is  $(A^T A)^{-1} \sigma^2$ . Since the mean square residual error is an unbiased estimator for  $\sigma^2$ , an estimate of the standard deviation of  $\hat{x}_i$ , the  $i$ th element of  $\hat{\underline{x}}$ , is

$$((\underline{\mu}_i^T (A^T A)^{-1} \underline{\mu}_i) \text{MSE})^{1/2}$$

where  $\underline{\mu}_i$  is the vector with 1 in the  $i$ th position and 0's elsewhere.

## 2.3 Modifications to the Least Squares Analysis Results

### 2.3.1 Astronomical argument and Greenwich Phase Lag

Instead of regarding each tidal constituent as the result of some particular component of the tidal potential, an artificial causal agent can be

attributed to each constituent in the form of a fictitious star which travels around the equator with an angular speed equal to that of its corresponding constituent. Making use of this conceptual aid, the astronomical argument,  $V(L,t)$ , of a tidal constituent can then be viewed as the angular position of this fictitious star relative to longitude  $L$ , and at time  $t$ . Although the longitudinal dependence is easily calculated, for historical reasons  $L$  is generally assumed to be the Greenwich meridian, and  $V$  is reduced to a function of one variable.

The Greenwich phase lag,  $g$ , is the difference between this astronomical argument for Greenwich and the phase of the observed constituent signal. Its value is dependent upon the time zone in which the hourly heights of the record were taken. This means that when phases at various stations, not necessarily in the same time zone, are compared, they must be reduced to a common zone in order to avoid spurious differences due to difference relative times. Specifically, if  $\sigma$  is the constituent frequency and  $g(j+\Delta_j)$  and  $g(j)$  are the Greenwich phase lags evaluated for time zones  $j+\Delta_j$  and  $j$  respectively (e.g. Pacific Standard Time is +8), then

$$g(j+\Delta_j) = g(j) + (\Delta_j)\sigma.$$

Although these adjustments are easily calculated, they can be tedious because each constituent must be handled individually. Therefore, to avoid possible misinterpretation of phases from nearby stations or subsequent phase alterations, it is suggested that all observations be recorded in, or converted to, GMT.

The calculation of  $g$  (see 2.3.3) requires that the astronomical argument need only be evaluated at one time, the central hour of the analysis period. For a particular main constituent, it is calculated as

$$V = i_0 \tau + j_0 S + k_0 H + l_0 P + m_0 N' + n_0 P'$$

where  $i_0, j_0, k_0, \ell_0, m_0, n_0$  are the Doodson numbers of the constituent and  $S, H, P, N', P'$  are the astronomical variables defined in 2.1.1.  $\tau$ , the number of mean lunar days from the absolute time origin of 000 ET January 1, 1976, is calculated as sum of the local mean solar time from this origin and  $(H-S)$ , and so need not be read from data cards.

For shallow water constituents, the astronomical argument is calculated as the linear combination of the coefficient number and the astronomical argument of the main constituents from which it is derived. For example,  $V_{MSN2} = V_{M2} + V_{S2} - V_{N2}$  and  $V_{2MK5} = 2 V_{M2} + V_{K1}$ .

### 2.3.2 Nodal corrections

Most of this section has been taken from the unpublished notes of G. Godin which were written subsequent to Cartwright's [1971,1973] recalculation of the tide generating potential. The material presented here is intended to give greater detail than that of section 2.1.3.

Due to the presence of satellites to the major contributor in a given cluster, it is known from tidal potential theory that the analyzed signal found at the frequency  $\sigma_j$  of the main constituent is actually the result of

$$a_j \sin (V_j - g_j) + \sum_k A_{jk} a_{jk} \sin (V_{jk} - g_{jk}) + \sum_{\ell} A_{j\ell} a_{j\ell} \cos (V_{j\ell} - g_{j\ell})$$

for the diurnal and terdiurnal constituents of direct gravitational origin, and

$$a_j \cos (V_j - g_j) + \sum_k A_{jk} a_{jk} \cos (V_{jk} - g_{jk}) + \sum_{\ell} A_{j\ell} a_{j\ell} \sin (V_{j\ell} - g_{j\ell})$$

for the slow and semidiurnal constituents.  $a$ ,  $g$  and  $V$  are the true amplitude, Greenwich phase, and astronomical argument at the central time of the record for all the constituents. Single  $j$  subscripts refer to the major contributor while  $jk$  and  $j\ell$  subscripts refer to satellites originating from tidal potential

terms of the second and third order respectively.  $A$  is the element of the interaction matrix resulting from the interference of a satellite with the main constituent.

It is the convention in tides and an assumption for our least squares fit that all constituents arise through a cosine term and positive amplitude. That is, the contribution for a constituent whose astronomical argument is  $V_j$  and whose Greenwich phase is  $g_j$ , is expected to be in the form  $a_j \cos (V_j - g_j)$  for  $a_j > 0$ . However, the diurnal and terdiurnal constituents, assuming that they are due to second order terms in the tidal potential, actually arise through a  $b_j \sin (V_j - g_j)$  term where  $b_j$  may be negative. Hence, a phase correction (variable SEMI read in data input iii) from logical unit 8) of either  $-1/4$  or  $-3/4$  cycles is necessary.

$$\begin{aligned} \text{i.e. } b_j \sin (V_j - g_j) &= |b_j| \cos (V_j - g_j - 1/4) \text{ if } b_j \geq 0 \\ &= |b_j| \cos (V_j - g_j - 3/4) \text{ if } b_j < 0. \end{aligned}$$

Similarly, an adjustment of  $1/2$  cycle will only be necessary for slow and semidiurnal main constituents if the tidal potential amplitude is negative.

Making these changes, the combined result of a constituent cluster in the diurnal and terdiurnal cases is

$$|a_j| \cos (V'_j - g_j) + \sum_k A_{jk} a_{jk} \cos (V'_{jk} + \alpha_{jk} - g_k) + \sum_\ell A_{j\ell} a_{j\ell} \cos (V'_{j\ell} + \alpha_{j\ell} - g_{j\ell})$$

where if  $a_j < 0$ ,  $V' = V - 3/4$ ,  $\alpha_{jk} = 1/2$  and  $\alpha_{j\ell} = 3/4$ ,

and if  $a_j > 0$ ,  $V' = V - 1/4$ ,  $\alpha_{jk} = 0$  and  $\alpha_{j\ell} = 1/4$ .

A further phase adjustment to satellite constituents can be made if we wish to ensure that their amplitudes are positive. This convention was adopted for the data package of Appendix 1 (variable PH read in data input iv) from logical unit 8). Replacing  $a_{jk}$  and  $a_{j\ell}$  by their absolute values we now see that

$$\begin{aligned} \alpha_{jk} &= 0 && \text{if both } a_{jk} \text{ and } a_j \text{ have the same sign,} \\ &= 1/2 && \text{otherwise;} \end{aligned}$$



$$\alpha_{j\ell} = 1/4 \quad \text{if both } a_{j\ell} \text{ and } a_j \text{ have the same sign,} \\ = 3/4 \quad \text{otherwise.}$$

Similarly, for the slow and semidiurnal constituents the cluster contribution can be rewritten as

$$|a_j| \cos (V'_j - g_j) + \sum_k A_{jk} |a_{jk}| \cos (V'_{jk} + \alpha_{jk} - g_{jk}) + \sum_\ell A_{j\ell} |a_{j\ell}| \cos (V'_{j\ell} + \alpha_{j\ell} - g_{j\ell})$$

$$\text{where} \quad V' = V + 1/2 \quad \text{if } a_j < 0, \\ \quad \quad \quad V \quad \quad \quad \text{otherwise;} \\ \alpha_{jk} = 0 \quad \quad \quad \text{if } a_{jk} \text{ and } a_j \text{ have the same sign,} \\ \quad \quad \quad 1/2 \quad \quad \quad \text{otherwise;} \\ \alpha_{j\ell} = -1/4 \quad \quad \text{if } a_{j\ell} \text{ and } a_j \text{ have the same sign} \\ \quad \quad \quad 1/4 \quad \quad \quad \text{otherwise.}$$

Special note should be made of the terdiurnal M3 because both it and its only satellite are due to third order terms in the tidal potential. Hence, both contribute directly through a cosine term and so behave as if they were second order semidiurnals.

In order to determine the amplitude and phase of the major contributor, we assume that the result actually found in the analysis was  $f_j a_j \cos (V'_j - g_j + u_j)$ , where  $f_j$  and  $u_j$  are called the nodal modulation corrections in amplitude and phase respectively. To avoid a possible misunderstanding, it is worth mentioning here that the term nodal modulation is actually a misnomer. It and the symbols  $f$  and  $u$  were first used before the advent of modern computers to designate corrections for the moons nodal progression that were not incorporated into the calculations of the astronomical argument for the main constituent. However, now the term satellite modulation is more appropriate because our correction is due to the presence of satellite constituents differing not only in the contribution of the lunar node to their astronomical argument, but also in the lunar and solar perigee effect.



For the purpose of calculating  $f_j$  and  $u_j$  it is assumed that the admittance is very nearly a constant over the frequency range within a constituent cluster, and so  $g_j = g_{jk} = g_{j\ell}$ ; and  $r_{jk} = |a_{jk}|/|a_j|$ ,  $r_{j\ell} = |a_{j\ell}|/|a_j|$  are equal to the ratio of the tidal equilibrium amplitudes of the satellite to the major contributor. These ratios are latitude dependent when satellites of the third order are involved, necessitating the correction factors mentioned in 2.1.3. However, the ratios are usually small and the correction is slight.

Dropping the 'prime' notation and grouping the second and third order terms in one summation, the relationship between the analysed results for a main constituent and the actual cluster contribution is

$$f_j |a_j| \cos (V_j + u_j - g_j) = |a_j| (\cos (V_j - g_j) + \sum_k A_{jk} r_{jk} \cos (V_j - g_j + \Delta_{jk} + \alpha_{jk}))$$

where  $\Delta_{jk} = V_{jk} - V_j$ .

Expanding this result and observing that it must be true for all  $V_j(t)$ , the following explicit formulae are found for  $f$  and  $u$ :

$$f_j = \sqrt{1 + \left( \sum_k A_{jk} r_{jk} \cos (\Delta_{jk} + \alpha_{jk}) \right)^2 + \left( \sum_k A_{jk} r_{jk} \sin (\Delta_{jk} + \alpha_{jk}) \right)^2},$$

$$u_j = \arctan \left[ \frac{\sum_k A_{jk} r_{jk} \sin (\Delta_{jk} + \alpha_{jk})}{1 + \sum_k A_{jk} r_{jk} \cos (\Delta_{jk} + \alpha_{jk})} \right].$$

For an analysis carried out over  $2N + 1$  consecutive observations,  $\Delta t$  time units apart,  $A_{jk}$  is given by  $A_{jk} = \frac{\sin [(2N+1)\Delta t (\sigma_{jk} - \sigma_j)/2]}{(2N+1) \sin [\Delta t (\sigma_{jk} - \sigma_j)/2]}$

where  $\sigma_j$  is the frequency of the main contributor and  $\sigma_{jk}$  is that of its satellite. However,  $A_{jk}$  is very nearly one even for a one year analysis and in the program is approximated by this value.

For a shallow water constituent whose frequency is calculated as  $\sum_{j=1}^{N_0} c_j \sigma_j$ , where  $\sigma_j$  is the frequency of the  $j^{\text{th}}$  main constituent from which it is derived and  $c_j$  is the linear coefficient, the nodal modulation corrections for amplitude and phase are computed as  $f = \frac{N_0}{\prod_{j=1} f_j} |c_j|$  and  $u = \sum_{j=1}^{N_0} c_j u_j$ .

### 2.3.3 Final amplitude and phase results

The result of the least squares analysis was to find for a constituent with frequency  $\sigma_j$ , the optimal amplitude  $A_j$  and phase  $\phi_j$  value for the tidal signal  $A_j \cos 2\pi (\sigma_j t - \phi_j)$ . However, due to nodal corrections, when the astronomical argument is calculated at the central time origin  $t = 0$  of the record, we know that the actual contribution of the constituent cluster is  $f_j a_j \cos 2\pi (V_j + u_j - g_j)$ . Hence, the amplitude and Greenwich phase lag of the constituent corresponding to frequency  $\sigma_j$  can be calculated as  $a_j = A_j / f_j$  and  $g_j = V_j + u_j + \phi_j$ .

### 2.3.4 Inferred constituents

In accordance with previous notation, tidal signals in this section are assumed to be real in nature. However an alternative presentation using complex numbers, and the basis for the following development is given by Godin [1972].

If the length of a specific tidal record is such that certain important constituents will not be included directly in the analysis, provision is made via the data input on logical unit 4 to include these constituents indirectly by inferring their amplitudes and phases from neighbouring constituents that are included. If accurate amplitude ratios and phase differences

are specified, inference has the effect of significantly reducing any periodic behaviour in the amplitudes and phases of the constituent used for the inference. This is due to the removal of interaction from the neighbouring inferred constituent. If it so happens that a constituent specified for inference is included directly in the analysis, the program will ignore the inference calculations.

The actual adjustments are as follows. Assume that the constituent with frequency  $\sigma_2$  is to be inferred from the constituent with frequency  $\sigma_1$ , and that the least squares fit analysis found the latter's contribution to be  $A_1^0 \cos 2\pi(\sigma_1 t - \phi_1^0)$ , where  $A_1^0$  and  $\phi_1^0$  are the amplitude and phase respectively ( $\sigma_1$  and  $\phi_1^0$  are measured in cycles/hour and cycles respectively). Letting

$VU_1$  be the astronomical argument + nodal modulation phase correction,

$g_1$  be the Greenwich phase lag,

$f_1$  be the nodal modulation amplitude correction factor,

and  $a_1$  be the corrected amplitude,

then from 2.3.3 we know that

$$-\phi_1 = VU_1 - g_1$$

$$\text{and } a_1 = A_1/f_1.$$

Assuming that  $A_1$  and  $\phi_1$  are the post-inference amplitude and phase for the constituent with frequency  $\sigma_1$ ,

$$r_{12} = a_2/a_1 = (A_2/f_2)/(A_1/f_1),$$

$$\text{and } \zeta = g_1 - g_2 = VU_1 + \phi_1 - VU_2 - \phi_2$$

(the latter two being data input variables R and ZETA respectively), then the presence of the inferred constituent in the analyzed signal yields the relationship:

$$\begin{aligned}
A_1^0 \cos 2\pi(\sigma_1 t - \phi_1^0) &= A_1 \cos 2\pi(\sigma_1 t - \phi_1) + A_2 \cos 2\pi(\sigma_2 t - \phi_2) \\
&= A_1 \cos 2\pi(\sigma_1 t - \phi_1) \left[ 1 + r_{12} \left( \frac{f_2}{f_1} \right) \cos 2\pi\{(\sigma_2 - \sigma_1)t + VU_2 - VU_1 + \zeta\} \right] \\
&\quad - A_1 \sin 2\pi(\sigma_1 t - \phi_1) \left[ r_{12} \left( \frac{f_2}{f_1} \right) \sin 2\pi\{(\sigma_2 - \sigma_1)t + VU_2 - VU_1 + \zeta\} \right].
\end{aligned}$$

Since the constituent with frequency  $\sigma_2$  was not chosen for inclusion in the least squares analysis,  $|\sigma_2 - \sigma_1| N \ll \text{RAY}$ , where  $N$  is the record length in hours and  $\text{RAY}$  is the Rayleigh criterion constant (usually 1.0). Assuming in general that  $|\sigma_2 - \sigma_1| N$  is small, good approximations to  $\cos 2\pi\{(\sigma_2 - \sigma_1)t + VU_2 - VU_1 + \zeta\}$  and  $\sin 2\pi\{(\sigma_2 - \sigma_1)t + VU_2 - VU_1 + \zeta\}$  are their average values over the interval  $[-N/2, N/2]$ , namely  $\sin [\pi N(\sigma_2 - \sigma_1)] \cos [2\pi(VU_2 - VU_1 + \zeta)] / \pi N(\sigma_2 - \sigma_1)$  and  $\sin [\pi N(\sigma_2 - \sigma_1)] \sin [2\pi(VU_2 - VU_1 + \zeta)] / \pi N(\sigma_2 - \sigma_1)$  respectively. Making these substitutions and setting

$$S = r_{12} \left( \frac{f_2}{f_1} \right) \sin [\pi N(\sigma_2 - \sigma_1)] \sin [2\pi(VU_2 - VU_1 + \zeta)] / \pi N(\sigma_2 - \sigma_1),$$

$$\text{and } C = 1 + r_{12} \left( \frac{f_2}{f_1} \right) \sin [\pi N(\sigma_2 - \sigma_1)] \cos [2\pi(VU_2 - VU_1 + \zeta)] / \pi N(\sigma_2 - \sigma_1),$$

we obtain

$$\frac{A_1^0}{A_1} \cos 2\pi(\sigma_1 t - \phi_1^0) = C \cos 2\pi(\sigma_1 t - \phi_1) - S \sin 2\pi(\sigma_1 t - \phi_1).$$

Expanding and regrouping this result yields

$$\begin{aligned}
\cos 2\pi\sigma_1 t \left[ \frac{A_1^0}{A_1} \cos 2\pi\phi_1^0 - C \cos 2\pi\phi_1 - S \sin 2\pi\phi_1 \right] = \\
\sin 2\pi\sigma_1 t \left[ -\frac{A_1^0}{A_1} \sin 2\pi\phi_1^0 + C \sin 2\pi\phi_1 - S \cos 2\pi\phi_1 \right].
\end{aligned}$$

Now since this relationship must hold for all  $t$ , both terms in brackets are equal to zero. Hence

$$\frac{A_1^0}{A_1} \cos 2\pi\phi_1^0 = C \cos 2\pi\phi_1 + S \sin 2\pi\phi_1,$$

$$\frac{A_1^0}{A_1} \sin 2\pi\phi_1^0 = C \sin 2\pi\phi_1 - S \cos 2\pi\phi_1,$$

and so

$$A_1 = A_1^0 / \sqrt{C^2 + S^2},$$

$$\phi_1 = \phi_1^0 + [\arctan (S/C)]/2\pi.$$

The relative phase and amplitude of the inferred constituent are then calculated as

$$\phi_2 = VU_1 - VU_2 + \phi_1 - \zeta,$$

and  $A_2 = r_{12} A_1 (f_2/f_1).$



### 3 USE OF THE TIDAL HEIGHTS PREDICTION COMPUTER PROGRAM

#### 3.1 General Description

This program produces tidal height values at a given location for a specified period of time. Amplitudes and Greenwich phase lags of the tidal constituents to be used in the prediction are required as input and either equally spaced heights or all the high and low values can be produced.

#### 3.2 Routines Required

- 1) MAIN.....reads in tidal station and time period information, amplitudes and Greenwich phases of constituents to be used in the prediction, and calculates the desired tidal heights.
- 2) ASTRO.....reads the standard constituent data package and calculates the frequencies, astronomical arguments, and nodal corrections for all constituents.
- 3) PUT.....controls the output for high-low predictions.
- 4) HPUT.....controls the output for equally spaced predictions.
- 5) CDAY.....returns the consecutive day number from a specific origin for any given date in the range 1901 to 1999, and vice versa.

#### 3.3 Data Input

All input data required by the tidal heights prediction program is from logical unit 8. A sample set is given in Appendix 4. Although data types i), ii) and iii) are identical to types ii), iii) and iv) expected on logical unit 8 by the analysis program, for completeness they are repeated here.

- i) Two cards specifying values for the astronomical arguments S0, H0, P0, ENPO, PPO, DS, DH, DP, DNP, DPP in the format (5F13.10).
- S0 = mean longitude of the moon (cycles) at the reference time origin.
- H0 = mean longitude of the sun (cycles) at the reference time origin.
- P0 = mean longitude of the lunar perigee (cycles) at the reference time origin.
- ENPO = negative of the mean longitude of the ascending node (cycles) at the reference time origin.
- PPO = mean longitude of the solar perigee (perihelion) at the reference time origin.
- DS, DH, DP, DNP, DPP are their respective rates of change over a 365 day period at the reference time origin.
- ii) At least one card for all the main tidal constituents specifying their Doodson numbers and phase shift along with as many cards as are necessary for the satellite constituents. The first card for each such constituent is in the format (6X,A5,1X,6I3,F5.2,I4) and contains the following information:
- KON = constituent name,
- II,JJ,KK,LL,MM,NN = the six Doodson numbers for KON,
- SEMI = the phase correction for KON,
- NJ = the number of satellite constituents.
- A blank card terminates this data type.
- If NJ > 0, information on the satellite constituents follows, three satellites per card, in the format (11X,3(3I3,F4.2,F7.4,1X,I1,1X)).
- For each satellite the values read are:

LDEL, MDEL, NDEL = the last three Doodson numbers of the main constituent subtracted from the last three Doodson numbers of the satellite constituent;

PH = the phase correction of the satellite constituent relative to the phase of the main constituent;

EE = the amplitude ratio of the satellite tidal potential to that of the main constituent;

IR = 1 if the amplitude ratio has to be multiplied by the latitude correction factor for diurnal constituents,

= 2 if the amplitude ratio has to be multiplied by the latitude correction factor for semi-diurnal constituents,

= otherwise if no correction is required to the amplitude ratio.

- iii) One card specifying each of the shallow water constituents and the main constituents from which they are derived. The format is (6X,A5,I1,2X,4(F5.2,A5,5X)) and the respective values read are:

KON = the name of the shallow water constituent,

NJ = the number of main constituents from which it is derived,

COEF, KONCO = combination number and name of these main constituents.

The end of these shallow water constituents is denoted by a blank card.

- iv) One card with the tidal station information ISTN, (NA(J),J=1,4), ITZONE, LAD, LAM, LOD, LOM in the format:

(5X,I4,1X,3A6,A4,A3,1X,I2,1X,I2,2X,I3,1X,I2).

ISTN = the station number.

(NA(J),J=1,4) = the station name.

ITZONE = the time zone reference for the 'Greenwich' phases.

LAD, LAM = the station latitude in degrees and minutes.

LOD, LOM = the station longitude in degrees and minutes.

- v) One card for each constituent to be included in the prediction, with the constituent name (KON), amplitude (AMP) and phase lag (G) in the format (5X,A5,28X,F8.4,F7.2). (This format is compatible with the analysis program results produced on output device 2). The phase lag units should be degrees (measured in time zone ITZONE) while the units of the predicted tidal heights will be the same as those of the input amplitudes. The last constituent is followed by a blank card.
- vi) One card containing the following information on the period and type of prediction desired. The format is (3I3,1X,3I3,1X,A4,F9.5).

IDY0, IM00, IYR0 = the first day, month, and year of the prediction period.

IDYE, IMOE, IYRE = the last day, month and year of the prediction period.

ITYPE = 'EQUI' if equally spaced predictions are desired,  
= 'EXTR' if all the high and low tide times and heights are desired.

DT = the time spacing of the predicted values if  
ITYPE = 'EQUI',  
= the time step increment used to initially bracket a high or low value if ITYPE = 'EXTR'.

Equally spaced predictions begin at DT hours on the first day and extend to 2400 hours (assuming 24 is a multiple of DT) of the last day. When ITYPE = 'EXTR', Godin and Taylor [1973] recommend using the following values for DT: 3 hours for a semi-diurnal tide, 6 hours for a diurnal tide, and 0.5 hours for a mixed tide.

Type vi) data may be repeated any number of times. One blank card following a type vi) record will return the program to type iv) input, while two blank cards will end the program execution.



### 3.4 Output

Two logical units are used for the output of results in the tidal heights prediction program. Device number 6 is the line printer and 10 is a data file. Both equally spaced and high-low predictions are put onto both devices with the same format. However the line printer also records the station name and location along with the amplitudes and phase lags of the constituents used in the prediction. Appendix 5 lists device 10 output resulting from the input of Appendix 4.

When daily high-low values are desired, the date, station number and a series of up to six heights and occurrence times are listed per record. Each record begins with the variable HL whose value is 0 if the first height for that day is a high (i.e. larger than the second height) and 1 if the first height is a low. If there are less than six high-low values for a day, they are padded up to six with the values 9999 and 99.9 for the times and heights respectively. On device 10, the format used for the variables HL, the station number, the day, month, year, and six times and heights is

(1X,I1,I5,2I3,I2,6(I5,F5.1)).

When equally spaced heights are requested, 8 values are listed on each record preceded by the station number, the time, day, month and year of the first value, and followed by the time increment between heights. On device number 10, the format for these variables is;

(1X,I4,F8.4,I3,2I2,8F6.2,F12.4).



### 3.5 Program Conversion, Modifications, Storage and Dimension Guidelines

The source program and constituent data package described in this manual were tested on the UNIVAC 1106 at Patricia Bay Institute of Ocean Sciences. Although the program was written in basic ASCII FORTRAN, there may be some changes needed before the program and data package can be used on other installations. These may include:

- i) converting the character code from EBCDIC to BCD.
- ii) deleting some or all the REAL\*8 declaration statements. Presently these are used only to permit alphanumeric strings longer than 4 characters (which is the ASCII FORTRAN single precision word length) to be read (eg. constituent names are read in A5 format). CDC installations should not require these double precision variables because there are no alphanumeric strings longer than 6 characters (which is the CDC word length) in the program.
- iii) switching the Chebyshev iteration formula to double precision in order to maintain accuracy. Tests performed on the UNIVAC demonstrate that this change is not necessary, however on less accurate installations, it may be (UNIVAC real variable single precision has 8.1 significant digits). As a test for machine accuracy, I suggest using the input of Appendix 4 and comparing the results with those listed in Appendix 5. In the event that more precision is needed, the following variables in the main program should be declared REAL\*8: CH,CHA, CHB, CHM, CHP, SUM TWOC, BTWOC, HGT, Z, ZA, ZB, ZP, ZM, DTPY;  
and all related assignments and library function calls should be altered accordingly (e.g. '=0.0' should become '0.D0' and SQRT should be DSQRT).

- iv altering the variable list structure for ENTRY statements and references to them.
- v) changing some or all of the logical unit (file reference) numbers from their present values in order to conform with local machine restrictions.

The program in its present form requires approximately 3000 and 15000 UNIVAC words for the storage of its instructions and arrays respectively. As with the analysis program, changing the number or type of constituents in the standard data package may require alteration to the dimensions of some arrays. Restrictions on the minimum dimension of all arrays are now given.

Let

MTAB be the total number of possible constituents contained in the data package (presently 146),

M be the number of constituents to be included in the prediction,

MCON be the number of main constituents in the standard data package (presently 45),

MSAT be the sum of the number of satellites for these main constituents and the number of main constituents with no satellites (presently  $162 + 8$ )

MSHAL be the sum for all shallow water constituents of the number of main constituents from which each is derived (presently 251),

and NITER be the number of iterations required to reduce the time interval within which it is known that a high or low tide exists, to a desired length (with the largest initial interval size of 6 hours and a 6 minute final interval, NITER is 6).

Then in the main program, arrays KONTAB, SIGTAB, V, U, and F should have minimum dimension MTAB; KON, SIG, AMP, G, INDX, TWOC, CH, CHP, CHA, CHB, CHM, ANGO and AMPNC should have minimum dimension M; and the two dimensional array BTWDC should have a minimum dimension of M by NITER. Array COSINE which stores pre-calculated cosine function values over the range of  $0^{\circ}$  to  $360^{\circ}$  and is used as a look-up table, presently has 2002 elements.

In subroutine ASTRO, the arrays KON, FREQ, V, U, F and NJ should have minimum dimension MTAB; arrays II, JJ, KK, LL, MM, NN and SEMI should have minimum dimension MCON; arrays EE, LDEL, MDEL, NDEL, IR and PH should have minimum dimension MSAT; and arrays KONCO and COEFF should have minimum dimension MSHAL.

In subroutine PUT, the dimensions of arrays HGTK and ITIME should be at least as large as the maximum number of high and low values per day (this is presently assumed to be 9).

In subroutine HPUT, the dimension of array H should be at least equal to the number of equally spaced tidal height values per output record of logical unit 10 or 6 (presently, this is 8).

In subroutine CDAY, both arrays NDM and NDP should have dimension 12.

#### 4. Tidal Heights Prediction Program Details

##### 4.1 Problem Formulation and the Equally Spaced Predictions Method

The tidal height,  $h(t)$ , at a particular station may be represented by the harmonic summation (see section 2.3.3)

$$h(t) = \sum_{j=1}^m f_j(t) A_j \cos(2\pi(V_j(t) + u_j(t) - g_j)) \quad , \quad (1)$$

where  $A_j, g_j$  = the amplitude and phase lag of constituent  $j$ ,

$f_j(t), u_j(t)$  = the nodal modulation amplitude and phase correction factors for constituent  $j$ ,

and  $V_j(t)$  = the astronomical argument for constituent  $j$ .

Expanding  $V(t)$  as in section 2.3.1 and using the first order Taylor approximations for the astronomical arguments as in section 2.1.1,  $V(t)$  can be re-expressed as

$$\begin{aligned} V(t) &= i\tau(t) + jS(t) + kH(t) + \ell P(t) + mN'(t) + nP'(t) \\ &= i\tau(t_0) + jS(t_0) + kH(t_0) + \ell P(t_0) + mN'(t_0) + nP'(t_0) \\ &\quad + (t-t_0) \frac{\partial}{\partial t} [i\tau(t) + jS(t) + kH(t) + \ell P(t) + mN'(t) + nP'(t)]_{t=t_0} \\ &= V(t_0) + (t - t_0)\sigma, \end{aligned}$$

where  $t_0$  is the reference time origin of 000 ET January 1 1976, and  $\sigma$  is the constituent frequency at this time origin. It follows from this result that  $V(t_2) = V(t_1) + (t_2 - t_1)\sigma$  for arbitrary times  $t_1, t_2$ , and so  $V_j(t)$  can be replaced in (1) by  $V_j(t_1) + (t - t_1)\sigma_j$  for some convenient time  $t_1$ .



From section 2.3.2 it is seen that  $f(t)$  and  $u(t)$  are time dependent only through the  $\Delta_{jk}(t)$  variable. Since satellites differ from main constituents in only the last three Doodson numbers (see section 2.1.3),

$$\begin{aligned}\Delta_{jk}(t) &= V_{jk}(t) - V_j(t) \\ &= \Delta l P(t) + \Delta m N'(t) + \Delta n P'(t) .\end{aligned}$$

Using the first order Taylor approximations for  $P, N'$ , and  $P'$ , it follows that over a time period  $[t_1, t_2]$  the change in  $\Delta_{jk}(t)$  is

$$\begin{aligned}\Delta_{jk}(t_2) - \Delta_{jk}(t_1) &= \Delta l (P(t_2) - P(t_1)) + \Delta m (N'(t_2) - N'(t_1)) + \Delta n (P'(t_2) - P'(t_1)) \\ &= (t_2 - t_1) \frac{d}{dt} [\Delta l P(t) + \Delta m N'(t) + \Delta n P'(t)]_{t=t_0} \\ &= (t_2 - t_1) (\sigma_{jk} - \sigma_j) .\end{aligned}$$

Since  $\frac{d}{dt} [P(t) + N'(t) + P'(t)]_{t=t_0}$  is .16668884 cycles/365 days and  $|\Delta l|, |\Delta m|, |\Delta n|$  are always less than or equal to 4, if  $|t_2 - t_1| \leq 16$  days,  $|\Delta_{jk}(t_2) - \Delta_{jk}(t_1)| \leq .03$  cycles. This small variation in  $\Delta_{jk}(t)$  leads to a similar behaviour in  $\cos(\Delta_{jk}(t))$  and  $\sin(\Delta_{jk}(t))$ , and hence  $f(t)$  and  $u(t)$ . Thus only a small loss in accuracy but a considerable calculation time saving will result if  $f(t)$  and  $u(t)$  are approximated by a constant value throughout the period of a month. Consequently  $f(t)$  and  $u(t)$  are assumed to equal their value at 000 hr of the 16th day of the month for the entire monthly period; and for convenience,  $V(t)$  is set to  $V(t_{16}) + (t - t_{16})\sigma$ , where  $t_{16}$  is this same time.



The procedure for calculating a series of tidal heights is then as follows. Since the tidal prediction data package does not contain constituent frequencies, they must be calculated via the astronomical variable derivatives and the constituent Doodson numbers.  $f$ ,  $u$  and  $V$  values are then calculated for the 16th day of the first month of the desired prediction period and, as required, for subsequent months. Tidal heights for the desired values of  $t$  can then be calculated as

$$h(t) = \sum_{j=1}^m f_j(t_{16}) A_j \cos(2\pi(V_j(t_{16}) + (t-t_{16})\sigma_j + u_j(t_{16}) - g_j)). \quad (2)$$

In order to avoid calling a trigonometric library function for each new value of  $t$ , when a sequence of equally spaced heights are required, the following Chebyshev iteration formula is used for each constituent contribution,

$$f(n+1) = 2 \cos(\sigma\Delta t) f(n) - f(n-1), \quad (3)$$

where  $f(n) = \cos(n\sigma\Delta t)$  or  $\sin(n\sigma\Delta t)$ .

## 4.2 The High and Low Tide Prediction Method

The material presented here is taken from Godin and Taylor [1973].

In 4.1 we saw that the tidal height at a given location can be represented by the harmonic sum

$$h(t) = \sum_{j=1}^m f_j(t_0) A_j \cos(2\pi(V_j(t_0) + (t-t_0)\sigma_j + u(t_0) - g_j)) \quad (1)$$

where:

$A_j, g_j, \sigma_j$  = the amplitude, phase lag and frequency of constituent  $j$ ,

$f_j(t_0), u_j(t_0)$  = the nodal modulation amplitude and phase correction

factors for constituent  $j$  at the time origin  $t_0$ ,

$V_j(t_0)$  = the astronomical argument for constituent  $j$  at the time origin  $t_0$ .

Letting  $D(t)$  be the derivative of  $h(t)$ , i.e.

$$D(t) = - \sum_{j=1}^m f_j(t_0) A_j 2\pi \sigma_j \sin(2\pi(V_j(t_0) + (t-t_0)\sigma_j + u(t_0) - g_j)) \quad , \quad (2)$$

the high-low tide prediction method uses the following calculus results. If  $D(t)$  is a continuous function on the interval  $[t_1, t_2]$  and  $t_k$  is a point in this interval, then:

- i)  $D(t_k) = 0$  if and only if  $t_k$  is an extreme point, or saddle point,<sup>1</sup> or  $h(t)$  is constant in the neighbourhood of  $t_k$ ;
- ii) if  $D(t_1)$  and  $D(t_2)$  have opposite signs then there exists a  $t_k$  in  $(t_1, t_2)$  with  $D(t_k) = 0$ .

---

<sup>1</sup> An example of a saddle point is  $x = 0$  for the function  $f(x) = x^3$ .

Now for computational purposes we can assume that saddle points do not exist. That is to say, due to accuracy limitations of the computer, a zero derivative will be approximated by a number with a very small absolute value, and thus perturb a saddle point so that it becomes either a maximum and minimum, or a near saddle point (in the neighbourhood of a 'near saddle point', the derivative is of constant sign and almost assumes the value zero). And since, from its definition, we can reasonably assume that  $h(t)$  is not constant over any arbitrarily small interval, the continuity of  $D(t)$  everywhere implies that an interval  $[t_1, t_2]$  with  $D(t_1)$  and  $D(t_2)$  having opposite signs contains an extremum.

However this result alone is not sufficient to guarantee the location of all extrema because, it does not eliminate the possibility of having more than one extremum in an interval whose endpoints have different signs, nor does it imply that if the endpoints have the same derivative sign there is no extremum in the interval. In order to ensure these conditions and thus be assured of bracketing all extreme values, it is necessary that a minimum interval size be specified in which we can assume that there exists at most one high or low tide.

Clearly the interval size  $\Delta t$  will be dependent upon the nature of the tide at a particular station. The time between successive high and low waters for predominantly semi-diurnal and diurnal tides is approximately 6 and 12 hours respectively. However if the tide is mixed, the extremal pattern is more complicated. FIGURE 2 shows the water level at Victoria, British Columbia between July 24 and 31, 1976. It is a mixed tide where the shorter period fluctuations override the major diurnal oscillations with a continuous shift in their position and amplitude.

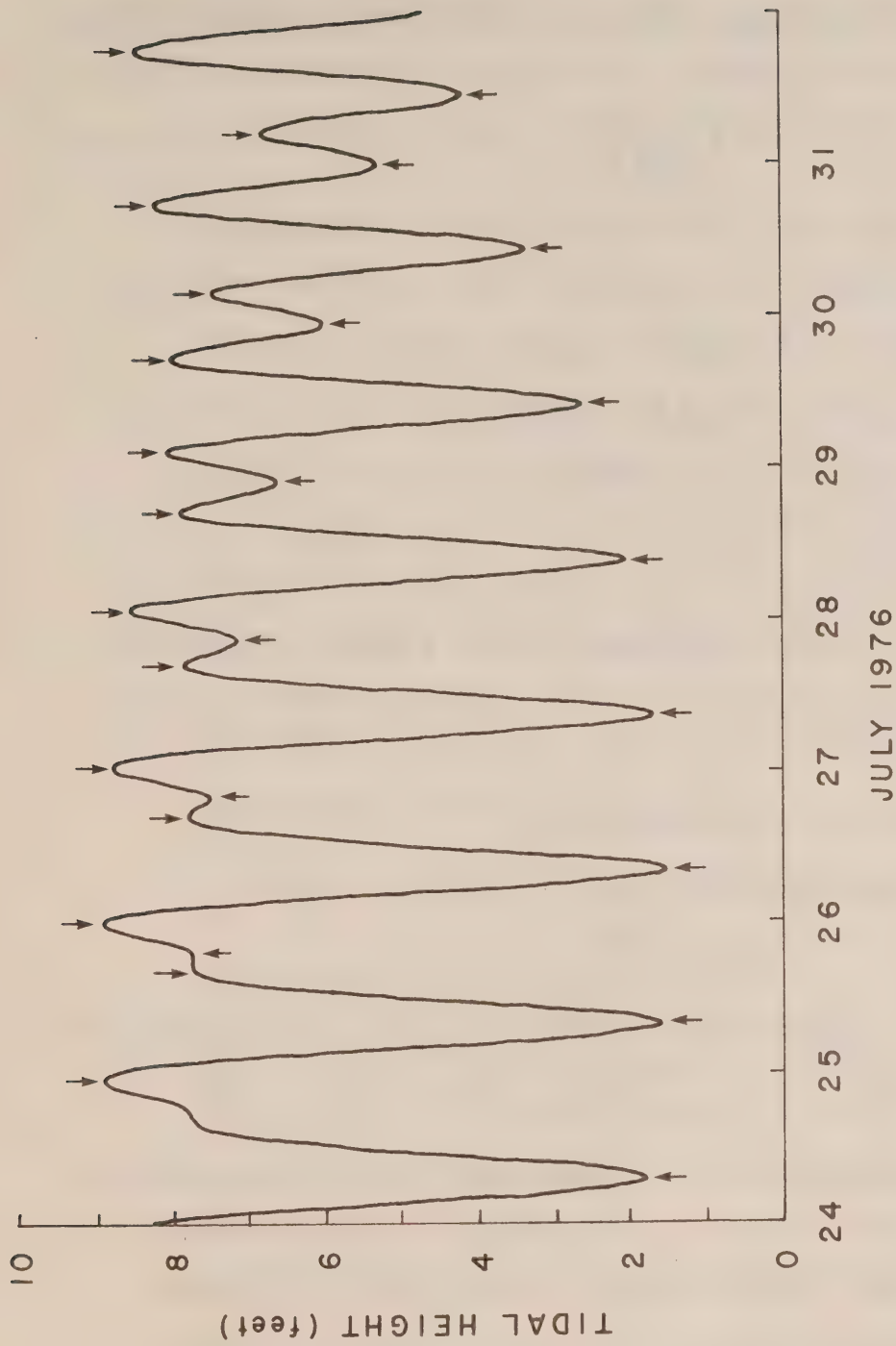


FIGURE 2

Synthesized water level at Victoria British Columbia over the period of July 24-31 1976. The tide is of a mixed character with  $F = 2.1$ . The arrows indicate the time and height of the extrema predicted using the method described in 4.2.

One characterization of the tide may be obtained by calculating the ratio of the amplitudes of the major harmonic constituents M2, S2, K1 and O1. This value is called the form number (Dietrich [1963]) and is defined precisely as

$$F = \frac{K1 + O1}{M2 + S2} .$$

The tide is then said to be

- i) semi-diurnal if  $0 \leq F \leq .25$ ,
- ii) mixed if  $.25 < F \leq 3.00$ ,
- iii) diurnal if  $F > 3.00$  .

For Victoria,  $F = 2.1$ .

In accordance with this determination Godin suggests the following maximum time interval values in which it can be assumed that there exists at most one extremum:

- i)  $\Delta t = 3$  hours for semi-diurnal tide,
- ii)  $\Delta t = .5$  hours for mixed tide,
- iii)  $\Delta t = 6$  hours for diurnal tide.

Although in fact, a mixed tide may have extrema closer than .5 hours, he feels that for practical purposes it is sufficient to note just one of them.

With these values of  $\Delta t$  we can then bracket all extrema by moving forward in time with steps of size  $\Delta t$ , and comparing signs of the interval endpoints. Once such upper and lower bounds have been found, the extreme point can be located exactly by any one of a number of search techniques. Because it requires a minimal amount of time, the one chosen is Bolzano's



method of bisection coupled with linear interpolation. Although the bisection method does not take the minimal number of iterations when compared to more sophisticated search techniques, it is able to make significant time savings by computing new sine function values as a linear combination of old ones, and thus, unlike the other methods, avoid calls to the fortran library function SIN.

In more detail, the search algorithm for an extremum is then as follows:

- i) move forward in time from the origin, or the last extremum, in steps of  $\Delta t$  until either a change in sign exists between the derivative values at the end points of the interval  $(t_a, t_b)$ , or  $t_b$  extends beyond the desired prediction period. Each constituent contribution in the summation  $D(t)$  is evaluated by the Chebyshev iteration formula (3) of 4.1. When an interval containing an extremum is located, set  $k = 1$  and proceed to ii).

- ii) calculate  $t_k = t_a + \frac{1}{2^k} \Delta t$ , and for each constituent in the sum, evaluate  $D(t_k)$  by using the formula

$$\sin(t_k) = (\sin(t_a) + \sin(t_b)) / (2 \cos(\frac{1}{2^k} \Delta t)).$$

If  $|D(t_k)| \leq 10^{-16}$ , set  $D(t_k) = 10^{-16}$ .

- iii) re-assign whichever of  $t_a$  or  $t_b$  has the same derivative sign as  $D(t_k)$ , by  $t_k$ . If the new interval length  $t_b - t_a$  is less than .1 hours, proceed to iv). Otherwise set  $k = k+1$  and return to ii).

- iv) use the following linear interpolation formula to find the extremum

$$t_E, \\ t_E = t_a + D(t_a)(t_b - t_a) / (D(t_a) - D(t_b)) ,$$

and evaluate  $h(t_E)$  via (1). For each constituent term in this sum, obtain the function value by using a pre-calculated stored table of 2002 cosine values with arguments in the range of  $0^\circ$  to  $360^\circ$ . Return to i).

FIGURE 3 illustrates an example of the sequence of steps involved in the search for an extreme value. It is easily calculated that the number of iterations required to reduce the bracketing interval from  $\Delta t$  to .1 hour is 6 for diurnal tides, 3 for mixed tides, and 5 for semi-diurnal tides.

Arrows in FIGURE 2 indicate the extrema predicted for Victoria using the technique just described; the shaft of the arrow locates the time abscissa while the tip ends at the predicted height. The predicted hourly heights and the times and heights of all extrema are listed in Appendix 5.

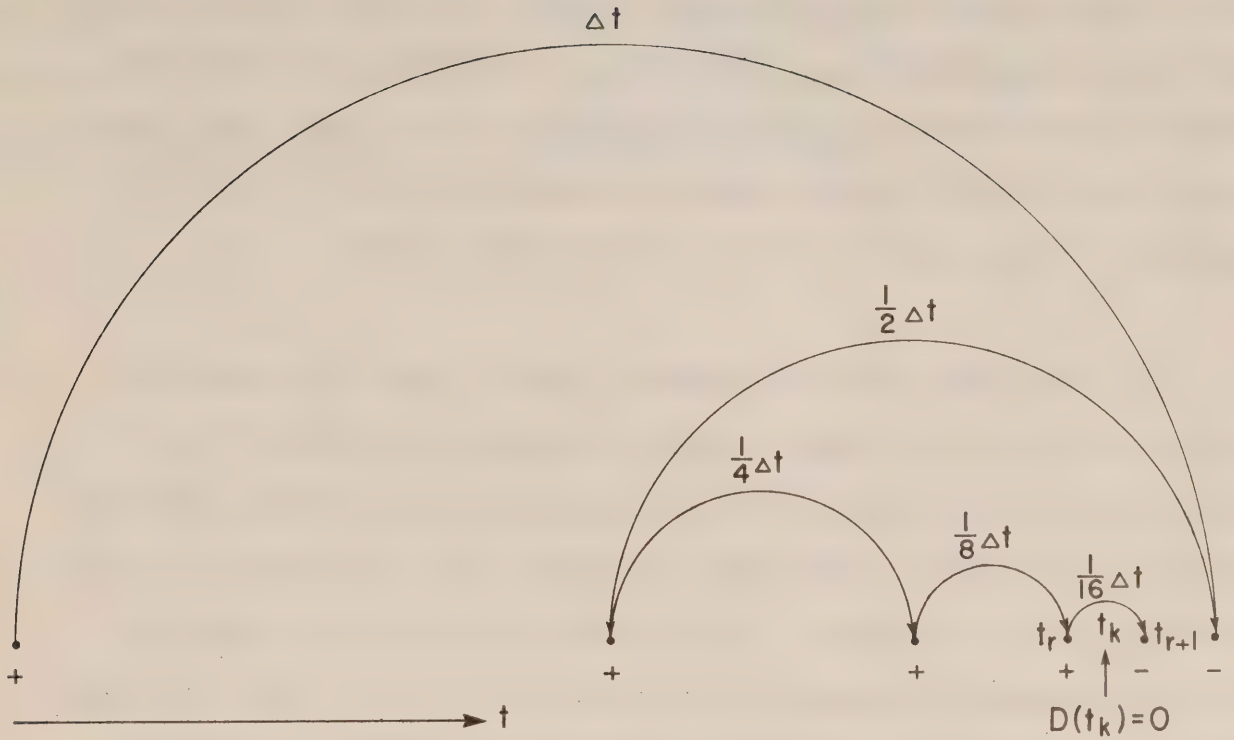


FIGURE 3

An example of the sequence of steps involved in locating a zero  $t_k$  of the derivative  $D(t)$ . The sign of  $D(t)$  at the various points tested is denoted by + or -. After a step  $\Delta t$ , the sign has changed; by a retrogression of  $\frac{1}{2}\Delta t$ , the sign has reverted to plus, forcing a forward step of  $\frac{1}{4}\Delta t$  where the sign is still unchanged. Two further forward steps of  $\frac{1}{8}\Delta t$  and  $\frac{1}{16}\Delta t$  locate the minimum width interval  $(t_r, t_{r+1})$  over which the position of  $t_k$  is determined by linear interpolation from the values of  $D(t)$  at  $t_r$  and  $t_{r+1}$ .

## 5. Consistency of the Analysis and Prediction Programs

Although consistency between the tidal heights analysis program and the tidal heights prediction program was a major objective in their revision, they do have one difference. In particular, if a pseudo-tidal record were generated by the prediction program and analysed using the same constituents, the amplitude and phase results given by the analysis program would not be identical to those used as input for the prediction program.

In a small part, this discrepancy is due to round-off accumulated during the calculations. However a test performed on the UNIVAC 1106 at Patricia Bay with a two month period of synthesized hourly heights indicates that such errors occur no sooner than the fourth digit. The remainder of the difference (which is, at worst, in the third digit) can be attributed to different approximating assumptions for the calculation of  $f$  and  $u$ , the nodal modulation amplitude and phase correction factors. Whereas the prediction program calculates these values at the 16th day of each month in the desired time period and keeps them constant throughout the entire month, the analyses program assumes them to be constant over the entire analyses period and equal to their true values at the central hour of that period.

It is important to note, though, that significantly different results can be expected in a similar test run if there is at least one more constituent used in the synthesis than analysis. This is because the least squares fit technique will adjust the amplitudes and phases of constituents included in the analysis to partially account for contributions due to constituents

included in the synthesis but not the analysis. In fact this will occur even if the extra constituents are inferred (e.g. P1 is included in the synthesis and in the analysis via inference from K1) because of small inaccuracies in the approximating inference assumptions. However, except for round-off errors and the slightly different  $f$  and  $u$  values, having more constituents in the analysis than the synthesis will not affect the results.



## Standard Constituent Input Data for the Tidal Heights Analysis Computer Program

This data is read by the program from logical unit 8

ZU	0.0	M2
SA	0.0001140741	SSA
SSA	0.0002281591	Z0
MSM	0.0013097808	MM
MM	0.0015121518	MSF
MSF	0.0028219327	Z0
MF	0.0030500918	MSF
ALP1	0.0343965699	2Q1
2Q1	0.0357063507	Q1
SI61	0.0359087218	2Q1
Q1	0.0372185026	O1
RH01	0.0374208736	Q1
O1	0.0387306544	K1
TAU1	0.0389588136	O1
BET1	0.0400404353	N01
N01	0.0402685944	K1
CHI1	0.0404709654	N01
PI1	0.0414385130	P1
P1	0.0415525871	K1
S1	0.0416666721	K1
K1	0.0417807462	Z0
PSI1	0.0418948203	K1
PHI1	0.0420089053	K1
THE1	0.0430905270	J1
J1	0.0432928981	K1
2P01	0.0443745198	
S01	0.0446026789	001
001	0.0448308380	J1
UPS1	0.0463429898	001
ST36	0.0733553835	
2NS2	0.0746651643	
ST37	0.0748675353	
ST1	0.0748933234	
0Q2	0.0759749451	EPS2
EPS2	0.0761773161	2N2

ST2	0.0764054753	
ST3	0.0772331498	
O2	0.0774613089	
2N2	0.0774870970	MU2
MU2	0.0776894680	N2
SNK2	0.0787710897	
N2	0.0789992488	M2
NU2	0.0792016198	N2
ST4	0.0794555670	
OP2	0.0802832416	
GAM2	0.0803090296	H1
H1	0.0803973266	M2
M2	0.0805114007	Z0
H2	0.0806254748	M2
MKS2	0.0807395598	M2
ST5	0.0809677189	
ST6	0.0815930224	
LDA2	0.0818211815	L2
L2	0.0820235525	S2
2SK2	0.0831051742	
T2	0.0832192592	S2
S2	0.0833333333	M2
R2	0.0834474074	S2
K2	0.0835614924	S2
MSN2	0.0848454852	ETA2
ETA2	0.0850736443	K2
ST7	0.0853018034	
2SM2	0.0861552660	
ST38	0.0863576370	
SKM2	0.0863834251	
2SN2	0.0876674179	
N03	0.1177299033	
M03	0.1192420551	M3
M3	0.1207671010	M2
NK3	0.1207799950	
S03	0.1220639878	MK3
MK3	0.1222921469	M3
SP3	0.1248859204	
SK3	0.1251140796	MK3
ST8	0.1566887168	

N4	0.1579984976	
3MS4	0.1582008687	
ST39	0.1592824904	M4
MN4	0.1595106495	
ST9	0.1597388086	
ST40	0.1607946422	M3
M4	0.1610228013	
ST10	0.1612509604	M4
SN4	0.1623325821	
KN4	0.1625607413	M4
MS4	0.1638447340	MS4
MK4	0.1640728931	S4
SL4	0.1653568858	
S4	0.1666666667	
SK4	0.1668948258	
MN05	0.1982413039	
2M05	0.1997534558	
3MP5	0.1999816149	
MNK5	0.2012913957	
2MP5	0.2025753884	M4
2MK5	0.2028035475	
MSK5	0.2056254802	
3KM5	0.2058536393	
2SK5	0.2084474129	2MK5
ST11	0.2372259056	
2NM6	0.2385098983	
ST12	0.2387380574	
2MN6	0.2400220501	M6
ST13	0.2402502093	
ST41	0.2413060429	2MK5
M6	0.2415342020	
MSN6	0.2428439828	
MKN6	0.2430721419	
ST42	0.2441279756	M6
2MS6	0.2443561347	2MS6
2MK6	0.2445842938	
NSK6	0.2458940746	
2SM6	0.2471780673	2MS6
MSK6	0.2474062264	2SM6
S6	0.2500000000	







K1	-2	-1	0	0	0.0002	-1	-1	0	0.75	0.0001R1	-1	0	0	.25	0.0007R1	
K1	-1	1	0	.75	0.0001R1	0	-2	0	.0	0.0001	0	-1	0	.50	0.0198	
K1	0	1	0	.0	0.1356	0	2	0	.50	0.0029	1	0	0	.25	0.0002R1	
K1	1	1	0	.25	0.0001R1											
PSI1	1	1	1	0	0	-1	-0.75	1								
PSI1	0	1	0	.0	0.0190											
PHI1	1	1	2	0	0	0	-0.75	5								
PHI1	-2	0	0	.0	0.0344	-2	1	0	0.0	0.0106	0	0	-2	.0	0.0132	
PHI1	0	1	0	.50	0.0384	0	2	0	.50	0.0185						
THE1	1	2	-2	1	0	0	-.75	4								
THE1	-2	-1	0	.00	.0300	-1	0	0	.25	0.0141R1	0	-1	0	.50	.0317	
THE1	0	1	0	.00	.1993											
J1	1	2	0	-1	0	0	-0.75	10								
J1	0	-1	0	.50	0.0294	0	1	0	0.0	0.1980	0	2	0	.50	0.0047	
J1	1	-1	0	.75	0.0027R1	1	0	0	.25	0.0816R1	1	1	0	.25	0.0331R1	
J1	1	2	0	.25	0.0027R1	2	0	0	.50	0.0152	2	1	0	.50	0.0098	
J1	2	2	0	.50	0.0057											
001	1	3	0	0	0	0	-0.75	8								
001	-2	-1	0	.50	0.0037	-2	0	0	.0	0.1496	-2	1	0	.0	0.0296	
001	-1	0	0	.25	0.0240R1	-1	1	0	.25	0.0099R1	0	1	0	.0	0.6398	
001	0	2	0	.0	0.1342	0	3	0	.0	0.0086						
UPS1	1	4	0	-1	0	0	-.75	5								
UPS1	-2	0	0	.00	0.0611	0	1	0	.00	0.6399	0	2	0	.00	0.1318	
UPS1	1	0	0	.25	0.0289R1	1	1	0	.25	0.0257R1						
0Q2	2	-3	0	3	0	0	0.0	2								
0Q2	-1	0	0	.25	0.1042R2	0	-1	0	.50	0.0386						
EPS2	2	-3	2	1	0	0	0.0	3								
EPS2	-1	-1	0	.25	0.0075R2	-1	0	0	.25	0.0402R2	0	-1	0	.50	0.0373	
2N2	2	-2	0	2	0	0	0.0	4								
2N2	-2	-2	0	.50	0.0061	-1	-1	0	.25	0.0117R2	-1	0	0	.25	0.0678R2	
2N2	0	-1	0	.50	0.0374											
MU2	2	-2	2	0	0	0	0.0	3								
MU2	-1	-1	0	.25	0.0018R2	-1	0	0	.25	0.0104R2	0	-1	0	.50	0.0375	
N2	2	-1	0	1	0	0	0.0	4								
N2	-2	-2	0	.50	0.0039	-1	0	0	1	.00	0.0008	0	-2	0	.00	0.0005
N2	0	-1	0	.50	0.0373											
NU2	2	-1	2	-1	0	0	0.0	4								
NU2	0	-1	0	.50	0.0373	1	0	0	.75	0.0042R2	2	0	0	.0	0.0042	
NU2	2	1	0	.50	0.0036											
GAM2	2	0	-2	2	0	0	-.50	3								



OP2	2	1.0	O1	1.0	P1	-1.0	S2	-1.0	K2
MKS2	3	1.0	M2	1.0	K2	-2.0	S2	-1.0	M2
ST5	3	1.0	M2	2.0	K2	-1.0	M2	-1.0	N2
ST6	4	2.0	S2	1.0	N2	-1.0	K2	-1.0	N2
2SK2	2	2.0	S2	-1.0	K2	-1.0	N2	-1.0	N2
MSN2	3	1.0	M2	1.0	S2	-1.0	S2	-2.0	N2
ST7	4	2.0	K2	1.0	M2	-1.0	M2	-1.0	M2
2SM2	2	2.0	S2	-1.0	M2	-1.0	N2	-2.0	N2
ST38	3	2.0	M2	1.0	S2	-1.0	M2	-1.0	M2
SKM2	3	1.0	S2	1.0	K2	-1.0	N2	-1.0	N2
2SN2	2	2.0	S2	-1.0	N2	-1.0	O1	-1.0	O1
NO3	2	1.0	N2	1.0	O1	-1.0	K1	-1.0	K1
MO3	2	1.0	M2	1.0	O1	-1.0	O1	-1.0	O1
INK3	2	1.0	N2	1.0	K1	-1.0	P1	-1.0	P1
SO3	2	1.0	S2	1.0	K1	-1.0	N2	-1.0	N2
MK3	2	1.0	M2	1.0	K1	-1.0	N2	-1.0	N2
SP3	2	1.0	S2	1.0	K1	-1.0	N2	-1.0	N2
SK3	2	1.0	S2	1.0	K1	-1.0	N2	-1.0	N2
ST8	3	2.0	M2	1.0	N2	-1.0	N2	-1.0	N2
IN4	1	2.0	N2	-1.0	S2	-1.0	N2	-1.0	N2
3MS4	2	3.0	M2	1.0	S2	-1.0	N2	-1.0	N2
ST39	4	1.0	M2	1.0	S2	-1.0	N2	-1.0	N2
IN4	2	1.0	M2	1.0	N2	-1.0	K2	-1.0	K2
ST40	3	2.0	M2	1.0	S2	-1.0	K2	-1.0	K2
ST9	4	1.0	M2	1.0	N2	-1.0	S2	-1.0	S2
M4	1	2.0	M2	1.0	K2	-1.0	S2	-1.0	S2
ST10	3	2.0	M2	1.0	N2	-1.0	N2	-1.0	N2
SN4	2	1.0	S2	1.0	N2	-1.0	N2	-1.0	N2
KN4	2	1.0	K2	1.0	S2	-1.0	L2	-1.0	L2
MS4	2	1.0	M2	1.0	K2	-1.0	N2	-1.0	N2
MK4	2	1.0	M2	1.0	K2	-1.0	N2	-1.0	N2
SL4	2	1.0	S2	1.0	L2	-1.0	N2	-1.0	N2
S4	1	2.0	S2	1.0	K2	-1.0	N2	-1.0	N2
SK4	2	1.0	S2	1.0	K2	-1.0	N2	-1.0	N2
MNO5	3	1.0	M2	1.0	O1	-1.0	P1	-1.0	P1
2MO5	2	2.0	M2	1.0	N2	-1.0	N2	-1.0	N2
3MP5	2	3.0	M2	-1.0	P1	-1.0	N2	-1.0	N2
MNK5	3	1.0	M2	1.0	N2	-1.0	K1	-1.0	K1
2MP5	2	2.0	M2	1.0	P1	-1.0	N2	-1.0	N2
2MK5	2	2.0	M2	1.0	K1	-1.0	N2	-1.0	N2

MSK5	3	1.0	M2	1.0	S2	1.0	K1	1.0	K1
3KM5	3	1.0	K2	1.0	K1	1.0	M2		
2SK5	2	2.0	S2	1.0	K1	-1.0	S2		
ST11	3	3.0	N2	1.0	K2				
2NM6	2	2.0	N2	1.0	M2				
ST12	4	2.0	N2	1.0	M2			-1.0	S2
ST41	3	3.0	M2	1.0	S2				
2MN6	2	2.0	M2	1.0	N2				
ST13	4	2.0	M2	1.0	N2			-1.0	S2
M6	1	3.0	M2						
MSN6	3	1.0	M2	1.0	S2				
MKN6	3	1.0	M2	1.0	K2				
2MS6	2	2.0	M2	1.0	S2				
2MK6	2	2.0	M2	1.0	K2				
NSK6	3	1.0	N2	1.0	S2				
2SM6	2	2.0	S2	1.0	M2				
MSK6	3	1.0	M2	1.0	S2				
ST42	3	2.0	M2	2.0	S2				
S6	1	3.0	S2						
ST14	3	2.0	M2	1.0	N2				
ST15	3	2.0	N2	1.0	M2				
M7	1	3.5	M2						
ST16	3	2.0	M2	1.0	S2				
3MK7	2	3.0	M2	1.0	K1				
ST17	4	1.0	M2	1.0	S2			1.0	O1
ST18	2	2.0	M2	2.0	N2				
3MN8	2	3.0	M2	1.0	N2				
ST19	4	3.0	M2	1.0	N2			-1.0	S2
M8	1	4.0	M2						
ST20	3	2.0	M2	1.0	S2				
ST21	3	2.0	M2	1.0	N2				
3MS8	2	3.0	M2	1.0	S2				
3MK8	2	3.0	M2	1.0	K2				
ST22	4	1.0	M2	1.0	S2			1.0	N2
ST23	2	2.0	M2	2.0	S2				
ST24	3	2.0	M2	1.0	S2				
ST25	3	2.0	M2	2.0	N2				
ST26	3	3.0	M2	1.0	N2				
4MK9	2	4.0	M2	1.0	K1				
ST27	3	3.0	M2	1.0	S2				







1	6485	17	775	60	50	50	61	84	111	135	149	154	154	143	122
2	6485	17	775	99	81	72	73	85	99	115	127	127	115	108	94
1	6485	18	775	78	59	50	50	64	81	100	132	164	184	188	179
2	6485	18	775	159	137	133	135	137	143	147	148	153	161	170	161
1	6485	19	775	147	141	142	128	130	143	160	177	193	211	230	236
2	6485	19	775	226	204	181	165	157	161	178	178	178	186	196	198
1	6485	20	775	201	190	172	155	138	130	136	156	174	199	227	245
2	6485	20	775	254	256	245	199	162	141	129	134	157	183	206	220
1	6485	21	775	219	222	210	194	182	169	171	183	206	240	255	265
2	6485	21	775	288	296	292	282	262	238	212	190	186	198	220	240
1	6485	22	775	259	268	271	264	249	228	203	184	187	206	230	257
2	6485	22	775	283	293	295	282	261	232	204	182	165	171	192	218
1	6485	23	775	232	247	255	249	230	205	181	158	148	152	180	209
2	6485	23	775	234	260	272	261	231	196	160	130	111	109	125	157
1	6485	24	775	187	209	224	231	209	181	155	125	110	111	130	159
2	6485	24	775	195	227	249	250	233	200	161	123	94	87	97	123
1	6485	25	775	153	183	196	202	195	174	138	101	71	58	60	87
2	6485	25	775	122	159	185	202	199	179	144	103	66	40	35	48
1	6485	26	775	75	104	132	151	160	155	129	98	66	39	34	47
2	6485	26	775	79	113	144	163	172	167	151	117	85	50	20	19
1	6485	27	775	39	74	107	136	148	158	141	118	89	54	29	16
2	6485	27	775	41	76	105	143	189	202	196	185	185	162	160	163
1	6485	28	775	168	187	222	254	260	275	281	268	256	241	221	198
2	6485	28	775	208	230	258	264	285	301	291	270	247	212	188	176
1	6485	29	775	183	200	224	245	256	269	280	270	243	216	194	164
2	6485	29	775	163	177	201	232	263	282	281	290	259	238	202	179
1	6485	30	775	179	184	205	226	242	272	281	279	263	233	205	279
2	6485	30	775	168	184	210	235	247	253	263	259	244	221	193	183
1	6485	31	775	180	176	194	208	215	224	235	243	241	225	207	188
2	6485	31	775	176											
1	875	1	875												
2	875	1	875												
1	875	2	875												
2	875	2	875												
3	875	3	875	97	83	68	56	51	54	75	95	118	118	116	108
2	875	3	875	133	120	103	87	71	56	52	66	81	98	109	107
1	875	4	875	98	77	49	28	14	4	7	17	44	70	94	110
2	875	4	875	117	116	107	88	71	55	46	44	60	84	108	125
1	875	5	875	133	136	114	86	70	62	62	79	113	143	175	208
2	875	5	875	238	256	266	240	203	179	143	117	118	146	167	186

1	6485	6	875	224	243	227	204	180	158	154	170	201	222	234	243
2	6485	6	875	254	260	247	231	211	188	160	143	137	145	167	195
1	6485	7	875	221	239	249	249	227	184	144	111	102	129	170	201
2	6485	7	875	233	255	260	252	227	195	156	123	107	118	149	180
1	6485	8	875	211	232	245	257	229	200	171	138	102	95	122	163
2	6485	8	875	207	253	295	338	369	353	318	285	221	184	165	175
1	6485	9	875	212	240	260	283	282	259	229	196	174	176	187	204
2	6485	9	875	244	288	329	356	369	370	324	281	289	294	293	287
1	6485	10	875	329	380	426	441	447	453	418	387	353	337	322	314
2	6485	10	875	342	365	404	438	470	482	487	456	441	423	438	448
1	6485	11	875	464	478	491	505	538	528	493	488	472	425	398	390
2	6485	11	875	393	408	421	438	444	433	412	379	337	300	262	247
1	6485	12	875	245	252	277	304	327	339	339	308	257	208	182	182
2	6485	12	875	203	235	260	281	319	315	297	273	237	198	168	158
1	6485	13	875	157	171	195	217	239	252	258	253	242	225	202	179
2	6485	13	875	167	172	190	217	242	257	266	263	244	217	187	155
1	6485	14	875	132	134	163	195	228	246	259	256	236	209	180	150
2	6485	14	875	129	122	136	161	184	200	207	205	195	177	158	136
1	6485	15	875	116	105	104	115	140	164	193	203	216	208	196	187
2	6485	15	875	159	142	147	164	175	183	197	202	202	202	192	176
1	6485	16	875	160	147	137	136	152	172	195	211	224	228	222	210
2	6485	16	875	199	186	171	165	163	169	180	190	201	203	200	193
1	6485	17	875	185	175	162	152	156	169	201	227	249	272	284	285
2	6485	17	875	295	280	259	241	225	211	211	226	247	268	286	297
1	6485	18	875	296	272	245	214	196	194	209	226	239	244	245	248
2	6485	18	875	246	239	229	218	201	183	165	158	160	183	207	221
1	6485	19	875	227	224	209	187	159	138	131	139	162	185	209	228
2	6485	19	875	239	242	233	212	183	152	129	119	132	167	193	218
1	6485	20	875	237	241	230	205	178	151	130	114	122	145	172	203
2	6485	20	875	226	237	237	223	197	165	131	108	103	118	144	173
1	6485	21	875	203	225	229	223	200	175	150	129	131	146	173	202
2	6485	21	875	236	258	263	256	233	198	165	137	127	133	159	190
1	6485	22	875	221	241	252	252	231	200	167	137	119	114	134	166
2	6485	22	875	201	234	256	264	249	212	176	140	111	103	115	140
1	6485	23	875	171	203	232	244	242	214	180	146	121	115	126	157
2	6485	23	875	187	211	235	249	247	229	194	151	114	88	87	110
1	6485	24	875	143	177	206	230	237	223	186	140	93	64	66	94
2	6485	24	875	129	165	197	215	220	205	177	144	112	84	80	100
1	6485	25	875	136	173	208	238	252	244	217	181	139	105	89	93
2	6485	25	875	121	159	188	199	200	185	155	121	84	64	45	28



1	6485	26	875	32	72	121	174	215	237	211	197	234	243	176	196
2	6485	26	875	250	219	272	361	391	376	355	389	370	321	300	285
1	6485	27	875	288	323	350	380	422	415	405	389	412	430	453	509
2	6485	27	875	557	559	548	560	576	557	513	489	462	422	388	383
1	6485	28	875	371	393	413	419	443	472	444	423	384	340	304	284
2	6485	28	875	280	286	300	309	312	324	319	299	270	227	203	181
1	6485	29	875	193	240	281	317	352	351	361	350	354	348	358	350
2	6485	29	875	326	317	316	324	327	313	298	283	264	244	230	215
1	6485	30	875	194	194	217	241	256	262	261	259	247	229	213	195
2	6485	30	875	175	163	168	177	187	198	203	204	191	171	144	119
1	6485	31	875	97	92	102	125	150	168	176	188	197	197	206	202
2	6485	31	875	191	186	192	200	197	199	206	205	207	208	205	198
1	6485	1	975	185	187	194	209	234	255	275	285	305	327	332	320
2	6485	1	975	301	295	291	275	277	294	312	328	344	335	321	328
1	6485	2	975	323	315	324	316	318	329	321	314	317	329	336	336
2	6485	2	975	327	316	301	284	263	245	236	231	233	240	250	262
1	6485	3	975	261	250	227	202	172	153	153	162	171	172	190	214
2	6485	3	975	226	228	214	186	160	143	142	155	173	201	236	255
1	6485	4	975	274	284	282	255	216	183	165	179	203	231	258	294
2	6485	4	975	327	364	353	332	299	262	227	207	219	240	256	275
1	6485	5	975	302	309	298	274	240	196	159	142	158	192	222	249
2	6485	5	975	270	280	282	269	239	197	154	110	99	125	159	187
1	6485	6	975	214	235	236	221	189	153	118	83	63	52	65	106
2	6485	6	975	132	151	165	175	169	148	115	74	42	18	5	30
1	6485	7	975	68	123	189	218	198	167	126	81	52	40	56	81
2	6485	7	975	121	173	203	211	199	173	137	100	72	58	57	92
1	6485	8	975	135	179	218	238	240	224	190	136	91	58	48	65
2	6485	8	975	99	140	173	194	195	175	141	96	57	33	30	50
1	6485	9	975	86	129	173	204	217	202	171	125	79	47	40	59
2	6485	9	975	88	121	173	204	217	202	171	125	79	47	40	59

## Appendix 3

Final analysis results arising from the input data of Appendix 2  
and the standard constituent data package of Appendix 1.

ANALYSIS OF HOURLY TIDAL HEIGHTS				STN	6485	16H	6/ 7/75 TO	14H	9/ 9/75
NO.OBS.=		1559	NO.PTS.ANAL.=	1559	MIDPT=	3H	8/ 8/75	SEPARATION =	1.00
NO	NAME	FREQUENCY	STN	M-Y/	M-Y/	A	G	AL	GL
1	Z0	.00000000	6485	775/ 975	775/ 975	1.9806	.00	1.9806	.00
2	MM	.00151215	6485	775/ 975	775/ 975	.2121	263.34	.2121	288.50
3	MSF	.00282193	6485	775/ 975	775/ 975	.1561	133.80	.1561	115.15
4	ALP1	.03439657	6485	775/ 975	775/ 975	.0152	334.95	.0141	180.96
5	2Q1	.03570635	6485	775/ 975	775/ 975	.0246	82.69	.0226	246.82
6	Q1	.03721850	6485	775/ 975	775/ 975	.0158	65.74	.0144	252.75
7	O1	.03873065	6485	775/ 975	775/ 975	.0764	74.23	.0694	284.43
8	N01	.04026859	6485	775/ 975	775/ 975	.0290	238.14	.0380	275.85
9	P1	.04155259	6485	775/ 975	775/ 975	.0465	71.76	.0468	252.20
10	K1	.04178075	6485	775/ 975	775/ 975	.1406	64.69	.1332	145.54
11	J1	.04329290	6485	775/ 975	775/ 975	.0253	7.32	.0234	103.62
12	001	.04483084	6485	775/ 975	775/ 975	.0531	235.74	.0463	358.47
13	UPS1	.04634299	6485	775/ 975	775/ 975	.0298	91.73	.0233	239.11
14	EPS2	.07617732	6485	775/ 975	775/ 975	.0211	184.59	.0216	109.98
15	MU2	.07768947	6485	775/ 975	775/ 975	.0419	83.23	.0428	30.06
16	N2	.07899925	6485	775/ 975	775/ 975	.0838	44.52	.0857	306.35
17	M2	.08051140	6485	775/ 975	775/ 975	.4904	77.70	.5007	4.40
18	L2	.08202355	6485	775/ 975	775/ 975	.0213	35.21	.0174	168.03
19	S2	.08333333	6485	775/ 975	775/ 975	.2195	126.65	.2193	36.74
20	K2	.08356149	6485	775/ 975	775/ 975	.0597	149.05	.0515	131.15
21	ETA2	.08507364	6485	775/ 975	775/ 975	.0071	246.05	.0059	235.38
22	M03	.11924206	6485	775/ 975	775/ 975	.0148	234.97	.0138	11.86
23	M3	.12076710	6485	775/ 975	775/ 975	.0123	261.57	.0126	331.91
24	MK3	.12229215	6485	775/ 975	775/ 975	.0049	331.60	.0048	339.15
25	SK3	.12511408	6485	775/ 975	775/ 975	.0023	237.69	.0022	228.64
26	MN4	.15951065	6485	775/ 975	775/ 975	.0092	256.47	.0096	85.00
27	M4	.16102280	6485	775/ 975	775/ 975	.0126	291.78	.0131	145.17
28	SN4	.16233258	6485	775/ 975	775/ 975	.0083	270.85	.0085	82.78
29	MS4	.16384473	6485	775/ 975	775/ 975	.0010	339.35	.0011	176.14
30	S4	.16666667	6485	775/ 975	775/ 975	.0047	299.56	.0047	119.75
31	2MK5	.20280355	6485	775/ 975	775/ 975	.0013	310.10	.0013	244.35



32 2SK5	•20844741	6485	775/ 975	•0045	104.00	•0043	5.04
33 2MN6	•24002205	6485	775/ 975	•0035	271.23	•0038	26.46
34 M6	•24153420	6485	775/ 975	•0017	158.88	•0018	298.97
35 2MS6	•24435613	6485	775/ 975	•0056	306.10	•0059	69.59
36 2SM6	•24717807	6485	775/ 975	•0023	298.92	•0023	45.80
37 3MK7	•28331495	6485	775/ 975	•0086	212.25	•0086	73.19
38 M8	•32204560	6485	775/ 975	•0030	42.43	•0033	109.22
39 M10	•40255700	6485	775/ 975	•0009	198.23	•0010	191.71

The following sample input for logical unit 8 will synthesize hourly heights, and the times and heights of all extrema at Victoria for the period of 0100 PST July 1 1976 to 2400 PST July 31 1976 inclusive. The output results are listed in Appendix 5.

.7428797055	.7771900329	.5187051308	.3631582592	.7847990160	000GMT 1/1/76
13.3594019864	.9993368945	.1129517942	.0536893056	.0000477414	INCR./365DAYS
Z0	0 0 0 0 0 0 0 0 0 0	0 0 0 0 0 0 0 0			
SA	0 0 1 0 0 0 -1 0 0 0	-1 0 0 0 0 0 0 0			
SSA	0 0 2 0 0 0 0 0 0 0	0 0 0 0 0 0 0 0			
MSM	0 1 -2 1 0 0 0 .00	0 0 0 0 0 0 0 0			
MM	0 1 0 -1 0 0 0 0 0 0	0 0 0 0 0 0 0 0			
MSF	0 2 -2 0 0 0 0 0 0 0	0 0 0 0 0 0 0 0			
MF	0 2 0 0 0 0 0 0 0 0	0 0 0 0 0 0 0 0			
ALP1	1 -4 2 1 0 0 -.25	2 0 0 0 0 0 0 0			
ALP1	-1 0 0 .75 0.0360R1	0 -1 0 .00 0.1906			
2Q1	1 -3 0 2 0 0 -0.25	5 0 0 0 0 0 0 0			
2Q1	-2 -2 0 .50 0.0063	-1 -1 0 .75 0.0241R1	-1 0 0 .75 0.0607R1		
2Q1	0 -2 0 .50 0.0063	0 -1 0 .0 0.1885			
SIG1	1 -3 2 0 0 0 -0.25	4 0 0 0 0 0 0 0			
SIG1	-1 0 0 .75 0.0095R1	0 -2 0 .50 0.0061	0 -1 0 .0 0.1884		
SIG1	2 0 0 .50 0.0087				
G1	1 -2 0 1 0 0 -0.25	10 0 0 0 0 0 0 0			
G1	-2 -3 0 .50 0.0007	-2 -2 0 .50 0.0039	-1 -2 0 .75 0.0010R1		
G1	-1 -1 0 .75 0.0115R1	-1 0 0 .75 0.0292R1	0 -2 0 .50 0.0057		
G1	-1 0 1 .0 0.0008	0 -1 0 .0 0.1884	1 0 0 .75 0.0018R1		
G1	2 0 0 .50 0.0028				
RH01	1 -2 2 -1 0 0 -0.25	5 0 0 0 0 0 0 0			
RH01	0 -2 0 .50 0.0058	0 -1 0 .0 0.1882	1 0 0 .75 0.0131R1		
RH01	2 0 0 .50 0.0576	2 1 0 .0 0.0175			
O1	1 -1 0 0 0 0 -0.25	8 0 0 0 0 0 0 0			
O1	-1 0 0 .25 0.0003R1	0 -2 0 .50 0.0058	0 -1 0 .0 0.1885		
O1	1 -1 0 .25 0.0004R1	1 0 0 .75 0.0029R1	1 1 0 .25 0.0004R1		
O1	2 0 0 .50 0.0064	2 1 0 .50 0.0010			









ST39	4	1.0	M2	1.0	S2	1.0	N2	-1.0	K2
MIN4	2	1.0	M2	1.0	N2				
ST40	3	2.0	M2	1.0	S2	-1.0	K2		
ST9	4	1.0	M2	1.0	N2	1.0	K2	-1.0	S2
M4	1	2.0	M2						
ST10	3	2.0	M2	1.0	K2	-1.0	S2		
SN4	2	1.0	S2	1.0	N2				
KN4	2	1.0	K2	1.0	N2				
MS4	2	1.0	M2	1.0	S2				
MK4	2	1.0	M2	1.0	K2				
SL4	2	1.0	S2	1.0	L2				
S4	1	2.0	S2						
SK4	2	1.0	S2	1.0	K2				
MN05	3	1.0	M2	1.0	N2	1.0	O1		
2M05	2	2.0	M2	1.0	O1				
3MP5	2	3.0	M2	-1.0	P1				
MNK5	3	1.0	M2	1.0	N2	1.0	K1		
2MP5	2	2.0	M2	1.0	P1				
2MK5	2	2.0	M2	1.0	K1				
MSK5	3	1.0	M2	1.0	S2	1.0	K1		
3KM5	3	1.0	K2	1.0	K1	1.0	M2		
2SK5	2	2.0	S2	1.0	K1	-1.0	S2		
ST11	3	3.0	N2	1.0	K2				
2NM6	2	2.0	N2	1.0	M2				
ST12	4	2.0	N2	1.0	M2	1.0	K2	-1.0	S2
ST41	3	3.0	M2	1.0	S2	-1.0	K2		
2MN6	2	2.0	M2	1.0	N2				
ST13	4	2.0	M2	1.0	N2	1.0	K2	-1.0	S2
M6	1	3.0	M2						
MSN6	3	1.0	M2	1.0	S2	1.0	N2		
MKN6	3	1.0	M2	1.0	K2	1.0	N2		
2MS6	2	2.0	M2	1.0	S2				
2MK6	2	2.0	M2	1.0	K2				
NSK6	3	1.0	N2	1.0	S2	1.0	K2		
2SM6	2	2.0	S2	1.0	M2				
MSK6	3	1.0	M2	1.0	S2	1.0	K2		
ST42	3	2.0	M2	2.0	S2	-1.0	K2		
S6	1	3.0	S2						
ST14	3	2.0	M2	1.0	N2	1.0	O1		
ST15	3	2.0	N2	1.0	M2	1.0	K1		

M7	1	3.5	M2	1.0	S2	1.0	O1
ST16	3	2.0	M2	1.0	K1	1.0	K2
3MK7	2	3.0	M2	1.0	S2	1.0	O1
ST17	4	1.0	M2	2.0	N2		
ST18	2	2.0	M2	1.0	N2		
3MN8	2	3.0	M2	1.0	N2		
ST19	4	3.0	M2	1.0	N2		
M8	1	4.0	M2	1.0	S2		
ST20	3	2.0	M2	1.0	N2		
ST21	3	2.0	M2	1.0	N2		
3MS8	2	3.0	M2	1.0	S2		
3MK8	2	3.0	M2	1.0	K2		
ST22	4	1.0	M2	1.0	S2		
ST23	2	2.0	M2	2.0	S2		
ST24	3	2.0	M2	1.0	S2		
ST25	3	2.0	M2	2.0	N2		
ST26	3	3.0	M2	1.0	N2		
4MK9	2	4.0	M2	1.0	K1		
ST27	3	3.0	M2	1.0	S2		
ST28	2	4.0	M2	1.0	N2		
M10	1	5.0	M2	1.0	N2		
ST29	3	3.0	M2	1.0	S2		
ST30	2	4.0	M2	1.0	S2		
ST31	4	2.0	M2	1.0	N2		
ST32	2	3.0	M2	2.0	S2		
ST33	3	4.0	M2	1.0	S2		
M12	1	6.0	M2	1.0	S2		
ST34	2	5.0	M2	1.0	N2		
ST35	4	3.0	M2	1.0	K2		
7120	VICTORIA	HARBOUR	BC	PST	48	23	123
Z0							22
Q1						6.067	000.0
O1						0.197	130.3
N01						1.211	137.0
P1						0.112	120.8
S1						0.674	148.5
K1						0.098	154.1
J1						2.070	149.4
N2						0.117	166.4
						0.294	63.4

M2  
S2

001007076 031007076 EQUI 1.0  
001007076 031007076 EXTR 0.5

1.213 87.0  
0.332 93.9

## Appendix 5

Tidal heights prediction results arising from the input data of Appendix 4. FIGURE 2 is a plot of these hourly heights over the period of 0100 PST July 24 1976 to 2400 PST July 31 1976.

STN	1ST HR	DATE	1	2	3	4	5	6	7	8	DT HRS
7120	1.0000	1 776	7.46	7.74	7.93	7.89	7.52	6.80	5.80	4.66	1.0000
7120	9.0000	1 776	3.58	2.76	2.36	2.47	3.07	4.05	5.23	6.39	1.0000
7120	17.0000	1 776	7.36	7.98	8.21	8.09	7.73	7.28	6.90	6.68	1.0000
7120	1.0000	2 776	6.66	6.82	7.05	7.22	7.19	6.89	6.30	5.48	1.0000
7120	9.0000	2 776	4.58	3.77	3.21	3.04	3.32	4.01	5.00	6.10	1.0000
7120	17.0000	2 776	7.12	7.90	8.31	8.34	8.02	7.48	6.68	6.35	1.0000
7120	1.0000	3 776	6.01	5.90	5.99	6.19	6.38	6.44	6.29	5.91	1.0000
7120	9.0000	3 776	5.36	4.75	4.21	3.90	3.91	4.29	5.00	5.93	1.0000
7120	17.0000	3 776	6.92	7.78	8.37	8.59	8.41	7.89	7.16	6.38	1.0000
7120	1.0000	4 776	5.68	5.20	4.98	5.01	5.22	5.50	5.72	5.81	1.0000
7120	9.0000	4 776	5.71	5.46	5.14	4.85	4.73	4.86	5.28	5.96	1.0000
7120	17.0000	4 776	6.80	7.65	8.36	8.77	8.80	8.42	7.71	6.77	1.0000
7120	1.0000	5 776	5.78	4.90	4.27	3.96	3.98	4.26	4.69	5.14	1.0000
7120	9.0000	5 776	5.51	5.72	5.76	5.69	5.60	5.60	5.78	6.18	1.0000
7120	17.0000	5 776	6.80	7.54	8.27	8.84	9.09	8.95	8.38	7.45	1.0000
7120	1.0000	6 776	6.30	5.10	4.05	3.29	2.94	3.00	3.41	4.05	1.0000
7120	9.0000	6 776	4.77	5.43	5.92	6.21	6.32	6.35	6.40	6.57	1.0000
7120	17.0000	6 776	6.93	7.48	8.13	8.76	9.21	9.33	9.02	8.26	1.0000
7120	1.0000	7 776	7.13	5.76	4.38	3.18	2.36	2.02	2.19	2.79	1.0000
7120	9.0000	7 776	3.67	4.66	5.58	6.29	6.74	6.95	7.01	7.05	1.0000
7120	17.0000	7 776	7.19	7.49	7.98	8.56	9.11	9.46	9.46	8.99	1.0000
7120	1.0000	8 776	8.05	6.72	5.18	3.65	2.38	1.56	1.31	1.65	1.0000
7120	9.0000	8 776	2.47	3.59	4.80	5.90	6.74	7.26	7.48	7.52	1.0000
7120	17.0000	8 776	7.51	7.59	7.85	8.29	8.83	9.32	9.58	9.46	1.0000
7120	1.0000	9 776	8.84	7.73	6.24	4.57	2.98	1.72	.99	.91	1.0000
7120	9.0000	9 776	1.44	2.48	3.80	5.16	6.35	7.21	7.70	7.86	1.0000
7120	17.0000	9 776	7.82	7.74	7.78	8.00	8.42	8.93	9.37	9.55	1.0000
7120	1.0000	10 776	9.30	8.55	7.31	5.72	4.00	2.44	1.28	.73	1.0000
7120	9.0000	10 776	.85	1.60	2.81	4.26	5.67	6.84	7.63	8.01	1.0000
7120	17.0000	10 776	8.06	7.92	7.78	7.78	8.00	8.40	8.88	9.26	1.0000
7120	1.0000	11 776	9.34	8.99	8.12	6.80	5.19	3.52	2.09	1.12	1.0000

7120	9.0000	11	776	.79	1.14	2.07	3.41	4.89	6.25	7.31	7.94	1.0000
7120	17.0000	11	776	8.16	8.08	7.85	7.66	7.64	7.85	8.24	8.68	1.0000
7120	1.0000	12	776	8.98	8.97	8.52	7.59	6.25	4.71	3.19	1.97	1.0000
7120	9.0000	12	776	1.26	1.18	1.74	2.81	4.18	5.59	6.82	7.68	1.0000
7120	17.0000	12	776	8.12	8.16	7.95	7.65	7.42	7.40	7.60	7.96	1.0000
7120	1.0000	13	776	8.33	8.55	8.45	7.93	6.99	5.73	4.34	3.05	1.0000
7120	9.0000	13	776	2.11	1.69	1.85	2.57	3.70	5.02	8.28	7.30	1.0000
7120	17.0000	13	776	7.94	8.16	8.04	7.71	7.36	7.11	7.08	7.25	1.0000
7120	1.0000	14	776	7.56	7.86	7.99	7.82	7.28	6.40	5.29	4.13	1.0000
7120	9.0000	14	776	3.14	2.50	2.35	2.72	3.54	4.64	5.83	6.89	1.0000
7120	17.0000	14	776	7.67	8.06	8.09	7.82	7.42	7.02	8.76	6.70	1.0000
7120	1.0000	15	776	6.83	7.06	7.28	7.34	7.14	6.64	5.89	4.99	1.0000
7120	9.0000	15	776	4.11	3.43	3.10	3.18	3.69	4.53	5.54	6.55	1.0000
7120	17.0000	15	776	7.38	7.91	8.08	7.93	7.55	7.08	6.65	6.36	1.0000
7120	1.0000	16	776	6.26	6.33	6.49	6.64	6.66	6.48	6.08	5.51	1.0000
7120	9.0000	16	776	4.87	4.30	3.91	3.83	4.09	4.67	5.46	6.33	1.0000
7120	17.0000	16	776	7.14	7.73	8.03	8.01	7.72	7.25	6.72	6.24	1.0000
7120	1.0000	17	776	5.91	5.76	5.77	5.87	5.98	8.02	5.92	5.68	1.0000
7120	9.0000	17	776	5.33	4.96	4.66	4.53	4.63	4.99	5.57	6.27	1.0000
7120	17.0000	17	776	6.98	7.58	7.96	8.06	7.88	7.47	6.91	6.32	1.0000
7120	1.0000	18	776	5.79	5.41	5.20	5.17	5.25	5.38	5.49	5.52	1.0000
7120	9.0000	18	776	5.47	5.35	5.23	5.15	5.21	5.43	5.82	6.34	1.0000
7120	17.0000	18	776	6.93	7.48	7.90	8.10	8.03	7.71	7.18	6.53	1.0000
7120	1.0000	19	776	5.85	5.27	4.84	4.60	4.56	4.68	4.89	5.13	1.0000
7120	9.0000	19	776	5.33	5.48	5.57	5.63	5.72	5.88	6.15	6.52	1.0000
7120	17.0000	19	776	6.98	7.46	7.87	8.13	8.17	7.95	7.49	6.83	1.0000
7120	1.0000	20	776	6.07	5.31	4.66	4.21	3.99	4.01	4.23	4.58	1.0000
7120	9.0000	20	776	4.98	5.37	5.69	5.94	6.12	6.29	6.49	6.75	1.0000
7120	17.0000	20	776	7.09	7.48	7.86	8.16	8.29	8.19	7.83	7.21	1.0000
7120	1.0000	21	776	6.41	5.53	4.69	4.00	3.56	3.41	3.55	3.94	1.0000
7120	9.0000	21	776	4.47	5.05	5.60	6.05	6.38	6.62	6.80	6.99	1.0000
7120	17.0000	21	776	7.22	7.52	7.86	8.19	8.40	8.42	8.18	7.65	1.0000
7120	1.0000	22	776	6.87	5.91	4.90	3.99	3.31	2.94	2.93	3.26	1.0000
7120	9.0000	22	776	3.85	4.58	5.32	5.98	6.49	6.84	7.05	7.20	1.0000
7120	17.0000	22	776	7.35	7.56	7.84	8.16	8.45	8.59	8.50	8.11	1.0000
7120	1.0000	23	776	7.41	6.44	5.33	4.22	3.28	2.66	2.43	2.63	1.0000
7120	9.0000	23	776	3.19	3.99	4.89	5.75	6.45	6.94	7.22	7.36	1.0000
7120	17.0000	23	776	7.45	7.57	7.77	8.06	8.39	8.65	8.74	8.53	1.0000
7120	1.0000	24	776	7.97	7.08	5.94	4.69	3.52	2.62	2.13	2.11	1.0000
7120	9.0000	24	776	2.54	3.34	4.34	5.36	6.25	8.92	7.32	7.49	1.0000



7120	17.0000	24	776	7.53	7.55	7.65	7.87	8.19	8.54	8.79	8.80	1.0000
7120	1.0000	25	776	8.47	7.75	6.68	5.39	4.06	2.90	2.11	1.81	1.0000
7120	9.0000	25	776	2.03	2.72	3.72	4.86	5.93	6.77	7.32	7.57	1.0000
7120	17.0000	25	776	7.60	7.53	7.50	7.59	7.85	8.23	8.61	8.83	1.0000
7120	1.0000	26	776	8.77	8.30	7.43	6.22	4.84	3.51	2.44	1.82	1.0000
7120	9.0000	26	776	1.76	2.23	3.14	4.30	5.49	6.52	7.24	7.61	1.0000
7120	17.0000	26	776	7.67	7.54	7.37	7.30	7.42	7.73	8.15	8.55	1.0000
7120	1.0000	27	776	8.74	8.60	8.02	7.04	5.76	4.37	3.11	2.21	1.0000
7120	9.0000	27	776	1.82	2.01	2.71	3.79	5.02	6.18	7.08	7.61	1.0000
7120	17.0000	27	776	7.76	7.62	7.33	7.07	6.98	7.12	7.48	7.93	1.0000
7120	1.0000	28	776	8.33	8.50	8.28	7.64	6.62	5.34	4.04	2.95	1.0000
7120	9.0000	28	776	2.27	2.13	2.55	3.44	4.60	5.81	6.86	7.56	1.0000
7120	17.0000	28	776	7.85	7.77	7.42	7.00	6.66	6.55	6.71	7.08	1.0000
7120	1.0000	29	776	7.56	7.95	8.08	7.85	7.20	6.22	5.05	3.92	1.0000
7120	9.0000	29	776	3.06	2.63	2.73	3.34	4.33	5.49	6.61	7.46	1.0000
7120	17.0000	29	776	7.93	7.97	7.66	7.13	6.57	6.17	6.02	6.17	1.0000
7120	1.0000	30	776	6.54	7.01	7.39	7.54	7.33	6.76	5.91	4.93	1.0000
7120	9.0000	30	776	4.05	3.44	3.26	3.56	4.28	5.29	6.38	7.34	1.0000
7120	17.0000	30	776	7.97	8.19	7.99	7.46	6.77	6.09	5.60	5.40	1.0000
7120	1.0000	31	776	5.52	5.87	6.32	6.72	6.90	6.79	6.38	5.74	1.0000
7120	9.0000	31	776	5.02	4.40	4.05	4.08	4.51	5.28	6.24	7.20	1.0000
7120	17.0000	31	776	7.96	8.37	8.36	7.94	7.22	6.37	5.58	4.99	1.0000

HL	STN	DATE	TIME	HGT	TIME	HGT	TIME	HGT	TIME	HGT	TIME	HGT
0	7120	1	776	322	7.9	1117	2.3	1907	8.2	9999	99.9	99.9
1	7120	2	776	33	6.6	424	7.2	1152	3.0	1933	8.4	9999
1	7120	3	776	200	5.9	550	6.4	1228	3.9	2002	8.6	9999
1	7120	4	776	321	5.0	759	5.8	1302	4.7	2034	8.8	9999
1	7120	5	776	426	3.9	1047	5.8	1332	5.6	2109	9.1	9999
1	7120	6	776	521	2.9	2148	9.3	9999	99.9	9999	99.9	99.9
1	7120	7	776	609	2.0	2230	9.5	9999	99.9	9999	99.9	99.9
1	7120	8	776	654	1.3	1547	7.5	1648	7.5	2313	9.6	9999
1	7120	9	776	737	.9	1611	7.9	1819	7.7	2358	9.5	9999
1	7120	10	776	819	.7	1639	8.1	1931	7.8	9999	99.9	99.9
0	7120	11	776	44	9.4	859	.8	1708	8.2	2035	7.6	9999
0	7120	12	776	129	9.0	937	1.1	1737	8.2	2137	7.4	9999
0	7120	13	776	214	8.6	1013	1.7	1806	8.2	2239	7.1	9999
0	7120	14	776	300	8.0	1047	2.3	1833	8.1	2347	6.7	9999

0	7120	15	776	346	7.3	1118	3.1	1900	3.1	9999	99.9	9999	99.9	9999	99.9
1	7120	16	776	102	6.3	433	6.7	1145	3.8	1926	8.1	9999	99.9	9999	99.9
1	7120	17	776	226	5.8	548	6.0	1205	4.5	1951	8.1	9999	99.9	9999	99.9
1	7120	18	776	345	5.2	754	5.5	1208	5.2	2015	8.1	9999	99.9	9999	99.9
1	7120	19	776	442	4.6	2040	8.2	9999	99.9	9999	99.9	9999	99.9	9999	99.9
1	7120	20	776	524	4.0	2106	8.3	9999	99.9	9999	99.9	9999	99.9	9999	99.9
1	7120	21	776	559	3.4	2136	8.4	9999	99.9	9999	99.9	9999	99.9	9999	99.9
1	7120	22	776	630	2.9	2210	8.6	9999	99.9	9999	99.9	9999	99.9	9999	99.9
1	7120	23	776	701	2.4	2250	8.7	9999	99.9	9999	99.9	9999	99.9	9999	99.9
1	7120	24	776	732	2.1	2333	8.8	9999	99.9	9999	99.9	9999	99.9	9999	99.9
1	7120	25	776	804	1.8	1638	7.6	1850	7.5	9999	99.9	9999	99.9	9999	99.9
0	7120	26	776	19	8.8	837	1.7	1643	7.7	1955	7.3	9999	99.9	9999	99.9
0	7120	27	776	107	8.7	910	1.8	1656	7.8	2055	7.0	9999	99.9	9999	99.9
0	7120	28	776	159	8.5	945	2.1	1714	7.9	2155	6.6	9999	99.9	9999	99.9
0	7120	29	776	254	8.1	1019	2.6	1736	8.0	2259	6.0	9999	99.9	9999	99.9
0	7120	30	776	356	7.5	1052	3.3	1800	8.2	9999	99.9	9999	99.9	9999	99.9
1	7120	31	776	7	5.4	509	6.9	1126	4.0	1828	8.4	9999	99.9	9999	99.9

# REFERENCES

- Cartwright, D.E. and R.J. Taylor, 1971. New Computations of the Tide-Generating Potential. *Geophys. J.R. Astr. Soc.* 23:45-74.
- Cartwright, D.E. and A.C. Edden, 1973. Corrected Tables of Tidal Harmonics. *Geophys. J.R. Astr. Soc.* 33:253-264.
- Davis, P.J. and P. Rabinowitz, 1961. Advances in Orthonormalizing Computation. *Advances in Computing.* 2:56-57.
- Dietrich, G., 1963. *General Oceanography.* Interscience Publishers. New York, London.
- Doodson, A.T., 1921. The Harmonic Development of the Tide-Generating Potential. *Proc. Roy. Soc. Series A.* 100:306-323. Re-issued in the *International Hydrographic Review*, May 1954.
- Faddeev, D.K. and V.N. Faddeeva, 1963. *Computational Methods of Linear Algebra.* W.H. Freeman and Company, San Francisco.
- Forsythe, G.E. and C.B. Moler, 1967. *Computer Solution of Linear Algebraic Systems.* Prentice-Hall, Englewood Cliffs, N.J.
- Godin, G., 1972. *The Analysis of Tides,* University of Toronto Press, Toronto.
- Godin, G. and J. Taylor, 1973. A Simple Method for the Prediction of the Time and Height of High and Low Water. Reprint from the *International Hydrographic Review.* Vol. L, N° 2, July 1973.
- Godin, G., 1974. Nodal Corrections (unpublished notes).
- Her Majesty's Nautical Almanac Office. *The Astronomical Ephemeris,* 1974. Her Majesty's Stationery Office, London.
- Her Majesty's Nautical Almanac Office, 1961. *Explanatory Supplement to the Astronomical Ephemeris and the American Ephemeris and Nautical Almanac.* Her Majesty's Stationery Office, London.
- Searle, S.R., 1971. *Linear Models.* John Wiley and Sons, New York.
- Wilkinson, J.H., 1967. The Solution of Ill-Conditioned Linear Equations in *Mathematical Methods for Digital Computers,* Vol. 2, edited by Ralston and Wilf.

















